Université de Montréal

Regulation of Sinoatrial Node and Pacemaking Mechanisms in Health and Disease

par Nabil El Khoury

Département de Pharmacologie et Physiologie
Faculté de Médecine

Thèse présentée en vue de l'obtention du grade de Doctorat
en Physiologie Moléculaire, Cellulaire et Intégrative

Décembre, 2016

Université de Montréal
Faculté de Médecine

Cette thèse intitulée :

Regulation of Sinoatrial Node and Pacemaking Mechanisms in Health and Disease

présentée par :
Nabil El Khoury

a été évaluée par un jury composé des personnes suivantes :

Dr Réjean Couture, président-rapporteur
Dre Céline Fiset, directrice de recherche
Dr Rémy Sauvé, membre du jury
Dr Alvin Shrier, examinateur externe
Dre Michèle Brochu, représentante de la doyenne

Résumé

Le nœud sinusal (NS) est le centre de l'automatisme cardiaque. Grâce à son activité électrique spontanée, il dicte la fréquence cardiaque (FC) en réponse aux demandes physiologiques. A ce jour, le NS demeure un sujet de recherche important puisque les mécanismes moléculaires responsables de sa régulation sont encore méconnus. Par exemple, les processus menant à la bradycardie sinusale et à la maladie du sinus (MS) chez les personnes âgées sont mécompris et présentement l'implantation d'un stimulateur cardiaque demeure le seul traitement disponible. Ainsi, l'objectif de cette thèse était de déterminer les changements moléculaires et cellulaires se produisant au niveau du NS en réponse à divers stimuli physiologiques et pathologiques afin d'établir leurs rôles potentiels dans la régulation de la FC et le développement de la MS.

Dans les deux premiers chapitres, la grossesse est présentée comme modèle physiologique. En effet, la réponse adaptative aux demandes croissantes de la mère et du fœtus engendre des changements physiologiques considérables au niveau du myocarde, dont une augmentation de la FC essentielle pour la perfusion adéquate des organes. Toutefois, cette augmentation peut aussi favoriser le développement d'arythmies.

Dans le troisième chapitre, l'inflammation, un facteur présent lors du vieillissement et dans plusieurs pathologies où la MS se manifeste, a fait l'objet d'une étude dans le but de déterminer son rôle dans le développement de la MS.

Les résultats obtenus dans cette thèse démontrent que la grossesse induit une hausse de la FC chez la souris gestante similaire à celle retrouvée chez la femme enceinte. Cette accélération était due à un remodelage électrique du NS. Plus spécifiquement, la fréquence des potentiels d'action ainsi que la densité et l'expression des courants *pacemaker* (I_f) et calcique de type L (I_{CaL}) étaient augmentées. De plus, une accélération des transitoires calciques spontanés et de la vitesse de relâche calcique du réticulum sarcoplasmique a été observée.

La régulation de l'automaticité par un stimulus pathologique, l'interleukine-1β, est abordée par la suite. L'interleukine-1β, une cytokine ayant un rôle majeur comme médiateur inflammatoire, se retrouve en concentrations élevées dans plusieurs maladies associées avec la

MS. Nos résultats démontrent que l'interleukine-1β engendre une diminution de l'automaticité associée à une réduction de I_f et I_{CaL} dans les cardiomyocytes humains de type nodal dérivés de cellules souches induites pluripotentes (hiPSC-CM). En parallèle, le phénotype électrophysiologique et moléculaire des hiPSC-CM a été caractérisé démontrant leur homologie avec les cellules du NS humain adulte, les validant comme modèle *in vitro* de cellules nodales humaines.

En conclusion, les études présentées dans cette thèse démontrent que le NS est plus qu'un simple tissu régulé par l'innervation autonome. En effet, son automaticité est dynamique et peut être influencée par des facteurs physiologiques ou pathologiques. Nos résultats contribuent ainsi à une meilleure compréhension des mécanismes sous-jacents à l'automaticité. Ces avancées sont importantes non seulement pour la santé des femmes, mais aussi pour les individus souffrant de la MS. À terme, nous espérons que ces résultats contribueront au développement de stratégies thérapeutiques pour traiter des complications liées aux troubles d'automaticité cardiaque.

Mots-clés : Nœud sinusal, maladie du sinus, automaticité, fréquence cardiaque, arythmies, grossesse, inflammation, interleukine-1β, hiPSC-CM

Abstract

The sinoatrial node (SAN) is the dominant cardiac pacemaker. With its spontaneous automaticity, it dictates rhythm and controls heart rate in response to varying physiological demands. Despite its modest size, the SAN is a very heterogeneous and complex structure that remains the topic of research efforts due, in part, to uncertainties in the mechanisms that regulate pacemaking in various conditions. For instance, the processes that lead to severe sinus bradycardia and SAN dysfunction (SND) in the elderly are unknown and to date, the implantation of electronic pacemaker remains the only SND treatment. Accordingly, the overall objective of this thesis was to explore and highlight the molecular and cellular changes that occur within the SAN in both physiological and pathological states, while determining how they contribute to regulation of heart rate and potentially SND.

In the first two chapters, we present pregnancy as a physiological model considering it is a period during which substantial adaptive changes to the myocardium and increases in heart rate occur. Paradoxically, the rapid rate, which is essential for adequate organ perfusion of both mother and foetus, may also increase vulnerability to certain arrhythmias.

In the third chapter, inflammation, a central process in pathology and common factor to several diseases and even ageing, was evaluated as potential underlying circumstance contributing to the development of sinus bradycardia and SND. Combinations of i*n vivo*, *ex vivo*, biochemical, molecular and cellular approaches were used in order to generate an integrated understanding of the models we examined.

Our data shows that in pregnant mice, an increase in heart rate similar to that of pregnant women occurs and was due to an electrical remodelling of the SAN. Specifically, an increase in action potential frequency of isolated individual SAN cells was observed. This was attributed to increased expression and density of pacemaker (I_f) and L-type Ca^{2+} currents (I_{CaL}) along with a rapid spontaneous Ca^{2+} transient rate and faster intracellular sarcoplasmic reticulum Ca^{2+} release.

We then demonstrate that the pro-inflammatory cytokine interleukin-1β which is a major inflammatory mediator that is upregulated in several diseases associated with SND,

dramatically slows automaticity by reducing I_f and I_{CaL} density in nodal-like cardiomyocytes derived from human-induced pluripotent stem cells (hiPSC-CM). Importantly, in that study, hiPSC-CMs were also physiologically and molecularly characterized revealing their high resemblance to adult human SAN and a potential use as a novel *in vitro* model to study pacemaking in humans.

In conclusion, the results of this thesis demonstrate that the SAN is not a simple, neurally controlled tissue, but a rather dynamic pacemaker that undergoes extensive intrinsic remodelling during states of health and disease. The results contribute to understanding physiological mechanisms of pacemaking and how they are altered by disease and may be relevant for both women's health and the individuals affected by SND. Ultimately, we hope these findings will be helpful in the development of therapeutic strategies to treat pacemaking-related complications.

Keywords : Sinoatrial node, sinus node disease, pacemaking, heart rate, arrhythmias, pregnancy, inflammation, interleukin-1β, hiPSC-CM.

Table of Contents

Figures List

List of Abbreviations and Acronyms

AF	Atrial Fibrillation
AKT	Protein Kinase B
ANP	Atrial Natiuretic Peptide
AP	Action Potential
APA	Action Potential Amplitude
APD	Action Potential Duration
AV node	Atrio-ventricular node
BMI	Body Mass Index
BPM	Beats per Minute
BSA	Bovine Serum Albumin
CaMKII	Ca2+ /calmodulin-dependent protein kinase II
cAMP	Cyclic adenosine monophosphate
CaV	Voltage-gated Ca2+ channel
cSNRT	Corrected Sinusnode Recovery Time
Cx	Connexin
DD	Diastolic depolarization
DDR	Diastolic depolarization rate
e.g.	example
EB	Embroyed Body
ECG	Electrocardiogram
END-2	visceral-endoderm-like
ePSC	Embryonic Pluripotent Stem Cells
ePSC-CM	Embryonic Pluripotent Stem Cells derived cardiomyocyte
eSC	Embryonic Stem Cells
etc.	etcetera
Eth	Threshold Potential
HCN	Hyperpolarization-activated cyclic nucleotide–gated channel

hiPSC	human induced Pluripotent Stem Cells
hiPSC-CM	human induced Pluripotent Stem Cells derived Cardiomyocytes
HIV	human immunodeficiency virus
i.e.	id est
ICaL	L-type Ca2+ current
ICaT	T-type Ca2+ current
If	Funny current
IL-1β	Interleukin 1
Kir	Inward rectifying K+ channel
Klf4	Kruppel-like factor 4
Kv	Voltage-gated K+ channel
LQTS	Long QT syndrome
MDP	Maximum Diastolic Potential
NANOG	Homeobox Transcription Factor
NaV	Voltage-gated Na+ channel
NCX	Sodium-calcium exchanger
N-hiPSC-CM	Nodal-like human induced Pluripotent Stem Cells derived Cardiomyocytes
NOD	Non-obese diabetic
Oct4	octamer-binding transcription factor 4
PDE	Phosphodiesterase
PDGF	Platelet-derived Growth Factor
PI3K(p110α)	Phosphatidylinositol-4,5-bisphosphate 3-kinase
PKA	Protein Kinase A
PLB	Phosphlamban
Rex-1	zinc finger protein 42
RyR	Ryanodine Receptor
SAN	Sinoatrial Node
SERCA	sarco/endoplasmic reticulum Ca2+-ATPase
Shox2	Short stature homeobox 2
SLE	Systemic Lupus Eythematosus

SND	Sinus Node Disease
SNRT	Sinus Node Recovery Time
Sox	Sry-related HMG box
SR	Sarcoplasmic Reticulum
SSEA-1	stage-specific embryonic antigen 1 or Cluster of Development 15
SSS	Sick Sinus Syndrome
Tbx	T-box transcription factor
TGF-β	Transforming Growth Factor Beta
TNFα	Tumour Necrosis factor alpha
WM-hiPSC-CM	working myocardium-like human induced Pluripotent Stem Cells derived Cardiomyocytes
Wnt	int/Wingless
zfp-42	zinc finger protein 42

To all the loving people that have offered me support throughout the years and filled my heart with joy.

Thank you.

Acknowledgments

Looking back at the experiences, scientific development, personal and professional growth that have reshaped my life during the last four years of my Ph.D., I cannot help realize how utterly remarkable this journey has been. And for this, I have first and foremost my mentor, Dr. Céline Fiset, to thank. Dr. Céline did not just teach me facts. She has given me something much more valuable: a complete mindset and a way of thinking that will remain with me long after the small scientific details have been forgotten. Through her knowledge, patience, consideration and trust, she has been able to awaken in me a high sense of scientific curiosity and critical thinking while constantly helping sharpen my skills throughout the years. I have been very fortunate to be awarded these life-long gifts and for that, I express my utmost appreciation and heartfelt gratitude.

By recognising the individual needs of every lab member and being flexible, Dr. Céline has created and nurtured an exceptionally professional and peaceful environment for all the lab members, allowing every person to find their own way in becoming the best version of themselves. This atmosphere also often managed to turn colleagues into friends. In that regard, I wish to extend my sincere thankfulness to Dr. Sophie Mathieu and Dr. Patrice Naud who have been of immense help both professionally and personally. And of course, Nathalie Ethier, who has not only been pretending to be my mother for all these years, but also acted accordingly. Thank you for relentlessly insisting on adopting me. I would also wish to thank Anh-Tuan Ton for his trust and help but especially for the entertaining and positive vibes he always brings; turning some of the most banal moments into hilarious memories.

Needless to say, none of the work presented here would have been possible without the dedication of present and former colleagues, trainees and collaborators who, I am fortunate to say, have become too many to name in one page. Thank you all!

Funding agencies have played a vital role in my education and I would like to thank the Fonds de Recherche en Santé du Québec, Université de Montréal and Institut de Cardiologie de Montréal for providing me scholarships, prizes, awards and investing in my capabilities throughout my Ph.D. years.

Reviewing a thesis is a long process requiring time and effort and is often taken for granted by students. Thus, I would also like to unequivocally acknowledge and thank all the members of the committee for taking some of their precious time to review this work and providing their much appreciated expert input.

Finally, I wish to extent my wholehearted gratefulness and love to my family, George, Gisèle and Laura who, through their endless support, have been a driving force in my life.

1 Introduction

Cardiac contraction is triggered by a finely coordinated electrical influx that propagates across the myocardial tissue. This electrical activity must remain synchronized and this is achieved thanks to various specialized structures within the heart that have evolved to transmit electrical impulses. Together, these tissues form what is known as the cardiac conduction system. The conduction system is comprised of both slow and fast conducting components: the sinoatrial node (SAN), a complete atrio-ventricular conduction axis which includes Bachmann's bundle as well as anterior, middle, and posterior internodal tracts that terminate at the atrio-ventricular (AV) node, the His bundle and branches and the Purkinje fibres (Figure 1).[1,2] While both nodes possess automaticity and are slow conducting, the SAN

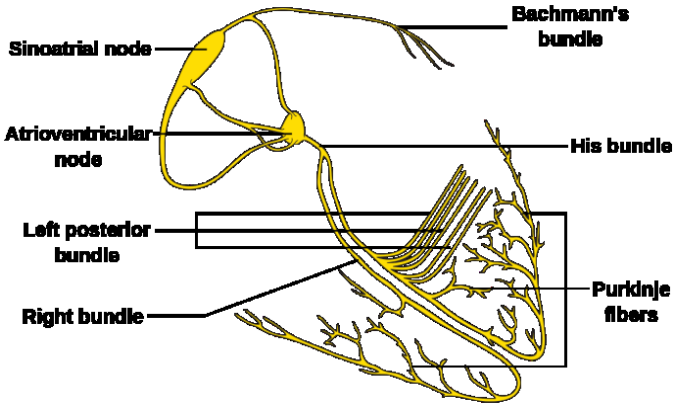

Figure 1. Representation of the human cardiac conduction system (Wikimedia commons).

is the dominant pacemaker that initiates the depolarization and the AV node may act as an accessory pacemaker if required. Thus, in case of SAN failure, the AV node is capable of stimulating the ventricles, albeit at much slower rate.[3] As the primary pacemaker, the SAN generates an impulse that is rapidly propagated across the atrial tissue before reaching the AV node where it gets delayed. This slowing in conduction allows the ventricles enough time to recover from the previous cardiac cycle before transmitting the electrical influx through the fast conducting His bundle and branches and the Purkinje fibre network.[4] The atrioventricular node is therefore the connecting point between the atrial and ventricular conduction pathways

and interestingly, in cases of rapid atrial pacing or fibrillation it can also block the impulse in order to protect the ventricles from arrhythmias. Once the impulse is transmitted to the ventricles, it spreads through the fast conducting and large network of fibres that allow propagation of the impulse deep within both ventricles simultaneously and in an apical to basal fashion i.e. from the base of the ventricles, upwards. The resulting cardiac contraction is thereby optimized for ejecting blood towards the pulmonary arteries and aorta.[3] Although the conduction system has been subject to investigation for more than a century now, much remains to be discovered. The work presented in this thesis will focus exclusively on the SAN, the specialized pacemaking cardiac tissue. After introducing the current state of knowledge, three articles related to SAN regulation will be presented. In brief, these studies delve into a relatively novel concept that portrays the SAN as an adaptive master regulator of heart rate. We propose that this specialized tissue is not static, but a rather dynamic pacemaker that can undergo extensive remodelling in response to both physiological and pathological stimuli. We present two models relevant healthy and pathological states, respectively, and by using a wide array of electrophysiological, cellular, molecular and imaging tools, we provide data showing how the pacemaking mechanisms were altered in each of these instances. Nonetheless, before presenting the data it will be important to review the SAN and place into its historical, anatomical and functional context.

1.1 The sinoatrial node: 110 years since its discovery

Sir Arthur Keith was a Scottish anatomist, anthropologist, evolutionary biologist and demonstrator at the London Hospital. Over the course of his career, he published numerous articles and books, held prestigious academic positions and through his work, presentations and honours became an internationally known scientist.[5] In the early 1900s, Keith was particularly interested by the heart and its anatomy. For years he thoroughly and meticulously examined cardiac preparations and specimens derived from various species including human and rodents. Eventually, this led him to believe that he knew everything about this fascinating biological pump.

Rather confidently, he decided one day to draft a letter to *The Lancet* denying the existence of a newly described cardiac feature, the AV node and conducting bundle, which he constantly failed to find in his preparations.[6] First extensively described by Sunao Tawara in 1906, the AV node discovery was published in German in a seminal paper entitled *Das Reizleitungssystem Des Säugetierherzens* (The conduction system of the mammalian heart). Tawara was a Japanese anatomist working under the supervision of pathologist Ludwig Aschoff in Germany and in his paper he described a structure at the end of the His bundle shaped into a "complex knotten" that, along with Purkinje fibers, formed a conduction system for the cardiac impulse.[5] Fortunately, after one additional search, Keith was finally able to find these structures and humbly admitted his oversights. He consequently amended the letter, which now corroborated Tawara's findings and sent it for publication.[7]

By the late summer 1906, Keith was still investigating cardiac anatomy in the study of his cottage in Kent, England. He actually transformed the study room into a laboratory, equipping it with ovens, microtomes, microscopes and a large supply of human and animal heart tissues. Quite unusual by today's standards, animals were mostly captured by traps and they included rats, mice, moles and hedgehogs, probably caught around the neighbouring gardens and vast parks of the Kent area. The idea behind this entire setup was to try and extend the work of Tawara, searching for irregular tissues within the heart. Keith had recruited a young fellow, Martin Flack, an Oxford graduate interested in pursuing a medical career.[6] Flack was the son of a local grocer and Keith was immediately delighted by his personality and ambition. One day after a hot summer bicycle ride with his wife, Keith came back to the cottage to find Flack staring at a peculiar structure under the microscope. It was near the sinus venosus region and while examining the hearts of the different species they had in their possession, they were always capable of tracing this structure right to the sino-atrial junction. In fact, it tremendously resembled the "knotten" previously described by Tawara, albeit, it was further upwards the AV node. The fibres of this section were somewhat striated, fusiform and densely packed in connective tissue. Keith and Flack also pointed out a close connection to the sympathetic and vagal nerves and a distinct artery irrigating the structure.[8] This was indeed the first documented evidence of the SAN as we know it today and the findings of this breakthrough by Keith and Flack were published in 1907. With this paper, the last piece of the

puzzle was finally added; solving, at least anatomically, the conduction system and answering many questions related to the beating of the heart.

Evidently, this was not the end, but merely the beginning of things. The SAN still needed functional validation and a few years later following its discovery, evidence elucidating the role of the SAN in the conduction system began to appear in the literature. Around 1909, using a setup consisting of a twin string galvanometer, Thomas Lewis was capable of measuring small electric currents at two locations on the heart simultaneously. By tracing the electrical impulse on a dog heart using this clever technique, he was able to pinpoint the exact location of the first electrical impulse. Sure enough, he found the SAN to be the precise site where the heart impulse was initiated. In 1924, when Einthoven, the inventor of the galvanometer for electrocardiography, was awarded the Nobel Prize, he heavily acknowledged Lewis and his findings which allowed the invention to serve a genuine purpose and actually be heard of.[5]

1.2 Anatomy, molecular determinants and physiology of the SAN

Fast forward to modern times and the SAN still fascinates many, including our group. There is still much to be learned and the SAN remains a source of discussion. Although nowadays, the debates have shifted from the old topics that questioned its importance in initiating the heartbeat to subjects related to the identity and contribution of various mechanisms within the SAN that are responsible for initiating the cardiac impulse. What are the molecular and electrophysiological characteristics on the SAN? How is the SAN regulated intrinsically and extrinsically? What role do physiological adaptations and disease play in regulating the SAN? These are only some of the fundamental questions being asked today; questions in which our laboratory has been particularly interested in and we hope, by the work presented herein, to provide some answers. Modern scientific tools including cellular, molecular and imaging techniques have allowed unprecedented insight into the SAN. With anatomy being one of the earliest investigated aspects of the SAN, the next section will debut by discussing the structure of the SAN and showing relatively recent computer-assisted data, resolving the 3-dimensional organization of the pacemaker tissue.

1.2.1 Basic anatomy of the SAN

The SAN is a small comma or crescent-shaped structure located at the junction of the right atrium and superior vena cava and extending down the crista terminalis. The cells within this structure do not resemble working myocardium myocytes but instead they are packed in connective and fibrous tissue, small and irregular in shape.[9,10] Indeed, in mice and other rodents, we find the average cellular capacitance of SAN cells to be around ~25-30 pF compared to ~70 and 150 pF for atrial and ventricular myocytes, respectively. When the SAN is enzymatically digested and cells released, the SAN cells are distinguishable by their heterogeneous morphology that falls into three different categories as shown in Figure 2.

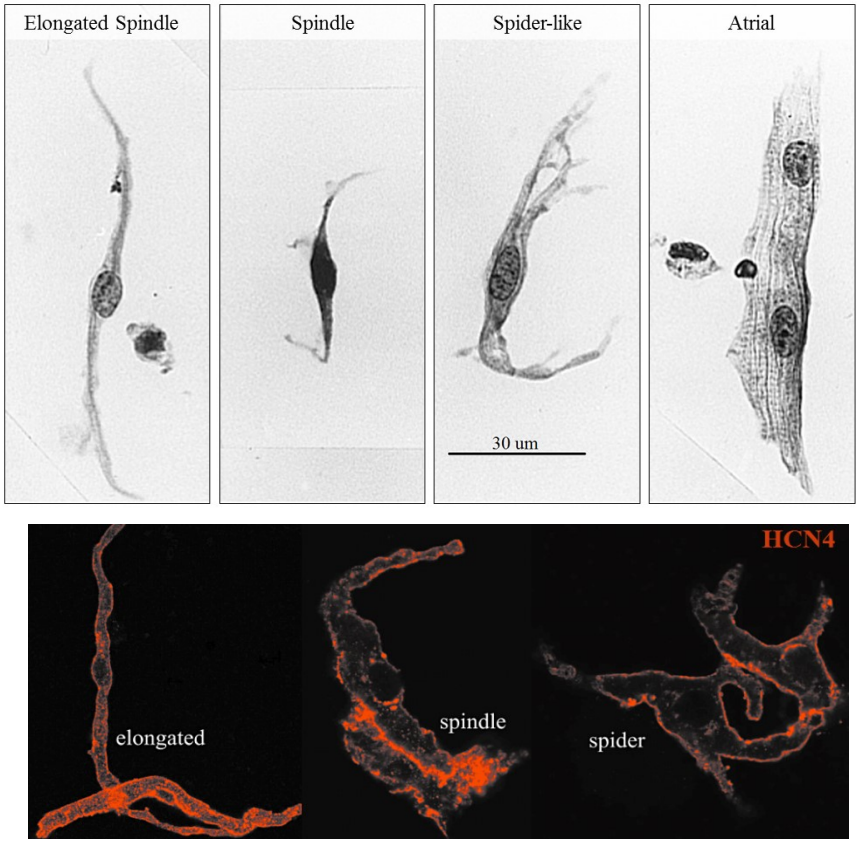

Figure 2. Morphology of isolated individual SAN cells. Following enzymatic digestion of the SAN individual nodal cells can be obtained. *Top*- Isolated rabbit SAN cells yield three distinct nodal cell shapes: elongated spindle, spindle and spider-like cells that differ drastically from atrial myocytes. SAN beat spontaneously under normal conditions. *Bottom*- Similar shapes are found in isolated mouse SAN cells. Cells are labelled in red for pacemaker ion channel HCN4, signature ion channel of the SAN. Modified from Verheijck et al. 1998 and Herrmann 2012.[10,25]

While the SAN has been classically reported as a nodule within the right atria, evidence suggests that its structure in humans is very heterogeneous and complex, even more so than in small mammals. Indeed it was reported that not only does the length of the SAN vary, but its location and orientation too, shifting from epicardial to endocardial.[11] Furthermore, the cells within the entire SAN region are also highly heterogeneous in shape and function while also varying amongst species. The SAN can be divided into two main distinct regions, so called a "head" and "tail". Closely surrounding the sinus node artery (Figure 3), cells have poorly structured myofilaments, low number of mitochondria and irregular shapes such as spindle and "spider" (Figure 2).[12,13] The myocytes in the head region are thought to form the dominant pacemaker, although under some circumstances, such as vagal stimulation, the leading pacemaker can shift to other areas of the SAN including the tail, which is lower, and runs parallel to the crista terminalis.[14] Nodal cells are evidently known for their distinct slow and spontaneous depolarization slope, depolarized potential and distinct action potential configuration that show sustained automaticity and of course, high expression

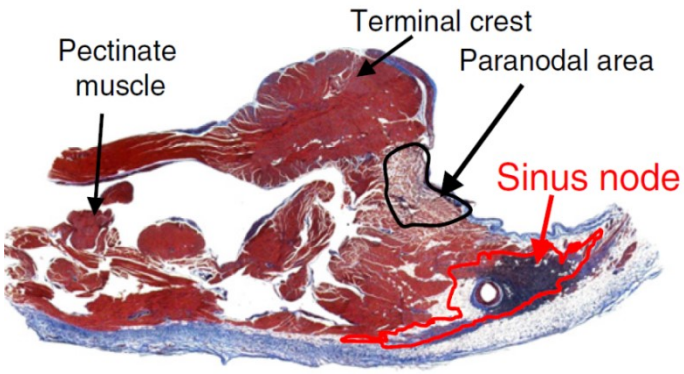

Figure 3. Histology of the SAN. Masson's trichrome stain of human SAN showing cardiac muscle in red and connective tissue in blue. The SAN body with its central sinus artery, packed in fibrous tissue, is encircled with a red line. The black line runs around a recently identified paranodal area. Modified from Dobrzynski H. et al. 2013.[2]

of hyperpolarization-activated pacemaker channels, HCN.[15] However, moving towards the periphery of the SAN, cells begin to have mixed nodal and atrial phenotype. The transition into peripheral myocytes occurs gradually as nodal cells begin to progressively acquire atrial traits such as bigger size, organized myofilaments and structure as well as expressing atrial ion channels and in fact, these cells have even been found to interweave with atrial myocytes at some levels (Figure 4).[11] Electrophysiological studies showed that these peripheral nodal cells have a certain degree of atrial electrophysiological properties as well, consistent with the gradient model of SAN heterogeneity, stating that nodal cells progressively acquire an increasing number of atrial traits the further they move away from the centre of the SAN.

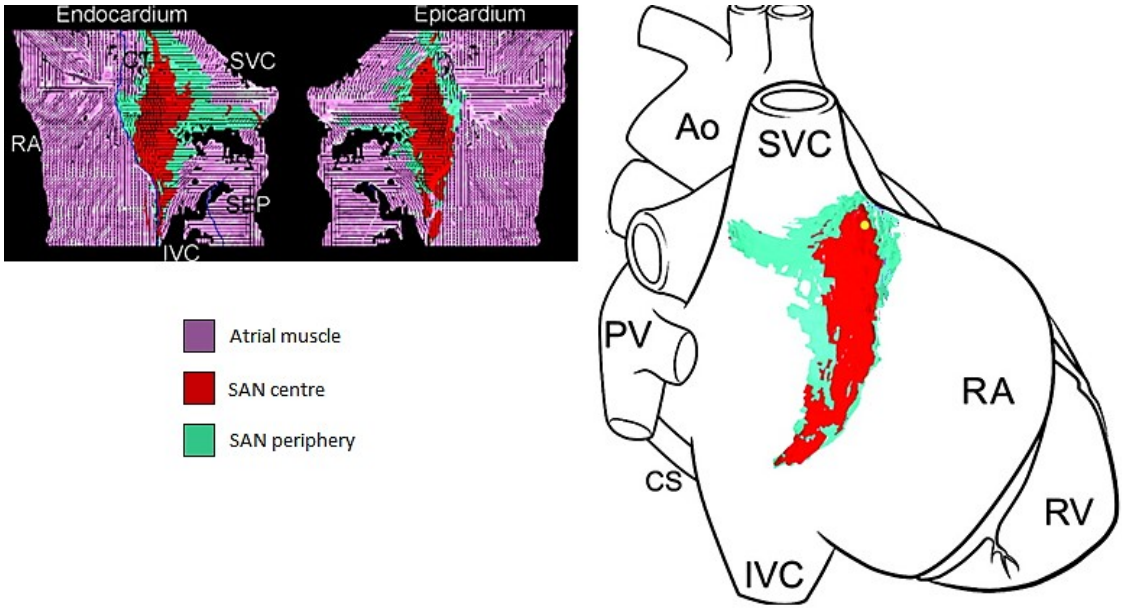

Figure 4. Computer reconstruction of rabbit SAN. *Left*- Location of the SAN within the right atria is shown from endocardium and epicardium views. Lines indicate cell orientation. *Right*- Schematic diagram of the SAN and its peripheral tissue in the heart. Ao indicates aorta; SVC, superior vena cava; PV, pulmonary vein; CS, coronary sinus; IVC, inferior vena cava; RA, right atria; RV, right ventricle. Modified from Dobrzynski et al. 2005.[3]

Indeed, although peripheral nodal myocytes retain their spontaneity, the action potential of these cells acquires faster, atrial-like phase 0 depolarization associated with higher expression of fast Na^+ channel[16] in addition to an increased expression of a major resting membrane potential channel Kir2.1, and fast-conducting connexin 43 compared to centre node cells (these channels will be discussed in more detail in the next sections).[17,18] It is important to note

that the peripheral SAN region also contains atrial myocytes. The presence of these myocytes along with nodal cells supports the mosaic effect model of SAN heterogeneity where the atrial/nodal cell proportion, but not individual properties, progressively increases with further distance from centre of the SAN.[12,19] Considering the SAN is surrounded by atrial tissue, these peripheral cells are thought to play a critical role in shielding the SAN from the inhibitory adjacent hyperpolarized potentials while preventing the centre of the node of becoming a source of re-entry in addition to efficiently regulating impulse exit and propagation towards the adjacent atria tissue.[17,20] While overall these various structures seem to be relatively conserved across species, in human SAN, they appear to be even more complex. A few years ago, a morphologically distinct paranodal region (Figure 3) was identified and characterized in human SAN preparations. With its mix of atrial and nodal myocytes, the paranodal region is hypothesized to serve an impulse exit function, analogous to the rabbit periphery SAN discussed above (Figure 4), although its exact role remains unknown (Figure 5).[9,21] The paranodal is peculiar in a sense that it is much larger than the actual SAN, thus, it extends far more than expected into surrounding atrial tissue. It has myocytes that are loosely packed in adipose tissue and has lower expression levels of the signature pacemaker channel HCN4.[9]

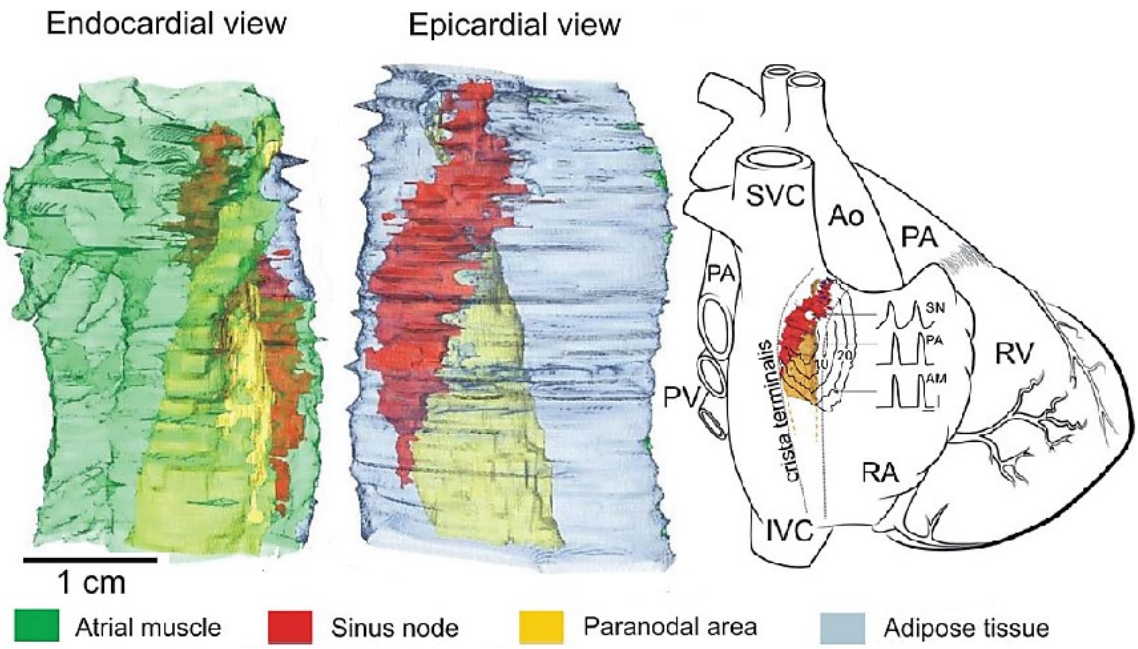

Figure 5. Computer reconstruction of human SAN and paranodal area. Reconstructed models of the paranodal area wrapped around the SAN are shown from different views. Schematic representation (right) shows the SAN and paranodal area in a human heart with electrical propagation into the right atria. Action potentials of varying morphology (SN: sinus node; PA: paranodal area; RA: right atria) are also shown on the activation front along with activation time (ms). They originate from the leading pacemaker site, shown as a white dot. Ao indicates aorta; SVC, superior vena cava; PA, pulmonary artery, PV, pulmonary vein; IVC, inferior vena cava; RA, right atria; RV, right ventricle. Modified from Chandler et al. 2011.[21]

1.2.2 Physiology and pacemaking mechanism of the SAN

The various genetic networks regulated during development and distinct expression pattern of ion channels, pumps and transporters are ultimately responsible for generating pacemaking capabilities within the SAN. Automaticity of the SAN can be electrically observed by recording action potentials (APs). Using the patch-clamp technique in current-clamp mode, individual, spontaneously beating SAN cells can be patched and recorded. We extensively use this technique in our laboratory; and under physiological conditions with no stimulation or current injection, we observe spontaneous APs that have a distinct configuration that is very different from typical atrial and ventricular myocytes APs. Indeed, the hallmark feature of the SAN AP is the presence of a diastolic depolarization slope (phase 4) which highly influences pacing rate.[22] During this phase, various voltage-gated channels and Ca^{2+}-dependent mechanisms participate in bringing membrane potential close to threshold potential of the AP by depolarizing the cell allowing it to fire an AP.[15] This is in clear contrast to working myocardium where Kir2.x channels impose a resting potential of around -80 mV, as the cell awaits the next stimulation.

These basic pacemaking mechanisms have been separated into two entities termed "voltage-clock" and "Ca^{2+}-clock". These clocks have, for years, fuelled heated debates over their individual importance and contribution to pacemaking.[23] Today, there is general agreement that both of these mechanisms are important in their own respective way, mostly because blocking either one severely disturbs pacemaking. Thus, the more recent term "coupled-clock" was coined to reflect the substantial contribution of both mechanisms to SAN automaticity. These two clocks will first be reviewed individually before discussing their integrated function.

1.2.2.1 Voltage-Clock

The voltage-clock, also known as M-clock, or membrane-clock consists of voltage-gated membrane ion channels, and their underlying currents, that control cell membrane potential in the SAN. It includes the pacemaker funny channels, HCN, L and T-type Ca2+ channels and repolarizing K^+ channels which are variable among species and include Kv4.3, Kv1.5, Kv7.1 and Kv11.1 (ERG).[9] In mouse SAN, mERG, plays a major role in repolarization and driving down membrane potential.[24]

Funny current (I_f): is encoded by HCN1-4, with HCN4 being the most importantly expressed isoform across several species, although HCN1 and 2 also contribute to human and mouse I_f, respectively.[9,17,25] The funny current has been originally described more than 35 years ago and tremendous amount of work has allowed it to evolve from a basic concept in cardiac physiology to a drug target for rate control with indications for angina and heart failure.[26,27] Termed "funny" at the time because the current counter-intuitively activated with hyperpolarization and was also found to be permeable to Na^+ despite its signature K^+ channel motif in the selectivity pore region. I_f plays a crucial role in the early phase of the diastolic depolarization (DD) also known as phase 4 of the AP. Indeed, the repolarization of the AP, bringing membrane potentials below -50 mV, triggers the activation of the HCN channels which generate a strong inward current through permeation of Na^+ and K^+ resulting in increases in membrane potential and the beginning of the depolarization phase.[15] A key feature of HCN channels is their regulation by cyclic nucleotides, notably cAMP which binds to a conserved cyclic nucleotide-binding domain (CNBD) in the C terminus. Increases and decreases of intracellular cAMP levels, through sympathetic and parasympathetic tones for instance, will modify voltage-dependency of HCN channels leading to an increase or decrease in current density at diastolic potential. Consequently, the steepening or lowering of the depolarization slope, results in acceleration or deceleration of AP frequency, respectively.[28,29] Although all HCN channels share common structural and functional features, the sensitivity to cAMP, the voltage-dependence and the kinetics of the different isoforms varies. Indeed, HCN1 channels have the fastest kinetics and lowest cAMP sensitivity compared to HCN4 that is the slowest to activate while having the highest sensitivity to cAMP. In addition, HCN1 is known to activate at more hyperpolarized voltages compared to HCN4.[26,30,31] HCN2 and 3 are

known to have intermediate properties that are found to be between those of HCN1 and 4. For instance, HCN2 has a lower cAMP sensitivity and activates faster than HCN4, although to a lesser extent than HCN1.[32] Through knockout studies in the mouse, HCN2 has been shown to have a functional role in regulating resting heart rate while accounting for about 30% of I_f current in SAN cells. The presence of HCN2 thus, plays a role in regulating overall sensitivity to cAMP as well as overall kinetics.[33]

T- and L- type Ca^{2+} currents (I_{CaT}, I_{CaL}): In the SAN both T-type channel transcripts $Ca_V3.1$ and $Ca_V3.2$ are found although transgenic approaches seem to support a major functional role only for $Ca_V3.1$. Indeed, in $Ca_V3.2^{-/-}$ knockout mice, no alterations in the ECG were noted while the $Ca_V3.1^{-/-}$ mice had bradycardia suggesting altered SAN function. Further analysis revealed that SAN AP firing rate was significantly reduced in $Ca_V3.1^{-/-}$ mice indicating a clear role for $Ca_V3.1$ in pacemaking.[34] Since I_{CaT} peaks rather negatively, at around -45 mV, its physiological role is thought to extend the I_f-induced depolarization (I_f conductance being close to nil at -40 mV), thereby bringing membrane potential further towards the activation threshold of L-type Ca^{2+} channels.[15] Thus, I_{CaT} is implicated in the mid DD phase and serves as an important link between I_f and I_{CaL} that are essential in the early and late DD, respectively. In the SAN, there is a particular enrichment in $Ca_V1.3$ transcripts compared to the working myocardium that is abundant in $Ca_V1.2$. Functionally, it is estimated that ~70% of I_{CaL} in the SAN is generated by $Ca_V1.3$.[9,35] Since $Ca_V1.3$ activates more rapidly and at more negative membrane potentials compared to $Ca_V1.2$, this allows I_{CaL} to have a more significant and efficient contribution to the diastolic depolarization in SAN cells. By beginning to activate towards -50 mV (close to peak I_{CaT}), I_{CaL} rapidly, drives the last end of the DD towards activation threshold and triggers the upstroke depolarization (phase 0) which also involves $Ca_V1.2$.[35]

ERG channels (I_{Kr}): In mouse SAN cells, the activation of the rapid component of the delayed rectifier K^+ current (I_{Kr}, encoded by mERG1) is very important for the repolarization of the AP. Considering there is virtually no Kir2.1 (I_{K1}) in the SAN and that stable resting potential cannot be achieved, the role of I_{Kr} and its deactivation become even more important for pacemaker depolarization.[24,36,37] Specifically, the degree to which I_{Kr} can drive the repolarization is critical considering it will directly influence the initial phase of the

pacemaker depolarization, i.e. I_f activation.[37,38] As such, block of I_{Kr} will not only result in prolongation of AP duration but it will also depolarize the maximal diastolic potential (MDP), which is usually around -60 mV in SAN, and as a result reduce the necessary activation of I_f and the other currents, further contributing to a lower AP frequency.

1.2.2.2 Ca^{2+}-clock mechanisms

Although the SAN expresses the same L-type Ca^{2+} channels and RyR isoforms as atrial or ventricular cells, the mechanisms and functional role of Ca^{2+} in the SAN is somewhat different. Indeed, in working myocytes, Ca^{2+} plays a critical role in inducing mechanical contraction of the cells.[39] The ultrastructure and organization of myocytes, featuring dense T-tubules, juxtaposing L-type Ca^{2+} and RyR channels ensure a rapid, efficient and cell-wide Ca^{2+} release to trigger contraction in a phenomenon termed Ca^{2+}-induced Ca^{2+}-release.[40] On the other hand, as a pacemaker, the SAN has arguably evolved to play a mostly electrical role as seen by the lack of T-tubules and contractile filaments.[39] Thus, the Ca^{2+}-induced Ca^{2+}-release by which L-type Ca^{2+} channels trigger the release of Ca^{2+} from the SR becomes essential for cellular depolarization and automaticity. Furthermore, this mechanism has been tweaked in the SAN to feature an additional component that is based of spontaneous Ca^{2+} releases and sparks. These Ca^{2+} sparks or local Ca^{2+} releases (LCRs) represent spontaneous releases of Ca^{2+} from the sarcoplasmic reticulum (SR) via RyR.[41] Collectively, the rhythmic oscillations of intracellular Ca^{2+} that contribute to automaticity are referred to as the Ca^{2+}-clock.

Similarly to other cardiomyocytes, the RyRs are sensitive to ryanodine-dependent block or caffeine-induced channel opening through lowering of the Ca^{2+} activation threshold.[42] Furthermore, SAN RyRs are particularly sensitive to cytosolic Ca^{2+} which can modulate amplitude and frequency of the spontaneous sparks. Compared to ventricular myocytes, it was found in the SAN that Ca^{2+}-spark frequency and amplitude were significantly higher, in support of a bigger role for LCRs in these cells.[43] Indeed, following Ca^{2+} entry through activation of I_{CaT}, there is a local rise in Ca^{2+} concentrations that increases the LCRs. As a result, the electrogenic Na^+/Ca^{2+} exchanger (NCX1) activates in forward mode exchanging 1 Ca^{2+} for 3 Na^+, resulting in a net positive charge that accelerates the late phase of the DD driving it faster towards threshold potential.[41,44] Once threshold is reached, opening of I_{CaL} and

subsequent phase 0 upstroke triggers a massive Ca^{2+} release from the SR, that is comparable to a Ca^{2+} -induced Ca^{2+}-release mechanism in working myocytes. Ca^{2+} is subsequently recaptured by SERCA2a, pumped into the SR as the remaining cytosolic Ca^{2+} gets extruded by NCX1. Overall, RyR2, NCX1, SERCA2a and its regulatory subunit phospholamban (PLB) are major proteins involved in the intracellular Ca^{2+} cycling in SAN and are essential for rhythmic activity.[23,41] Figure 6 summarizes these two pacemaking mechanisms and their related proteins.

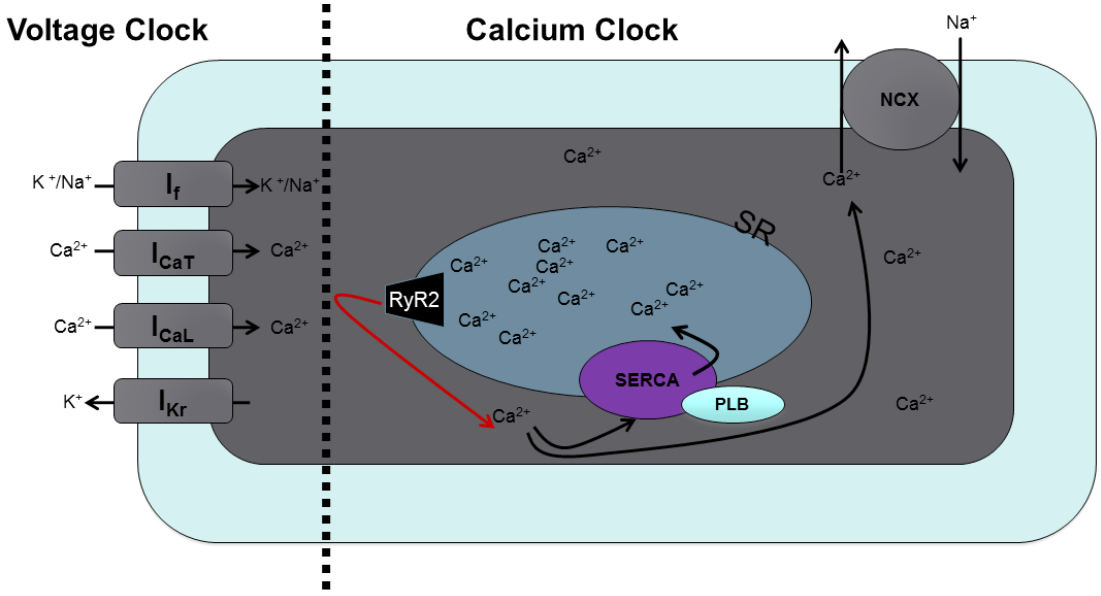

Figure 6. Schematic representation of SAN cell with voltage and Ca^{2+} clocks illustrated. Membrane-bound voltage gated ion channels are shown on the left while SR-Ca^{2+} cycling is shown on the right.

1.2.2.3 Coupled-clock model of pacemaking

The coupled-clock model of SAN pacemaking proposes that both of the previously discussed mechanisms are important for automaticity. This model is most likely to be a concrete representation of physiological pacemaking as it integrates two large concepts and presents the SAN as sole pacemaker unit that can be finely regulated.[45] While Figure 6 shows the various components of the two clocks, Figure 7 illustrates their functional interaction. This interlock of the two systems is particularly noticeable when altering either of the components and realizing that it results in termination or altered automaticity. For instance, ivabradine, the HCN selective-blocker, results in a reduction of AP rate while application of ryanodine also results in a similar effect.[46] Another important aspect of the coupling relates to control of automaticity by external factors including sympathetic and parasympathetic tones, β-

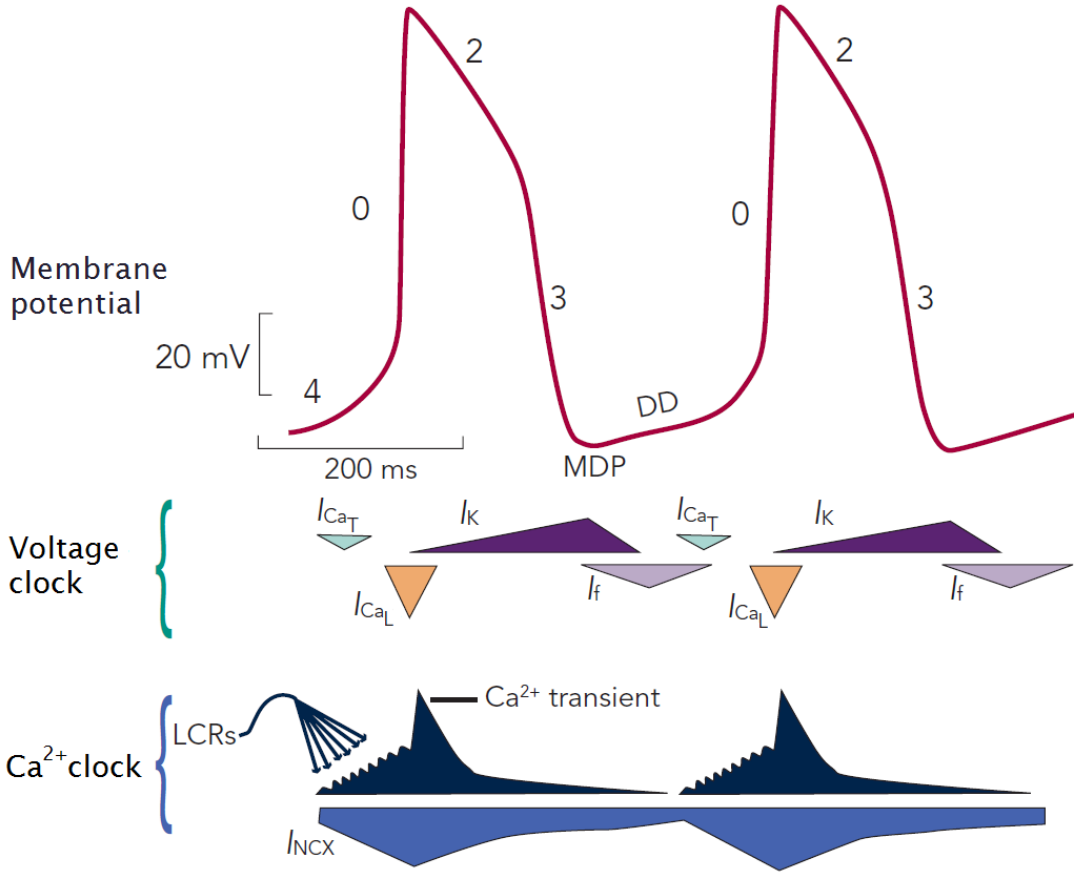

Figure 7. Schematic representation of SAN automaticity. Typical nodal action potentials are shown on top, chronologically aligned with corresponding voltage-gated ionic currents and Ca^{2+} mechanisms during AP each phase. LCR indicate local Ca^{2+} release; MDP, maximal diastolic potential; DD, diastolic depolarization. Modified from Choudhury et al. 2015.[20]

adrenergic and muscarinic agonist. Thus, second messengers such as Ca^{2+} and cAMP and cAMP-dependent pathways which include Protein Kinase A (PKA), Phosphodiesterase (PDE), Ca^{2+} /calmodulin-dependent protein kinase II (CaMKII), affect both membrane-bound ion channels and a big part of the Ca^{2+} handling components, providing further evidence that it is essential that both mechanisms be regulated concomitantly to sustain an accelerated or slow pacing rate.[47,48]

1.2.3 Molecular determinants of the SAN

Following transition and maturation from the embryonic to the adult stage, the complex network of transcription factors and gene program would have been responsible for the regulation of thousands of genes including fundamental targets, such as ion channels, transporters and pumps that allow the SAN to fulfill its pacemaking function. Molecular analysis of these genes and proteins also reveal a distinct signature for various tissues surrounding the SAN. As a general observation, there is a striking contrast in the expression of various ion channels and transporters between the central SAN and the atria while the peripheral SAN is somewhat in between both, showing a mixed expression profile.[9] Interestingly, analysis of the human SAN showed high consistency with expression studies from smaller mammals including rabbit and mouse indicating great conservation of the basic pacemaking mechanism with the differences being mostly confined to voltage-gated K^+ channel isoforms. Indeed, compared to the right atria, the human SAN shows higher expression of pacemaker funny channel HCN4, L-type Ca^{2+} channel α-subunit $Ca_V1.3$, T-type channel α-subunit $Ca_V3.1$ and slow conducting gap junction connexin 30.2. Conversely, it shows lower expression of L-type Ca^{2+} channel α-subunit $Ca_V1.2$, cardiac Na^+ channel α-subunit $Na_V1.5$, inward rectifier channel Kir2.1, ryanodine receptor RyR2, sarcoplasmic reticulum Ca^{2+} ATPase pump SERCA2a as well as the fast conducting gap junctions, connexin 40 and 43.[9,17] The absence of fast conducting connexins in the SAN is thought to protect the SAN from the hyperpolarized adjacent atrial tissue where conduction velocity is much higher. Having low conduction connexins in the centre (Cx45 and 30.2) and gradually increasing expression of Cx40 and Cx43 towards the periphery, facilitates the unidirectional

exit of the cardiac impulse.[12] Of note, although Cx45 expression is high in the SAN, it has also been shown to be equally high in the atria, thus, the overall conduction velocity is likely to be dependent on a balance of fast/slow connexins. Lastly, another interesting observation was the dramatic increase in RyR3 expression in the SAN compared to the atria.[9,49] It has been hypothesized that in frog muscle RyR3 may act as a leak Ca^{2+} channel[50] however, the functional consequence and role of RyR3 in the SAN remains completely unknown.

It has been long been suspected that the distinct morphological features of the SAN arise from differential gene programming compared to other cardiac tissue such as the atrium. Over the last couple of decades, meticulous analyses have revealed a distinct molecular signature for the different subparts of the SAN. Recently, genetic lineage tracing revealed that the head, which comprises up to 75% of the total volume of the mouse SAN, retains the embryonic sinus venosus molecular signature from which it is initially derived.[51] The function of the various transcription factors that were mapped within the SAN region will be discussed in more detail below, nonetheless, the classic signatures known today are $Tbx3^+$, $Tbx18^+$, $Shox2^+$ and $Nkx2.5^-$ in the SAN head, while the tail is $Tbx3^+$, $Tbx18^-$, $Shox2^+$ and $Nkx2.5^{+/-}$. The expression profile of these transcription factors is in striking contrast to that of the atrium which is $Tbx3^-$, $Tbx18^-$, $Shox2^-$ and $Nkx2.5^+$.[51,52] Tbx, T-box family of transcription factors, are critical and absolutely necessary in early embryogenesis as they are responsible for organogenesis, tissue differentiation and even limb formation.[53] As early transcription factors, they are upstream a wide range of genes and in the SAN, Tbx18 was shown to be necessary for the formation of the SAN head and its structure. On the other hand, Tbx3 was required for SAN differentiation by increasing expression of nodal (e.g. HCN4) and suppressing atrial genes including Nkx2.5, connexin 40/43, natriuretic peptide A (ANP) and $Na_V1.5$.[51] In short, while both Tbx18 and 3 control different developmental stages, both are required for full maturation and differentiation of the SAN. Interestingly, it was recently been shown that ectopic expression of Tbx18 into rodent adult cardiomyocytes, directly transforms them into a sinoatrial phenotype with pacemaker function and morphology through control of Shox2, Tbx3 and Tbx5, indicating that Tbx18 is likely upstream of all these targets.[54] Tbx5 is also important in SAN development as it positively regulates Tbx3 and Shox2.[55] Shox2 is a homeobox DNA-binding protein and transcription factor that controls morphogenesis, it is

known to be a negative regulator of Nkx2.5, and thus essential for SAN differentiation.[56] Indeed, Nkx2.5 is another cardiac transcription factor involved in encoding structural, functional and regulatory proteins of cardiomyocytes. During embryogenesis it actively participates in morphogenesis, septation and chamber differentiation and it is upstream a wide range of other transcription factors responsible for expression of contractile proteins and ion channels in working cardiomyocytes such as α-actin, MEF-2C, NCX1, connexin 40, and ANP.[57,58] Inhibition of Nkx2.5 by Shox2 is, therefore, crucial for maturation of the SAN. The basic molecular signatures and transcription factor network are summarized in Figure 8.

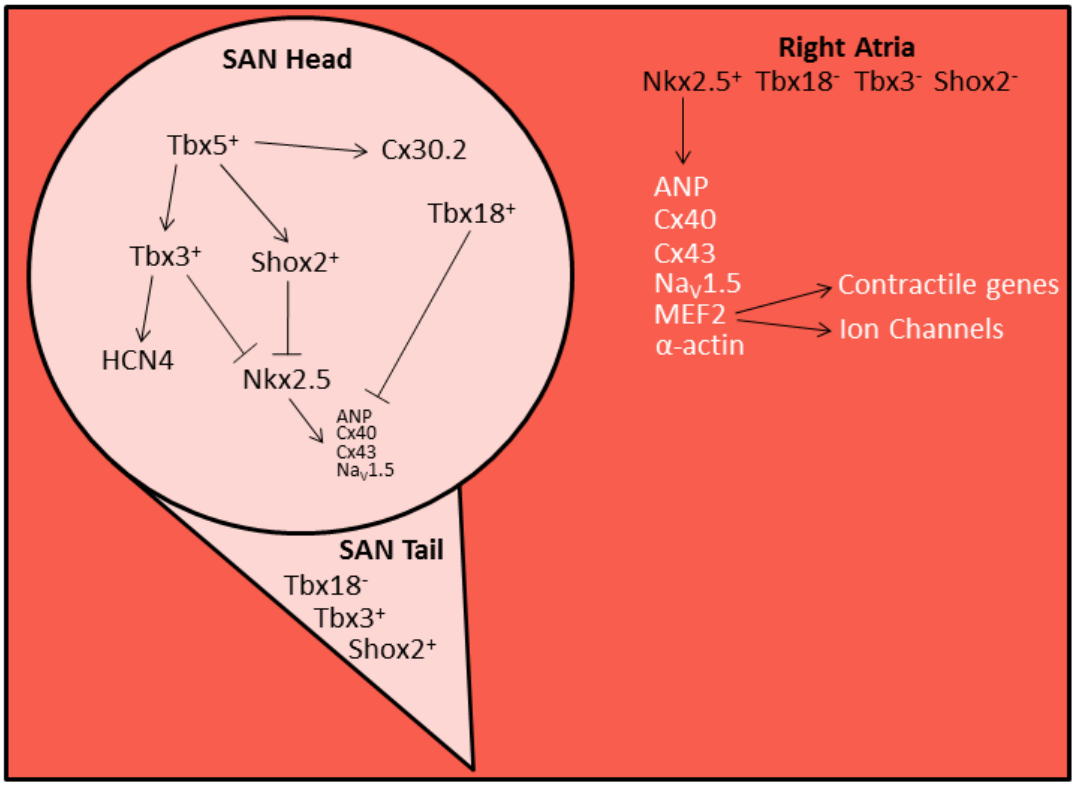

Figure 8. Transcription factor network of the SAN and right atria. Schematic representation shows the basic molecular signature of each structure and corresponding downstream gene targets, which can include other transcription factors. E.g. MEF2 regulates hundreds of genes implicated in myocyte contractility and ion channels.

1.3 Regulation of automaticity in models of health and disease

Having now covered an important part of the SAN normal anatomy and function, the next sections will provide contextualization and essential knowledge on various subjects that revolve around on the main themes of this thesis. Regulation of cardiac automaticity is a critical process in the maintenance of a healthy cardiovascular system. Through a fine regulation of its rate, the heart can provide an appropriate response to a varying range of physiological demands such as exercise, resting or stress. One can thus, easily imagine how tipping the heart rate balance towards increased or decreased resting rate or even worse, losing this homeostatic control could prove to be detrimental.[59,60] The SAN therefore remains the master controller of heart rate and in order to understand how the pacemaking mechanisms are affected by certain cases of health and disease we chose two models that illustrate these conditions. Specifically, we chose pregnancy as a model of healthy physiological adaptation and in this context, we were the first to examine the SAN and its pacemaking functions. Pregnancy is an important period during which the body goes through a complex array of changes to ensure sustained growth and wellbeing of the foetus.[61] The changes that are brought about extend to the vasculature and the heart and are in big part thought to be triggered by major changes in hormonal levels. Although, the maternal heart has been morphologically and functionally examined during the various stages of pregnancy, much remains to be known, especially in terms of changes in electrophysiological parameters.[62] Indeed, cardiac electrophysiological properties in women are strongly influenced by pregnancy as they also need to adapt and function in tandem with the cardiac structural changes in order to cope with the larger blood volume and provide sufficient perfusion to the organs and foetus.[63] These cardiac changes have often been paralleled to the changes observed in the athlete's heart, yet unfortunately, in some women pregnancy also results in electrical instability leading to several cardiac complications.[64] The SAN being central to heart rate regulation and initiation of the cardiac impulse we thus, asked how does the SAN adapt to pregnancy and how are the pacemaking parameters altered accordingly? In addition, how can these changes relate to electrical instability and arrhythmia vulnerability in some cases and is there any role for hormones in this regulation? We believe understanding the pathways that regulate cardiac electrical activity in the context of pregnancy and hormones is essential as it

provides invaluable knowledge on a physiological adaptation that can affect close to half the population. This knowledge becomes a setting stone for also understanding how these mechanisms can become deregulated in some cases, thereby contributing to the advancement of women's health and paving the way for eventual novel therapies.

At the other end of the spectrum, pathophysiology and disease drive a large part of cardiovascular research: heart failure, ischemia, hypertension, congenital heart disease and arrhythmias, to name a few topics, are still subjects of intense investigation. Worryingly, the SAN has been shown to be sensitive to several of these conditions that alter its function.[20] Although more of a process than a disease, we have chosen inflammation as a model to represent pathophysiology. Inflammation is today recognized as a key process implicated in countless conditions, including cardiovascular ailments. Indeed, heart failure, atherosclerosis, diabetes and several other diseases have been strongly linked to inflammation, which is characterized by the secretion of a complex array of cytokines, chemokines and immune system modulators.[65–67] These factors have the ability to circulate systemically, binding to cell surface receptors on many cells and triggering a response. Although in the heart the role of inflammatory processes in hypertrophy and heart failure has been examined,[68] very little is known on how these factors alter cardiac electrophysiological parameters. In one of our first studies, we have shown that pathophysiological levels of a cytokine (IL-1β) can alter ventricular ionic currents[69] which lead us to ask the question, are cytokines able to alter the ionic current of the SAN, hence affect pacemaking? If yes, could it be the link between SAN dysfunction observed in patients suffering from inflammatory conditions or even ageing, a process now known to implicate chronic low-grade inflammation? Sinus node dysfunctions (SND) currently represent a group of pathologies with varied aetiologies that affect the SAN and the causes of SND remain largely unknown.[20] In our studies, we propose that inflammation might be central to the development of SND by contributing to electrical remodelling of the SAN and perhaps even its senescence.

By using these two models, we hope to be able to understand how the SAN responds to various stimuli and how dynamic it is. Specifically, we will be able to analyse and compare the electrophysiological remodelling that could occur in both of these instances and conclude on the regulation of pacemaking function. By including *in vivo* and human cells in our studies,

we also hope that this work will further in help identifying pathways that could be targeted in order to prevent SAN dysfunction.

1.3.1 Physiological adaptations of pregnancy

Pregnancy is an important time during which the body undergoes important adaptations in preparation and in order to support of a new life. The mother's body goes through several adjustments including changes in hormonal balance, weight gain due to acquisition of fat, water and muscle as well as metabolic changes that need to be supported by appropriate nutrition and supplementation. Almost every organ system and functions from respiratory to gastrointestinal are affected including of course, the cardiovascular system which also witnesses an increase in its overall functional capacity and efficiency.[70,71] These changes will be discussed below in more detail.

1.3.1.1 Cardiovascular changes associated with pregnancy

Within the early stages of pregnancy, the cardiovascular system begins undergoing extensive remodelling. These changes are essential in order to ensure adequate supply of oxygen and nutrients to the uteroplacental regions and the growing foetus while preserving an uncompromised function to the mother.[61] Hemodynamic measurements have shown that during pregnancy blood volume increase (up to 40%), cardiac output is nearly doubled and arterial compliance is increased by ~30%.[62,64,72,73] Furthermore, total vascular resistance, a measure that depends on blood viscosity and flow rate through small calibre vessels, is decreased while systolic and diastolic blood pressures are mostly maintained normal or with a tendency towards a slight (10 mm Hg) reduction in some instances.[74] The larger blood volumes, outputs and overall cardiac work require the heart to adapt as well and accordingly, there is significant structural remodelling of the atria and ventricles. Indeed, left atrial diameter and ventricular wall thickness are increased by up to 25% while the left ventricular mass is increased by 50%.[75,76] Of note, this cardiac hypertrophy has been shown to be highly correlated with body mass index and body surface. Furthermore, in pregnant rats heart-to-body weight ratios were actually reduced, indicating efficient cardiac function and overall

adaptation. This is in clear contrast to heart failure for example, where the heart-to-body ratio is much higher since for a same -or even declining- body weight, the heart keeps growing larger in an attempt to counteract its inherent inefficiency.[77,78] Interestingly, with the increased capacity to pump blood, the resting heart rate is also increased during pregnancy by up to 25%.[79,80] Although physiologically essential, this increase in resting heart rate can have several electrophysiological impacts. As stated earlier, tipping the homeostatic balance of heart rate control in either direction can be detrimental and in this case sustaining fast rates has been known to increase the risk of electrical disturbances.[81] Perhaps unsurprisingly, numerous studies have shown that during pregnancy there is a significant increase in the risk of a wide range of arrhythmias.[64,80,82,83]

1.3.1.2 Arrhythmias during pregnancy

It is now well established that during pregnancy, there is a significant increase in the risk of certain types of arrhythmias. The fast heart rates associated with sinus tachycardia are commonly observed disturbances and throughout pregnancy more than half of the pregnant women will have manifestations of some form of electrical disturbance including ectopic beats, palpitations and other non-sustained arrhythmias.[80] Although rarely life-threatening, the frequency of arrhythmias remains relatively high and can cause complications. Indeed, premature ventricular and supraventricular ectopic beats are observed in nearly 60% of patients while the incidence of paroxysmal supraventricular tachycardia also increases, making it one of the most common arrhythmias during pregnancy.[84,85] Supraventricular arrhythmias refer to a group of electrical disturbances that affects the heart's upper chambers i.e. the atria and their conduction pathways and studies show that pregnancy increases the risk of *de novo* supraventricular arrhythmias notably tachycardia, by 34% while also exacerbating pre-existing supraventricular tachycardia cases by about 50%.[64,79,86] On the other hand, ventricular tachycardia and ventricular arrhythmias, with the exception of ectopic beats, are uncommon in otherwise healthy young women and only appear when underlying structural problems such as congenital heart disease, exist.[87] For instance, ventricular arrhythmias become problematic in women suffering from congenital long QT syndrome; as the fast heart rate of pregnancy provides temporary relief from the syndrome, a sudden loss of protection and complications are induced following delivery thus, appropriate screening becomes

essential for management of these patients.[88] Lastly, arrhythmias such as bradycardia and ventricular tachycardia leading to sudden cardiac death have also been reported in pregnancy however due to their peculiar aetiologies and rarity they will not be further discussed.[82]

1.3.1.3 Mechanisms underlying arrhythmias in pregnancy

Despite the frequency of electrical disturbances during pregnancy, the underlying cellular and molecular mechanisms have been rarely explored and instead, arrhythmias have been attributed to factors such as changes in autonomic tone, electrolyte balance, hemodynamic alterations and effects of hormones on ion channels.[89] Several of these factors will be evaluated in this work and discussed in the subsequent chapter where they were investigated. Nonetheless, hormones have an important role and have long been known to alter expression and function of various ion channels. During pregnancy the surge of oestrogen, progesterone and thyroid hormones is likely to modulate cardiac electrical properties by exerting specific effects on individual channels. Several studies have shown that oestrogen is able to regulate K^+ channel Kv4.3 in the heart, affecting repolarization. Furthermore, oestrogen was also shown to alter the excitability of neurones through modulation of HCN, L- and T-type Ca^{2+} channel expression. [78,90–93] It is therefore possible that a similar regulation exists in the heart and specifically in the SAN which sees its automaticity modulated through an oestrogen-dependent change in ion channel function or expression. Although the role of progesterone is less defined and requires further investigation, thyroid hormones have also been shown to regulate a broad range of ion channel α and β subunits in the heart including those of K^+, Ca^{2+} and HCN channels and may therefore be highly implicated in the electrical remodelling observed during pregnancy.[94,95]

In conclusion, pregnancy represents a complex state of physiological adaptations that dramatically affect the cardiovascular system. The heart becomes subject to a wide range of external factors that affect it structurally, mechanically and electrically. Although, these changes are normal and essential they do come with some potential complications, notably arrhythmias. Unfortunately, with the increase in comorbidities, cardiovascular disease and median age of pregnancy, the magnitude of these complications is estimated to become progressively bigger. The SAN being the dominant pacemaker and controller of heart rate

therefore becomes a key player in regulating electrical stability and arrhythmia risk. With two pregnancy-related studies, the aim of a major part of this work will therefore be to try to understand how pregnancy alters the SAN and pacemaking and how these changes can lead to arrhythmia vulnerability.

1.3.2 Pathology of the SAN and its dysfunctions

The second important part of the work presented here will be focused on the pathology of the SAN. SAN disease or SAN dysfunction (SND) also referred to as sick sinus syndrome (SSS) is a group of SAN disorders clinically characterized by poor SAN function related to either deficient impulse formation, i.e. the SAN is incapable of pacing, or has trouble in conducting electrical impulse outside the SAN, also known as SAN exit block.[96] The mechanisms of SND remain elusive and have begun only recently to be investigated. It is thought that intrinsic and/or extrinsic factors play a role in the development of SND however, the aetiology and molecular underpinnings of the disease are still vague. In the next sections, a summary of current SND knowledge will be presented.

1.3.2.1 Clinical presentation, epidemiology and risk factors

The single most important manifestation of SND is bradycardia (heart rate < 60 bpm) with a sluggish return to sinus rhythm pacemaking following electrophysiological right atrial pacing. The time it takes to resume spontaneous automaticity can be measured on the ECG and reported as a corrected SAN recovery time (cSNRT).[97,98] As such, low heart rates along with an increased cSNRT represent the most robust and widely used parameters to diagnose SND. The diagnosis of SND usually involves a general clinical examination, enquiring about symptoms which might include fatigue, lethargia, syncope and hypoperfusion. The presence of such symptoms can then be correlated with 12 lead ECGs or Holter data which might uncover SAN arrhythmias, predominantly bradycardia in addition to sinus pauses, sinus arrests, exit blocks and surprisingly even supraventricular tachycardia, in a phenomenon now termed tachy-brady syndrome.[97,99] Additional electrophysiological, exercise and pharmacological testing might also be performed for further validation, especially when multiple confounding

variables and symptoms exist. These tests should reveal a high cSNRT as well as a lack of chronotropic response to exercise while pharmacological testing will determine if the SND is related to modifications in autonomic activity.[100]

Owing to the complexity, presence of intrinsic and extrinsic factors and the overlapping symptoms of the disease, the epidemiology of SND is difficult to assess. For instance most patients with a cardiovascular condition are already taking some form of treatment consisting of antiarrhythmics, β-blockers, Ca^{2+} channel blockers, etc., which are known to induce bradycardia. In these instances, SND will be considered due to extrinsic factors if it can be corrected following removal of drugs that are interfering with pacemaking.[96,100] However, this would require the aforementioned additional testing in order to reveal the root cause of SND, a feat that is unfeasible for already multifaceted studies. Nonetheless, in a pooled analysis of about 20000 individuals followed over 17 years, 291 cases of SND were confirmed with a positive correlation with body mass index, prior cardiovascular events, hypertension and advanced age which was in fact, the highest risk factor for SND.[97] It is very likely that the study has missed many cases of SND due to difficult and inappropriate diagnosis as stated earlier, meaning the incidence of SND in the general population is probably higher. However, age has been confirmed to be a major contributor to the development of SND and in patients over the age of 65, SND affects 1 in every 600 individuals.[96] Indeed, even in the otherwise healthy population the correlation between age and lower heart rate has already been observed, as shown on Figure 9.[101]

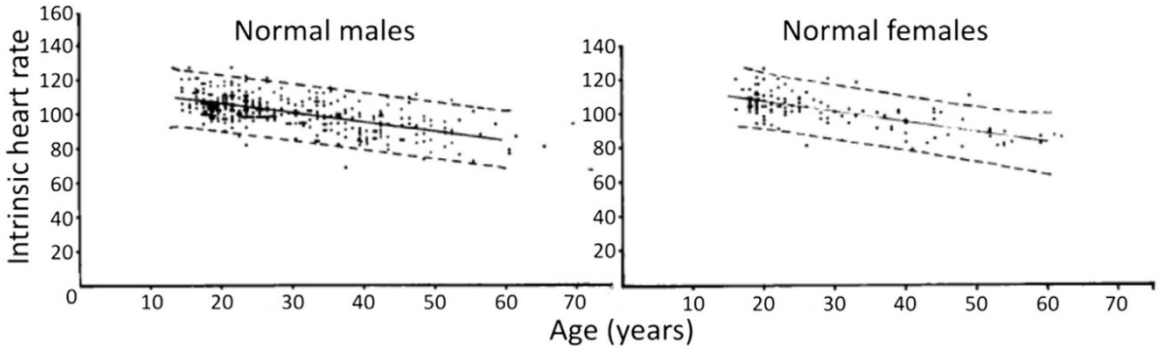

Figure 9. Analysis of intrinsic heart rate in men and women. Heart rates obtained by pharmacological autonomic blockade reveal an age-dependent decrease in rate that is similar between both sexes, hinting at a potential age-induced development of SND (see mechanisms below). Modified from Jose et al. 1970.[101]

1.3.2.2 Mechanisms of Sinus Node Dysfunction

Currently, the only available treatment for SND is the invasive implantation of electronic pacemaker.[102] SND and associated bradycardia can not only result in hypoperfusion, syncope, dizziness and chronotropic incompetence but can also favour the development of threatening supraventricular tachyarrhythmias such as atrial fibrillation (AF).[100] Indeed, in some SND patients, structural and electrical remodelling notably, atrial enlargement and decrease in conduction velocity have been observed. These changes are thought to increase the risk of re-entry and consequently AF.[103] The complications associated with SND are therefore wide-ranging and with the single invasive current treatment that is available, understanding the mechanisms of SND is becoming increasingly important. As pointed out earlier, SND is thought to develop through the influence of intrinsic or extrinsic factors. Extrinsic factors include medication that alters pacemaking mechanisms such as antiarrhythmic drugs, electrolyte imbalance or changes in autonomic tone which may favour parasympathetic stimulation[104,105] thereby inducing bradycardia. Although these extrinsic causes are frequent in SND patients they are mostly observed in individuals taking rate-altering medication as well as younger patients with no organic heart disease and purely extrinsic cases are often reversible or treatable. We will therefore discuss in the following section the so-called idiopathic cases of SND that remain mostly elusive mechanistically. In these complex cases although extrinsic factors can to some extent contribute to the disease, it appears nonetheless, that intrinsic factors weigh much heavier on the development of the pathology.

Genetic causes of SND- The coupled-clock model for pacemaking is a robust yet finely regulated mechanism consisting of multiple key players that rely on each other for precise and flawless pacemaking. It is therefore expected that mutations affecting any of the individual components of the clocks might result in faulty pacemaking and subsequent development of SND. Indeed, in several families with idiopathic SND, genetic screening has revealed mutations in ion channel and Ca^{2+} handling genes.[100] Subsequent introduction of these mutations *in vitro* and *in vivo* recapitulated the SND phenotype of patients revealing potential mechanisms of SND. Congenital SND cases represent a small fraction of idiopathic SND, featuring relatively straight-forward mechanisms and will not be discussed in broad details.

Accordingly, only a highlight of the most characterized mutations will be presented. Several Na^+ channel mutations have been associated with SND and patients with loss-of-function mutations also have multiple ECG and rhythm abnormalities considering $Na_V1.5$ channels are widely expressed in the heart.[106] Although Na^+ channels are not found in the centre, they are expressed at the periphery of the SAN where they help in impulse propagation towards atrial tissue. Mutations in $Na_V1.5$ therefore lead to SAN exit block and arrest in addition to the other complications in impulse conduction.[20] Another set of widely recognized SND-related mutations that have previously been described are in the HCN4.[107–109] Unsurprisingly, mutating a hallmark in SAN pacemaking mechanism does leads to SND. These mutations alter various biophysical properties of HCN4 channels including channel activation kinetics, voltage-dependence, activation, cAMP-regulation and current density. Overall, the lower conductance results in deficient pacemaking, bradycardia and several associated arrhythmias. Lastly, mutations in calsequestrin 2 and ankyrin-B that directly or indirectly affect Ca^{2+} handling have also been described. These mutations known to cause catecholaminergic polymorphic ventricular tachycardia were also shown to induce bradycardia through inappropriate Ca^{2+} handling and subsequent reduction in expression of several channels including $Ca_V1.3$ in the SAN.[110,111]

Congestive Heart Failure and Myocardial Infarction- In patients suffering from heart failure, there is a significant increase in the risk of SND. Electrophysiological and anatomical mapping of the SAN and surrounding atrial region revealed important shifts in leading SAN pacemaker, sinus arrests, and increases in conduction and recovery time in these tissues.[112,113] Subsequent animal studies using both ischemic and non-ischemic models of heart failure recapitulated some of these phenotypes and reported a reduction in expression of HCN and repolarizing K^+ channels along with altered Ca^{2+} handling in the SAN.[114–116] Of note, not all heart failure patients will suffer from SND and while a correlation exists, the exact pathways in which heart failure induces electrophysiological changes in the SAN remain unknown and will require further elucidation. In patients suffering from acute myocardial infarction in the inferior wall, angiogram analysis combined with electrophysiological testing revealed a strong correlation between degree of sinus node artery occlusion and reduction in intrinsic heart rate.[117] This highlights the particular importance of the SAN artery in maintaining normal

sinus rhythm and its occlusion through poor compliance, emboli, or atherosclerotic events may lead to an ischemia of the SAN leading to bradycardia and SND.[118]

Ageing and fibrosis- Considering SND affects in a large proportion the elderly population, one of the earliest causes of SND was hypothesized to be a fibrosis of the SAN and its senescence as it ages. Indeed, some of the initial studies confirming this hypothesis were conducted in 1977 and featured post-mortem histological analysis of patient hearts clinically diagnosed with chronic SND.[119,120] The results of these studies revealed not only increased fibrosis, but atrophy of the SAN. In addition, there was a decrease in SAN volume and SAN cell count, a report of amyloid depositions, fatty tissue infiltration within the SAN and narrowing of coronary sinus artery.[121] In the most severe cases of SND this remodelling and lesions also affected the AV node and other parts of the conduction system and additional fibrosis in adjacent atrial tissue was also observed, in correlation with tachy-brady arrhythmias. It is important to mention that these histological observations were not widespread across every analysed tissue sample. While there were strong correlations between the histological changes and SND, some patients with fibrotic or atrophied SAN had normal sinus rhythm and some with normal SAN structure had sinus rhythm problems. It is therefore concluded that the aetiology of SND appears to be multifactorial and it will be important to separate normal ageing-induced remodelling from the one that causes pathological SND.

Accordingly, studies comparing young and old animals were subsequently performed in order to examine the specific changes occurring within the SAN. In old rats and guinea pigs, studied at 24 and 38 months of age respectively (24 is thought to be the equivalent of ~70 years of age in humans while 38 months corresponds to the near end of lifespan) there was a significant down-regulation of $Na_V1.5$ and Cx43 in the periphery of the SAN.[122,123] These changes were responsible for a decrease in conduction velocity and SAN exit block. Furthermore, in aged rodents a hypertrophy of SAN cells was noted along with a reduction in expression of $Ca_V1.2$, RyR2 as well as I_f, T- and L-type Ca^{2+} currents associated with increased SNRT, decreased conduction velocity and diastolic depolarization slope. Structurally, increased interstitial fibrosis attributable to decreased matrix metallopeptidase expression was also observed.[123–127] It appears thus, that ageing brings about an electrophysiological and structural remodelling that causes perturbation in action potential

generation and propagation from the SAN and towards atrial tissue. It should be mentioned that in some of these studies hypertrophy of SAN cells and enlargement of the SAN were observed, which is inconsistent with human data that mostly suggests ageing-induced atrophy of the SAN and although the electrophysiological changes of ageing seem consistent with SND, their mechanisms remain unknown. In other words, how does ageing trigger all of these changes? Why is there such variability between different human tissues analysed and why do experimental studies show variable changes in expression/function of ion channels? How does one differentiate normal SAN ageing from remodelling that favours the development of SND?

Inflammation- Inflammation can play an important role in regulating automaticity of the SAN. Inflammatory mediators through complex pathways can affect various parts of the cardiovascular system, directly or indirectly impacting the SAN. For instance, through its role in plaque formation in atherosclerotic disease and its effects on coronary arteries, inflammation can potentially compromise SAN artery function or even cause its occlusion leading to SAN ischemia and SND.[118] However, inflammation and inflammatory factors, notably cytokines and specific antibodies, have been reported in several studies to have much more direct roles in altering pacemaking. Indeed, in the case of infectious diseases, including diphtheritic myocarditis, Chagas' disease and Lyme disease, severe arrhythmias associated with bradycardia and conduction blocks have been reported in infected patients.[128–131] Interestingly, we previously reported that in an HIV mouse model, bradycardia and sinus pauses were present along with several other electrophysiological changes.[132,133] Although these mice suffer from HIV symptoms that are very similar to HIV patients, they are pathogen free and not infected with the virus; instead, they simply express a small fragment of the HIV-1 genome which is enough to trigger the immune inflammatory response. We were then able to recapitulate several of the electrophysiological phenotypes of these HIV mice through *in vitro* treatments and injection in healthy control mice of pro-inflammatory cytokines that were upregulated in the model (i.e. IL-1β and TNFα).[69,134] Overall, these clinical observations along with the experimental data strongly support a role for inflammation and cytokines in regulating electrophysiological properties of the heart, including those of the SAN, thereby contributing to the development of SND.

While a case was made for SND in inflammation associated with infectious diseases, other notable examples of SND in sterile inflammatory conditions also exist. Indeed, in patients suffering from systemic lupus erythematosus (SLE), an autoimmune disease featuring multi-systemic inflammation of various tissues and the production of antibodies to components of the cell nucleus, bradycardia, SND and conduction disturbances have been well documented and are considered to be an important cardiac complication of adult SLE.[135,136] Since bradycardia can be completely resolved with anti-inflammatory treatment, the elevated level of various cytokines in SLE patients is thought to be essential in the etiopathology of the disease although the underlying mechanisms of cardiac dysfunction have not been completely clarified. Interestingly, gene expression data have shown significant changes in expression profile of the IL1 family genes in SLE patients, namely in IL1β, suggesting its involvement in SLE.[137–139] We have previously shown that IL-1β to be a potent suppressor of L-type Ca^{2+} current and thus, it is likely that inflammation causes bradycardia and SND, at least in one way, through suppression of SAN Ca^{2+} currents that are essential for the DD and upstroke phase of the AP.

A global working hypothesis that we are testing through multiple projects in our laboratory is that inflammation might be the common culprit between various pathologies that will result in SND. While bradycardia is clearly visible in inflammatory diseases, we believe that in conditions not classically strongly linked to inflammation such as heart failure or even ageing, chronic low grade inflammation might also be responsible for remodelling of the SAN both structurally and electrically. For instance, pro-inflammatory cytokines such as TGF-β are well known to induce fibrosis[140] and can be upregulated in various heart disease conditions. However, several other cytokines are also released in the circulation and we believe they can exert multiple effects on ion channels. In ageing, the presence of low-grade inflammation correlates with higher level of IL-1β and a higher incidence of sinus bradycardia and SAN dysfunction.[124,141,142] Thus, based on clinical and experimental evidence it appears that inflammation and notably IL-1β is a common feature of seemingly unrelated diseases that end up affecting cardiac electrical properties and predisposing individuals to arrhythmias.

Accordingly, the third study presented in this thesis will be focused specifically on the role of IL-1β in inducing SAN dysfunction. The strong clinical associations between bradycardia and IL-1β levels warrant such investigation and in addition, in a previous study, we demonstrated that IL-1β is a potent regulator of ion channel function in the ventricle.[69] This study will represent the foundation work of the larger SND/inflammation project that will eventually explore the role of other cytokines and pathways in SND. The data of this project was obtained from a new *in vitro* model, consisting of human cardiomyocytes and nodal cells derived from induced pluripotent stem cells. The ability to work with human myocytes provides a novel and exciting opportunity and in the next section we will present an overview of stem cells and their potential and how biotechnology and cell culture techniques permitted the procurement of cardiomyocytes from these cells.

1.4 Pluripotent stem cells: biotechnology and cardiac applications

Pluripotent stem cells have two main characteristics that differentiate them from all other cells: the ability for constant self-renewal and a capacity to differentiate into any of the three germ layers: endoderm, mesoderm and ectoderm.[143] Pluripotent stem cells are formed not long after fertilisation of the egg with the sperm. First, the resulting zygote goes into a division cycle forming a morula. The morula is a very early stage of mammalian embryonic development and is formed of blastomeres contained in a glycoprotein membrane termed zona pellucida. Blastomeres are totipotent stem cells, meaning a single cell can give rise to all the different cell types of the body. As the morula continues to mature it forms the blastocyst: a 200-300 cellular structure composed of an inner cell mass (embryoblast) in a cavity surrounded by a cellular membrane known as the throphoblast. This inner cell mass or embryoblast subsequently forms the embryo and the throphoblast becomes the placenta.[144] Since the inner cell mass gives rise to an embryo in later stages it therefore contains all the cells required to form an organism. These cells are thus classified as pluripotent stem cells and are subject to manipulation in order to create transgenic animals for instance. Alternatively, they are also the source of embryonic pluripotent stem cells (ePSC or eSC) that can be used for biotechnology purposes. As such, the pluripotency of the cells can be used to our

advantage. By driving their differentiation into specific fates it is possible, at least theoretically, to obtain any desired cell type of the body by applying of the right protocols and conditions. The development of cell culture techniques using complex media often containing proprietary mixes of growth factors, hormones and cytokines allows these ePSC to retain their pluripotency and divide *in vitro*. Furthermore, it is possible, although development of the technology is still needed, to favour their reprogramming and differentiation into any of the three germ layers: endoderm that forms intestinal tract and lung cells, the mesoderm that differentiates into muscle, bone and blood tissues and finally the ectoderm, the precursor of epidermal tissues and nervous system.[145] Our focus will however be on cardiac cells, which will be discussed in the next section.

1.4.1 Pluripotent Stem Cells and their Derived Cardiomyocytes

Mouse ePSC were one of the first to be isolated. They are readily available and can relatively be cheap to obtain. It is of course also possible to isolate human ePSC, albeit this comes with substantial ethical concerns and fierce debate related to issues such as whether the inner cell mass is already a living human. Nevertheless, when cultured using special protocols such as hang-drop protocol where 20 µL drops of ePSC are seeded on a plastic cover dish and reversed upside down, an "artificial" development takes place. The ePSC drops contain media supplemented with high foetal bovine serum and other additives such as bone morphogenic factor 4 to favour mesoderm and cardiac lineage development. Within five days embryoid bodies (EB), which are aggregates of cells, form. These EB can then be collected, plated and cultured on adhesive substrates with addition of factors such as retinoic or ascorbic acid for a few more days where eventually local spontaneously contracting foci will be observed. Manual picking of these foci and subsequent re-culturing gives rise to a cardiomyocyte population that has therefore developed from the ePSC. Of note, since the differentiation technique is rather to assist spontaneous differentiation and not fully or exclusively favour cardiac cells development, the rest of the EB also contains cells with neuronal and intestinal markers considering the EB gives rise to the three germ layers. In a good preparation, and technique optimization up to 30% cardiomyocytes could be observed at day 12.[145] Alternatively, is it also possible to induce differentiation into cardiomyocytes through co-culture of the PSCs on mouse visceral-endoderm-like cells (END-2). These END-2 cells

secrete several endodermal factors, including bone morphogenetic factors, nodal/activin A, fibroblast growth factors, and repressors of Wnt/β-catenin pathways thereby favouring cardiac lineage development nevertheless the efficiency of this protocol is rather low.[146] Lastly, it is possible to combine these two techniques, for instance ePSC can be were plated into drops to form EBs then these EBs can be subsequently plated on END-2 cells.[147] Beating aggregates, containing cardiomyocytes, 15-18 days post plating could then be isolated and dispersed with collagenase and used for experimentation.

1.4.2 Induced Pluripotent Stem Cells (iPSC)

In 2012, the Nobel Prize for Physiology or Medicine was awarded to Shinya Yamanaka and Sir John B. Gurdon for their discovery of iPSC technology that allowed reprogramming of mature somatic cells, such as fibroblasts, into pluripotent stem cells hence, the "i" in iPSC refers to the induction of somatic cells to stem cells.[148] First discovered nearly ten years ago, the discovery was essentially about reintroducing a handful of genes into a mature somatic cell which were enough to reprogram its fate and re-activate pluripotency. Since different stages in embryonic development are characterized by strikingly different expression profiles of transcription factors, the required transcription factors to induce pluripotency were discovered by assaying gene expression during various developmental stages. It was found that as early as 3.5 days post-coitum markers and transcription factors such as Oct4 (octamer-binding transcription factor 4 or POU5F1), Sox2 (sex determining region Y-box 2), FGF-2 (Basic fibroblast growth factor) and SSEA-1 (stage-specific embryonic antigen 1 or CD15) are highly expressed and are sufficient to reverse the fate of somatic cells back to pluripotency. Today, these factors are available commercially in ready to go vectors in order to induce pluripotency in all kinds of terminally differentiated cells. The main transcription factors used are Oct4, Sox2, Klf4 (Kruppel-like factor 4), NANOG (Homeobox Transcription Factor) and c-Myc. While different combinations of these factors have been used, one study showed that Oct4 alone was sufficient to induce pluripotency, although in most instances varying combination of Oct4, Sox2, Kfl4 and NANOG have been routinely used with avoidance of c-Myc due to its oncogenic potential.[149]

Briefly explained, these transcription factors act as very broad regulators of early stage embryogenesis. Oct4 and Sox2 are essential and critical in self-renewal of undifferentiated ePSC and insuring pluripotency, together they can also induce the gene expression of NANOG and Rex-1 (zfp-42; zinc finger protein 42). Thus, in a rather poorly understood mechanism, these genes act cooperatively within a regulated network to control global gene expression and favour genetic events that reverse cell fate back to its embryonic stages of pluripotency while promoting an autoregulatory-loop that sustains their pluripotency.[145]

Investigators working on iPSC need to go through stringent quality control tests to prove the pluripotency state of their cells. Consequently, experiments such as *in vitro* differentiation and screening or injection of these iPSC into immunodeficient mice typically non-obese diabetic (NOD mice) followed by teratoma analysis through staining for markers of the three germ layers are essential.[143]

1.4.3 Induced and embryonic PSC-derived cardiomyocytes (iPSC-CM, ePSC-CM)

The remarkable finding that cardiomyocytes could be generated from iPSC sparked a big interest in the cardiac research community since the long sought-after source of cardiomyocytes could have potentially been found. Since iPSC technology was going through rapid development it was now possible to obtain patient specific cardiomyocytes, generated from a skin graft, known as hiPSC-CM. This paved a new road for cardiac regenerative medicine pushing the field to new limits of tissue engineering and patient-specific cellular therapies. When differentiated into cardiomyocytes, these clusters of hiPSC-CM exhibited an interesting spontaneous electrical activity and beating[145,147] but also raised several fundamental questions. Do these cells resemble actual adult human cardiomyocytes electrically and mechanically? Which ion channels are expressed and what about the Ca^{2+} handling and contractile machinery? In essence, it was important to determine whether these cells constitute a good model to study electrophysiological or even contractile parameters of human cardiomyocytes. Over the last few years, investigational work and characterization of these cells reached the conclusion that overall, these cells are relatively immature and resemble mostly embryonic or foetal cardiomyocytes. Structurally and morphologically, iPSC-

CMs do not resemble adult cardiomyocytes. They are flat, often spread out widely, mostly polygonal in shape and heterogeneous in sizes and shape unlike rod-shaped adult cardiomyocytes. Furthermore, ultrastructure analyses reveal that these cells lack highly developed T-tubules. They have underdeveloped and relatively disorganized sarcomeres and also rely on IP_3 Ca^{2+} mechanisms instead of excitation-contraction coupling with Ca^{2+}-induced Ca^{2+}-release. Mitochondrial numbers are also much lower therefore indicating overall, that these cells are not the structurally organized powerhouse adult cardiomyocytes.[145]

Electrophysiologically, these cells became more interesting as they expressed all the human ion channels responsible for generation of AP that are consistent with adult human myocyte AP durations even though the expression level for several channels including Na^+ and Ca^{2+} is not identical to the adult heart.[150] Furthermore, AP and ionic current analysis of these iPSC-CMs revealed that the cell population is composed of cardiomyocytes with different electrical properties and action potential configurations allowing their classification into nodal-, atrial- and ventricular-like cells.[151,152] Electrophysiological data showed that nodal-like cells had a spontaneous diastolic depolarisation phase in their action potentials with presence of I_f, indicating HCN expression. On the other hand quiescent cells, found in much larger proportions, had either long or short plateau phases which were used to determine whether they fell into the atrial or ventricular-like groups, respectively. While AP duration and shape can be somewhat useful, it is arguable that there are too many intermediate phenotype cells with AP duration at the limits of the designated cut-off values. Thus, simply AP durations are not sufficient to classify cells into an atrial or ventricular category. Instead, several groups, including our own, prefer to call these myocytes working myocardial cells.

Interestingly, to date there has been tens of studies investigating arrhythmia-related pathologies in iPSC-CM with the large majority of these, especially the ones investigating LQTS, finding results consistent with animal and human data. This indicates that these cells could be useful to investigate human mutations of electrical disturbances.[153] While these findings have not specifically led to discovery of new mechanisms they did confirm previous findings from animal and cell culture models. This step is essential in validating the functional impact of these cells. By having a benchmark or standard for comparison, hiPSC-CMs are

starting to fill an important missing gap in cardiac experimental models: cultivable and manipulable terminally-differentiated human cardiomyocytes.

To summarize, hiPSC-CM appear to be immature cardiomyocytes. Nonetheless, they express all the adult ion channels and Ca^{2+} handling proteins albeit, at different levels from the adult cardiomyocyte. Their use as a model for LQTS and drug discovery has been warranted and validated several times already however, much more development and research is still needed in order for these cells to reach full potential. For instance, several groups are exploring ways to mature these iPSC-CMs in order to faithfully recapitulate the adult myocyte.[154,155]

It was previously mentioned that AP analysis of these cells revealed some nodal-like AP configuration. Indeed, these cells usually constitute about 10% of the entire iPSC-CM population and have been largely overlooked.[152] While efforts have been focused on getting working myocardium cells to resemble as much as possible adult cardiomyocytes or regenerative therapies for the ventricles and LQTS studies, we are particularly interested in the minority of cells within this population. It appears that this minority does not require maturation or complex protocols and accordingly, we are exploring the potential of these nodal-like cells as a relatively easy and robust human *in vitro* cellular model of the adult SAN. The broad scheme of this project, of which a part will be presented here, is to obtain a full characterization of these cells. This will include determining the molecular signatures, electrophysiological and Ca^{2+} handling properties of the cells and compare them to mouse and human SAN. Should the results be entirely favourable, these cells, as human SAN-like, provide a highly interesting potential to study the mechanisms of different SAN diseases and effects of various molecules on pacemaking. Furthermore, if we were to parallel the ever-growing interest in regenerating the myocardium, these cells could perhaps one day constitute a source of SAN cells useful for repair of sick SANs. Our interest in the pathology of the SAN has led us to begin the studies in nodal hiPSC-CM cells.

Overall, as an *in vitro* model, nodal hiPSC-CM cells constitute an excellent starting point from an investigational standpoint. It will allow for a reasonable amount of cells to go through testing of multiple inflammatory mediators of interest (e.g. IL-1β) while facilitating the subsequent mechanistic work. As a human cell model, it provides the advantage of a

human molecular machinery thus, an increased translational potential for the data. Certainly, these cells cannot replace *in vivo* models and validation; however they will provide a highly interesting and valuable complement to experimental studies.

1.5 Hypothesis and Objectives

As demonstrated throughout the introduction, the SAN appears to be a complex and dynamic tissue that is subject to a wide range of regulatory signals that modulate its function. The overall aim of this work was to shed light on some of the key changes that affect the SAN during states of health and diseases. Specifically, three studies are presented. The first two studies employ pregnancy as a model of physiological adaptation where we hypothesized that intrinsic electrophysiological changes to the SAN occur. The objective was to determine and characterize these changes while establishing how they relate to heart rate control and arrhythmia susceptibility. The first study presents the mouse model of pregnancy and examines changes in the pacemaker current and channels, the second examines the role of Ca^{2+} homeostasis in the SAN and how they are modulated in pregnancy.

The subject of the third study was the pathological regulation of the SAN and its relation to poor pacemaking and bradycardia. The objective here was to determine how cytokines, which are elevated in numerous disease states, are capable of affecting pacemaking. Specifically, the pro-inflammatory mediator IL-1β was tested and the adverse electrophysiological remodelling it induces and its relation to bradycardia were presented and discussed. Furthermore, a molecular and electrophysiological characterization of a relatively new human SAN cell model in which the effects of IL-1β were tested is also presented.

2 Upregulation of the Hyperpolarization-Activated Current Increases Pacemaker Activity of the Sinoatrial Node and Heart Rate During Pregnancy in Mice

Nabil El Khoury, MSc*; Sophie Mathieu, BSc*; Laurine Marger, PhD*; Jenna Ross, PhD; Gracia El Gebeily, MSc; Nathalie Ethier, MSc; Céline Fiset, PhD

Circulation. 2013 May 21;127(20):2009-20. doi: 10.1161/CIRCULATIONAHA.113.001689

*These authors contributed equally

Author contribution:

N.E.K: Patch-clamp recording protocols development, data acquisition, data analysis, technique optimization for mouse SAN RNA and protein extractions, SAN Western blot technique development, manuscript writing and proofing.
S.M.: Patch-clamp data acquisition and analysis, contribution to SAN Western blot technique development, manuscript text input and reviewing.
L.M.: SAN cell isolation technique, patch-clamp data acquisition, manuscript text input.
J.R.: Patch-clamp data acquisition, SAN cell isolation, manuscript proofing.
G.E.G: Contribution to original manuscript idea, *in vivo* and *ex vivo* electrophysiology.
N.E.: SAN cell isolation, patch-clamp, data acquisition and analysis, qPCR.
C.F.: Corresponding author and principal investigator, original manuscript idea, complete data reviewing with study conceptualization and design, manuscript writing and proofing.

Outline- The first study presented explores the role of pacemaker current (I_f) in the heart rate increase during pregnancy. This is the first study to our knowledge to demonstrate that an electrophysiological remodelling of the SAN is an adaptive mechanism of pregnancy. The study also evaluates the contribution of previously suspected mechanisms to heart rate increase and introduces the mouse model of pregnancy. Presenting a wide array of data and techniques including *in vivo*, *ex vivo* and cellular electrophysiology, along with associated molecular work this study was accompanied by an editorial featuring a mathematical model of accelerated SAN automaticity based on the study data. (Circulation, 2013, 21;127(20):2003-5).

2.1 Résumé

La grossesse est associée à une fréquence cardiaque (FC) plus rapide, qui est un facteur de risque d'arythmies. Toutefois, les mécanismes sous-jacents à cette augmentation de la FC demeurent mal compris. Ainsi, l'objectif de cette étude était d'obtenir une base mécanistique expliquant l'augmentation de la FC induite par la grossesse.

En étudiant des ECG de surface, nous avons observé que les souris gestantes (SG) ont une FC plus rapide (531 ± 14 battements par minute (bpm) comparativement aux souris non gestantes (SNG) (470 ± 27 bpm, P<0,03). Les résultats obtenus avec des cœurs perfusés en mode Langendorff ont montré que cette différence persistait en l'absence d'une innervation par le système nerveux autonome (SNG, 327 ± 16 bpm ; SG, 385 ± 18 bpm, P<0,02). Les potentiels d'action spontanés des cellules du nœud sinusal (NS) des souris gestantes présentent une automaticité plus élevée (SNG, 292 ± 13 bpm, SG, 330 ± 12 bpm, P = 0,047) et une pente de dépolarisation diastolique plus forte (SNG, 0,20 ± 0,03 V/s ; SG 0,40 ± 0,06 V/s, P = 0,004). La grossesse augmente la densité du courant activé par l'hyperpolarisation (I_f) (à -90mV: SNG, -15,2 ± 1,0 pA / pF; G, -28,6 ± 2,9 pA / pF; P = 0,0002) dans les cellules du NS. La dépendance au voltage de la courbe d'activation de I_f et les concentrations intracellulaires d'AMPc restent inchangées dans les cellules du NS des SG. En outre, l'expression protéique du canal HCN2 est augmentée sans que l'expression de HCN4 ne soit changée. Le déplacement maximal de la courbe d'activation de I_f induit par l'isoprotérénol était atténué pendant la grossesse. Cette réponse réduite à l'isoprotérénol peut être attribuable à une moindre sensibilité à l'AMPc de l'isoforme HCN2 par rapport à HCN4.

Cette étude montre qu'une augmentation de la densité de I_f contribue à l'accélération de l'automaticité du NS et explique en partie la FC plus rapide observée durant la grossesse.

2.2 Study

ABSTRACT

Background - Pregnancy is associated with a faster heart rate (HR), which is a risk factor for arrhythmias. However, the underlying mechanisms for this increased HR are poorly understood. Therefore, this study was performed to gain mechanistic insight into the pregnancy-induced increase in HR. **Methods and Results -** Using surface ECG we observed that pregnant (P) mice have faster HR (531±14bpm) compared to non-pregnant (NP) mice (470±27bpm, $p<0.03$). Results obtained with Langendorff-perfused hearts showed that this difference persisted in the absence of autonomic nervous innervation (NP: 327±16bpm, P: 385±18bpm, $p<0.02$). Spontaneous action potentials of sino-atrial node (SAN) cells from pregnant mice exhibited higher automaticity (NP: 292±13bpm, P: 330±12bpm, $p=0.047$) and steeper diastolic depolarization (NP: 0.20±0.03V/s, P: 0.40±0.06V/s, $p=0.004$). Pregnancy increased the density of the hyperpolarization-activated current (I_f) (at -90mV, NP: -15.2±1.0pA/pF, P: -28.6±2.9pA/pF, $p=0.0002$) in SAN cells. Voltage-dependence of the I_f activation curve and the intracellular cAMP levels were unchanged in SAN cells of pregnant mice. However, there was a significant increase in HCN2 channel protein expression with no change in HCN4 expression. Maximal depolarizing shift of the I_f activation curve induced by isoproterenol was attenuated in pregnancy. This reduced response to isoproterenol may be attributable to the lower cAMP sensitivity of HCN2 isoform compared to that of HCN4. **Conclusions -** This study shows that an increase in I_f current density contributes to the acceleration of SAN automaticity and explains, in part, the higher HR observed in pregnancy.

Keywords: Heart rate; ion channels; pacemakers; pregnancy; sino-atrial node.

INTRODUCTION

In women, cardiovascular function is strongly influenced by pregnancy and undergoes significant changes such as alterations in cardiac electrical function and higher vulnerability to arrhythmias.[1, 2] During pregnancy, there is an increased risk of onset of new supraventricular tachycardia or exacerbation of pre-existing arrhythmia, which may compromise the wellbeing of the mother and the fetus.[3-5] Furthermore, pregnancy is also associated with a higher resting heart rate (HR), which is a known risk factor for arrhythmias.[4, 6, 7] This increase in HR suggests an influence of pregnancy on cardiac autonomic regulation and/or the automaticity of the heart.

Changes in cardiac autonomic modulation play a central role in the adaptation of the cardiovascular system to various hemodynamic changes required for a normal pregnancy.[8-10] The heart is innervated by both the sympathetic and parasympathetic divisions of the autonomic nervous system. Stimulation of the sympathetic nerve fibers results in the release of norepinephrine that increases the automaticity of the sino-atrial node (SAN), the cardiac pacemaker. This is reflected on the electrocardiogram (ECG) by a faster HR. In contrast, parasympathetic stimulation by means of the vagus nerve releases acetylcholine and slows the pacemaker activity of the SAN.[11]

The automaticity of the SAN is responsible for initiating heart rhythm. The diastolic depolarization phase of the spontaneous action potential (AP) generated in SAN cells is a major determinant of cardiac automaticity. Multiple mechanisms are involved in the diastolic depolarization of SAN cells. These include a hyperpolarization-activated current (I_f), T- and

L-type calcium currents (I_{caT}, I_{CaL}), the delayed rectifier K^+ current (I_{Kr}), Na^+-Ca^{2+} exchanger current (I_{NCX}) and spontaneous Ca^{2+} release from the sarcoplasmic reticulum.[12-14] While intracellular Ca^{2+} signaling is important in the generation of the late diastolic depolarization,[15] I_f plays a crucial role in the early phase of the diastolic depolarization of SAN cells.[15] In mouse SAN, the hyperpolarization-activated cyclic nucleotide-gated (HCN) channel isoforms, HCN1, HCN2 and particularly HCN4, contribute to the native I_f current.[16, 17] Regulation of HCN by sympathetic and parasympathetic stimulation represents one of the main mechanisms by which the autonomic nervous system controls HR.[18] A direct interaction of cyclic AMP (cAMP) with an intracellular cyclic nucleotide binding domain is known to regulate the voltage dependence of HCN channels. Indeed, β-adrenergic agonists increase the levels of cAMP, which positively shifts the HCN voltage dependence. The positive shift in the I_f activation curve results in an increase in current density. In contrast, muscarinic stimulation decreases cAMP levels and has the opposite effect on I_f voltage dependence.[19]

Elevated HR can increase the susceptibility to arrhythmias; therefore, a better understanding of the mechanisms responsible for the increased cardiac automaticity associated with pregnancy is clinically important. As mentioned above, several mechanisms are involved in the automaticity of the heart. Since I_f initiates the first part of the diastolic depolarization, the present study focused on the regulation of this ionic current during pregnancy. We therefore hypothesized that the increased physiological demands during pregnancy may lead to changes in I_f channel expression and/or current density as well as I_f response to stimulation by the autonomic nervous system. In turn, these modifications could increase the automaticity of the SAN and, in part, explain the mechanisms of elevated HR associated with pregnancy.

Accordingly, the objectives of the present study were (1) to investigate the effect of pregnancy on HR in mice under control conditions and in the absence of autonomic nervous tone, and (2) to examine the effects of pregnancy on the automaticity of single SAN cells, and (3) to explore the mechanisms underlying the HR changes and how they relate to I_f.

MATERIAL AND METHODS

Animals

All experiments were performed on adult female CD1 mice (2-3 months old) obtained from Charles River (St-Constant, QC, Canada). Non-pregnant (NP) and late pregnant (P: 18-19 gestation days, gd) mice were used. All experiments were performed in accordance to the guidelines of the Canadian Council on Animal Care and the *Guide for the Care and Use of Laboratory Animals* published by the US National Institutes of Health (NIH Publication No 85-23, revised 1996). Experiments were also approved by the Montreal Heart Institute Animal Care Committee (approval reference number 2009-80-02).

Surface electrocardiograms (ECG)

Lead I surface ECGs were conducted in anaesthetized NP and P mice for 5 minutes at a rate of 2kHz after baseline period. Additional surface ECG recordings were obtained on mice before and after intravenous (IV) injection of isoproterenol (0.1ng/g) through the right jugular vein.[20] Further information is presented in the online supplemental material.

Langendorff-perfused heart

Experiments were performed as previously described.[21] After rapid excision, the heart was hung on a modified Langendorff apparatus and retrogradely perfused through the aorta. ECG recordings were obtained after an equilibration perfusion period; ECG parameters were calculated as explained in the supplemental material.

Hemodynamic measurements

Mice were anaesthetized with isoflurane before a pressure catheter was inserted into the right carotid artery. Systolic, diastolic and mean arterial blood pressures were measured by a Millar Mikro-Tip Catheter Transducer (model SPR-671, 2F, Millar Instruments, TX, USA) and data were analyzed with the program IOX, version 2.5.1.6 (EMKA Technologies).

Catecholamine and cAMP measurements

Plasma epinephrine and norepinephrine levels were measured using the 2-cat (A-N) Research ELISA kit (Rocky Mountain Diagnostics, CO, USA) following the manufacturer's instructions. SAN intracellular cAMP concentrations were measured using a LANCE® cAMP 384 ELISA kit (PerkinElmer, Waltham, MA, USA) following the manufacturer's instructions.

Sino-atrial cell isolation

Mice were anaesthetized by inhalation of isoflurane and then sacrificed by cervical dislocation. The SAN cells were isolated using an adaptation of the protocol previously described by Mangoni *et al.*[22] Briefly, SANs were dissected in normal HEPES-buffered Tyrode's and digested by enzymatic dissociation. Cells were then obtained by trituration and kept in "Kraft-Brühe" (KB) solution until use. Isolated mouse SAN cells were identified as small spindle-type cells spontaneously beating in normal Tyrode's solution.[22] Details on the digestion protocol are presented in the supplemental material.

Electrophysiological data

Current- and voltage-clamp recordings. For I_f recordings, 1 mM $BaCl_2$ (Sigma) was added to the external solution to block the inward rectifier K^+ current, I_{K1}. All recordings were carried out at 35±1°C. Pipette resistance was between 3-5MΩ. The I_f IV curve was obtained in whole-

cell configuration while the action potential and activation curves were obtained using perforated patch-clamp technique with nystatin (350ng/ml). To account for differences in cell size, current amplitudes were normalized to cell capacitance and expressed as densities (pA/pF). Solution composition and protocols are available in the supplemental material.

Current- and voltage-clamp protocols and data analysis. Current-voltage relationships for the hyperpolarized current (I_f) were constructed using records elicited by 2-s voltage steps from -120 to -20mV in 10mV increments from a holding potential of -30mV at a frequency rate of 0.2Hz. The density of I_f was measured at the end of the hyperpolarizing steps. Activation curves were obtained using a protocol in which 2-s voltage steps from -35 to -130mV were applied from a holding potential of -35mV, followed by a 1.5-s step at -90mV and a 1-s step at +5mV. To obtain voltage dependent steady-state activation curves, tail currents were determined as the difference between the peak current and the steady-state current (tail current at -90mV). Tail currents were normalized by the maximal tail current (Imax) and plotted against test voltage. The normalized plot of tail currents versus test voltages were fitted with a Boltzmann equation: $I/Imax=1/(1+\exp[V-V_{1/2}]/k)$, where V is the test voltage, $V_{1/2}$ is the mid-activation voltage and k is the slope factor.[23, 23, 24]

Real time RT-PCR

Total RNA extraction and real-time PCR (qPCR) for the HCN channels were conducted using previously published protocols,[16, 25] which are detailed in the online supplemental material.

Western blot

Protein samples were extracted from 3 SANs of non-pregnant and pregnant mice. Protocols used for protein isolation and Western blot analysis are described in the online supplemental material.

Statistical analysis

All data are presented as mean ± SEM. "*n"* refers to the number of experiments and "*N*" the number of mice. $p<0.05$ was considered significantly different. Statistical analyses are detailed in the online supplemental material.

RESULTS

Surface ECG parameters

To determine whether pregnancy in mice is associated with an increase in HR as seen in humans, lead I surface ECG data were obtained from anaesthetized non-pregnant and pregnant female mice under baseline conditions. ECG parameters were compared between both groups and representative examples are illustrated in Figure 1A. Pregnant mice exhibit a significantly higher resting HR compared to non-pregnant mice (NP: 470±27bpm and P: 531±14bpm, p=0.03). HR was also assessed in pregnant mice at gd 12-13 to determine whether the increased HR observed in late pregnancy was present at an earlier stage of gestation. Interestingly, the HR was already increased in pregnant mice at gd 12-13 (514±15bpm, n=9). These findings are consistent with reports in humans which show that the change in resting HR begins in early pregnancy.[5, 6, 9, 26, 27] Mean data for the PR, QT and QTc intervals are also summarized in Figure 1A. The PR interval was significantly shorter in pregnant mice without any change in P wave duration (data not shown). The QT interval was on average 10ms shorter in pregnant mice; however, after adjustment for the difference in HR, this trend was no longer present as illustrated by the comparable QTc intervals measured in the two groups.

Arterial blood pressure

Using a Millar catheter we compared arterial blood pressure in anaesthetized non-pregnant and pregnant mice to confirm that the increase in HR associated with pregnancy was not secondary to a reduction in blood pressure. Results summarized in Table 1 show that systolic, diastolic and mean arterial blood pressures were similar in both groups.

Stimulation by the autonomic nervous system

Catecholamine levels. The contribution of the autonomic nervous system to the pregnancy-induced increase in HR was then explored. Data presented in Table 1 indicate that plasma concentrations of norepinephrine and epinephrine were not increased in pregnant mice.

ECG parameters on Langendorff-perfused heart. Additional ECG recordings were performed on Langendorff-perfused hearts isolated from non-pregnant and pregnant mice. As illustrated in Figure 1B, the HR measured in the Langendorff-perfused heart preparation was significantly slower than that obtained with surface ECGs. The slower HR measured in the Langendorff-perfused heart preparation reflects the intrinsic HR and is explained by the absence of sympathetic stimulation. Similar to what was seen in the surface ECG studies, the HR measured in the Langendorff experiments was significantly faster in pregnant (385±18bpm) compared to non-pregnant (327±16bpm, p=0.02) mice, indicating that the increased HR seen in pregnant mice was not due to alterations in the autonomic tone. The table in Figure 1B presents mean data for PR, QT and QTc intervals obtained from both groups. The PR interval was also significantly shorter in pregnant mice and this faster AV conduction time was still independent of atrial conduction since the P wave duration was unaltered (data not shown). Similar to the surface ECG data, the shorter QT interval in pregnant mice was also explained by a faster HR as there was no difference in QTc intervals between non-pregnant and pregnant mice. Results presented thus far indicate that HR is altered in pregnant mice and that this difference does not result from changes in blood pressure, circulating levels of catecholamines or autonomic nervous tone but rather reflects a change intrinsic to the heart.

Influence of pregnancy on the spontaneous automaticity of the SAN cells

Accordingly, the next series of experiments were performed to explore the cellular mechanism underlying the increased HR observed in pregnant mice. Spontaneous APs were recorded using freshly isolated single SAN cells from non-pregnant and pregnant mice. The morphology of the SAN cells was similar between both groups and had comparable cellular capacitance (NP: 30.2±1.5pF, n=42 and P: 29.4±1.1pF, n=46, p=0.66). Figure 2A compares spontaneous APs and the corresponding first derivative of the AP (dV/dt) waveform recorded from SAN cells obtained from a non-pregnant and pregnant mouse. Detailed analysis of the AP parameters is summarized in Figure 2B. The frequency of spontaneous SAN AP was increased in cells from pregnant mice (330±12bpm) compared to non-pregnant mice (292±13bpm, p=0.047). Diastolic depolarization rate (DDR) was increased in cells from pregnant mice. As also reported in Figure 2B, pregnancy was also associated with a more positive AP threshold (Eth). On the other hand, the maximum diastolic potential (MDP), the maximal velocity of the AP upstroke (Vmax), the AP amplitude (APA), the AP duration (APD) and the waveform of dV/dt during AP repolarization were not affected by pregnancy.

Influence of pregnancy on I_f density and its voltage-dependence of activation

Considering the importance of I_f for the initiation of the diastolic depolarization of the SAN we then compared the density of I_f in SAN cells from non-pregnant and pregnant mice. Data reported in Figure 3 (A-B) show that the density of I_f was significantly higher in the SAN cells of pregnant mice compared to non-pregnant mice from voltages of -40 to -120mV (at -90mV, NP: -15.2±1.0, P: -28.6±2.9pA/pF, p=0.0002). Of note, I_f was recorded in Tyrode's solution containing $BaCl_2$ to eliminate the inwardly rectifying K^+ current, I_{K1} (see Methods). It is worth

mentioning that only a very small Ba^{2+}-sensitive K^+ current was activated in SAN cells from non-pregnant mice (at -90 mV, -4.5±0.9pA/pF, n=7). Furthermore, there was no influence of pregnancy on the density of I_{K1} (-4.8±1.0pA/pF, n=8, p=0.83) which is consistent with the absence of differences in the MDP of the spontaneous SAN AP. We then compared the voltage-dependence of the I_f activation curve and found that neither the voltage at half-maximal activation ($V_{1/2}$) (NP: -102.8±1.5mV and P: -103.6±1.5mV, p=0.69) nor the slope factor (NP: 10.2±0.4 and P: 9.7±0.3, p=0.33) significantly differed between either group, suggesting that a change in the I_f activation kinetics cannot explain the increased density of I_f.

I_f response to relaxin and SAN cAMP levels are unchanged in pregnancy

In the next series of experiments, we compared the voltage-dependence of I_f activation in SAN cells from non-pregnant and pregnant mice in the presence of relaxin (80nM), which has been reported to modulate other ionic currents by increasing intracellular cAMP.[28] Data presented in Figure 4A and B show that relaxin shifted the activation curve to more depolarized potentials; however, the I_f voltage-dependence of activation and the change ($\Delta V_{1/2}$= relaxin $V_{1/2}$ – baseline $V_{1/2}$) was similar between the two groups (NP: $\Delta V_{1/2}$ 2.8±0.6mV and P: $\Delta V_{1/2}$ 2.3±0.3mV, p=0.46). The effect of relaxin on the slope factor was also comparable (NP: Δ1.3±0.3mV and P: Δ1.4±0.1mV, p=0.73). Thus, the data suggests that the basal cAMP level is not elevated in SAN from pregnant mice. These results are in agreement with the cAMP data reported in Figure 4C, where similar intracellular cAMP content was found in SANs isolated from non-pregnant and pregnant mice. Together these findings indicate that the increased I_f density in SAN cells of pregnant mice cannot be explained by a positive shift in the I_f voltage-dependence due to higher intracellular cAMP levels.

The sensitivity of I_f to isoproterenol is blunted during pregnancy

To determine whether the responses of I_f to β-adrenergic stimulation was modified by pregnancy, we measured the voltage-dependence of the I_f activation curve in the presence of the β-adrenergic agonist, isoproterenol (100nM). We found that the maximal isoproterenol-induced shift to more positive voltages was attenuated in pregnancy (NP: $\Delta V_{1/2}$ 4.8±0.6mV and P: $\Delta V_{1/2}$ 2.8±0.5mV, p=0.02) (Figure 5A-D). Isoproterenol did not affect the slope factor in non-pregnant mice, (Δ0.1±0.5mV, p=0.75) but the slope was slightly increased in SAN cells from pregnant mice (from 9.6±0.6 to 10.9±0.6mV, Δ1.4±0.3mV, p=0.007) although this change did not reach statistical significance compared to the change (Δ0.1±0.5mV) in non-pregnant mice (p=0.06 NP vs P). In addition, another set of surface ECG experiments was performed on non-pregnant and pregnant mice before and after IV injection of isoproterenol (Figure 5E). Consistent with a lower I_f isoproterenol-induced response, data presented in Figure 5F indicates that although isoproterenol significantly accelerated the heart rate in both groups, the increase was lower in pregnant (Δ72±15bpm) compared to non-pregnant mice (Δ132±24bpm).

I_f response to muscarinic stimulation is unchanged during pregnancy

We then examined the effect of pregnancy on the voltage-dependence of the I_f activation curve after the application of acetylcholine (1μM). Figure 6 shows that the hyperpolarizing shift in I_f activation caused by acetylcholine was similar in non-pregnant and pregnant mice (NP: $\Delta V_{1/2}$ -1.3±0.4mV, P: $\Delta V_{1/2}$ -1.7±0.3mV, p=0.52). No change in slope was found in the presence of acetylcholine in either group (NP: Δ -0.1±0.3mV, P: Δ -0.1±0.2mV, p=0.89).

Influence of pregnancy on HCN channel expression

To further explore the mechanisms for the increased I_f current density in pregnancy, we measured the mRNA levels of the three HCN channel isoforms expressed in mouse SAN (HCN1, HCN2 and HCN4) using qPCR analysis (Figure 7A). Results of these experiments reveal that the transcript levels of the three HCN isoforms did not differ between non-pregnant and pregnant animals. Additionally, we performed Western blot analysis to examine the protein expression of the HCN isoforms and found that although the protein level of HCN4 was not altered, the expression of HCN2 was significantly increased in pregnancy (Figure 7B). Taken together with the electrophysiological data described above, these expression studies indicate that an increase in HCN2 protein expression, with no change in the voltage-dependence of the I_f activation curve, contributes to the increased I_f density in pregnancy.

DISCUSSION

Summary of main findings. In the present study, we provide the first mechanistic insight into the increase in HR associated with pregnancy. First, we show that in a mouse model of pregnancy the increased HR is not secondary to alterations in autonomic tone, arterial blood pressure or circulating catecholamine levels. We then demonstrate that the higher HR in pregnancy is associated with accelerated automaticity of SAN cells, steeper diastolic depolarization rate, and enhanced density of I_f, one of the major ionic currents modulating pacemaker activity of the heart. The increased I_f density could be explained by higher protein expression of HCN2 channels with no change in the voltage-dependence of the I_f activation curve. Together, these findings demonstrate that I_f upregulation is a major mechanism in the increase in HR during pregnancy.

Our mouse model of pregnancy reproduces the increased HR observed during pregnancy in humans. This effect is present even in the absence of autonomic nervous system input, suggesting that the pregnancy-induced increase in HR reflects changes intrinsic to the heart. Similar explanations have also been proposed for the increased HR observed in pregnant women.[9, 29] In addition, clinical studies have shown that women have a higher resting HR than men,[2, 30-33] and this difference is preserved after autonomic blockade.[34] Interestingly, the faster HR in pregnant mice is accompanied by a shorter PR interval with no change in P wave duration. A shorter PR interval could be a direct consequence of the increased HR. However, since the SAN and AV node share similar ion channels, it is possible that the AV node also undergoes remodelling mechanisms similar to the SAN. However, further studies will be required to assess the effects of pregnancy on AV node.

Elevated levels of cAMP lead to a positive shift in the I_f activation curve and hence increase its current density. However, this study rules against a cAMP-dependent regulation of I_f as a potential explanation for the enhanced I_f density in pregnancy. Indeed, there was no change in the voltage-dependence of the I_f activation curve or cAMP levels in SAN cells from pregnant mice. Results obtained with relaxin also support this conclusion. As mentioned above, relaxin has been shown to rapidly elevate cAMP content in various tissues.[28, 35, 36] Therefore, if SAN cells from pregnant mice had a higher basal cAMP level, addition of relaxin should only minimally increase cAMP content. This would result in a much smaller shift in the I_f activation curve. However, the similar response of I_f to relaxin obtained in both groups does not support this hypothesis. Thus, it appears that mechanisms independent of cAMP participate in the upregulation of I_f in the SAN during pregnancy.

In the present study, the higher density of I_f is associated with an increased protein expression of HCN2 channel isoform. Previous studies have shown that HCN4 is the most highly expressed HCN isoform in mouse SAN whereas HCN2 and HCN1 are detected at moderate and low levels, respectively.[37] HCN4 is considered to be the main component of I_f in murine SAN; however, evidence also supports a functional role, although to a lesser extent, for HCN2.[37] Findings reported here show that HCN2 protein level is increased in SAN from pregnant mice suggesting that the contribution of this channel isoform to mouse SAN I_f would be enhanced during pregnancy. In support of this notion, the maximal isoproterenol-induced shift in the I_f activation curve was attenuated in pregnancy. This observation agrees with an increased expression of HCN2 since this channel isoform is known to have a lower cAMP

sensitivity than HCN4.[37] Considering that HCN2 channels have faster activation kinetics compared to HCN4, it is tempting to speculate that an increase in HCN2 channels is essential in order to support the elevated HR needed to compensate for the greater physiological demand associated with pregnancy. Indeed, exponential fits of the I_f activation trace at -60 mV reveal that the activation time constant was significantly reduced in pregnant mice (NP: 883±120 ms and P: 596±73 ms p=0.04). This is consistent with an increase in the HCN2 mole fraction in HCN heteromultimers of pregnant mice. As a result, a more rapid activation of the current near the diastolic potentials is observed. It is also worthwhile mentioning that the frequency of cells where I_f was not activated at -60 mV was much higher in the non-pregnant mice. Although we were able to detect HCN1 transcripts, this isoform was not detectable at the protein level in SAN isolated from either experimental groups. This could be due to low sensitivity of the antibody used or reflects a low expression level of HCN1 in the mouse SAN as previously reported,[37] suggesting that this isoform may not make an important contribution to I_f in mouse SAN.

Besides the increased HCN2 expression, other factors could also contribute to the increase in I_f density. In fact, various factors are known to modulate I_f in SAN cells, such as auxiliary subunits and cytoskeletal proteins, which functionally interact with HCN channels.[15, 38, 39] Interestingly, the expression of HCN1 and HCN2 was upregulated when these isoforms were co-expressed with MinK-related protein 1 (MiRP1).[38] Therefore, future studies are required to explore the contribution of these factors on the upregulation of I_f in pregnancy.

It is plausible that the increase in HR itself may lead to an upregulation of I_f. Consistent with this idea, previous studies have shown that in response to HR acceleration, other cardiac ionic

currents, such as L-type calcium currents (I_{CaL}) and ATP-sensitive K^+ current (I_{KATP}), are also upregulated.[40, 41] For instance, in human cardiac myocytes it has been reported that the density of I_{CaL} can be increased by high rates of cell stimulation. This increase was attributed to an incomplete inactivation of I_{CaL} at rapid pacing frequencies, which may also involve phosphorylation of Ca^{2+} channels. This process was thought to be crucial in the adaptation of the beating heart to stress and exercise.[40] Pregnancy is also associated with accelerated HR as part of the adaptive response to the increased physiological requirements. Therefore, rate-dependent upregulation of I_f may also be mediated by similar mechanisms where an initial increase in the frequency of activation of I_{CaL}, as well as changes in I_{CaL} gating kinetics, (e.g., slowing of I_{CaL} decay) increases Ca^{2+} influx. The elevated intracellular Ca^{2+} levels could then trigger intracellular events upregulating I_f. In support of this hypothesis, a report in rat hippocampal CA1 cells showed that a Ca^{2+}-dependent modulation of the hyperpolarization-activated current (I_h, the neuronal equivalent of I_f) controls the synchronized thalamocortical rhythms.[42] Thus, a rise in intracellular Ca^{2+} may promote the I_f–dependent pacemaker mechanisms and in addition modulate the Ca^{2+}-dependent pacemaker process referred to as the "Ca^{2+} clock," in which the rhythmic SR Ca^{2+} release plays a major role in the SAN automaticity. These functional interactions between the two pacemaker mechanisms may provide additional means to accelerate HR as part of the adaptation to pregnancy.

Hormonal changes that occur during pregnancy are likely to be involved in the increased automaticity of the heart during pregnancy.[28, 43, 44] It is also noteworthy that sex-specific hormonal fluctuations increase the inducibility of arrhythmias, which has been correlated with gestation, menopause, and even changes in the menstrual cycles.[26, 45, 46] In other cell types,

pregnancy or sex steroid hormones have been shown to regulate hyperpolarization-activated inward currents. For instance, during pregnancy, uterine smooth muscle cells also exhibit a hyperpolarization-activated inward current similar to I_f in SAN cells. This current is believed to contribute to the spontaneous automaticity and enhanced myometrial contractility that occurs near parturition.[47] In the brain, I_h also plays a critical role in many rhythmic neurons. Specifically, 17β-estradiol regulates the density of I_h in GnRH neurons. In these cells, rising levels of 17β-estradiol also increase mRNA expression of multiple ion channels, such as HCN, T- and L-type Ca^{2+} channels, which increase the overall excitability of GnRH neurons.[48] Additionally, ovariectomy was shown to reduce the number of action potentials in hippocampal CA1 pyramidal neurons, supporting a role for female hormones on neuronal automaticity.[49] Taken together, these data support the notion that hormonal changes occurring during pregnancy can contribute to the higher HCN2 channel expression and increased I_f density.

Upregulation of I_f is most likely not the only change associated with enhanced automaticity of the heart during pregnancy. In fact, regulation of other ionic currents by pregnancy-related hormonal changes has been previously reported.[28] It is therefore plausible that other mechanisms involved in the diastolic depolarization could also contribute to the steeper diastolic depolarization. Furthermore, the fact that the AP threshold was more positive in pregnant mice also suggests that additional mechanisms are involved in the AP remodelling of the SAN during pregnancy. Conceivably, alterations in ionic mechanisms such as Ca^{2+} currents, Na^{+}-Ca^{2+} exchanger and spontaneous SR Ca^{2+} release could also contribute to these changes. Interestingly, Elzwiei F. *et al* recently reported that the α1 isoform of the Na^{+}-K^{+}

pump expression and flux are reduced in pregnant rats. The consequences were an accumulation of Na^+ which drove the Na^+-Ca^{2+} exchanger into reverse mode, thereby increasing intracellular Ca^{2+}.[50] Thus, it is possible that a similar scenario occurs in the SAN where increases in intracellular Ca^{2+} cycling would act in concert with an enhanced I_f density in order to sustain the elevated HR during pregnancy. Future studies will be required to explore the contribution of these ionic and Ca^{2+} mechanisms on the increased HR in pregnancy.

Conclusion

In conclusion, our data provide evidence that the accelerated heart rate in pregnant mice is associated with higher HCN2 channel protein expression leading to increased I_f density and automaticity of SAN. Our results demonstrate novel and functionally important ionic mechanisms, which contribute to the well-known pregnancy-induced increase in HR. Additional work will be directed toward examining how these changes in I_f may predispose the heart to initiation of arrhythmias during pregnancy.

ACKNOWLEDGMENTS

The authors wish to express their thanks to A. Douillette, M.A. Gillis and N. Duquette for expert technical assistance and A. Fortier from Biostatistics, Montreal Heart Institute Coordinating Center for the statistical analyses.

FUNDING SOURCES

This study was supported by an operating grant from Canadian Institutes of Health Research to C. Fiset (CIHR-MOP-64344). C. Fiset was a Research Scholar of the Fonds de la Recherche en Santé du Québec (FRSQ).

DISCLOSURES

None

REFERENCES

(1) Rashba EJ, Zareba W, Moss AJ, Hall WJ, Robinson J, Locati EH, Schwartz PJ, Andrews M. Influence of pregnancy on the risk for cardiac events in patients with hereditary long QT syndrome. LQTS Investigators. *Circulation* 1998;97:451-6.

(2) Larsen JA, Kadish AH. Effects of gender on cardiac arrhythmias. *J Cardiovasc Electrophysiol* 1998;9:655-64.

(3) Wolbrette D. Treatment of arrhythmias during pregnancy. *Curr Womens Health Rep* 2003;3:135-9.

(4) Gowda RM, Khan IA, Mehta NJ, Vasavada BC, Sacchi TJ. Cardiac arrhythmias in pregnancy: clinical and therapeutic considerations. *Int J Cardiol* 2003;88:129-33.

(5) Hunter S, Robson SC. Adaptation of the maternal heart in pregnancy. *Br Heart J* 1992;68:540-3.

(6) Adamson DL, Nelson-Piercy C. Managing palpitations and arrhythmias during pregnancy. *Heart* 2007;93:1630-6.

(7) Burkart T, Conti J. Cardiac Arrhythmias during Pregnancy. *Cur Treat Opt Cardiovasc Med* 2010;12:457-71.

(8) Thornburg KL, Jacobson SL, Giraud GD, Morton MJ. Hemodynamic changes in pregnancy. *Semin Perinatol* 2000;24:11-4.

(9) Speranza G, Verlato G, Albiero A. Autonomic changes during pregnancy: Assessment by spectral heart rate variability analysis. *J Electrocardiol* 1998;31:101-9.

(10) Ekholm EM, Erkkola RU. Autonomic cardiovascular control in pregnancy. *Eur J Obstet Gynecol Reprod Biol* 1996;64:29-36.

(11) Opthof T. The normal range and determinants of the intrinsic heart rate in man. *Cardiovasc Res* 2000;45:177-84.

(12) Irisawa H, Brown HF, Giles W. Cardiac pacemaking in the sinoatrial node. *Physiological Reviews* 1993;73:197-227.

(13) Vinogradova TM, Zhou YY, Maltsev V, Lyashkov A, Stern M, Lakatta EG. Rhythmic Ryanodine Receptor Ca^{2+} Releases During Diastolic Depolarization of Sinoatrial Pacemaker Cells Do Not Require Membrane Depolarization. *Circ Res* 2004;94:802-9.

(14) Maltsev VA, Vinogradova TM, Lakatta EG. The Emergence of a General Theory of the Initiation and Strength of the Heartbeat. *J Pharmacol Sci* 2006;100:338-69.

(15) Mangoni ME, Nargeot J. Genesis and Regulation of the Heart Automaticity. *Physiol Rev* 2008;88:919-82.

(16) Marionneau C, Couette B, Liu J, Li H, Mangoni ME, Nargeot J, Lei M, Escande D, Demolombe S. Specific pattern of ionic channel gene expression associated with pacemaker activity in the mouse heart. *J Physiol* 2005;562:223-34.

(17) Baruscotti M, Bucchi A, Viscomi C, Mandelli G, Consalez G, Gnecchi-Rusconi T, Montano N, Casali KR, Micheloni S, Barbuti A, DiFrancesco D. Deep bradycardia and

heart block caused by inducible cardiac-specific knockout of the pacemaker channel gene Hcn4. *Proc Natl Acad Sci U S A* 2011;108:1705-10.

(18) Baruscotti M, Barbuti A, Bucchi A. The cardiac pacemaker current. *J Mol Cell Cardiol* 2010;48:55-64.

(19) DiFrancesco D, Tortora P. Direct activation of cardiac pacemaker channels by intracellular cyclic AMP. *Nature* 1991;351:145.

(20) Berul CI, McConnell BK, Wakimoto H, Moskowitz IP, Maguire CT, Semsarian C, Vargas MM, Gehrmann J, Seidman CE, Seidman JG. Ventricular arrhythmia vulnerability in cardiomyopathic mice with homozygous mutant Myosin-binding protein C gene. *Circulation* 2001;104:2734-9.

(21) Brouillette J, Lupien MA, St Michel C, Fiset C. Characterization of ventricular repolarization in male and female guinea pigs. *J Mol Cell Cardiol* 2007;42:357-66.

(22) Mangoni ME, Nargeot J. Properties of the hyperpolarization-activated current (If) in isolated mouse sino-atrial cells. *Cardiovasc Res* 2001;52:51-64.

(23) Qu Y, Whitaker GM, Hove-Madsen L, Tibbits GF, Accili EA. Hyperpolarization-activated cyclic nucleotide-modulated 'HCN' channels confer regular and faster rhythmicity to beating mouse embryonic stem cells. *J Physiol* 2008;586:701-16.

(24) Harzheim D, Pfeiffer KH, Fabritz L, Kremmer E, Buch T, Waisman A, Kirchhof P, Kaupp UB, Seifert R. Cardiac pacemaker function of HCN4 channels in mice is

confined to embryonic development and requires cyclic AMP. *EMBO J* 2008;27:692-703.

(25) Grandy SA, Trepanier-Boulay V, Fiset C. Postnatal Development has a Marked Effect on Ventricular Repolarization in Mice. *Am J Physiol* 2007;293:H2168-H2177.

(26) Clapp JF, Capeless E. Cardiovascular Function Before, During, and After the First and Subsequent Pregnancies. *Am J Cardiol* 1997;80:1469-73.

(27) Ekholm EM, Erkkola RU, Piha SJ, Jalonen JO, Metsala TH, Antila KJ. Changes in autonomic cardiovascular control in mid-pregnancy. *Clin Physiol* 1992;12:527-36.

(28) Han X, Habuchi Y, Giles WR. Relaxin increases heart rate by modulating calcium current in cardiac pacemaker cells. *Circ Res* 1994;74:537-41.

(29) Bootsma M, Swenne CA, Van Bolhuis HH, Chang PC, Cats VM, Bruschke AV. Heart rate and heart rate variability as indexes of sympathovagal balance. *Am J Physiol* 1994;266:H1565-H1571.

(30) Rautaharju PM, Zhou SH, Wong S, Calhoun HP, Berenson GS, Prineas R, Davignon A. Sex differences in the evolution of the electrocardiographic QT interval with age. *Can J Cardiol* 1992;8:690-5.

(31) Peters RW, Gold MR. The influence of gender on arrhythmias. *Cardiol Rev* 2004;12:97-105.

(32) Bazett H. An analysis of the time-relations of electrocardiograms. *Heart* 1920;7:353-70.

(33) Burke JH, Goldberger JJ, Ehlert FA, Kruse JT, Parker MA, Kadish AH. Gender differences in heart rate before and after autonomic blockade: Evidence against an intrinsic gender effect. *Am J Med* 1996;100:537-43.

(34) Ng AV, Callister R, Johnson DG, Seals DR. Age and gender influence muscle sympathetic nerve activity at rest in healthy humans. *Hypertension* 1993;21:498-503.

(35) Fei DTW, Gross MC, Lofgren JL, Mora-Worms M, Chen AB. Cyclic AMP response to recombinant human relaxin by cultured human endometrial cells - A specific and high throughput in vitro bioassay. *Biochem Biophys Res Commun* 1990;170:214-22.

(36) Osheroff PL, Ling VT, Vandlen RL, Cronin MJ, Lofgren JA. Preparation of biologically active 32P-labeled human relaxin. Displaceable binding to rat uterus, cervix, and brain. *J Biol Chem* 1990;265:9396-401.

(37) Moosmang S, Stieber J, Zong X, Biel M, Hofmann F, Ludwig A. Cellular expression and functional characterization of four hyperpolarization-activated pacemaker channels in cardiac and neuronal tissues. *European Journal of Biochemistry* 2001;268:1646-52.

(38) Qu J, Kryukova Y, Potapova IA, Doronin SV, Larsen M, Krishnamurthy G, Cohen IS, Robinson RB. MiRP1 Modulates HCN2 Channel Expression and Gating in Cardiac Myocytes. *J Biol Chem* 2004;279:43497-502.

(39) Altomare C, Terragni B, Brioschi C, Milanesi R, Pagliuca C, Viscomi C, Moroni A, Baruscotti M, DiFrancesco D. Heteromeric HCN1-HCN4 channels: a comparison with

native pacemaker channels from the rabbit sinoatrial node. *The Journal of Physiology* 2003;549:347-59.

(40) Piot C, Lemaire S, Albat B, Seguin J, Nargeot J, Richard S. High Frequency-Induced Upregulation of Human Cardiac Calcium Currents. *Circulation* 1996;93:120-8.

(41) Zingman LV, Zhu Z, Sierra A, Stepniak E, Burnett CML, Maksymov G, Anderson ME, Coetzee WA, Hodgson-Zingman DM. Exercise-induced expression of cardiac ATP-sensitive potassium channels promotes action potential shortening and energy conservation. *J Mol Cell Cardiol* 2011;51:72-81.

(42) Luthi A, McCormick DA. Modulation of a pacemaker current through Ca(2+)-induced stimulation of cAMP production. *Nat Neurosci* 1999;2:634-41.

(43) Eghbali M, Deva R, Alioua A, Minosyan TY, Ruan H, Wang Y, Toro L, Stefani E. Molecular and functional signature of heart hypertrophy during pregnancy. *Circ Res* 2005;96:1208-16.

(44) Song M, Helguera G, Eghbali M, Zhu N, Zarei MM, Olcese R, Toro L, Stefani E. Remodeling of Kv4.3 Potassium Channel Gene Expression under the Control of Sex Hormones. *J Biol Chem* 2001;276:31883-90.

(45) Clapp JF, III. Maternal heart rate in pregnancy. *Am J Obstet Gynecol* 1985;152:659-60.

(46) Myerburg RJ, Cox MM, Interian A, Jr., Mitrani R, Girgis I, Dylewski J, Castellanos A. Cycling of inducibility of paroxysmal supraventricular tachycardia in women and its

implications for timing of electrophysiologic procedures. *Am J Cardiol* 1999;83:1049-54.

(47) Miyoshi H, Yamaoka K, Garfield R, Ohama K. Identification of a non-selective cation channel current in myometrial cells isolated from pregnant rats. *Pflug Arch* 2004;447:457-64.

(48) Chu Z, Takagi H, Moenter SM. Hyperpolarization-activated currents in gonadotropin-releasing hormone (GnRH) neurons contribute to intrinsic excitability and are regulated by gonadal steroid feedback. *J Neurosci* 2010;30:13373-83.

(49) Wu WW, Adelman JP, Maylie J. Ovarian hormone deficiency reduces intrinsic excitability and abolishes acute estrogen sensitivity in hippocampal CA1 pyramidal neurons. *J Neurosci* 2011;31:2638-48.

(50) Elzwiei F, Bassien-Capsa V, St-Louis J, Chorvatova A. Regulation of the sodium pump during cardiomyocyte adaptation to pregnancy. *Experimental Physiology* 2013;98:183-92.

FIGURES

Figure 1

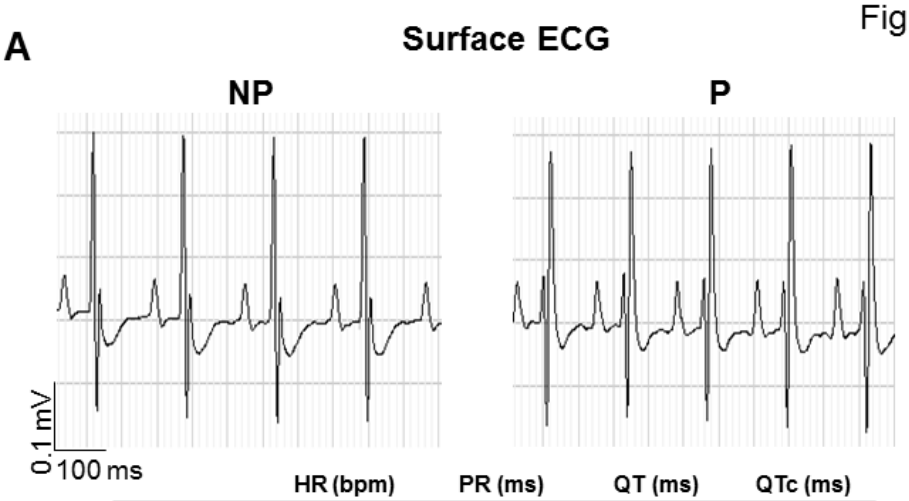

	HR (bpm)	PR (ms)	QT (ms)	QTc (ms)
NP	470 ± 27	43.5 ± 1.4	56.5 ± 6.7	48.5 ± 3.9
P	531 ± 14*	34.8 ± 0.7*	45.9 ± 1.4	43.2 ± 1.6
***p*-value**	0.03	< 0.0001	0.06	0.14

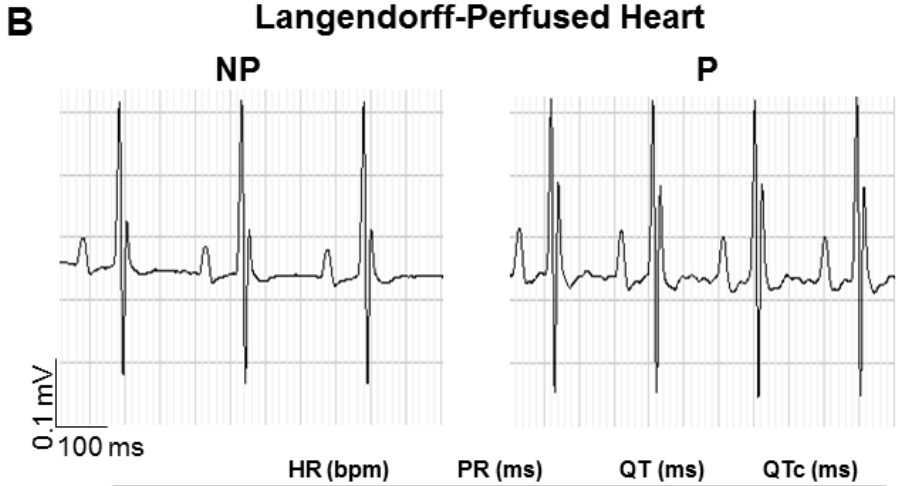

	HR (bpm)	PR (ms)	QT (ms)	QTc (ms)
NP	327 ± 16	44.3 ± 1.8	98.2 ± 6.7	71.5 ± 4.5
P	385 ± 18*	38.3 ± 2.3*	80.9 ± 7.6	62.4 ± 4.3
***p*-value**	0.02	< 0.0001	0.052	0.11

Figure 1. Pregnancy is associated with increased HR and shortened PR interval in surface ECG and Langendorff-perfused heart experiments. (A) Typical examples of surface ECG traces from anaesthetized NP and P mice. Table comparing mean data for HR, PR, QT and QTc intervals in NP and P mice show that HR is significantly increased and PR interval shortened in P mice (NP; N=10 and P; N=15). **(B)** Representative epicardial ECG recordings from Langendorff-perfused hearts in NP and P mice. Table comparing mean ECG parameters reveals a faster HR and a shorter PR interval in P mice (NP; N=10 and P; N=11).

Figure 2

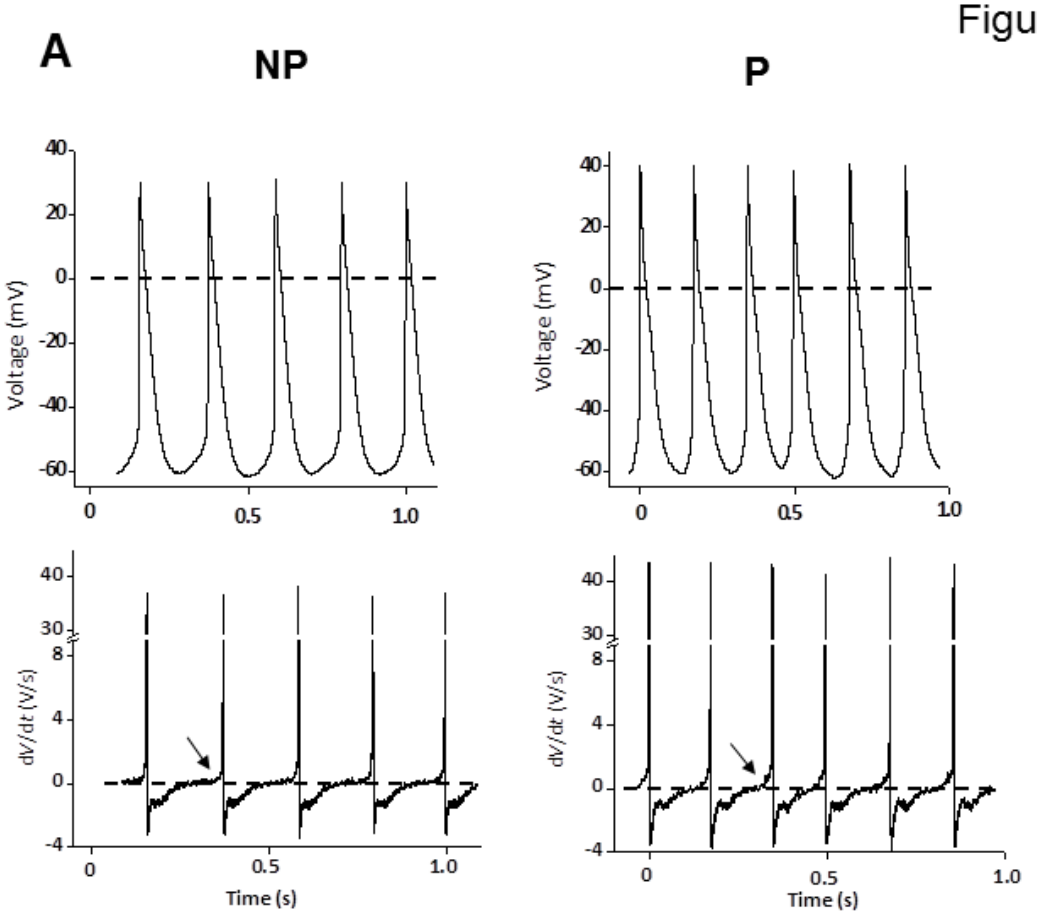

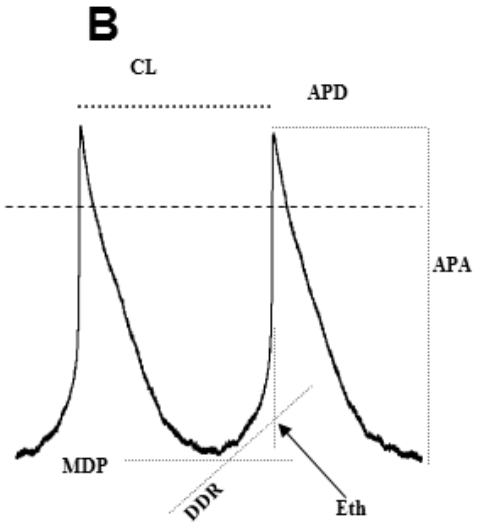

	NP	P	*p*-value
Pacing rate (bpm)	292 ± 13	330 ± 12*	0.047
DDR (V/s)	0.20 ± 0.03	0.40 ± 0.06*	0.004
Eth (mV)	-45.8 ± 1.3	-41.5 ± 1.4*	0.03
MDP (mV)	-58.7 ± 1.2	-56.8 ± 1.6	0.34
Vmax (V/s)	44.3 ± 5.2	58.8 ± 7.0	0.10
APA (mV)	97 ± 5	97 ± 4	0.96
ADP (ms)	119 ± 4	110 ± 3	0.11

Figure 2. Pacemaker activity of isolated SAN cells is increased in pregnant mice. (A) Representative spontaneous APs (top) and their first derivative (bottom) recorded using perforated patch-clamp configuration in SAN cells isolated from NP (left) and P (right) mice. Arrows indicate diastolic depolarization while the hatched line indicates 0 mV in this and subsequent figures. (**B)** Measurements of the intrinsic cycle length (CL), diastolic depolarization rate (DDR), AP threshold (Eth), maximum diastolic potential (MDP), maximal velocity of AP upstroke (V_{max}), AP amplitude (APA) and AP duration (APD) of SAN cell APs were made as shown by the dotted lines and arrows on the AP (left). Summary table of AP parameters from NP (n=17, N=9) and P mice (n=12, N=8).

Figure 3

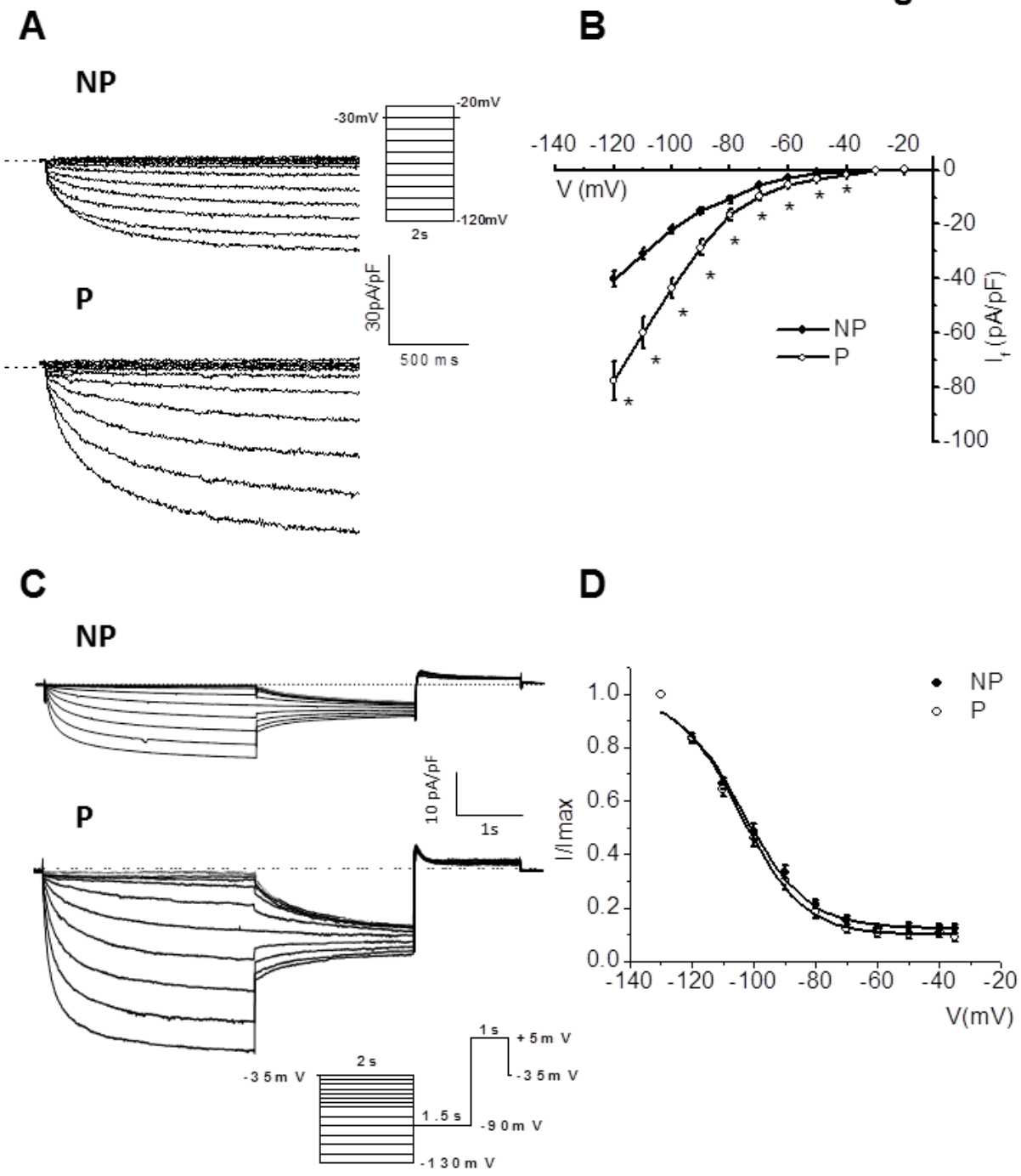
A
NP
-30mV
-20mV
-120mV
2s
30pA/pF
500 ms
P
B
-140 -120 -100 -80 -60 -40 -20
V (mV)
0
-20
-40
-60
-80
-100
NP
P
I_t (pA/pF)
C
NP
10 pA/pF
1s
P
1 s
+ 5 m V
-3 5 m V
2 s
-3 5 m V
1 .5 s
-9 0 m V
-1 3 0 m V
D
NP
P
1.0
0.8
0.6
0.4
0.2
0.0
I/I max
-140 -120 -100 -80 -60 -40 -20
V(mV)

Figure 3. Electrophysiological properties of I_f in SAN cells of non-pregnant and pregnant mice. (A) Typical examples of I_f current recorded in whole-cell configuration in SAN cells isolated from NP and P mice. Insets depict recording protocols. (**B)** Mean data for the current-voltage (I-V) relationship for I_f in SAN cells of NP (n=26, N=18) and P (n=26, N=17) mice (*p<0.05). **(C)** Typical examples of I_f current recorded in perforated patch configuration using a tail current protocol *(shown in inset)* in SAN cells isolated from NP and P mice. **(D)** Mean data for the steady-state I_f activation curves of SAN cells in NP (n=18, N=12) and P (n=17, N=8) mice. Tail currents were determined by substracting the peak current from the steady-state current (tail current at -90mV), normalized and plotted against test voltage. The relationships were fitted with the Boltzmann equation.

Figure 4

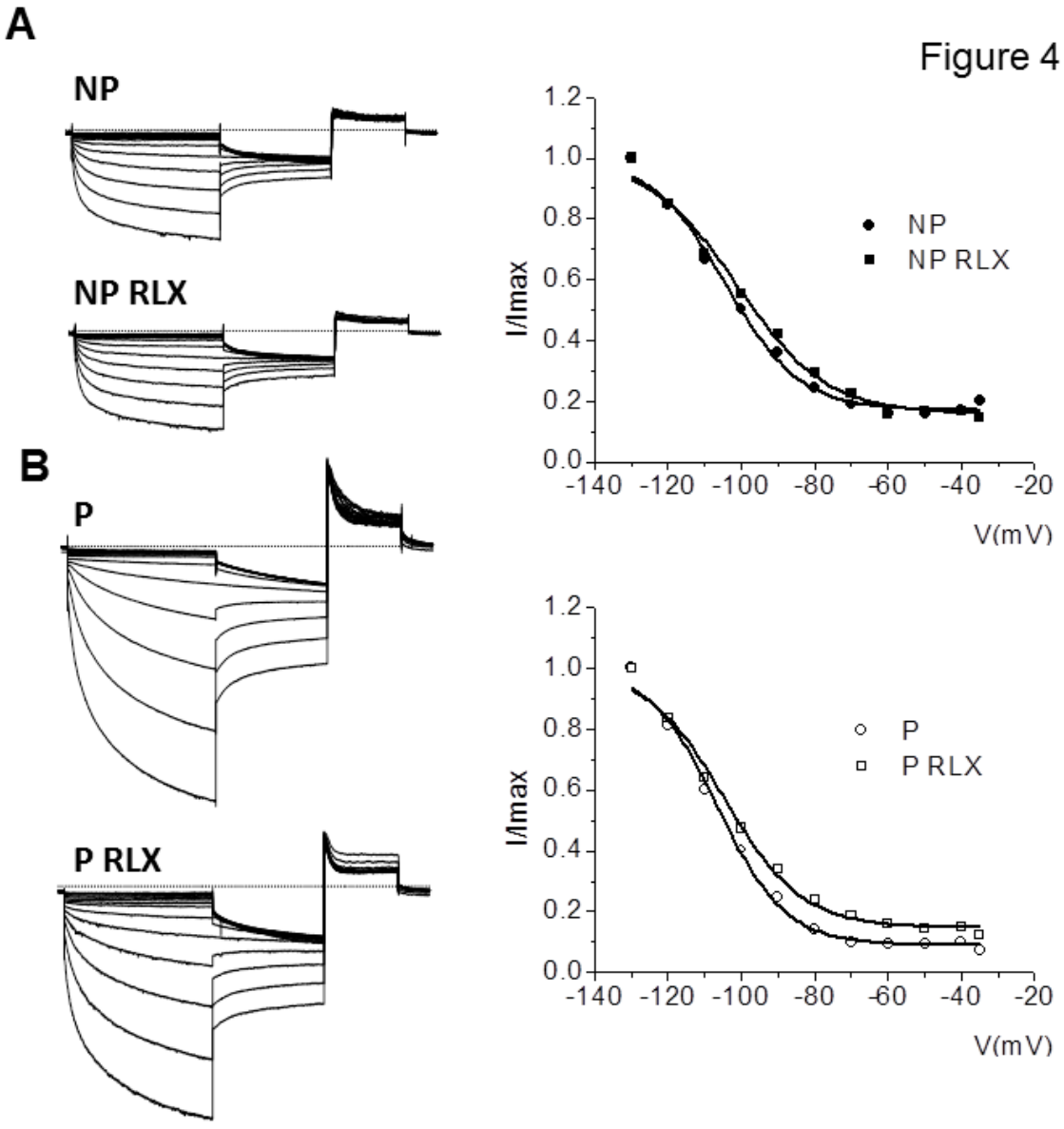
A
NP
NP RLX
B
P
P RLX
I/Imax
1.2
1.0
0.8
0.6
0.4
0.2
0.0
-140 -120 -100 -80 -60 -40 -20
V(mV)
NP
NP RLX
P
P RLX
C
SAN cAMP Level (pmol/mg protein)
10
5
0
NP
P

Figure 4. I_f response to relaxin is similar in pregnant and non-pregnant mice. (A) Typical examples of I_f current traces from NP mice (left) and corresponding steady-state I_f activation curves (right) before and after application of relaxin (RLX, 80nM). **(B)** Typical examples of I_f current traces from P mice (left) and corresponding steady-state I_f activation curves (right). Similar results were obtained in n=5 SAN cells from N=3 mice for each group. **(C)** Bar graph summarizing cAMP assay results on SAN derived from NP and P mice (N=10 in both groups, p=0.07).

Figure 5

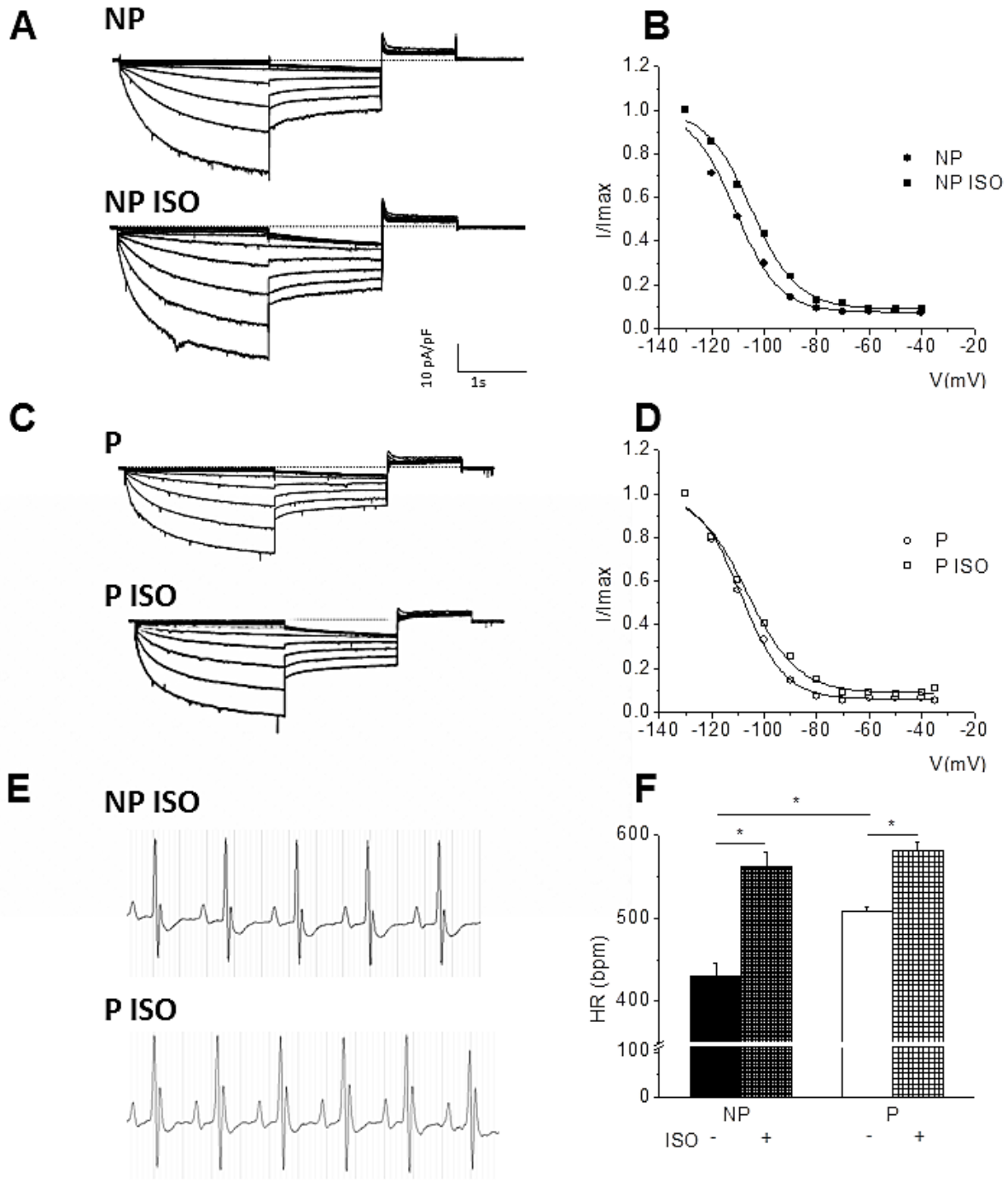
A
NP
NP ISO
10 pA/pF
1s
B
I/Imax
V(mV)
NP
NP ISO
C
P
P ISO
D
I/Imax
V(mV)
P
P ISO
E
NP ISO
P ISO
F
HR (bpm)
NP
P
ISO

Figure 5. Effect of isoproterenol on I_f is not affected by pregnancy. (A) Representative examples of I_f recorded in SAN cells of a NP mouse in the absence or presence of isoproterenol (ISO, 100nM). **(B)** Corresponding I_f activation curve. **(C)** Representative examples of I_f recorded in SAN cells of a P mouse in absence or presence of isoproterenol (ISO, 100nM). **(D)** Corresponding I_f activation curve. Similar results were obtained from n=5, N=4 in NP and n=6, N=3 in P groups. **(E)** Typical surface ECG recordings from anaesthetized NP (top) and P mice (bottom) in presence of ISO. **(F)** Bar graphs presenting the mean data for HR obtained on surface ECGs from anaesthetized NP and P mice before and after ISO (NP: ΔHR +132±24, N=6 and P: ΔHR +72±15, N=7).

Figure 6

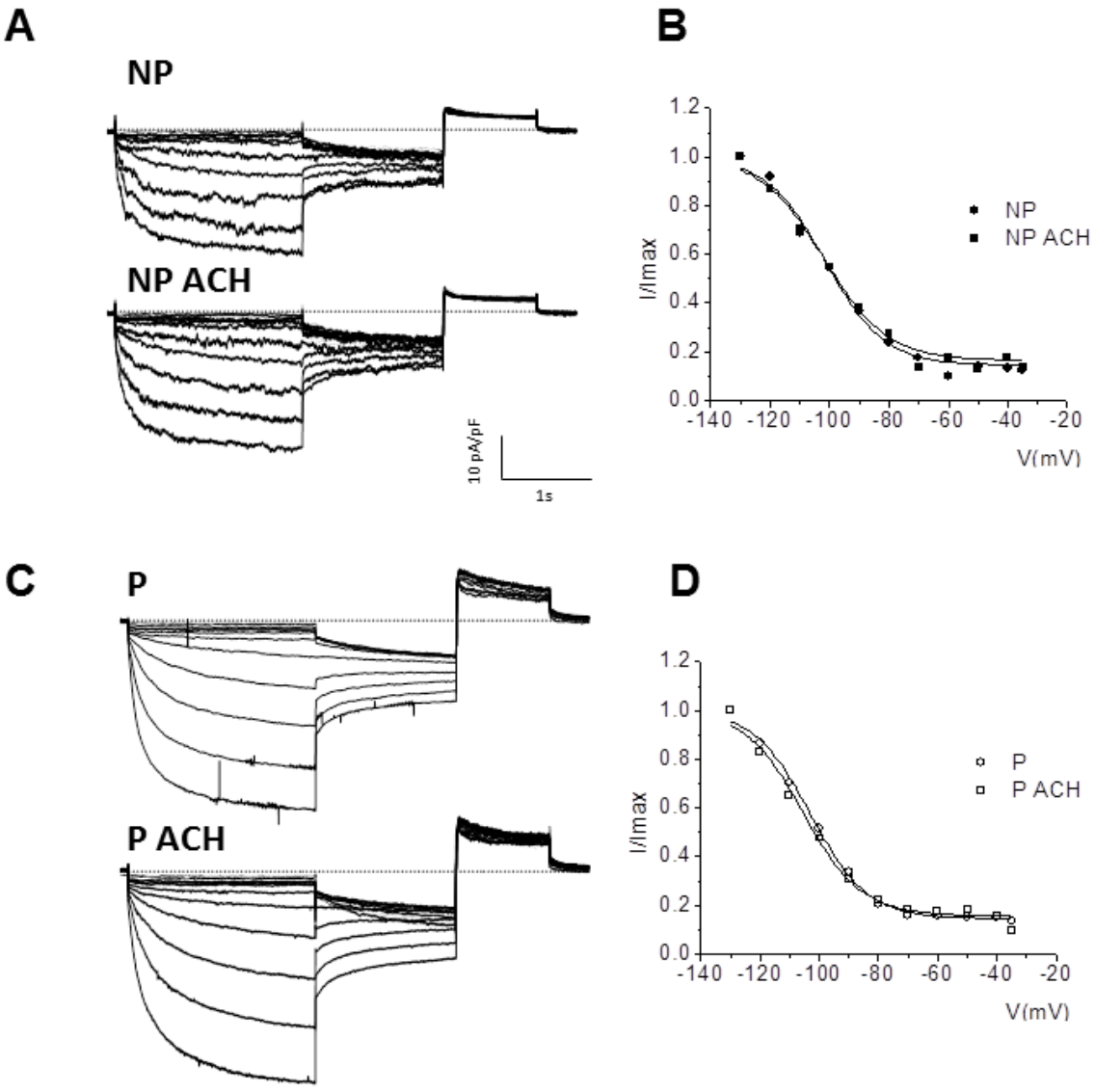
A
NP
NP ACH
10 pA/pF
1s
B
I/Imax
V(mV)
NP
NP ACH
C
P
P ACH
D
I/Imax
V(mV)
P
P ACH

Figure 6. Response of I_f to acetylcholine is similar in SAN cells of pregnant and non-pregnant mice. (A) Representative examples of I_f recorded in SAN cells of a NP mouse in absence or presence of acetylcholine (ACH, 1μM). **(B)** Corresponding I_f activation curve. Similar results were obtained in n=8 SAN cells from N=4 mice. **(C)** Representative examples of I_f recorded in SAN cells of a P mouse in absence or presence of acetylcholine (ACH, 1μM). **(D)** Corresponding I_f activation curve. Similar results were obtained in n=6 SAN cells from N=2 mice.

Figure 7

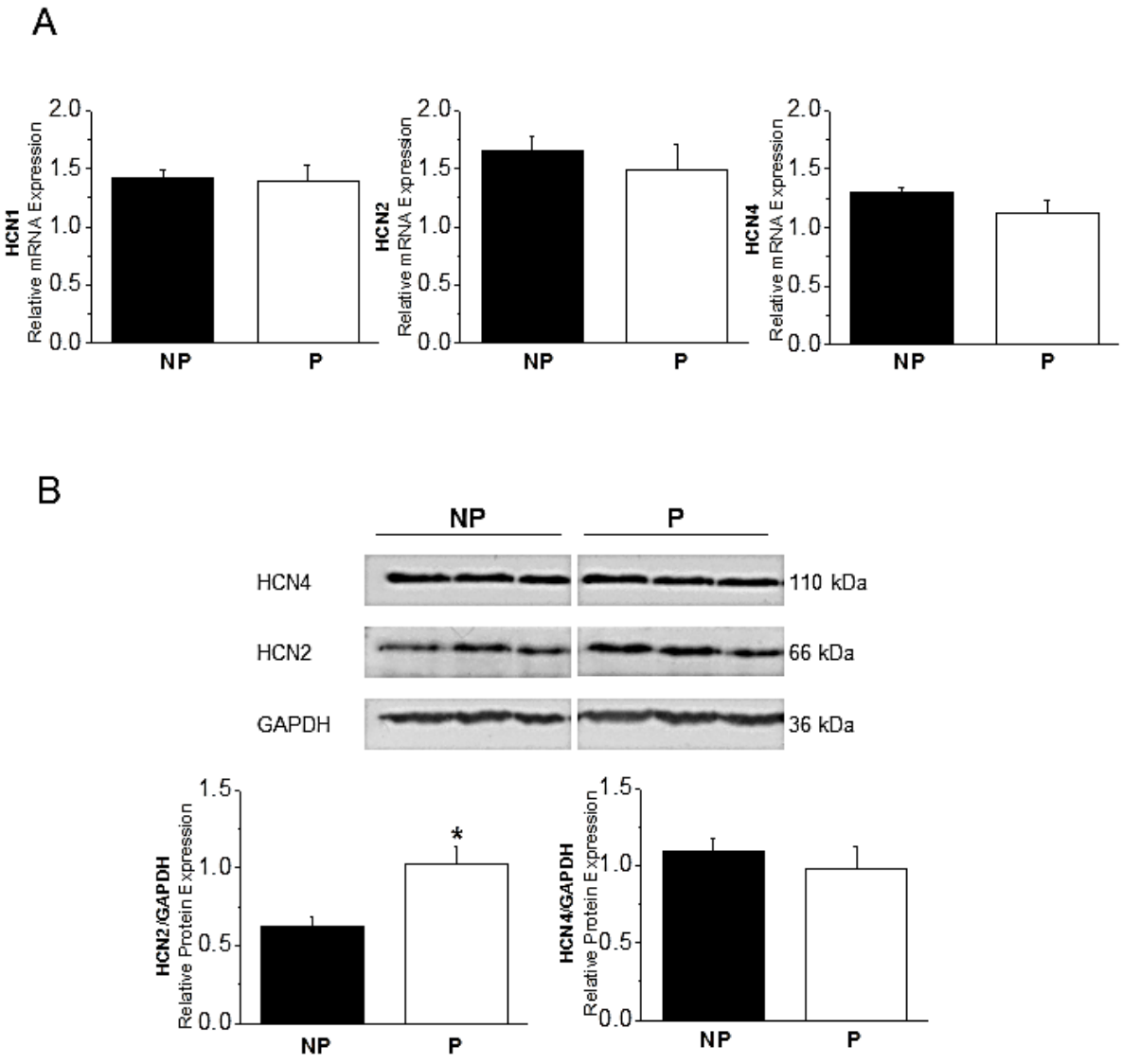
A
HCN1
Relative mRNA Expression
2.0
1.5
1.0
0.5
0.0
NP
P
HCN2
Relative mRNA Expression
HCN4
Relative mRNA Expression
B
NP
P
HCN4
HCN2
GAPDH
110 kDa
66 kDa
36 kDa
HCN2/GAPDH
Relative Protein Expression
*
HCN4/GAPDH
Relative Protein Expression

Figure 7. qPCR and Western blot analysis of HCN channel isoforms from pregnant and non-pregnant mouse SAN.

(A) Mean qPCR data showing relative mRNA expression of HCN1, HCN2 and HCN4 in SAN of NP and P mice. Each bar graph represents mean data of 6 samples, each analyzed in triplicate. 10-12 SAN were pooled per sample (HCN1, p=0.88, HCN2, p=0.55, HCN4, p=0.14).

(B) Western blot analysis for HCN2 and HCN4 on SAN from P and NP mice (top) and bar graph summarizing mean data for relative protein expression (bottom) (n=3 for both groups, 3 SANs were pooled per n, *p=0.04).

Table 1. Arterial Blood Pressure and Catecholamine Levels in Non-Pregnant and Pregnant Mice.

	Non-Pregnant	Pregnant	*p*-value
Arterial Blood Pressure			
Systolic pressure (mm Hg)	99.5 ± 1.4 (8)	100.8 ± 3.1 (7)	0.68
Diastolic pressure (mm Hg)	70.0 ± 1.8 (8)	70.3 ± 3.0 (7)	0.95
Mean blood pressure (mm Hg)	79.0 ± 1.5 (8)	79.7 ± 3.0 (7)	0.85
Plasma Catecholamines			
Epinephrine level (ng/ml)	2.0 ± 0.5 (6)	2.8 ± 0.8 (5)	0.37
Norepinephrine level (ng/ml)	9.8 ± 1.0 (6)	10.8 ± 1.3 (7)	0.55

Numbers in parenthesis represent numbers of mice

Clinical Perspectives

An increased incidence of cardiac arrhythmias is observed during pregnancy. This may have significant consequences on the wellbeing of the mother and the fetus. In fact, during pregnancy the heart rate significantly increases thus raising the susceptibility to arrhythmias. This is particularly true in the third semester where sinus tachycardia becomes very common. Indeed, more than 50% of pregnant women exhibit a form of arrhythmia and ectopic beats. The mechanisms for the increase in heart rate and subsequent arrhythmia risks have been largely unexplored. In the present study we used a mouse model of pregnancy to explore the positive chronotropic effect in pregnancy and we report one of the main underlying ionic mechanisms responsible for heart rate increase. First, we show that our mouse model of pregnancy reproduces the increased heart rate observed in pregnancy in humans and importantly that this increase is intrinsic to the heart and not secondary to alterations in autonomic tone, arterial blood pressure or circulating catecholamine levels. We then demonstrate that pregnancy is associated with accelerated automaticity of the sino-atrial node cells through enhanced density of the funny current (I_f), one of the major ionic currents modulating pacemaker activity of the heart. Our results thus, provide novel and functionally insight into mechanisms of pregnancy-induced increase in heart rate. Additional work will be directed toward examining how these changes may initiate arrhythmias during pregnancy. As the number of pregnancies in women at an advanced maternal age, -with more comorbidity- continues to rise, this issue is becoming even more relevant.

Online data Supplement

Upregulation of the hyperpolarization activated channels increases pacemaker activity of the sinoatrial node and heart rate during pregnancy in mice

Corresponding author: C. Fiset

MATERIAL AND METHODS

Surface electrocardiograms (ECG)

Mice were anaesthetized with isoflurane. Body temperature was maintained at 37°C using a heating pad. Platinum electrodes positioned subcutaneously were connected to a Biopac System MP100 (EMKA Technologies, France). Surface ECGs were recorded in lead I configuration at a rate of 2 kHz and performed for 5 minutes of continuous experimental recording at the end of a baseline period. The signal was filtered at 100Hz (low pass) and 60kHz (notch filter). Data were analyzed using ECG-auto 1.7 (EMKA Technologies). RR, PR, and QT intervals were calculated manually by a blinded observer from signal averaged ECG recordings (500-1000 cardiac cycles). QT intervals were corrected (QTc) for HR using the correction formula for mice ($QTc=QT/(RR/100)^{1/2}$).[1] Additional surface ECG recordings were obtained on anaesthetized mice before and after intravenous (IV) injection of isoproterenol (0.1ng/g) through the right jugular vein.[2] After the maximal isoproterenol effect occurred (within 1-2 minutes), ECG parameters were measured as described above.

Langendorff-perfused heart

Experiments were performed as previously described.[3] Mice were heparinized (1 U/kg, IP) 20 minutes prior to sacrifice. They were then anaesthetized with isoflurane and sacrificed by cervical dislocation. The heart was rapidly excised and hung on a modified Langendorff

apparatus and retrogradely perfused through the aorta at a constant perfusion pressure of 75mmHg with a Krebs-Henseleit buffer at 37°C and constantly gassed with 95% O_2/ 5% CO_2 containing (mM) 11.2 glucose, 118.5 NaCl, 25 $NaHCO_3$, 4.7 KCl, 2.45 $MgSO_4$, 1.2 KH_2PO_4, 1.2 $CaCl_2$. Epicardial ECG recordings were obtained by placing one silver electrode at the base of the heart under the right atrium and another in the apex of the left ventricle. After an equilibration perfusion period, epicardial ECG measurements were recorded and ECG parameters were calculated as above.

Sino-atrial cell isolation

Mice were anaesthetized by inhalation of isoflurane and then sacrificed by cervical dislocation. The SAN cells were isolated using an adaptation of the protocol previously described by Mangoni *et al.*[4] Briefly, SANs were dissected in normal HEPES-buffered Tyrode's solution containing (mM): 140 NaCl, 5.4 KCl, 1.8 $CaCl_2$**,** **1** $MgCl_2$, 5 HEPES and 5.5 glucose (pH=7.4 with NaOH). SAN tissue was cut into small pieces and rinsed twice for 4 minutes in a Ca^{2+}-free Tyrode's solution containing (mM) 0.5 $MgCl_2$, 1.2 KH_2PO_4, 50 taurine and 0.1% bovine serum albumin (BSA Fraction V, Sigma, St. Louis, MO, USA) (pH=6.9 with NaOH). The tissue strips were then digested at 36±1°C for 20-30 minutes with the same solution supplemented with collagenase type IV (229U/ml, Worthington, Lakewood, NJ, USA), elastase (1.9U/ml, Worthington), protease type XIV (0.9U/ml, Sigma) and 200µM $CaCl_2$. The SAN tissue was then washed three times and transferred into "Kraft-Brühe" (KB) solution (mM): 100 K^+-glutamate, 10 K^+-Aspartate, 25 KCl, 10 KH_2PO_4, 2 $MgS0_4$, 20 taurine, 5 creatine, 0.5 EGTA, 5 HEPES, 0.1% BSA, 20 glucose (pH=7.2 with KOH). The tissue was triturated gently with a Pasteur pipette until single SAN cells were obtained, usually within 2-3 minutes. Physiological extracellular Ca^{2+} concentration was gradually restored. Isolated mouse SAN

cells were identified as small spindle-type cells spontaneously beating in normal Tyrode's solution.[4]

Electrophysiological data

Current- and voltage-clamp recordings. An aliquot of SAN cell solution was placed in a recording chamber (volume 200µl) mounted on the modified stage of an inverted microscope and superfused with a normal Tyrode's solution containing (mM): 140 NaCl, 5.4 KCl, 1.8 $CaCl_2$, 1 $MgCl_2$, 5 HEPES and 5.5 glucose (pH=7.4 with NaOH). For I_f recordings, 1 mM $BaCl_2$ (Sigma) was added to the external solution to block the inward rectifier K^+ current, I_{K1}.Bath was perfused with continuously gassed (100% O_2) at 35±1˚C. Current- and voltage-clamp recordings were obtained using the Axopatch 200B patch-clamp amplifier (Molecular Devices, Sunnyvale, CA, USA). Pipettes were pulled from borosilicate glass (World Precision Instruments, Sarasota, FL, USA), and had resistance of 3-6 MΩ when filled with the following solution (mM): 100 K^+-aspartate, 30 KCl, 10 NaCl, 2 MgATP, 6.6 Na_2phosphocreatine, 0.1 Na_2GTP, 0.04 $CaCl_2$, 1 $MgCl_2$ and 5 HEPES (pH=7.2 with KOH). Voltage-clamp recordings were low-pass filtered at 10kHz (4-pole Bessel), digitized and analyzed using pCLAMP 10.2 software (Molecular Devices). Capacitive transients were elicited by a 10-ms voltage step of ± 10 mV from a holding potential (HP) of -30mV. Cell capacitances were measured by integrating the area of the capacitive transients. Junction potential was not corrected.

Real time RT-PCR

Total RNA extraction and real-time PCR (qPCR) for the HCN channels were conducted using previously published protocols.[5, 6] For each sample, 10-12 SANs were pooled and used to isolate total RNA from NP and P mice. Total RNA was isolated using TriReagent® and treated

with DNase I as previously described.[5] cDNA was then synthesized with SuperScript™ III Reverse Transcriptase (Life Technologies). mRNA was transcribed using pdN6 random primers. Gene specific primers and conditions for PCR reactions were used for HCN1 and HCN4 as previously described.[6] The following primers specific to HCN2 were designed (forward: GCTGGGTGTCCATCAACAAC, reverse: AGATGTCTGTCATGCTCTCG) and the PCR reactions were cycled using a 3-step procedure (denaturation at 95ºC for 30s, annealing at 55ºC for 60s, elongation at 72ºC for 60s). The qPCR was performed with Platinum SYBR Green qPCR Supermix (Life Technologies) using a real-time PCR system (MX3005P QPCR system, Stratagene). Quantitative measurements were performed in triplicate and normalized to the average of three housekeeping genes (18S, lamin C, and succinate dehydrogenase complex subunit A (SDHA)).

Western blot

The protein samples were extracted from SAN tissues of non-pregnant and pregnant mice for Western blot analysis. For each sample, 3 SANs were pooled for protein isolation. SANs were pulverized in liquid nitrogen and were then resuspended in ice cold extraction buffer containing 1% Triton-X100 and a cocktail of protease and phosphates inhibitors and agitated 1 hour at 4^{o}C. Samples were subsequently centrifuged at 12,000g and the supernantant containing the proteins was recovered, quantified using the Bradford assay and stored at -80^{o}C for later use. Proteins (25 μg) were loaded and separated on 10% SDS-PAGE, blotted on a PVDF membrane (Millipore) and probed with anti-rabbit HCN2 and HCN4 specific antibody (1:1000) (Alomone Labs, Israel). After secondary antibody incubation, chemiluminescence

analysis using an ECL system (PerkinElmer) was performed. All bands were normalized to GAPDH (Fitzgerald, Acton, MA, USA).

Drugs

Recombinant Human Relaxin-2 (H2 Relaxin; B-29/A24) was purchased from R&D Systems, Minneapolis, MN USA. All other compounds were obtained from Sigma. Isoproterenol and acetylcholine were prepared in water while relaxin was prepared in sterile PBS. Stock solutions of all drugs were then diluted in Tyrode's solution to achieve their respective final concentration. Isoproterenol was protected from degradation by the addition of ascorbic acid (100μM) to the final solution.

Statistical analysis

All data are presented as mean ± SEM. "*n"* refers to the number of experiments and "*N*" the number of mice. Descriptive statistics were used to compare ECG parameters. A Mann-Whitney Test was used to either compare data between NP and P mice obtained with ECG recording methods under control conditions and after treatment with isoproterenol. A Wilcoxon Signed Ranks test was used to compare HR in the same group before and after isoproterenol (Fig. 1,5F). Unpaired t-tests were used to compare blood pressure, catecholamine and cAMP levels, cellular electrophysiology, mRNA and protein data between NP and P mice (Table 1, Fig. 2-4 and 7). Electrophysiological data in NP and P mice obtained before and after pharmacological manipulations were compared using two-way ANOVA for repeated measures, no adjustment was used for multiple comparisons (Fig. 3-6). Non parametric analyses were conducted using SAS9.2. T-tests and ANOVA were performed with Origin 8.0 (OriginLab, MA, USA). $p<0.05$ was considered significantly different.

References

(1) Mitchell GF, Jeron A, Koren G. Measurement of heart rate and QT interval in the conscious mouse. *Am J Physiol* 1998;274:H747-H751.

(2) Berul CI, McConnell BK, Wakimoto H, Moskowitz IP, Maguire CT, Semsarian C, Vargas MM, Gehrmann J, Seidman CE, Seidman JG. Ventricular arrhythmia vulnerability in cardiomyopathic mice with homozygous mutant Myosin-binding protein C gene. *Circulation* 2001;104(22):2734-9.

(3) Brouillette J, Lupien MA, St Michel C, Fiset C. Characterization of ventricular repolarization in male and female guinea pigs. *J Mol Cell Cardiol* 2007;42(2):357-66.

(4) Mangoni ME, Nargeot J. Properties of the hyperpolarization-activated current (If) in isolated mouse sino-atrial cells. *Cardiovasc Res* 2001;52(1):51-64.

(5) Grandy SA, Trepanier-Boulay V, Fiset C. Postnatal Development has a Marked Effect on Ventricular Repolarization in Mice. *Am J Physiol* 2007;293(4):H2168-H2177.

(6) Marionneau C, Couette B, Liu J, Li H, Mangoni ME, Nargeot J, Lei M, Escande D, Demolombe S. Specific pattern of ionic channel gene expression associated with pacemaker activity in the mouse heart. *J Physiol* 2005;562(Pt 1):223-34.

3 Alterations in sinoatrial node Ca^{2+} homeostasis sustain an accelerated heart rate during pregnancy in mice

Nabil El Khoury, Ph.D., Jenna Ross, Ph.D., Valérie Long, Simon Thibault, Nathalie Ethier, M.Sc., Céline Fiset, Ph.D.

In preparation for Circulation, 2017

Author contribution:

N.E.K: Patch-clamp recording protocols development, data acquisition and analysis, technique optimization for mouse SAN RNA extractions, study design, manuscript writing and proofing.

J.R.: Patch-clamp and fluorescent microscopy data acquisition, SAN cell isolations, manuscript text input.

S.T.: Fluorescent microscopy data acquisition.

V.L.: Fluorescent microscopy data acquisition.

N.E.: SAN cell isolation, patch-clamp data acquisition and analysis, qPCR, fluorescent microscopy data acquisition.

C.F.: Corresponding author and principal investigator, original manuscript idea, complete data reviewing with study conceptualization and design, manuscript writing, reviewing and proofing.

Outline- The second study has been completed and is in the last stages of preparation and proofing. It will be submitted to Circulation shortly. Based on the previous paper, this study explores the role of Ca^{2+} in contributing to the heart rate increase during pregnancy. Featuring *in vivo* and cellular electrophysiology, Ca^{2+} imaging, and gene expression data we demonstrate how SAN Ca^{2+} homeostasis and regulation, that is critical to pacemaking function, adapts to sustain an elevated heart rate. Additionally, new evidence relating to arrhythmia risk and the reversal of the SAN adaptations following delivery is presented.

3.1 Résumé

L'augmentation de la fréquence cardiaque (FC) pendant la grossesse est potentiellement associée à un risque accru d'arythmies ou d'exacerbation de conditions cardiaques préexistantes, mettant en danger à la fois la mère et le fœtus. L'homéostasie calcique joue un rôle important dans la régulation de l'automaticité du nœud sinusal (NS), toutefois, sa contribution à l'accélération de la FC pendant la grossesse demeure inconnue. En utilisant des cellules isolées du NS, nous démontrons que le courant de Ca^{2+} de type L (I_{CaL}), qui joue un rôle majeur dans l'automaticité du NS, est augmenté de 42% chez les souris gestantes (SG) par rapport aux non gestantes (SNG) tandis que le courant Ca^{2+} de type T demeure inchangé. Conformément à ces résultats, l'analyse de qPCR du gène codant $Ca_V1.3$ montre une expression presque doublée chez les SG comparées aux SNG.

Nous avons également étudié l'homéostasie calcique dans les cellules du NS en évaluant les oscillations du Ca^{2+} intracellulaire qui dépendent des récepteurs à la ryanodine (RyR2), de la pompe Ca^{2+} du réticulum sarcoplasmique (SERCA2a), du phospholamban (PLB) et de l'échangeur Na^+/Ca^{2+} (NCX1). Les données montrent que la fréquence des transitoires Ca^{2+} et la vélocité de la phase ascendante étaient significativement plus élevées chez les SG et elles étaient à une associées une plus forte expression génique de RyR2 tandis que l'expression celle de SERCA2a, PLB et NCX1 restait inchangée. L'évaluation de la susceptibilité aux événements arythmiques, déterminée à l'aide de protocoles de stimulation électrique programmée a permis de mettre en évidence que les SG étaient plus susceptibles (25%) de souffrir d'arythmies que les SNG. Enfin, nous avons montré que toutes les modifications observées pendant la grossesse étaient réversibles après la parturition.

Ces résultats suggèrent que des modifications de l'homéostasie Ca^{2+} intracellulaire du NS particulièrement, une augmentation de I_{CaL} et la libération spontanée de Ca^{2+} du réticulum sarcoplasmique par les RyR2 peuvent contribuer à l'accélération de l'automaticité chez les SG.

3.2 Study

ABSTRACT

During pregnancy there is a significant increase in heart rate (HR) potentially associated with an increased risk of arrhythmias or exacerbation of pre-existing cardiac conditions endangering both mother and fetus. Calcium homeostasis plays an important role in regulating automaticity of the sinoatrial node (SAN) however, its contribution to the accelerated HR during pregnancy remains unknown. Using isolated SAN cells, we show that L-type Ca^{2+} current (I_{CaL}), which plays a major role in SAN automaticity, is increased by 42% in pregnant (P) compared to non-pregnant (NP) mice, while T-type Ca^{2+} current was unchanged. Congruent with these results, qPCR analysis for $Ca_v1.3$ was increased approximately 2 fold in P compared to NP mice. Ca^{2+} homeostasis in SAN cells mediated by oscillations of intracellular Ca^{2+} concentrations by means of ryanodine receptors (RyR2), sarcoplasmic reticulum (SR) Ca^{2+}-ATPase (SERCA2a), phospholamban (PLB) and the Na^+/Ca^{2+} exchanger (NCX1) was examined. Data shows that Ca^{2+} transient frequency and Ca^{2+} release were significantly higher in P mice along with a higher mRNA expression of RyR2. SERCA2a, PLB and NCX1 expression remained unchanged. Assessment of arrhythmic events using programmed electrical stimulation protocols revealed that P mice are more likely to suffer from supraventricular arrhythmias compared to NP. Lastly, we showed that all of the reported modifications associated with pregnancy are rapidly reversible following delivery. Together, these results suggest that an increase in I_{CaL} and spontaneous Ca^{2+} release from the SR through RyR2 in SAN cells contribute to the acceleration in SAN automaticity in pregnant mice by altering intracellular Ca^{2+} homeostasis.

Keywords: Heart rate; Ca^{2+} handling; pacemaker; pregnancy; sinoatrial node.

INTRODUCTION

Pregnancy brings about drastic changes to physiological functions of many organ systems including the vasculature and the heart that undergo extensive remodeling.[1] Indeed, throughout normal pregnancy in women, the substantial increase in blood volume, metabolism and fetal needs require the cardiovascular system to undergo major adjustments to meet the growing demand of both the mother and the fetus.[2,3] During the second to fifth week of pregnancy, the heart rate (HR) can increase up to 25% and remain elevated throughout the remainder of gestational period. Elevated HR or sinus tachycardia are often seen in pregnant women and are a known risk factor for arrhythmias notably supraventricular arrhythmias.[2,4–7] During pregnancy, the prevalence of arrhythmias is high and they may occur *de novo* or become exacerbated if an underlying cardiac condition exists, thereby posing an increased risk to both the mother and the fetus.[5,7]

This HR increase in women suggests that pregnancy directly influences the automaticity of the heart. Indeed, cardiac automaticity is regulated by the sinoatrial node (SAN), which is responsible for initiating and controlling the HR making it a fundamental aspect of normal cardiac physiology.[8,9] A major determinant of cardiac automaticity is the spontaneous diastolic depolarization phase of the action potential (AP) in SAN cells where the rate of firing is determined by the slope of the diastolic depolarization.[8–10] Two main mechanisms are thought to regulate spontaneous activity of SAN cells: a voltage-sensitive component comprised of several voltage-gated membrane ion channels including the L-type and T-type Ca^{2+} channels along with the pacemaker channels that encode the pacemaker current (I_f). These channels work in concert with a Ca^{2+} cycling mechanism that relies on a spontaneous and rhythmic

release of Ca^{2+} from the sarcoplasmic reticulum (SR) during the late diastolic depolarization in the form of Ca^{2+} sparks and transients.[9,11–14] The localized increase in intracellular Ca^{2+} initiates membrane depolarization largely through activation of the sodium-calcium exchanger (NCX1).[12,13] The small electrogenic current produced by forward-mode NCX1 contributes to an acceleration of the late diastolic depolarization phase and spontaneous activity of the SAN. Recent evidence from numerous studies has shown that intracellular Ca^{2+} handling and membrane voltage-gated ion channels are locked in together and subject to crosstalk forming a complex pacemaking mechanism.[15,16] Specifically, in SAN cells, T- and L-type Ca^{2+} currents (I_{CaT} and I_{CaL}) and their underlying voltage-gated channels $Ca_V3.1$ and $Ca_V1.2/1.3$ respectively, play a critical role in the second half of the diastolic depolarization. Indeed, the activation of I_{CaT} then I_{CaL} following the spontaneous I_f-mediated depolarization, causes a localized Ca^{2+} release from the SR and therefore both currents are important in the late diastolic depolarization phase and pacemaking.[8,17,18] Intracellular Ca^{2+} cycling in SAN cells is also tightly regulated by various Ca^{2+} handling proteins. The major players include the SR-bound ryanodine receptor (RyR2), the SR Ca^{2+}-ATPase pump (SERCA2a) as well as the NCX1, which in concert, regulate SAN automaticity and HR.

In order to explain the increase in HR during pregnancy several hypotheses related to hemodynamic changes and catecholamines have been put forth. Nonetheless, the exact mechanisms underlying this increase in HR and the underlying molecular mechanisms of this adaptation have been, until recently, largely unexplored. We proposed the hypothesis that pregnancy leads to an intrinsic electrophysiological remodeling of the SAN resulting in an increased automaticity. Consequently, in our previous study examining the influence of

pregnancy on the SAN, we have shown that pregnancy induces an important upregulation of the pacemaker current I_f in SAN and contributes to faster automaticity of the SAN in mice.[19] However, we now report that although block of I_f reduces AP rate, it fails to completely eliminate the increase observed in SAN cells of pregnant mice, suggesting that other mechanisms are at play and hinting a possible role for Ca^{2+} in regulating HR during pregnancy.

Accordingly, in light of the fundamental importance of Ca^{2+} in automaticity of the SAN, we sought to determine in this study the role that intracellular Ca^{2+} cycling plays in regulating HR during pregnancy. In the first objective, we aimed to determine whether pregnancy alters I_{CaT} and I_{CaL} in isolated SAN cells. We then examined the effects of pregnancy on global Ca^{2+} transient homeostasis, identifying affected Ca^{2+} handling proteins and we tested how these changes can relate to an increased HR and arrhythmia vulnerability. Finally, we also explore in this study the effects of delivery on the various pacemaking mechanisms and we show that post-partum is an important period that triggers a rapid reversal of the changes in SAN automaticity induced by pregnancy.

MATERIALS AND METHODS

Animals

This study was performed in accordance to the guidelines of the Canadian Council on Animal Care (Ottawa, ON, Canada) and the *Guide for the Care and Use of Laboratory Animals* published by the US National Institute of Health (NIH Publication No 85-23, revised 1996); the Montreal Heart Institute Animal Care Committee approved all experiments (approval reference number 2012-80-02 and 2015-80-04). Adult CD1 female non-pregnant (NP, 2-3 months old), pregnant (P, 18-19 gestation days) and post-partum (PP, 1-2 days post-delivery) mice were used for all experiments and were purchased from Charles River (St-Constant, QC, Canada).

Sinoatrial cell isolation

For several experiments, isolated mouse sinoatrial (SAN) cells were obtained using previously published protocols.[19] Briefly, mice were anaesthetized with isoflurane and killed by cervical dislocation. Hearts were rapidly excised and placed in normal HEPES-buffered Tyrode's solution gassed with 100% O_2 containing (in mM): 140 NaCl, 5.4 KCl, 1 $CaCl_2$, 1 $MgCl_2$, 5 HEPES and 5.5 glucose (pH = 7.4 with NaOH). Atrial tissue was excised, exposing the SAN. A cut, running parallel to the crista terminalis, was then performed in order to isolate the SAN. SAN pieces were rinsed twice for 4 minutes in a modified Ca^{2+}-free Tyrode's solution containing (in mM): 140 NaCl, 5.4 KCl, 0.5 $MgCl_2$, 5 HEPES, 1.2 KH_2PO_4 and 50 Taurine. (36 ± 1°C, pH = 6.9 with NaOH). The SAN tissue was then placed in the same Ca^{2+}-free Tyrode's solution supplemented with 0.1% bovine serum albumin (BSA Fraction V, Sigma, St. Louis, MO, USA), collagenase type IV (229 U/mL, Worthington, Lakewood, NJ, USA),

elastase (1.9 U/mL, Worthington), protease type XIV (0.9 U/mL, Sigma) and 200 μM $CaCl_2$ for 25-30 minutes. After the digestion period, the tissue was removed, rinsed three times and transferred into Kraft-Brühe (KB) solution containing (in mM): 100 K^+-glutamate, 110 K^+-Aspartate, 25 KCl, 10 KH_2PO_4, 2 $MgSO_4$, 20 taurine, 5 creatine, 0.5 EGTA, 5 HEPES, 0.1% BSA, and 20 glucose (36 ± 1°C, pH = 7.2 with KOH) for 4 minutes. The tissue was then gently triturated with a glass-fired Pasteur pipette for approximately 3-5 minutes until single SAN cells were obtained. The SAN cell suspension was then stored at 4°C until use. Individual mouse SAN cells were identified as small, spindle-like cells that were spontaneously beating in normal Tyrode's solution.

Electrophysiological data

Current-clamp recordings. A drop of SAN cells containing solution was placed in a recording chamber (volume 200 μL) mounted on the modified stage of an inverted microscope and superfused with a normal Tyrode's solution containing (mM): 140 NaCl, 5.4 KCl, 1.8 $CaCl_2$, 1 $MgCl_2$, 5 HEPES and 5.5 glucose (pH = 7.4 with NaOH). Bath was perfused with the solution that was continuously gassed (100% O_2) at 36 ± 1˚C. Pipettes were pulled from borosilicate glass (World Precision Instruments, Sarasota, FL, USA), and had resistance of 2-4 MΩ when filled with the following solution (mM): 100 K^+-aspartate, 30 KCl, 10 NaCl, 2 MgATP, 6.6 Na_2-phosphocreatine, 0.1 Na_2GTP, 0.04 $CaCl_2$, 1 $MgCl_2$ and 5 HEPES (pH = 7.2 with KOH).

Spontaneous AP recordings using perforated-patch clamp technique with nystatin (350 ng/mL) in current-clamp mode were obtained using the Axopatch 200B patch-clamp amplifier and digitized using Digidata 1550 (Molecular Devices, Sunnyvale, CA, USA). For some experiments, the same external solution containing ivabradine (3 μM) was perfused while

spontaneous APs were being recorded. Effects of ivabradine on a rate were assessed following a stabilization period of 3-5 minutes.

Ca^{2+} Current recordings. SAN cell suspension was placed in a recording chamber (200 μL) and perfused with external Ca^{2+} solution containing (in mM): 10 CsCl, 0.5 $MgCl_2$, 1 $CaCl_2$, 5 HEPES, 145 TEA-Cl and 5.5 glucose (pH = 7.4 with CsOH). All recordings were performed at 36 ± 1°C. Currents were recorded with borosilicate microelectrodes that had a resistance of 2-4 MΩ when filled with the following solution (in mM): 130 CsCl, 10 EGTA, 25 HEPES, 3 Mg-ATP and 0.4 Na-GTP (pH = 7.2 with CsOH). Capacitive transients, elicited by a 10 ms step of ±10 mV, were used to calculate cell capacitance and normalize current amplitudes expressed as current densities (pA/pF). Data acquisition was performed using the same Axopatch 200B patch-clamp amplifier and Digidata 1550 digitizer (Molecular Devices).

Current recording protocols and analysis. Current-voltage (I-V) relationships were all obtained in whole-cell configuration. I_{CaL} I-V curves were obtained using stimulation protocol eliciting 250 ms voltage steps in 5-10 mV increments from -50 mV to +50 mV from a holding potential of -50 mV. I_{CaT} I-V relationships curves were obtained by subtraction of I_{CaL} from total Ca^{2+} current traces ($I_{CaTotal}$). $I_{CaTotal}$ was obtained using stimulation protocols with 250 ms voltage steps from -90 to +50 in 5-10mV increments from a holding potential of -90mV. Current protocols were generated and analyzed using the Axon pCLAMP 10 electrophysiology data acquisition and analysis Software (Molecular Devices).

In vivo heart rate assessment. HRs were obtained from anesthetized NP, P and PP mice using RR intervals obtained from surface ECGs in lead I configuration. Details can be found in the online supplemental data.

Programmed in vivo electrophysiological stimulation protocols (EPS). Arrhythmia risk was assessed using EPS in anaesthetized mice (2% isoflurane). Body temperature of the mice was monitored and kept at 37°C by use of a heating pad. An octapolar electrophysiology catheter (1.9F) designed for rodent electrophysiology (Transonic Scisense Inc.) was introduced into the heart via the right jugular vein and bipolar recordings were obtained from the distal two electrode pairs. Right atrial pacing was performed by triggering a stimulus at *twice diastolic* threshold using a custom-built computer-based stimulator (509 Stimulator, Grass-Telefactor). The induction of supraventricular arrhythmias was tested using 8 consecutive burst stimulation protocols (5 s at S1S1: 50-10 ms, 10 ms stepwise reduction). Pacing stimulation duration was set at 1 ms. Arrhythmias of supraventricular type featuring rapid, irregular rhythm, lasting for at least 1s were quantified and analyzed.[20–22] All mice underwent the identical pacing stimulation protocol in the same controlled conditions.

Quantitative real-time PCR (qPCR)

RNA Extraction. Extraction of RNA and (qPCR were performed using protocols that were previously published.[19] RNA isolation was performed using the NucleoSpin RNA XS isolation kit (Macherey-Nagel, Bethlehem, PA, USA) following manufacturer instructions. RNA quantity was assessed using NanoDrop spectrophotometric analysis. Superscript™ III Reverse Transcriptase (Life Technologies, Carlsbad, CA, USA) and pdN6 non-specific primers were used to synthesize cDNA. A total of 5-6 SANs were used for each sample to isolate RNA from NP, P and PP mice.

Quantitative PCR. Primers for $Ca_V1.2$, $Ca_V1.3$ and $Ca_V3.1$, RyR2, SERCA2a, PLB and NCX1 were designed and sequences are presented in the data supplemental. PCR reactions were performed with a three steps cycle of denaturation (95^{o}C for 30s), annealing (55^{o}C for 60s) and elongation (72^{o}C for 60s). Quantitative PCR was performed using Platinum SYBR Green qPCR Supermix (Life Technologies) and a real-time PCR system (MX3005P qPCR, Agilent technologies, Mississauga, ON, Canada). In all experiments, quantitative analysis was performed in triplicate and the geometric mean of three housekeeping genes (18S, succinate dehydrogenase complex subunit A (SDHA) and hypoxanthine-guanine phosphoribosyltransferase (HPRT)) was used for normalization. Expression data were obtained following the $2^{-\Delta\Delta Ct}$ method.

Calcium Transients

Spontaneous Ca^{2+} transients were obtained using adaptation of previously published protocol.[23] Briefly, isolated SAN cells loaded for 20 min with 5 μM of Fluo-4 AM (Molecular

Probes) were placed in a bath perfused with 36°C Tyrode's solution and mounted on a Zeiss LSM 710 confocal microscope. Following a washout period, spontaneous activity was observed and transients were recorded by live imaging. Following a 10-second recording of spontaneous transients, a 10 mM caffeine solution was applied to the SAN cell via a precision perfusion stylus in the bath to evoke large SR Ca^{2+} release. Spontaneous and caffeine transients were then analyzed using ImageJ software and various transient parameters were calculated by adapting formulas from previously published studies.[24] Specifically, we reported rate of spontaneous release, time-to-peak, Ca^{2+} transient amplitude $(F-F_0)/F_0$, time to 90% decay as well as SR fractional release, defined as ratio of spontaneous transient to caffeine-induced transient $(F-F_0)/F_0$ transient / $(F-F_0)/F_0$ caffeine).

Chemicals

All chemicals were purchased from Sigma-Aldrich, unless otherwise stated. Fluo-4 AM and nystatin were first dissolved in anhydrous DMSO.

Statistical analysis

Analyses were performed with Origin 8.0 (OriginLab, MA, USA). The value of 'n' represents the number of cells or experiments and 'N' the number of mice. All data are presented as mean ± SEM. Data were compared using unpaired t-test or one-way ANOVA with Tukey or Fisher LSD post-hoc comparison where appropriate. p-values <0.05 were considered significantly different.

RESULTS

Pregnancy accelerates action potential frequency

We have previously reported that upregulation of I_f during pregnancy contributes to an acceleration of spontaneous action potential (AP) firing rate in isolated SAN cells.[19] In order to determine the functional impact of I_f on pacing frequency of SAN cells, we applied the specific HCN channel blocker ivabradine. Results presented on Figure 1 show that ivabradine reduced AP pacing rate in both P and NP mice, however, the reduction in pacing rate was significantly larger in NP group. Since AP frequency is higher in P group[19] and was reduced to a lesser extent by ivabradine application, we conclude that when I_f is blocked, cardiac automaticity is still faster in P mice suggesting that mechanisms other than I_f are playing an important role in the pregnancy-induced enhanced automaticity. Considering Ca^{2+} homeostasis is a fundamental mechanism of pacemaking in the SAN, we devised accordingly the next series of experiments to determine the role of Ca^{2+} currents and Ca^{2+} handling function in contributing to the increased SAN automaticity and consequent acceleration of HR during pregnancy.

Influence of pregnancy on Ca^{2+} currents

As previously stated, Ca^{2+} currents play an important role in the late diastolic depolarization phase of the sinoatrial node AP, thereby contributing to automaticity of the heart. To determine if pregnancy resulted in any change in Ca^{2+} current density, I_{CaL} and I_{CaT} from P and NP isolated SAN myocytes were recorded and compared. The typical recordings and I-V curves on Figure 2A and B respectively, show that peak I_{CaL} was significantly increased in SAN cells from P compared to NP mice (at -10 mV in pA/pF, NP: -5.3 ± 0.3, P: -7.5 ± 0.5,

*p<0.01). On the other hand, I_{CaT}, which was obtained through subtraction of I_{CaL} from total Ca^{2+} currents, remained comparable between the two groups (Figure 2C and D). Furthermore, we subsequently measured I_{CaL} in post-partum (PP) mice in order to determine whether delivery would reverse the increase in current density. Recordings on Figure 2A and the mean I-V curve (Figure 2B) demonstrate comparable current densities between the PP and the NP group. Overall, the voltage-clamp data show that pregnancy specifically increases L-type Ca^{2+} current in the SAN, making it a likely contributor to faster automaticity of the SAN during pregnancy. In addition, this upregulation was completely reversible 24h following delivery, returning to NP values.

Transcriptional upregulation of L-type Ca^{2+} channels by pregnancy

In the following set of experiments mRNA expression of Ca^{2+} channel α-subunits in whole SAN tissue was evaluated. Specifically, we examined the two isoforms of L-type Ca^{2+} channels ($Ca_V1.2$ and $Ca_V1.3$) as well as the major isoform of T-type Ca^{2+} channels $Ca_V3.1$. Results shown on Figure 3 indicate that mRNA expression of $Ca_V1.3$ but not $Ca_V1.2$ was significantly increased in the P group compared to NP. Congruent to the previous voltage-clamp data on I_{CaT}, mRNA abundance of $Ca_V3.1$ was not affected by pregnancy (Figure 3) thereby indicating that pregnancy induces a selective transcriptional upregulation of $Ca_V1.3$ leading to increased I_{CaL} in the SAN. Interestingly, qPCR analysis in PP mice (Figure 3) also reveals that following delivery $Ca_V1.3$ expression reverts to NP levels indicating, in clear concordance with the voltage-clamp data, a key role of pregnancy in transcriptionally regulating $Ca_V1.3$ L-type Ca^{2+} channels in the SAN.

Pregnancy accelerates spontaneous Ca^{2+} transient rate

Following these observations we sought next to determine whether pregnancy altered intracellular SAN Ca^{2+} handling. Using SAN cells isolated from P, NP and PP mice that were loaded with the Ca^{2+} probe Fluo-4AM, we examined spontaneous Ca^{2+} transients in the various groups. Data in Figure 4 shows that the rate of spontaneous transients in SAN cells from P mice were significantly increased (19%). Furthermore, there was a decrease in the Ca^{2+} transient time-to-peak and time to 90% decay in the P group (Figure 4). The results also show that these adaptations, specifically, rate and time-to-peak but not the time to 90% decay were also reversed in the PP group highlighting yet again the specific effect of pregnancy in regulating Ca^{2+} homeostasis. The PP group also showed a tendency for higher spontaneous Ca^{2+} transient amplitude ($(F-F_0)/F_0$) although it did not reach statistical significance. Of note, similarly to the time-to-peak parameter during spontaneous pacing, it was found that in the P group the time-to-peak in the caffeine-induced transient was also smaller and caffeine-induced Ca^{2+} transient amplitude in the PP group became significantly different from NP and P groups (Figure 5). Furthermore, data on Figure 5 shows no changes in fractional release or time to 90% decay. Thus, these data indicate that pregnancy results in changes in multiple Ca^{2+} handling parameters notably, a faster Ca^{2+} transient rate associated to a faster SR- Ca^{2+}content release.

Influence of pregnancy on Ca^{2+} handling proteins gene expression

In order to determine the molecular mechanisms responsible for the increase in Ca^{2+} transient rate during pregnancy we conducted qPCR experiments on isolated SAN tissues from the various groups. The mRNA levels of the major Ca^{2+} handling proteins expressed in mouse

SAN were analyzed to determine which components were altered. Figure 6 shows that while mRNA expression of NCX1, SERCA2a and PLB were all unaffected by pregnancy, expression of RyR2 was significantly increased in SAN from P mice compared to NP mice. In addition, we noted that the effects of pregnancy on increased RyR2 expression were also reversed to pre-pregnancy levels following delivery while all the other examined genes remained stable in PP mice (Figure 6). Taken together, the findings of the last experiments suggest that pregnancy enhances the rate of SR Ca^{2+} release as indicated by the smaller time-to-peak values through a transcriptional upregulation of RyR2 in the SAN. The faster time to 90% decay was not associated with transcriptional upregulation of SERCA2a nor PLB in the P group indicates that the pump is most likely functionally modulated through second messengers.

Cellular and *in vivo* electrophysiological studies

In order to evaluate how the cellular and molecular changes observed thus far translated functionally we started by comparing heart rates between NP, P and PP mice. The *in vivo* HR analysis by ECG measurements shown on Figure 7A revealed that P mice had a significantly higher HR compared to the NP, consistent with our previous study. Furthermore, we report that the PP had HR values comparable to the NP, indicating a return to baseline rates shortly after delivery. Interestingly, a similar observation was made on the cellular level. When AP frequency of isolated SAN cells were measured, as expected P group had the highest frequency and 24h following delivery there was a rapid reversal in automaticity of the SAN as seen by the slower AP frequency in PP that was comparable to the NP group (Figure 7B; in bpm, NP: 292 ± 13, n=17; P: 330 ± 12*, n=12; PP: 306 ± 27, n=7, *$p<0.05$ vs NP and PP).

Furthermore, following the ECG measurements, programmed *in vivo* electrophysiological stimulations were used to determine whether the increase in SAN automaticity we observed in P mice might contribute to an increased arrhythmia risk, a well observed phenomenon in pregnant women. Our *in vivo* EPS data on Figure 7C shows that the probability of inducing a sustained supraventricular arrhythmia, expressed as incidence of arrhythmia, was increased by ~50% in P mice compared to NP. Data also shows that arrhythmia risk in PP mice was reduced, indicating that the near complete reversal in the increased SAN automaticity mechanisms and HR translated into reversal to baseline arrhythmia inducibility (Figure 7C). Collectively, results from this set of experiments indicate that pregnancy induces changes in several Ca^{2+} handling parameters that result in faster SAN automaticity and HR that are associated with significant increase in the risk of arrhythmias and remarkably these parameters were reversed within 24h following delivery.

DISCUSSION

During pregnancy, cardiac remodeling is considered an essential physiological adaptation that helps provide adequate delivery of nutrients and oxygen to the growing fetus.[2] Along with the structural changes such as hypertrophy, there is an up to 25% increase in resting HR,[25] indicating that effects of pregnancy also extend to electrophysiological parameters. While investigating these changes, we have previously found that the increase in HR in pregnant mice was independent of changes in autonomic tone, blood pressure or circulating catecholamines and was instead attributable to cardiac electrical remodeling. Specifically, we showed that there was a significant increase in the density and expression of the pacemaker current I_f that was associated with faster automaticity of the SAN[15]. In the present study, we show that blockade of I_f, using the selective HCN channel blocker ivabradine, affected differently P and NP mice. Indeed, while the SAN cells firing frequency was reduced in both groups, P mice had a rate that remained significantly higher after application of ivabradine, indicating that pacemaking mechanisms other that I_f are contributing to HR control during pregnancy and sustaining elevated rates. We report here that Ca^{2+} homeostasis is also regulated to support an accelerated HR. Our data shows that, in the SAN, pregnancy induces a transcriptional upregulation of $Ca_V1.3$ and RyR2 channels. This upregulation resulted in an increase in I_{CaL} current along with a faster Ca^{2+} extrusion from the SR measured during spontaneous and caffeine-induced Ca^{2+} transients. This increase in both $Ca_V1.3$ and RyR2 may be critical to sustain the faster HR by allowing a quicker spontaneous transient rate through accelerated Ca^{2+} entry and subsequent intracellular Ca^{2+} release. Interestingly, in the SAN of pregnant mice, there was no increase in $Ca_V1.2$ and the L-type Ca^{2+} current peaked at a relatively hyperpolarized -10 mV, consistent with the greater role for $Ca_V1.3$ in the SAN.

Indeed, as previously reported $Ca_V1.3$ constitutes the major L-type Ca^{2+} channel isoform in the mouse SAN and in support of this observation, recent studies have shown that deletion of $Ca_V1.3$ in the SAN results in bradycardia and dysrhythmic SAN pacemaking. Furthermore, $Ca_V1.3$ was demonstrated to play a critical role in modulating intracellular Ca^{2+} dynamics by regulating Ca^{2+} release from the SR.[26–28] Since it was shown that $Ca_V1.3$ deletion resulted in an inhibition of Ca^{2+} transients, it is very likely that the increase in $Ca_V1.3$ we observed here, along with the increase in RyR2, serves the opposite purpose: increasing Ca^{2+} transient rate and robustness of the $Ca_V1.3$/RyR2 coupling, thereby sustaining the elevated HR during pregnancy. Interestingly, this upregulation in the molecular underpinnings of HR control occurs early on in pregnancy. In women, the increase in HR is observed as early as 12 weeks,[29,30] while we previously reported an increase in HR in pregnant mice at earlier pregnancy days (12-13).[19] The mechanisms behind these rapid changes remain to be examined however, pregnancy is a time during which important fluctuations in hormonal levels occur, including changes in estrogen, progesterone, thyroid and relaxin which might contribute to the electrophysiological remodeling.[19] In support of this notion, it was previously shown that increased levels of 17β-estradiol can upregulate various ion channels including L-type Ca^{2+} channels in the ventricle and other cell types.[31–33] Additionally, in the SAN, relaxin was shown to cause rapid increases in pacemaking rate attributable to an increase in Ca^{2+} current[34], while thyroid hormone has also been known for many years to have a role in regulating cardiac ion channels.[35–37]

It is noteworthy to mention that the substantial fluctuations in the levels of these hormones that take place in various phases of pregnancy, such as during early, late pregnancy and the

early postpartum period, coincide with important changes in cardiac automaticity. For instance, following delivery, there is a sharp drop in estrogen and progesterone levels and pre-pregnancy HR level is restored within the first two weeks.[1] In this study, we also report a novel finding that HR in pregnant mice reverts to control values as early as 24h following delivery. The reversal in HR was also observed at the cellular and molecular level of the SAN with a return of Ca^{2+} current density to control levels and a normalization of transient rate, $Ca_V1.3$ and RyR2 expression levels. Of note, time to 90% decay in the PP group remained lower indicating that SERCA2a activity is still high. Since transcriptionally, SECRA2a and PLB were not affected, it appears that the functional modulation of SERCA2a requires more than 24h to revert to baseline function. Interestingly, we also examined the pacemaker current I_f in PP mice, and we found that its density also reverted to pre-pregnancy values, becoming comparable to that of control recordings we previously obtained (Supplemental Figure 1).[19] This rapid reversal of electrophysiological and several critical Ca^{2+} handling parameters to baseline levels would be therefore consistent with a hormonal effect on ion channels during pregnancy.

Understanding the mechanisms underlying the electrophysiological changes during pregnancy is becoming increasingly important. Indeed, as the average maternal age and proportion of pregnant women suffering from comorbidities including diabetes, hypertension and various cardiovascular conditions increase,[38,39] pregnancy-related complications and mortality are becoming complex issues requiring fundamental understanding of their underlying mechanisms. For instance, as previously noted, the increase in HR is a known risk factor for arrhythmias and during pregnancy there is a significant increase in the risk of electrical

disturbances notably supraventricular and sinus node arrhythmias, comprising more than 70% of total arrhythmia occurrences.[40] While changes in sympathetic tone, hormones and stress have been thought to contribute to the increased arrhythmia susceptibility,[39] little mechanistic evidence has been proposed. In our study and previous report[19] we showed that the HR during pregnancy increases due to major electrophysiological remodelling of the SAN. Furthermore, we showed that the murine model of pregnancy was also associated with an increased risk of arrhythmias and although it was previously demonstrated that reversal of structural changes is relatively slow, the modifications in electrophysiological parameters we observed were rapidly reversed following delivery, similarly to women. These observations are consistent with the idea that electrophysiological changes due to direct regulation of ion channels and not cardiac structural remodeling are a major cause of arrhythmic events. In further support to this notion, it was previously reported that the increase in HR during pregnancy is protective in women with long QT syndrome and is associated with lower arrhythmia risk. However, in postpartum women, with the reduction of HR comes a loss of the protective effect of pregnancy and a significant increase in arrhythmia susceptibility and torsades de pointes.[41]

CONCLUSION

In conclusion, our study highlights an important role for pregnancy in regulating SAN function and pacemaking. Specifically, we demonstrated a major role for Ca^{2+} homeostasis, as well as pacemaker current, in the increased HR during pregnancy. This illustrates a notable case where key players in the SAN Ca^{2+} and voltage clocks are mutually entrained and regulated. These findings also portray the SAN as a dynamic pacemaker that can intrinsically and rapidly adjust to changing physiological requirements as witnessed by the rapid reversal

of pacemaking function following delivery. In conclusion, understanding the cellular and molecular mechanisms that drive the SAN, HR control and arrhythmias during pregnancy is essential not only for expanding our knowledge of the regulatory pathways within the SAN but also for appropriate management of pregnant women and a step forward in progressing women's health.

ACKNOWLEDGMENTS

The authors wish to express their thanks to Dr. Sophie Mathieu, Dr. Philippe Comtois, Marc-Antoine Gillis, and Louis Villeneuve for expert technical assistance as well as Charlotte Guinard and Gabriella Broncheva for assistance with the calcium transient and *in vivo* electrophysiology experiments.

FUNDING SOURCES

This study was supported by an operating grant from the Heart and Stroke Foundation of Canada. El Khoury N. holds a PhD student scholarship from the Fonds de Recherche du Québec en Santé (FRQS).

DISCLOSURES

None

REFERENCES

1. Melchiorre K, Sharma R, Thilaganathan B. Cardiac structure and function in normal pregnancy. *Curr Opin Obstet Gynecol*. 2012;24:413–421.

2. Hunter S, Robson SC. Adaptation of the maternal heart in pregnancy. *Br Heart J*. 1992;68:540–543.

3. Thornburg KL, Jacobson SL, Giraud GD, Morton MJ. Hemodynamic changes in pregnancy. *Semin Perinatol*. 2000;24:11–14.

4. Larsen JA, Kadish AH. Effects of gender on cardiac arrhythmias. *J Cardiovasc Electrophysiol*. 1998;9:655–664.

5. Wolbrette D. Treatment of arrhythmias during pregnancy. *Curr Womens Health Rep*. 2003;3:135–139.

6. Gowda RM, Khan IA, Mehta NJ, Vasavada BC, Sacchi TJ. Cardiac arrhythmias in pregnancy: clinical and therapeutic considerations. *Int J Cardiol*. 2003;88:129–133.

7. Adamson DL, Nelson-Piercy C. Managing palpitations and arrhythmias during pregnancy. *Heart*. 2007;93:1630–1636.

8. Irisawa H, Brown HF, Giles W. Cardiac pacemaking in the sinoatrial node. *Physiol Rev*. 1993;73:197–227.

9. Mangoni ME, Nargeot J. Genesis and Regulation of the Heart Automaticity. *Physiol Rev*. 2008;88:919–982.

10. DiFrancesco D, Ferroni A, Mazzanti M, Tromba C. Properties of the hyperpolarizing-activated current (if) in cells isolated from the rabbit sino-atrial node. *J Physiol*. 1986;377:61–88.

11. Imtiaz MS, von der Weid PY, Laver DR, van Helden DF. SR Ca^{2+} store refill--a key factor in cardiac pacemaking. *J Mol Cell Cardiol*. 2010;49:412–426.

12. Lakatta EG, DiFrancesco D. What keeps us ticking: a funny current, a calcium clock, or both? *J Mol Cell Cardiol*. 2009;47:157–170.

13. Lakatta EG, Maltsev VA, Vinogradova TM. A Coupled SYSTEM of Intracellular Ca^{2+} Clocks and Surface Membrane Voltage Clocks Controls the Timekeeping Mechanism of the Heart' Pacemaker. *Circ Res*. 2010;106:659–673.

14. Gao Z, Chen B, Joiner M ling, Wu Y, Guan X, Koval OM, Chaudhary AK, Cunha SR, Mohler PJ, Martins JB, Song L sheng, Anderson ME. If and SR Ca^{2+} release both contribute to pacemaker activity in canine sinoatrial node cells. *J Mol Cell Cardiol*. 2010;49:33–40.

15. Sirenko SG, Maltsev VA, Yaniv Y, Bychkov R, Yaeger D, Vinogradova T, Spurgeon HA, Lakatta EG. Electrochemical Na^{+} and Ca^{2+} gradients drive coupled-clock regulation of automaticity of isolated rabbit sinoatrial nodal pacemaker cells. *Am J Physiol Heart Circ Physiol*. 2016;311:H251–H267.

16. Yaniv Y, Lakatta EG, Maltsev VA. From two competing oscillators to one coupled-clock pacemaker cell system. *Front Physiol*. 2015;6:28.

17. Vinogradova TM, Zhou YY, Maltsev V, Lyashkov A, Stern M, Lakatta EG. Rhythmic Ryanodine Receptor Ca^{2+} Releases During Diastolic Depolarization of Sinoatrial Pacemaker Cells Do Not Require Membrane Depolarization. *Circ Res*. 2004;94:802–809.

18. Vinogradova TM, Lyashkov AE, Zhu W, Ruknudin AM, Sirenko S, Yang D, Deo S, Barlow M, Johnson S, Caffrey JL, Zhou YY, Xiao RP, Cheng H, Stern MD, Maltsev VA, Lakatta EG. High basal protein kinase A-dependent phosphorylation drives rhythmic internal Ca^{2+} store oscillations and spontaneous beating of cardiac pacemaker cells. *Circ Res*. 2006;98:505–514.

19. El Khoury N, Mathieu S, Marger L, Ross J, El Gebeily G, Ethier N, Fiset C. Upregulation of the hyperpolarization-activated current increases pacemaker activity of the sinoatrial node and heart rate during pregnancy in mice. *Circulation*. 2013;127:2009–2020.

20. Stockigt F, Brixius K, Lickfett L, Andrie R, Linhart M, Nickenig G, Schrickel JW. Total beta-adrenoceptor knockout slows conduction and reduces inducible arrhythmias in the mouse heart. *PLoS One*. 2012;7:e49203.

21. Schrickel JW, Bielik H, Yang A, Schimpf R, Shlevkov N, Burkhardt D, Meyer R, Grohe C, Fink K, Tiemann K, Luderitz B, Lewalter T. Induction of atrial fibrillation in mice by rapid transesophageal atrial pacing. *Basic Res Cardiol*. 2002;97:452–460.

22. Schrickel JW, Brixius K, Herr C, Clemen CS, Sasse P, Reetz K, Grohe C, Meyer R, Tiemann K, Schroder R, Bloch W, Nickenig G, Fleischmann BK, Noegel AA, Schwinger

RH, Lewalter T. Enhanced heterogeneity of myocardial conduction and severe cardiac electrical instability in annexin A7-deficient mice. *Cardiovasc Res*. 2007;76:257–268.

23. Rivard K, Grandy SA, Douillette A, Paradis P, Nemer M, Allen BG, Fiset C. Overexpression of type 1 angiotensin II receptors impairs excitation-contraction coupling in the mouse heart. *Am J Physiol Heart Circ Physiol*. 2011;301:H2018–H2027.

24. Fares E, Pyle WG, Ray G, Rose RA, Denovan-Wright EM, Chen RP, Howlett SE. The impact of ovariectomy on calcium homeostasis and myofilament calcium sensitivity in the aging mouse heart. *PLoS One*. 2013;8:e74719.

25. Clapp JF, Capeless E. Cardiovascular Function Before, During, and After the First and Subsequent Pregnancies. *Am J Cardiol*. 1997;80:1469–1473.

26. Mangoni ME, Couette B, Bourinet E, Platzer J, Reimer D, Striessnig J, Nargeot J. Functional role of L-type Cav1.3 Ca^{2+} channels in cardiac pacemaker activity. *Proc Natl Acad Sci U A*. 2003;100:5543–5548.

27. Torrente AG, Mesirca P, Neco P, Rizzetto R, Dubel S, Barrere C, Sinegger-Brauns M, Striessnig J, Richard S, Nargeot J, Gomez AM, Mangoni ME. L-type Cav1.3 channels regulate ryanodine receptor-dependent Ca^{2+} release during sino-atrial node pacemaker activity. *Cardiovasc Res*. 2016;109:451–461.

28. Mesirca P, Bidaud I, Mangoni ME. Rescuing cardiac automaticity in L-type Cav1.3 channelopathies and beyond. *J Physiol*. 2016;594: 5869–5879.

29. Atkins AF, Watt JM, Milan P, Davies P, Crawford JS. A longitudinal study of cardiovascular dynamic changes throughout pregnancy. *Eur J Obstet Gynecol Reprod Biol*. 1981;12:215–224.

30. Carruth JE, Mivis SB, Brogan DR, Wenger NK. The electrocardiogram in normal pregnancy. *Am Heart J*. 1981;102:1075–1078.

31. Yang X, Chen G, Papp R, DeFranco DB, Zeng F, Salama G. Oestrogen upregulates L-type Ca^{2+} channels via oestrogen-receptor-a by a regional genomic mechanism in female rabbit hearts. *J Physiol*. 2012;590:493–508.

32. Song M, Helguera G, Eghbali M, Zhu N, Zarei MM, Olcese R, Toro L, Stefani E. Remodeling of Kv4.3 potassium channel gene expression under the control of sex hormones. *J Biol Chem*. 2001;276:31883–31890.

33. Bosch MA, Tonsfeldt KJ, Ronnekleiv OK. mRNA expression of ion channels in GnRH neurons: Subtype-specific regulation by 17b-estradiol. *Mol Cell Endocrinol*. 2013;10:85–97.

34. Han X, Habuchi Y, Giles WR. Relaxin increases heart rate by modulating calcium current in cardiac pacemaker cells. *Circ Res*. 1994;74:537–541.

35. Rajagopalan V, Gerdes AM. Role of thyroid hormones in ventricular remodeling. *Curr Heart Fail Rep*. 2015;12:141–149.

36. Dillmann WH. Cellular action of thyroid hormone on the heart. *Thyroid*. 2002;12:447–452.

37. Shimoni Y, Fiset C, Clark RB, Dixon JE, McKinnon D, Giles WR. Thyroid hormone regulates postnatal expression of transient K+ channel isoforms in rat ventricle. *J Physiol*. 1997;500.1:65–73.

38. Berg CJ, Callaghan WM, Syverson C, Henderson Z. Pregnancy-related mortality in the United States, 1998 to 2005. *Obstet Gynecol*. 2010;116:1302–1309.

39. Page RL, Hamdan MH, Joglar JA. Arrhythmias occurring during pregnancy. *Card Electrophysiol Rev*. 2002;6:136–139.

40. Li JM, Nguyen C, Joglar JA, Hamdan MH, Page RL. Frequency and outcome of arrhythmias complicating admission during pregnancy: experience from a high-volume and ethnically-diverse obstetric service. *Clin Cardiol*. 2008;31:538–541.

41. Rashba EJ, Zareba W, Moss AJ, Hall WJ, Robinson J, Locati EH, Schwartz PJ, Andrews M. Influence of pregnancy on the risk for cardiac events in patients with hereditary long QT syndrome. LQTS Investigators. *Circulation*. 1998;97:451–456.

DATA SUPPLEMEMENT

SUPPLEMENTAL FIGURE 1

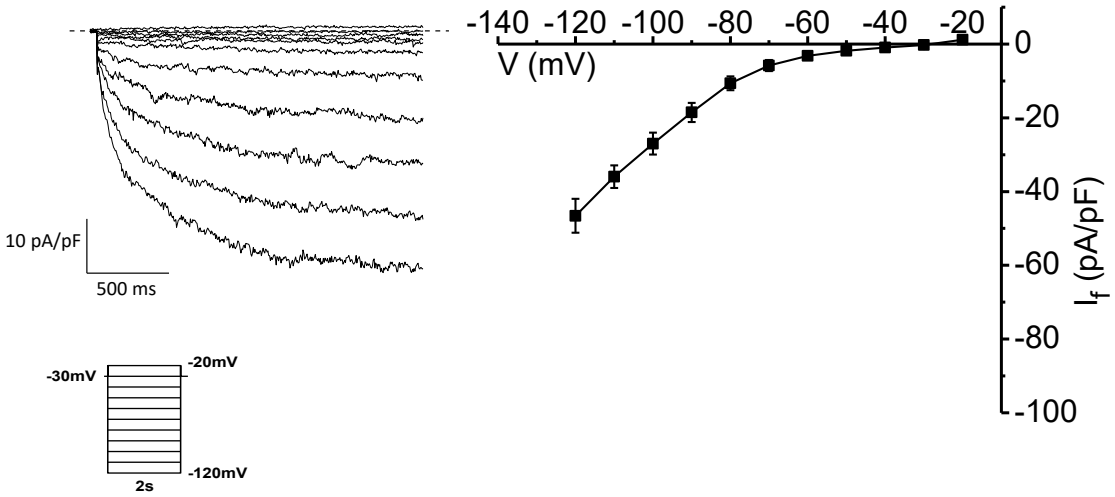

Supplemental Figure 1. **I_f current in SAN cells of post-partum CD-1 mice:** Left panel; Typical example of I_f current recorded in whole-cell configuration in SAN cells isolated from PP mice. Insets depict recording protocol. Right panel; Mean data for the current-voltage (I-V) relationship for I_f in SAN cells from PP (n=7, N=6) mice shows current densities that are similar to previously obtained values from control mice.[3]

SUPPLEMENTAL MATERIAL AND METHODS

Surface electrocardiograms (ECG)

Surface electrocardiograms were performed in order to determine heart rate. Mice were anaesthetized with 2% isoflurane. Body temperature was maintained at 37°C using a heating pad. Platinum electrodes positioned subcutaneously were connected to a Biopac System MP100 (EMKA Technologies, France). Surface ECGs were recorded in lead I configuration at a rate of 2 kHz and performed for 5 minutes of continuous experimental recording at the end of a baseline period. The signal was filtered at 100Hz (low pass) and 60kHz (notch filter). Data were analyzed using ECG-auto 1.7 (EMKA Technologies). RR intervals were calculated manually by a blinded observer from signal averaged ECG recordings (500-1000 cardiac cycles).

Real time RT-PCR

Total RNA extraction and real-time PCR (qPCR) for the Ca^{2+} handling channels were conducted using adaptation of previously published protocols.[1,2] For each sample, 5-6 SANs were pooled and used to isolate total RNA from NP, P and PP mice. Total RNA was isolated using TriReagent® and treated with DNase I as previously described.[3] cDNA was then synthesized with SuperScript™ III Reverse Transcriptase (Life Technologies) using pdN6 random primers. Gene-specific primers and conditions for PCR reactions were used for the genes figuring in table below. The qPCR was performed with Platinum SYBR Green qPCR Supermix (Life Technologies) using a real-time PCR system (MX3005P QPCR system, Stratagene). Quantitative measurements were performed in triplicate and normalized to the

average of three housekeeping genes (18S, hypoxanthine-guanine phosphoribosyltransferase (HPRT), and succinate dehydrogenase complex subunit A (SDHA)).

Table 1. Primer List

Primers	**Sequences**
$Ca_v1.2$	Forward: 5'ACAACCTGGCTGATGCGGA3' Reverse: 5'TCACTGGGCTGGAGGTCATC3'
$Ca_v1.3$	Forward: 5'TCCGAAGAGCCTGCATTAGT3' Reverse: 5'ATGCAGCAACAGTCCATACG3'
$Ca_v3.1$	Forward: 5'GTCTCCGCACGGTCTGTAAC3' Reverse: 5' CCACAGCAAAGAAAGGCAAAG3'
RyR2	Forward: 5'CATGAGAATGCTGGCCTTGT3' Reverse: 5'TAGCAGTATCGCTGGAGGTT3'
SERCA2a	Forward: 5'GTCCTGGCAGATGACAACTT3' Reverse: 5'ATGTCCAGGTCTGGAGGATT3'
PLB	Forward: 5'TCTCCCTACTTTTGCCTTCCTG3' Reverse: 5'GATGCAGATCAGCAGCAGACATA3'
NCX1	Forward: 5'AGAGGAGGAGAGGCGCATTG3' Reverse: 5'CGCTGACAGTGATGGCTTCG3'
HPRT	Forward: 5'TGAATCACGTTTGTGTCATTAGTGA3' Reverse: 5'TTCAACTTGCGCTCATCTTAGG3'
18s	Forward: 5'TTGACGGAAGGGCACCACCAG3' Reverse: 5'GCACCACCACCCACGGAATCG3'
SDHA	Forward: 5'GAGGAAGCACACCCTCTCATA3' Reverse: 5'GCACAGTCAGCCTCATTCAA3'

References

1. Rivard K, Grandy SA, Douillette A, Paradis P, Nemer M, Allen BG, Fiset C. Overexpression of type 1 angiotensin II receptors impairs excitation-contraction coupling in the mouse heart. *Am J Physiol Heart Circ Physiol*. 2011;301:H2018–H2027.

2. Marionneau C, Couette B, Liu J, Li H, Mangoni ME, Nargeot J, Lei M, Escande D, Demolombe S. Specific pattern of ionic channel gene expression associated with pacemaker activity in the mouse heart. *J Physiol*. 2005;562:223–234.

3. El Khoury N, Mathieu S, Marger L, Ross J, El Gebeily G, Ethier N, Fiset C. Upregulation of the hyperpolarization-activated current increases pacemaker activity of the sinoatrial node and heart rate during pregnancy in mice. *Circulation*. 2013;127:2009–2020.

FIGURES

Figure 1

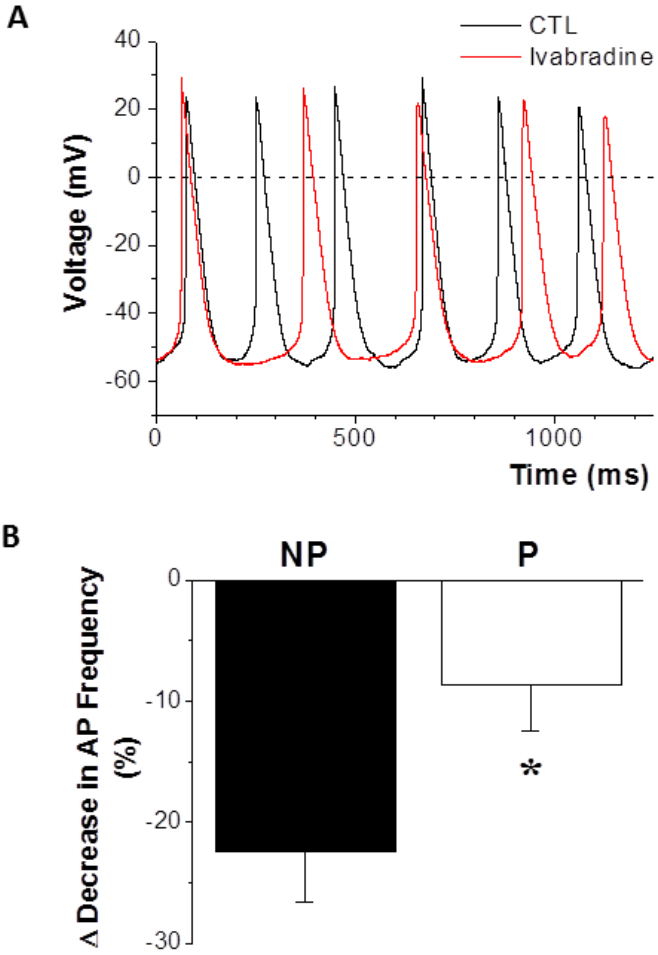

Figure 1. Ivabradine differentially reduces AP frequency in isolated SAN cells. A. The effects of ivabradine (3 μM) on AP frequency are shown for SAN cells isolated from NP mice. **B.** Mean Δ decrease in frequency was obtained by averaging the Δ frequencies from individual cells before and after application of ivabradine to SAN cells from NP and P (NP: n=7, N=3; P: n=6, N=3) (* $p<0.05$). Recordings were all obtained by whole-cell perforated current-clamp technique and a t-test on log transformed values of Δ change was performed.

Figure 2

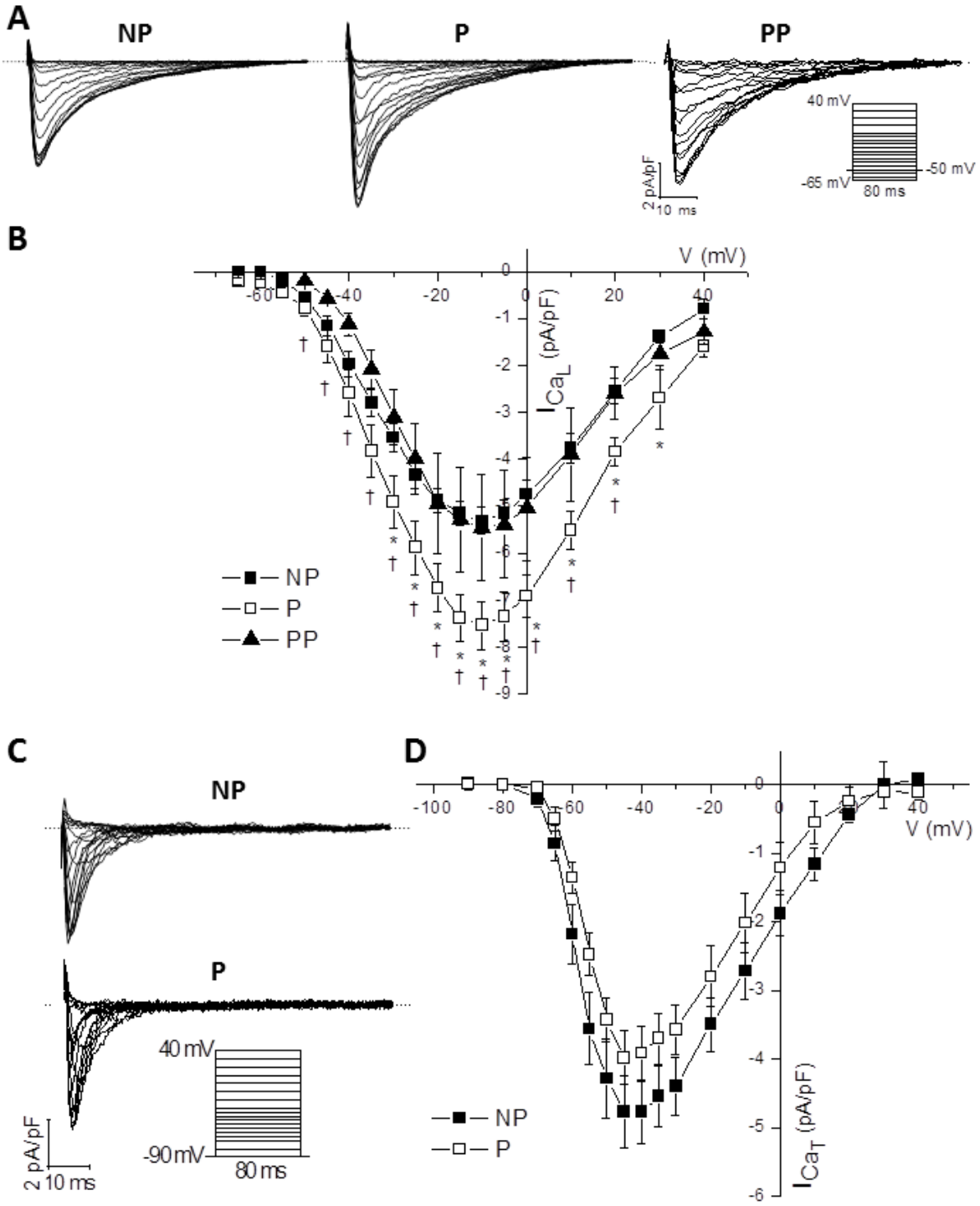
A
NP
P
PP
40 mV
-50 mV
-65 mV
80 ms
2 pA/pF
10 ms
B
V (mV)
I_{Ca_L} (pA/pF)
NP
P
PP
C
NP
P
40 mV
-90 mV
80 ms
2 pA/pF
10 ms
D
V (mV)
I_{Ca_T} (pA/pF)
NP
P

Figure 2. Pregnancy selectively increases L-type Ca^{2+} currents in isolated SAN cells. A. Typical I_{CaL} traces recorded from SAN cells of NP, P and PP mice (*inset shows protocol*). **B.** Mean data for the I-V relationship for I_{CaL} in SAN cells from P (n=11, N=9) mice show increased current density compared to NP (n=12, N=9) and PP mice (n=8, N=2) (*p<0.05 vs NP; †p<0.05 vs PP, ANOVA with Fisher LSD post-hoc test). **C.** Representative examples of T-type Ca^{2+} currents (I_{CaT}) traces recorded from SAN cells of NP and P mice were determined by subtracting I_{CaL} from the total Ca^{2+} current trace for each cell. **D.** Mean I-V relationship data from I_{CaT} recordings show no effect of pregnancy on current density (NP: n=12, N=7; P: n=11, N=6).

Figure 3

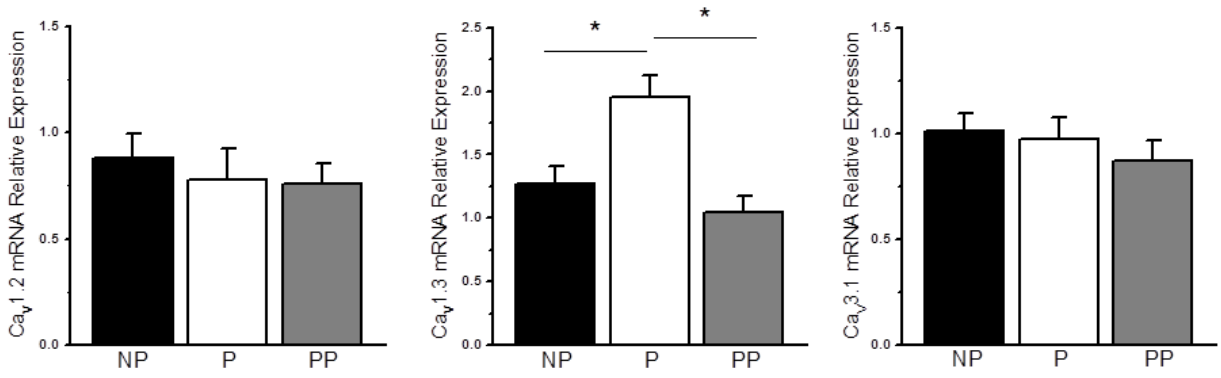

Figure 3. qPCR analysis of Ca^{2+} channel isoforms from isolated SAN shows a selective increase in $Ca_V1.3$ mRNA expression in the pregnant mice.

Mean qPCR results showing relative mRNA expression of $Ca_V1.2$ (*left*) and $Ca_V1.3$ (*middle*) in SAN from NP, P and PP mice (*p<0.05). While $Ca_V1.2$ is unchanged, pregnancy significantly increases mRNA expression of $Ca_V1.3$. *Right*- Consistent with voltage-clamp data, mRNA expression results show that α subunit of T-type Ca^{2+} channel $Ca_V3.1$ is unaffected by pregnancy (n=3, N=5-6 SAN per sample, analyzed in triplicate, ANOVA with Tukey post-hoc test).

Figure 4

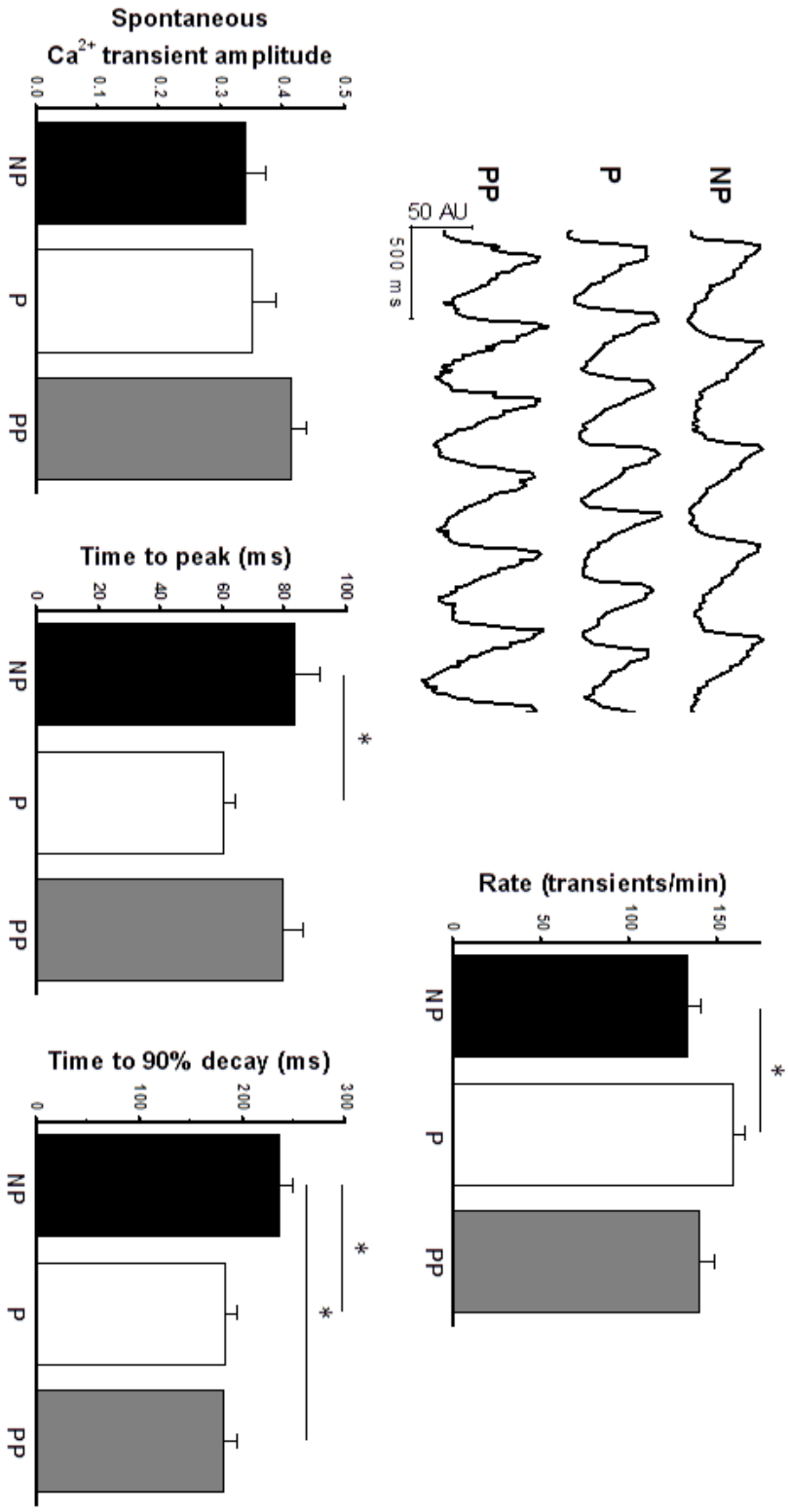
NP
P
PP
50 AU
500 ms
Rate (transients/min)
0
50
100
150
*
Spontaneous
Ca2+ transient amplitude
0.0
0.1
0.2
0.3
0.4
0.5
Time to peak (ms)
0
20
40
60
80
100
Time to 90% decay (ms)
0
100
200
300
*

Figure 4. Spontaneous Ca^{2+} transient parameters obtained from NP, P and PP mice.

Top left panel shows typical examples of spontaneous Ca^{2+} transients recorded by confocal microscopy that were obtained from individual SAN cells loaded with Fluo-4AM and beating spontaneously. Mean data for computed parameters from spontaneous Ca^{2+} transient recordings include transient rate, spontaneous Ca^{2+} transient amplitude ($(F-F_0)/F_0$), time-to-peak and time to 90% decay are shown for NP (n=16-17, N=6), P (n=16-18, N=7) and PP (n=14-16, N=6-7) groups (*$p<0.05$, ANOVA with Tukey post-hoc test).

Figure 5

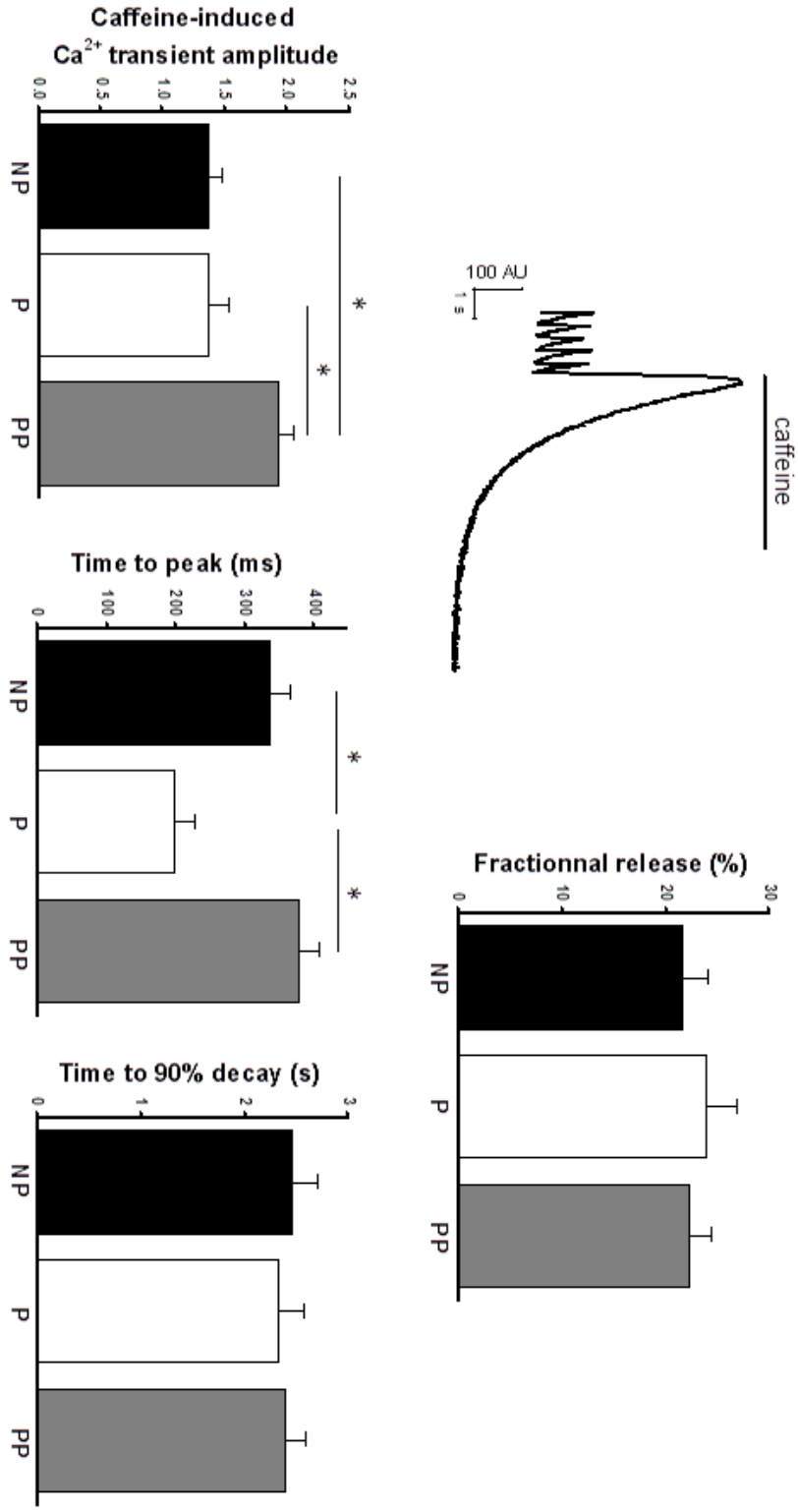
Caffeine-induced
Ca2+ transient amplitude
0.0
0.5
1.0
1.5
2.0
2.5
NP
P
PP
*
*
100 AU
1 s
caffeine
Time to peak (ms)
0
100
200
300
400
NP
P
PP
*
*
Fractionnal release (%)
0
10
20
30
NP
P
PP
Time to 90% decay (s)
0
1
2
3
NP
P
PP

Figure 5. Caffeine-induced Ca^{2+} transient parameters obtained from P, NP and PP mice. Mean data for caffeine-induced Ca^{2+} transient parameters are shown for the 3 groups. Application of caffeine (10 mM) resulted in SR-Ca^{2+} depletion and the following parameters were calculated: amplitude of caffeine-induced transient, fractional release, time-to-peak and time to 90% decay (NP: n=10-12, N=5; P: n=10-12, N=5; PP: n=10-11, N=6, *$p<0.05$, ANOVA with Tukey post-hoc test).

Figure 6

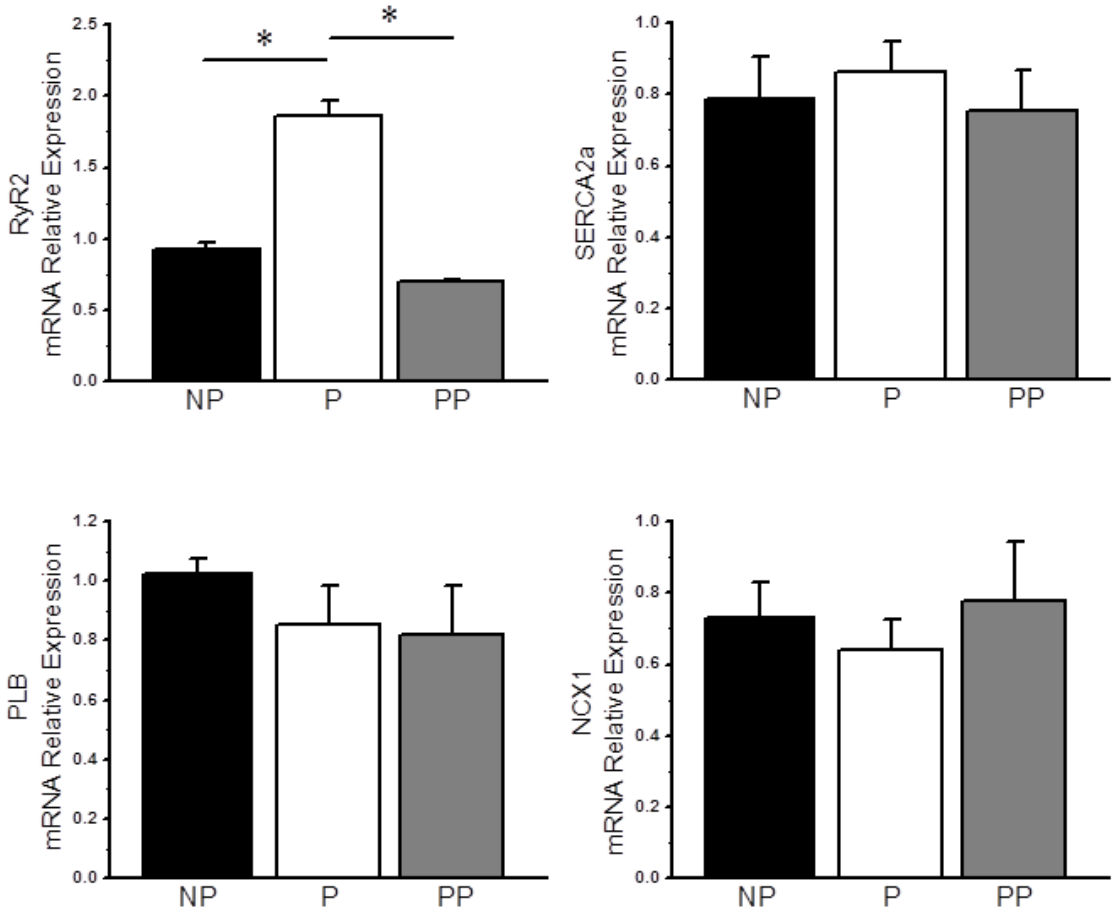

Figure 6. qPCR analysis of Ca^{2+} handling genes from SAN of NP, P and PP mice. Mean qPCR data for relative mRNA expression of RyR2, NCX1, SERCA2a and PLB in whole SAN from P, NP and PP mice are shown. (*$p<0.01$, ANOVA with Tukey post-hoc test). All bar graphs represent n=3-5 samples from 5-6 pooled SANs, all analyzed in triplicate.

Figure 7

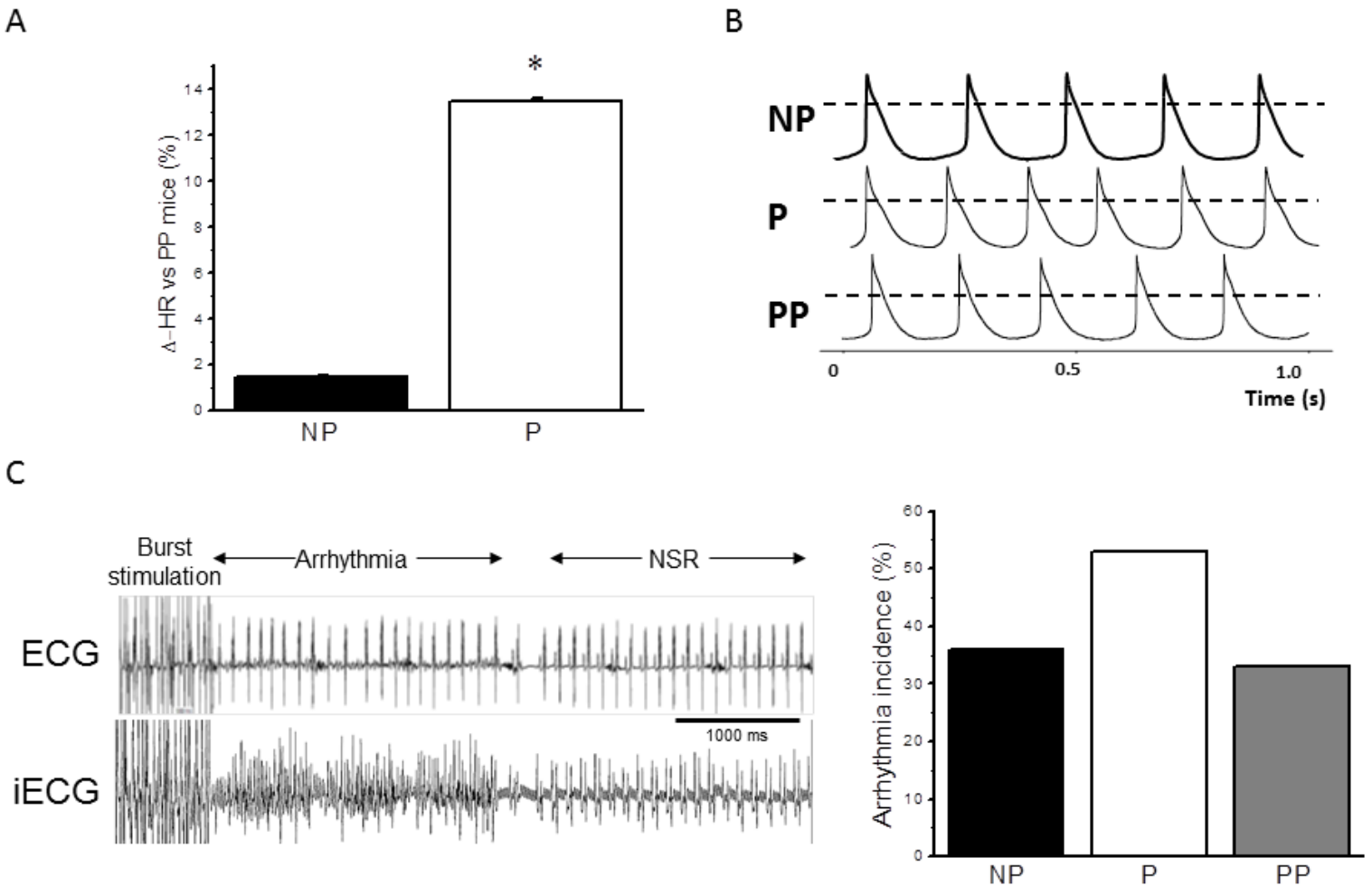
A
*
Δ-HR vs PP mice (%)
14
12
10
8
6
4
2
0
NP
P
B
NP
P
PP
0
0.5
1.0
Time (s)
C
Burst stimulation
Arrhythmia
NSR
ECG
iECG
1000 ms
Arrhythmia incidence (%)
60
50
40
30
20
10
0
NP
P
PP

Figure 7. *In vivo* electrophysiological studies and arrhythmia susceptibility in NP, P and PP mice.

A. The HR of PP mice obtained by lead I surface ECG was compared to that of previously obtained values from NP and P mice.[19] Data shows similar HR between PP and NP however there was a significant difference in HR between PP and P mice. PP, N=9, *p<0.05). **B**. Typical examples of spontaneous AP recordings of obtained from SAN cells of NP, P and PP mice reveal a comparable rate between PP and NP, compared to P. Mean AP rate for PP was comparable to previously obtained values from NP.[19] **C.** *Left*-Representative surface and intracardiac ECGs showing programmed electrical stimulations using burst protocol to trigger supraventricular arrhythmia followed by restoration of normal sinus rhythm (NSR). *Right*-Mean arrhythmia incidence data shows that the increased HR in P group was associated with a higher susceptibility to arrhythmias that was normalized following delivery, as seen by comparable arrhythmic events between the NP and PP groups (NP, N=14; P, N=15; PP, N=6).

4 Interleukin-1β contributes pacemaking dysfunction in human nodal myocytes derived from pluripotent stem cells

Nabil El Khoury, Ph.D., Patrice Naud, Ph.D., Céline Fiset, Ph.D.

In preparation for Circulation Arrhythmia and Electrophysiology, 2017

Author contribution:

N.E.K: Original idea, hiPSC-CM culture, patch-clamp recording, data acquisition and analysis, contribution to development of single cell qPCR technique in hiPSC-CM, study design, manuscript writing and proofing.

P.N.: Development of single-cell qPCR technique for hiPSC-CM applications.

C.F.: Corresponding author and principal investigator, original idea, complete data reviewing with study conceptualization and design, manuscript writing, reviewing and proofing.

Outline- This study represents the second theme of the thesis focused on pathology of the SAN. Inflammation being a key player in the development of diseases and ageing, we provide evidence on how inflammatory mediators can be implicated in adverse remodelling of pacemaker cells. Indeed, based on our previous study (El Khoury N. et al J Biol Chem, 2014), we show here that IL-1β is a pro-inflammatory cytokine with potent electrophysiological effects. In addition, we provide a novel characterization of human nodal like myocytes derived from pluripotent stem cells and demonstrate their potential in serving as a novel *in vitro* model of human SAN. More data is currently being generated and will be added to this study shortly in order to further consolidate its current results.

4.1 Résumé

La maladie du sinus (MS) regroupe différentes maladies complexes affectant le nœud sinusal (NS) et entraîne des troubles de l'automaticité. Les mécanismes sous-jacents à la forme idiopathique de la MS demeurent largement inconnus et nous avons émis l'hypothèse que l'inflammation chronique associée au vieillissement et à diverses pathologies contribue à la détérioration de l'activité pacemaker, conduisant finalement à la MS. Nous avons précédemment montré que l'interleukine-1 bêta (IL-1β) était un puissant modulateur des courants ioniques. En utilisant des cardiomyocytes de type nodal dérivés de cellules souches pluripotentes induites humaines (N-hiPSC-CM), préalablement caractérisés afin de valider leur phénotype, nous avons examiné l'influence de l'IL-1β sur les mécanismes de l'activité pacemaker de ces cellules.

Les N-hiPSC-CMs ont une morphologie distincte et les qPCR sur cellule unique y révèlent une plus grande abondance en ARNm des gènes marqueurs du NS: HCN4, HCN2 et Cx45 et une expression moindre des gènes ANP, Nkx2.5, Cx43 et $Na_V1.5$ comparativement aux hiPSC-CMs de type ventriculaires. Les potentiels d'action (PA) spontanés des N-hiPSC-CM présentaient une grande similarité avec les propriétés de PA du NS humain adulte. Dans les N-hiPSC-CMs traités à l'IL-1β, une réduction significative de la fréquence des PA est associée à une pente de dépolarisation diastolique (DD) plus lente et une hyperpolarisation du potentiel diastolique maximum. Les enregistrements des courants pacemaker (I_f) et Ca^{2+} de type L (I_{CaL}), deux acteurs clés de la DD, ont montré que l'IL-1β entraîne une réduction drastique de la densité de I_{CaL} et I_f. De plus, l'IL-1β induit un déplacement de la courbe d'activation de I_f vers des voltages plus hyperpolarisés, concordant avec une DD plus lente. Enfin, les effets de l'IL-1β étaient indépendants de l'expression de l'ARNm des canaux sous-jacents, suggérant une régulation post-transcriptionnelle.

En conclusion, les N-hiPSC-CM représentent un modèle approprié de cellules humaines du NS dans lesquelles un traitement à l'IL-1β est capable d'induire des troubles de l'automaticité.

4.2 Study

ABSTRACT: Sinus node dysfunction (SND) is a group of complex diseases that affect the sinoatrial node (SAN) resulting in pacemaking disorders. The mechanisms underlying idiopathic form of SND remain largely unknown and we hypothesized that chronic inflammation associated to various pathologies and ageing contributes to deterioration of pacemaking, eventually leading to SND. Previously, we showed IL-1β to be a potent modulator of ionic currents. Accordingly, using nodal-like cardiomyocytes derived from human-induced pluripotent stem cells (N-hiPSC-CM) that were first characterized in order to validate their phenotype, we examined the influence of IL-1β on pacemaking mechanisms of these cells. Results show that, compared to working myocardium cells (WM-hiPSC-CM), N-hiPSC-CMs have a distinct morphology while single-cell qPCR revealed higher mRNA abundance of hallmark SAN genes HCN4, HCN2 and Cx45 with repressed expression of ANP, Cx43 and $Na_V1.5$. Electrophysiologically, N-hiPSC-CM spontaneous action potentials (AP) exhibited high resemblance to properties of adult human pacemaker AP. Furthermore, in IL-1β-treated N-hiPSC-CMs, a significant reduction in AP frequency associated with slower diastolic depolarization rate (DDR) and hyperpolarized maximum diastolic potential was noted. Recordings of L-type Ca^{2+} (I_{CaL}) and pacemaker (I_f) currents, two key contributors to the DDR, showed that IL-1β induces a dramatic reduction in density of I_{CaL} and I_f. . In addition, IL-1β negatively shifted the I_f activation curve, consistent with slower DDR. Effects of IL-1β were independent of mRNA expression changes of underlying channels suggesting post-transcriptional regulation. We conclude that N-hiPSC-CMs represent a suitable model of human SAN cell in which IL-1β was shown to induce pacemaking disturbances.

Keywords: sinus node disease, pacemaking, inflammation, hiPSC-CM.

INTRODUCTION

The sinoatrial node (SAN) is a crescent-shaped structure located at the junction of the right atrium and superior vena cava representing the uppermost point of the conduction system that features a spontaneous electrical activity and acts as the dominant pacemaker in the heart.[1] Within the SAN, clusters of individual pacemaker myocytes are densely packed into collagen rich, fibrous connective tissue and a fatty outer matrix surrounding the peripheral SAN cells that interlock with some atrial myocytes. These features provide shielding from the automaticity-suppressing effects of the hyperpolarized atrial membrane potentials and favour impulse propagation towards the atrium.[2,3] Pacemaking relies on a complex interplay of membrane ion channels and intracellular Ca^{2+} cycling mechanisms found in every SAN cell. Considering there is no substantial expression of inward rectifying channels (Kir2.x) or currents in the SAN, no stable resting membrane potential can be achieved[4,5] and the lowest hyperpolarized level is defined as the maximum diastolic potential (MDP). The MDP is a critical parameter in pacemaking since it can alter the required time to reach threshold, noticeable through either a prolonged or shortened spontaneous diastolic depolarization (DD) phase. Indeed, the diastolic depolarization rate (DDR) is a major determinant of automaticity that controls SAN AP frequency hence, heart rate.[6] Hyperpolarization-activated cyclic nucleotide–gated (HCN) channels encoding the funny current I_f drive the early DDR phase of the AP. The progressive membrane depolarization results in activation of T-type Ca^{2+} channels that facilitate the attaining of depolarization threshold and subsequent activation of L-type Ca^{2+} channels ($Ca_V1.2/1.3$) that trigger the rapid AP upstroke.[7,8] The DD depolarization is also facilitated by spontaneous Ca^{2+} release from the sarcoplasmic reticulum (SR) that drives an electrogenic current through the Na^+/Ca^{2+} exchanger (NCX1) contributing to the DDR.

Ultimately, an SR Ca^{2+} release synchronized with the AP upstroke is elicited. This bringing soon after the AP into its repolarization phase that is driven by K^+ extrusion and Ca^{2+} reuptake.[9] Owing to the importance of proper heart rate control, the pacemaking system can be finely tuned by a wide range of factors including autonomic input and second messengers that convey the necessary cardiac response to varying physiological needs.[1] Unfortunately, there are numerous conditions that can adversely affect the SAN leading to deficient pacemaking, trouble in SAN impulse exit, chronotropic incompetence, bradycardia and other arrhythmias including atrial fibrillation. These conditions are collectively referred to as sinus node dysfunction (SND).[10] Although both extrinsic and intrinsic factors are thought to cause SND, intrinsic cases are irreversible, mostly idiopathic and severe cases have very limited treatment options mostly restricted to the invasive implantation of electronic pacemaker.[11] Idiopathic SND has therefore been the subject of investigation recently in order to grasp the underlying mechanisms which remain largely elusive. Idiopathic SND correlates well with age and is highly prevalent in the elderly where fibrosis and electrical remodelling have been shown to depress pacemaker function.[4,10] Indeed, in aged rodents, an age-dependent decline in several membrane ionic currents including L-type Ca^{2+} (I_{CaL}), T-type Ca^{2+} (I_{CaT}) and I_f has been previously reported to cause bradycardia, lowering shifts in lead pacemaker and depressed excitability of the SAN.[12–14] Interestingly, in autoimmune inflammatory conditions such as systemic lupus erythematous and rheumatoid arthritis, severe complications in conduction and SAN function have also been reported.[15–17] Furthermore, in infectious pathologies, where inflammatory cascades are highly activated, including Chaga's and Lyme disease, bradycardia and SND has also been observed and previously, we showed rhythm irregularities and sinus pauses in a mouse model of HIV.[10,18] Together, these observations indicate that inflammation

might play a major role in the development of SND. In this study, we propose the notion that inflammation, be it elevated as seen in autoimmune and inflammatory disease or the chronic low grade type associated with ageing, may be a common factor between these pathologies that contributes to the development of SND.[19]

Inflammation is intrinsically linked to production of various active immunomodulating peptides such as cytokines. In particular, pro-inflammatory cytokines have been well known to affect the heart in various ways including extracellular matrix remodelling and regulation of ion channels.[20–24] Moreover, interleukin 1β (IL-1β) a key pro-inflammatory cytokines at the top of the inflammatory cascade is classically known to be implicated in the development of chronic diseases associated with low-grade systemic inflammation.[25,26] However, IL-1β also appears to be highly implicated in the pathogenesis of several heart diseases such as myocardial infarction and atherosclerosis and its blockade has even been tested in patients.[27–30] Recently, we showed that IL-1β is a potent suppressor of ventricular I_{CaL}, a current that also plays a critical role in SAN AP depolarization and triggering.[31,32] Considering the important role of IL-1β in cardiac disease and its high circulating levels in inflammatory conditions where bradycardia is observed we tested in this study the effects of chronic IL-1β treatment on pacemaking function of nodal-like human induced pluripotent stem cells-derived cardiomyocytes (hiPSC-CM). The development of hiPSC-CM has been shown to produce the three major myocyte types referred to as nodal-, atrial and ventricular-like in unequal proportions with nodal-like constituting the minority of cells.[33] While various efforts have been focused on enriching and maturing ventricular-type, little attention has been given to nodal-like cells. Accordingly, in this study we provide an electrophysiological and molecular characterization of these cells and demonstrate their similarity to adult human SAN cells.

Considering the extremely limited availability of human SAN tissues and relatively low yield of SAN cells from animals compared to atrial and ventricular preparations, nodal like hiPSC-CM (N-hiPSC-CM) may represent a highly interesting *in vitro* human model of SAN cells that can be maintained in culture in high numbers for relatively long periods of time. Thus, our objectives were to validate and characterize N-hiPSC-CMs and subsequently determine the effect of a chronic IL-1β treatment on the pacemaking function of these cells in order to uncover the potential role of this cytokine inducing SND.

MATERIALS AND METHODS

Cell culture of hiPSC-CM

Vials of hiPSC-CM (iCell® Cardiomyocytes^2) and their maintenance medium that was purchased from Cellular Dynamics International were thawed and plated following manufacturer's instructions. Briefly, hiPSC-CM were rapidly thawed and resuspended in provided plating media then plated on fibronectin coated glass coverslips. Cells were cultured in a water-jacketed incubator at 37°C/5% CO_2 for a maximum of two weeks. Media was refreshed every day for control (CTL) and recombinant human IL-1β (1 ng/mL, Life Sciences) groups. Treatments were performed for a 72h prior to experimentation.

Single-cell qPCR

Single cell qPCR was performed with Single Cell-to-CT™ qRT-PCR Kit following manufacturer's instruction and protocol (Thermofisher, # 4458237). Briefly, two to five N-hiPSC-CMs and WM-hiPSC-CMs were individually collected using a large tip glass micro-pipet and then deposited in a 0.2 mL PCR micro-tube containing the lysis solution. A stop

solution was applied to the samples that were subsequently stored at -20°C until the next step. A retro-transcription step was then performed, followed by a gene-specific pre-amplification of the cDNA. The qPCR was run with the pre-amplified cDNA and Taqman probes and primers for genes of interest. Real-time PCR reactions were completed on a Stratagene MXPro3005 system with a two-steps amplification phase (Denaturation 95°C, 5s; annealing and elongation 60°C, 1 min). Tested genes included HCN4 (Hs00975492_m1), HCN2 (Hs00606903_m1), Cx45 (Hs00271416_s1), Cx43 (Hs00748445_s1), ANP (Hs00383230_g1), $Ca_V1.2$ (Hs00167681_m1), $Ca_V1.3$ (Hs00167753_m1) and NaV1.5 (Hs00165693_m1). All genes have N=3-5 consisting of n=2-5 pooled cells in each N. All the reactions were done in duplicates and HPRT1 (Hs99999909_m1) and 18S (Hs99999901_s1) were used as a reference genes. All data represent expression values analyzed according to the $2^{-\Delta ct}$ method.

Human tissue RNA Extraction and qPCR

Human tissues (left atria, left ventricle and SAN) were obtained from the Montreal Heart Institute tissue bank (Research Ethics Committee approval #2007-43, 924). Isolation of total RNA was performed using TriReagent® and treated with DNase I. A purification step was added using the Macherey-Nagel Total RNA isolation kit following manufacturer instructions. RNA quantity was assessed using NanoDrop spectrophotometric analysis. Maxima First Strand cDNA synthesis kit (ThermoFisher Scientific) was used to synthesize cDNA. Real-time PCR (qPCR) was performed using protocols that were previously published.[34] Briefly, qPCR was performed with Platinum SYBR Green qPCR Supermix (Life Technologies) using a real-time PCR system (MX3005P QPCR system, Stratagene). PCR reactions were performed with a three steps cycle of denaturation (95°C for 30s), annealing (50°C for 60s) and elongation

(72°C for 60s). Quantitative measurements were performed in duplicate and normalized to the geometric mean of three housekeeping genes (hypoxanthine-guanine phosphoribosyltransferase (HPRT), Beta2-microglobulin (B2M) and GAPDH). Expression data were obtained following the 2-ΔCt method.

Electrophysiological data

AP recordings. Spontaneous APs were recorded from N-hiPSC-CM placed in recording chamber (200 μL) on a modified stage of an inverted microscope and perfused with Tyrode's solution containing (mM): 140 NaCl, 5.4 KCl, 1.8 $CaCl_2$, 1 $MgCl_2$, 5.0 HEPES and 5.5 glucose (pH=7.4 with NaOH). All recordings were carried out at 35±1°C using perforated patch-clamp technique with nystatin (350 ng/mL). Pipettes were pulled from borosilicate glass (World Precision Instruments, Sarasota, FL, USA) and had a resistance between 3 to 5 MΩ when filled with the following solution (mM): 100 K^+-aspartate, 30 KCl, 10 NaCl, 2 Mg-ATP, 6.6 Na_2-phosphocreatine, 0.1 Na_2-GTP, 0.04 $CaCl_2$, 1.0 $MgCl_2$ and 5.0 HEPES (pH=7.2 with KOH). All current protocols, data acquisitions and analysis were conducted on the ClampEx suite featuring pClamp 10.3 and Clampfit 10.3 software using an Axopatch 200B patch-clamp amplifier and Digidata 3000 digitizer (Molecular Devices, Sunnyvale, CA, USA).

I_f recordings. The I_f recordings from N-hiPSC-CMs were acquired following AP recordings keeping the same conditions. Current-voltage (IV) relationship curves for I_f were obtained by eliciting 2-s voltage steps from −120 to −20 mV in 10 mV increments from a holding potential of −30 mV at a frequency rate of 0.2 Hz. The density of I_f was measured at the end of the hyperpolarizing steps. Macroscopic activation curves were generated by normalizing current density at a given voltage by maximal current density. Data were plotted against test voltage

and fitted with a Boltzmann equation $I/I\text{max}=1/(1+\exp[V-V_{1/2}]/k)$, where V is the test voltage, $V_{1/2}$ is the mid-activation voltage, and k is the slope factor.

Ca^{2+} Current recordings. L-type Ca^{2+} currents (I_{CaL}) were obtained in whole-cell configuration using the extracellular solution containing (in mM): 10 CsCl, 0.5 $MgCl_2$, 2.0 $CaCl_2$, 5 HEPES, 145 TEA-Cl and 5.5 glucose (pH = 7.4 with CsOH) while the pipettes were filled with the following solution (in mM): 130 CsCl, 10 EGTA, 25 HEPES, 3 Mg-ATP and 0.4 Na-GTP (pH = 7.2 with CsOH). IV relationship curves for I_{CaL} were obtained using stimulation protocol eliciting 250 ms voltage steps in 5-10 mV increments from -50 mV to +60 mV from a holding potential of -80 mV with a 50 ms prepulse at -50 mV. To account for differences in cell size, current amplitudes for all recordings were normalized to cell capacitance and expressed as densities (pA/pF).

RESULTS

Morphological characteristics of N-hiPSC-CMs

The use of N-hiPSC-CM as an *in vitro* model is a potentially interesting prospect that could allow the study of cellular and molecular mechanisms governing human SAN pacemaking. However, most of the actual studies have been focused on working-myocardium type cells and except for few spontaneous AP measurements and some ionic currents recordings, modest information related to the nodal-like myocyte exists. Accordingly, in the first series of experiment we characterized the N-hiPSC-CM population. Morphologically, individual cultured N-hiPSC-CMs appear very different from the other cell types and have a particular shape that allows them to be relatively easily detectable within the WM-hiPSC-CM

population. As shown on Figure 1A, compared to WM-hiPSC-CMs, N-hiPSC-CMs cells are smaller, round, with a large darker central zone corresponding to the nucleus. Their smaller size translates into smaller cellular capacitance, averaging 77.8 ± 8.6 pF, n=20, compared to WM-hiPSC-CMs at 284.5 ± 24.5 pF, n=18, $p<0.01$ (Figure 1B). N-hiPSC-CMs were noted to be relatively poorly developed structurally with no visible evidence of striation or T-tubules. They were flat, except over the central nucleus, with a smooth round shape and overall differing strikingly from the polygonal shaped WM-hiPSC-CMs. Furthermore, under normal physiological conditions they beat spontaneously although contractions are mostly limited to a twitchy motion.

Molecular characteristics of N-hiPSC-CMs

Using single-cell qPCR technique, gene expression of individual N-hiPSC-CMs and WM-hiPSC-CMs was then performed and the results compared. Specific and robust markers that were previously demonstrated to be positive or negative for human SAN were tested.[5] Specifically, data on Figure 2A shows that in N-hiPSC-CMs there is a significant enrichment in expression of three hallmark human SAN genes, pacemaker channels HCN4 and HCN2 and slow conducting connexin 45 (Cx45). Furthermore, N-hiPSC-CMs were shown to be negative for working myocardium markers atrial natriuretic peptide (ANP), fast conducting Cx43 and Na^+ channel $Na_V1.5$ that was higher expressed in working myocardium cells. Interestingly, qPCR analysis on ventricular, atrial and SAN tissues isolated from a freshly explanted human heart, we also observed the expected enrichment in HCN isoforms, including HCN4 and HCN2 in the SAN compared to both atrial and ventricular tissues (Figure 2B).

Electrophysiological characteristics of N-hiPSC-CM

Analysis of spontaneous APs recorded from individual *N-hiPSC-CM* cells reveal very similar AP configuration to mathematical model predictive of human SAN with comparable maximum diastolic potential (MDP), depolarization rate, amplitude and lack of atrial or ventricular-like plateau phase which can be observed in paranodal and SAN peripheral zones.[5,35] The basic AP configuration also resembles murine SAN APs[34] although cycle length and duration of different parameters varies drastically, consistent with the divergent heart rates between mice and humans. The various analyzed parameters including frequency, DDR, MDP, threshold of activation (Eth), AP amplitude (APA) and AP duration (APD) are summarized in Figure 3B. Of note, mean AP frequency of N-hiPSC-CM of 91.5 ± 4.2 bpm was found to be consistent with adult human intrinsic heart rates determined by either pharmacological autonomic blockade or complete denervation of SAN, thereby supporting the pacemaker role of N-hiPSC-CM cells.[36,37]

IL-1β depresses pacemaking in N-hiPSC-CM cells

Following the characterization and validation of molecular and electrophysiological phenotype of N-hiPSC-CMs, in the next series of experiments we tested the effects of a chronic IL-1β treatment on pacemaking mechanisms of these cells. Spontaneous APs from N-hiPSC-CM cells were obtained and typical AP recordings from control (CTL) and IL-1β-treated (IL-1β), shown on Figure 3A, indicate that IL-1β causes a significant reduction in AP frequency. Mean data for the various analyzed AP parameters (Figure 3B) reveal that IL-1β significantly reduces AP rate while slowing the DDR and hyperpolarizing MDP and Eth. Furthermore, in IL-1β-treated cells, an increase in overall APA and AP duration (APD) was also noted.

Overall, these data show that IL-1β reduces AP frequency and induces multiple changes to the AP configuration that are consistent with decreased automaticity, suggesting that IL-1β has a substantial effect on pacemaking mechanisms of N-hiPSC-CMs.

IL-1β reduces pacemaker current I_f in N-hiPSC-CMs.

Since the DDR is a critical determinant of AP rate, two major contributors to the DDR, I_f and I_{CaL}, were subsequently analyzed. Indeed, I_f is a main contributor to the early phase of the DDR and has a fundamental role in pacemaking.[6] I_f currents recordings from N-hiPSC-CM under CTL and IL-1β-treated conditions were obtained and typical examples of recordings are illustrated on Figure 4A while panel B shows the mean IV curve data for both groups. Although no change in maximal current density was noted, there was a dramatic reduction in current density close to the MDP range. In fact, very significant current reductions varying between 64 to 71% were observed at the -40 to -60 mV range. A strong tendency for reduction persisted beyond the MDP range down until -80 mV and thereafter current densities became comparable. This reduction in I_f is very consistent with a change in the channel's voltage dependency that is also observed when decreasing cAMP levels for instance.[38] Accordingly, macroscopic steady-state activation curves fitted with Boltzmann function were computed in order to determine whether IL-1β caused any shifts in voltage dependency. Data reported on Figure 4C shows that IL-1β induces a significant leftward shift in activation voltage that is consistent with the observed current reduction. Indeed, midpoint of activation voltage ($V_{1/2}$) shifted from -88.4 to -93.2 mV ($n=7\text{-}8$, $p<0.01$) in IL-1β-treated cells indicating functionally that close to the MDP range, HCN channel availability is significantly reduced resulting in a slower DDR.

IL-1β reduces L-type Ca^{2+} current N-hiPSC-CMs

I_{CaL} was also subsequently evaluated considering it plays a crucial role in the DDR and contributes to the AP upstroke. Typical examples of I_{CaL} recordings illustrated on Figure 5A show a reduction in current density in IL-1β-treated cells compared to CTL. Mean IV curve data shown on panel B indicates that chronic IL-1β results in a 40% reduction in peak I_{CaL} density. Interestingly, analysis of macroscopic steady-state activation of I_{CaL} shown of Figure 4C, reveals that similarly to I_f, IL-1β induces a significant leftward shift in the activation curve of I_{CaL} indicating opening of these channels at more hyperpolarized voltages and earlier activation during the DD phase, despite the lower current density. Overall, the electrophysiological results indicate that the slower AP frequency observed in IL-1β-treated N-hiPSC-CM is a result of a significant reduction in two main contributors to the DDR, I_f and I_{CaL}.

Effects of IL-1β on N-hiPSC-CM automaticity on ion channel transcription

In order to determine the mechanism by which IL-1β caused a reduction in current density we used the single cell technique on treated and control N-hiPSC-CM. Data for the major genes underlying I_f and I_{CaL} in the SAN are shown on Figure 6. Gene expression results indicate that expression of HCN4, $Ca_V1.2$ and $Ca_V1.3$ is not globally altered by IL-1β treatment. Although $Ca_V1.2$ seems to be augmented, $Ca_V1.3$ is equally reduced, indicating no overall change in the transcription level of these α subunit encoding for I_{CaL}. Therefore, these results suggest that IL-1β does not reduce current density by transcriptionally regulating HCN and $Ca_V1.2/1.3$ channels, but mediates its effects through post-transcriptional modifications. Indeed, these

findings are consistent with our previous results showing that IL-1β does not alter expression of ventricular $Ca_V1.2$, despite lowering its density by up to 40%.[31]

DISCUSSION

In this study, we hypothesized that inflammation and pro-inflammatory cytokines that are elevated in various pathologies, contribute to SND by affecting pacemaking. The rationale behind this notion comes from multiple clinical and experimental observations. Indeed, in individuals affected by inflammatory autoimmune or infectious diseases several cases of SND have been reported.[10,16,17] Importantly, chronic low grade inflammation has also been linked to ageing, cardiovascular disease, diabetes and metabolic syndromes; conditions that represent some of the most important risk factors for the development of SND.[4,12,19,39–45] Although inflammation is a complex state where a myriad of cytokines and immunomodulating factors interact, the pro-inflammatory cytokine IL-1β is pivotal to the inflammatory cascades and was shown to be implicated in a wide range of pathologies ranging from arthritis to cardiovascular disease.[25–27,29] Previously, we found IL-1β to be a potent modulator of ionic currents. Specifically, levels of circulating IL-1β were shown to be particularly elevated in an HIV mouse model that suffered from sinus pauses and bradycardia. Furthermore, treatment of ventricular myocytes with IL-1β was shown to have strong inhibitory effect on I_{CaL} density, a key cardiac current that also plays a major role in SAN pacemaking.[18,31] Accordingly, we tested in this study the potential of IL-1β in contributing to the pathogenesis of the SAN and development of SND.

Our data shows that chronic IL-1β treatment induces several major changes to the spontaneous AP configuration. We highlight a lower DDR, a hallmark feature of bradycardia, but also

hyperpolarized MDP and AP threshold. While a hyperpolarization associated with a more negative MDPs contributes to bradycardia by increasing time to reach threshold,[46,47] we have found the threshold in IL-1β-treated cells to also be reduced thus, a complete negative shift in AP voltage range was observed. A possible explanation for the lower threshold is the negative shift in activation of I_{CaL} that was highly significant from -50 to -35 mV. Even though current density was reduced by ~40%, the earlier activation of I_{CaL} would result in sufficient depolarization to trigger AP upstroke at more hyperpolarized voltages. On the other hand, lower current densities of I_{CaL} combined with that of a reduced I_f contribute to the slowing of the DD phase thereby, lowering AP frequency. Interestingly, activation of I_f was also shifted negatively, explaining its significantly reduced density (up to 70%) at the MDP voltage range. Overall, the resulting slowing in AP rate of ~20% induced by IL-1β is even more pronounced than the effects of classic bradycardic agent ivabradine that was previously shown to reduce AP rate by ~16%,[46] demonstrating that IL-1β produces very potent effects on pacemaking and may induce bradycardia in settings where its levels are elevated. Moreover, another contributing factor to bradycardia might be the longer AP repolarization revealed by higher APD observed in IL-1β-treated cells. Thus, the effects of IL-1β likely extend to repolarizing K^+ channels in N-hiPSC-CMs in support of the strong bradycardic influence of this cytokine.

While exploring the underlying mechanisms of IL-1β-induced bradycardia, no significant effects on channel mRNA expression were found, indicating that IL-1β likely exerts its effects through post-transcriptional mechanisms. Interestingly, it was previously demonstrated that IL-1β contributed to inducing an inotropic effect in ventricular myocytes by reducing intracellular cAMP and uncoupling β-adrenergic response through activation of inhibitory G protein $G_{\alpha i}$.[48,49] Moreover, in ventricular myocytes treated with IL-1β we have found pertussis

toxin, an inhibitor of $G_{\alpha i}$, rescues I_{CaL} density reverting it to control values (unpublished data). These finding would be consistent with a negative shift in I_f activation induced by a decrease in intracellular cAMP concentration. It is also possible that IL-1β indirectly reduces cAMP levels by affecting ATP synthesis. For instance, in retinal neurones it was shown that IL-1β resulted in loss of mitochondrial membrane potential and depleted intracellular ATP.[50] Conceivably, the reduced ATP would not only reduce cAMP, indirectly affecting I_f and I_{CaL}, but could also trigger activation of I_{KATP} and hyperpolarize the MDP, as it was observed. In support of this notion, it was previously demonstrated that SAN cells expressed the ATP-sensitive K^+ current and that potent I_{KATP} activators cromakalim and pinacidil hyperpolarized MDP and abolished or slowed the pacemaker activity.[51] Nonetheless, in one study it was shown that in aged mice although increasing cAMP does somewhat rescue the slow AP firing rate; it does not completely reverse the ageing phenotype suggesting that there are other non-identified factors at play that contribute to bradycardia.[52]

Another important finding reported here is the use of N-hiPSC-CMs as a model of human SAN cells. While most of the efforts have been focused at maturing working myocardium in order to obtain adult-like myocytes suitable for experimental studies and regenerative medicine applications[53–55], nodal-like, beating cells have been mostly overlooked. Using the novel single-cell qPCR technique we were able to analyze expression of key genes in N-hiPSC-CM and compare them to working myocardium type cells as well as adult human SAN. Our results have revealed enrichment of SAN markers in N-hiPSC-CM specifically, HCN2, HCN4 and Cx45 while a lower expression of atrial and working myocardium genes ANP, Cx43 and $Na_V1.5$ was observed. Thus, we conclude that N-hiPSC-CM represent a highly interesting *in vitro* model that shares a molecular a physiological signature with the human

SAN. Unquestionably, several of these markers are also shared with the atrioventricular node (AVN) owing to high resemblance in properties of the two nodes.[56] Nevertheless, the AVN has been shown to have high Nkx2.5 expression compared to the ventricles, which is not the case in N-hiPSC-CM (data not shown).[56] Furthermore, their rapid AP rate is consistent with the fast, dominant pacemaker role of the SAN and with intrinsic human heart rates.[36,37] It is possible that a subpopulation with more AVN properties exist, however this will require substantial experimentation to be validated. Of note, several of the tested markers such as HCN4 and HCN2 also showed high expression levels in working-myocardium cells. While this does not invalidate the N-hiPSC-CMs it hints at the well-known immature phenotype of working hiPSC-CMs.[55] Indeed, various lineage tracing and cardiac embryology studies have shown that the SAN develops early on and retains a pacemaker gene program through expression of several transcription factors that suppress differentiation. As such, mature SAN cells resemble immature and developing working myocardium cells,[57–59] which is likely the case of hiPSC-CM where evidence of automaticity or spontaneous DDR has been observed in myocytes regardless of their individual types.[33,54]

In conclusion, this study highlights a new role for N-hiPSC-CMs as a powerful model of adult SAN cells featuring the appealing advantage of human molecular machinery they hold. Automaticity of N-hiPSC-CMs was shown to be strongly affected by IL-1β, providing explanations on its potential role in inducing sinus bradycardia and promoting the development of SND in various pathologies where its levels are elevated. Naturally, owing to the complex inflammatory cascades, IL-1β cannot be solely accountable for inducing SND as several other pro-inflammatory cytokines have been shown to alter electrophysiological properties of cardiac cells while other have been shown to promote fibrosis.[20,22–24,31,60] It will

therefore be important in the future to determine the role of IL-1β in inducing bradycardia in a complex disease setting where several other factors are at play.

ACKNOWLEDGMENTS

We wish to thank Nathalie Ethier for excellent technical assistance, Anh-Tuan Ton for critical review of the manuscript and Cellular Dynamics International for providing hiPSC-CMs.

FUNDING

This study was funded by a Fondation de l'Institut de Cardiologie grant awarded to C. Fiset. N. El Khoury holds a PhD student scholarship from the Fonds de Recherche en Santé du Québec.

REFERENCES

1. Monfredi O, Dobrzynski H, Mondal T, Boyett MR, Morris GM. The anatomy and physiology of the sinoatrial node--a contemporary review. *Pacing Clin Electrophysiol*. 2010;33:1392–1406.

2. Joyner RW, van Capelle FJ. Propagation through electrically coupled cells. How a small SA node drives a large atrium. *Biophys J*. 1986;50:1157–1164.

3. Dobrzynski H, Li J, Tellez J, Greener ID, Nikolski VP, Wright SE, Parson SH, Jones SA, Lancaster MK, Yamamoto M, Honjo H, Takagishi Y, Kodama I, Efimov IR, Billeter R, Boyett MR. Computer Three-Dimensional Reconstruction of the Sinoatrial Node. *Circulation*. 2005;111:846–854.

4. Choudhury M, Boyett MR, Morris GM. Biology of the Sinus Node and its Disease. *Arrhythmia Electrophysiol Rev*. 2015;4:28–34.

5. Chandler NJ, Greener ID, Tellez JO, Inada S, Musa H, Molenaar P, DiFrancesco D, Baruscotti M, Longhi R, Anderson RH, Billeter R, Sharma V, Sigg DC, Boyett MR, Dobrzynski H. Molecular Architecture of the Human Sinus Node: Insights Into the Function of the Cardiac Pacemaker. *Circulation*. 2009;119:1562–1575.

6. DiFrancesco D. The role of the funny current in pacemaker activity. *Circ Res*. 2010;106:434–446.

7. Mangoni ME, Nargeot J. Genesis and Regulation of the Heart Automaticity. *Physiol Rev*. 2008;88:919–982.

8. Mesirca P, Torrente AG, Mangoni ME. Functional role of voltage gated Ca(2+) channels in heart automaticity. *Front Physiol*. 2015;6:19.

9. Lakatta EG, Maltsev VA, Vinogradova TM. A Coupled SYSTEM of Intracellular Ca2+ Clocks and Surface Membrane Voltage Clocks Controls the Timekeeping Mechanism of the Heart' Pacemaker. *Circ Res*. 2010;106:659–673.

10. Monfredi O, Boyett MR. Sick sinus syndrome and atrial fibrillation in older persons - A view from the sinoatrial nodal myocyte. *J Mol Cell Cardiol*. 2015;83:88–100.

11. Mangrum JM, DiMarco JP. The Evaluation and Management of Bradycardia. *N Engl J Med*. 2000;342:703–709.

12. Jones SA, Boyett MR, Lancaster MK. Declining into failure: the age-dependent loss of the L-type calcium channel within the sinoatrial node. *Circulation*. 2007;115:1183–1190.

13. Larson ED, St Clair JR, Sumner WA, Bannister RA, Proenza C. Depressed pacemaker activity of sinoatrial node myocytes contributes to the age-dependent decline in maximum heart rate. *Proc Natl Acad Sci U S A*. 2013;110:18011–18016.

14. Moghtadaei M, Jansen HJ, Mackasey M, Rafferty SA, Bogachev O, Sapp JL, Howlett SE, Rose RA. The impacts of age and frailty on heart rate and sinoatrial node function. *J Physiol*. 2016;

15. Ahern M, Lever JV, Cosh J. Complete heart block in rheumatoid arthritis. *Ann Rheum Dis*. 1983;42:389–397.

16. Yilmazer B, Sali M, Cosan F, Cefle A. Sinus node dysfunction in adult systemic lupus erythematosus flare: A case report. *Mod Rheumatol*. 2015;25:472–475.

17. Lin Y, Liou YM, Chen JY, Chang KC. Sinus node dysfunction as an initial presentation of adult systemic lupus erythematosus. *Lupus*. 2011;20:1072–1075.

18. Grandy SA, Brouillette J, Fiset C. Reduction of ventricular sodium current in a mouse model of HIV. *J Cardiovasc Electrophysiol*. 2010;21:916–922.

19. Candore G, Caruso C, Jirillo E, Magrone T, Vasto S. Low grade inflammation as a common pathogenetic denominator in age-related diseases: novel drug targets for anti-ageing strategies and successful ageing achievement. *Curr Pharm Des*. 2010;16:584–596.

20. Dobaczewski M, Chen W, Frangogiannis NG. Transforming growth factor (TGF)-β signaling in cardiac remodeling. *J Mol Cell Cardiol*. 2011;51:600–606.

21. Kaur K, Zarzoso M, Ponce-Balbuena D, Guerrero-Serna G, Hou L, Musa H, Jalife J. TGF-beta1, released by myofibroblasts, differentially regulates transcription and function of sodium and potassium channels in adult rat ventricular myocytes. *PLoS One*. 2013;8:e55391.

22. Liao CH, Akazawa H, Tamagawa M, Ito K, Yasuda N, Kudo Y, Yamamoto R, Ozasa Y, Fujimoto M, Wang P, Nakauchi H, Nakaya H, Komuro I. Cardiac mast cells cause atrial fibrillation through PDGF-A-mediated fibrosis in pressure-overloaded mouse hearts. *J Clin Invest*. 2010;120:242–253.

23. Grandy SA, Fiset C. Ventricular K+ currents are reduced in mice with elevated levels of serum TNFa. *J Mol Cell Cardiol*. 2009;47:238–246.

24. Musa H, Kaur K, O'Connell R, Klos M, Guerrero-Serna G, Avula UMR, Herron TJ, Kalifa J, Anumonwo JMB, Jalife J. Inhibition of platelet-derived growth factor-AB signaling prevents electromechanical remodeling of adult atrial myocytes that contact myofibroblasts. *Heart Rhythm*. 2013;10:1044–1051.

25. Dinarello CA. Interleukin-1 in the pathogenesis and treatment of inflammatory diseases. *Blood*. 2011;117:3720–3732.

26. Dinarello CA. Blocking IL-1 in systemic inflammation. *J Exp Med*. 2005;201:1355–1359.

27. Dinarello CA, Pomerantz BJ. Proinflammatory cytokines in heart disease. *Blood Purif*. 2001;19:314–321.

28. Abbate A, Kontos MC, Grizzard JD, Biondi-Zoccai GG, Van Tassell BW, Robati R, Roach LM, Arena RA, Roberts CS, Varma A, Gelwix CC, Salloum FN, Hastillo A, Dinarello CA, Vetrovec GW. Interleukin-1 blockade with anakinra to prevent adverse cardiac remodeling after acute myocardial infarction (Virginia Commonwealth University Anakinra Remodeling Trial [VCU-ART] Pilot study). *Am J Cardiol*. 2010;105:1371–1377.

29. Abbate A, Van Tassell BW, Biondi-Zoccai G, Kontos MC, Grizzard JD, Spillman DW, Oddi C, Roberts CS, Melchior RD, Mueller GH, Abouzaki NA, Rengel LR, Varma A,

Gambill ML, Falcao RA, Voelkel NF, Dinarello CA, Vetrovec GW. Effects of Interleukin-1 Blockade With Anakinra on Adverse Cardiac Remodeling and Heart Failure After Acute Myocardial Infarction [from the Virginia Commonwealth University-Anakinra Remodeling Trial (2) (VCU-ART2) Pilot Study]. *Am J Cardiol*. 2013;111:1394–1400.

30. Van Tassell BW, Toldo S, Mezzaroma E, Abbate A. Targeting interleukin-1 in heart disease. *Circulation*. 2013;128:1910–1923.

31. El Khoury N, Mathieu S, Fiset C. Interleukin-1β reduces L-type Ca2+ current through protein kinase Cϵ activation in mouse heart. *J Biol Chem*. 2014;289:21896–21908.

32. Irisawa H, Brown HF, Giles W. Cardiac pacemaking in the sinoatrial node. *Physiol Rev*. 1993;73:197–227.

33. Ma JG Liang Fiene, Steve. High purity human-induced pluripotent stem cell-derived cardiomyocytes: electrophysiological properties of action potentials and ionic currents. *Am J Physiol - Heart Circ Physiol*. 2011;301:H2006–H2017.

34. El Khoury N, Mathieu S, Marger L, Ross J, El Gebeily G, Ethier N, Fiset C. Upregulation of the hyperpolarization-activated current increases pacemaker activity of the sinoatrial node and heart rate during pregnancy in mice. *Circulation*. 2013;127:2009–2020.

35. Tellez JO, Dobrzynski H, Greener ID, Graham GM, Laing E, Honjo H, Hubbard SJ, Boyett MR, Billeter R. Differential Expression of Ion Channel Transcripts in Atrial Muscle and Sinoatrial Node in Rabbit. *Circ Res*. 2006;99:1384–1393.

36. Strobel JS, Epstein AE, Bourge RC, Kirklin JK, Kay GN. Nonpharmacologic validation of the intrinsic heart rate in cardiac transplant recipients. *J Interv Card Electrophysiol Int J Arrhythm Pacing*. 1999;3:15–18.

37. Opthof T. The normal range and determinants of the intrinsic heart rate in man. *Cardiovasc Res*. 2000;45:177–184.

38. Wainger BJ, DeGennaro M, Santoro B, Siegelbaum SA, Tibbs GR. Molecular mechanism of cAMP modulation of HCN pacemaker channels. *Nature*. 2001;411:805–810.

39. Hasslacher C, Wahl P. Diabetes prevalence in patients with bradycardiac arrhythmias. *Acta Diabetol Lat*. 1977;14:229–234.

40. Grimm W, Langenfeld H, Maisch B, Kochsiek K. Symptoms, cardiovascular risk profile and spontaneous ECG in paced patients: a five-year follow-up study. *Pacing Clin Electrophysiol PACE*. 1990;13:2086–2090.

41. Stout MB, Justice JN, Nicklas BJ, Kirkland JL. Physiological Aging: Links Among Adipose Tissue Dysfunction, Diabetes, and Frailty. *Physiol Bethesda Md*. 2017;32:9–19.

42. Haffner SM. The Metabolic Syndrome: Inflammation, Diabetes Mellitus, and Cardiovascular Disease. *Am J Cardiol*. 2006;97:3–11.

43. Rana JS, Nieuwdorp M, Jukema JW, Kastelein JJP. Cardiovascular metabolic syndrome – an interplay of, obesity, inflammation, diabetes and coronary heart disease. *Diabetes Obes Metab*. 2007;9:218–232.

44. Movahed M-R, Hashemzadeh M, Jamal MM. Increased prevalence of third-degree atrioventricular block in patients with type II diabetes mellitus. *Chest*. 2005;128:2611–2614.

45. Soltysinska E, Speerschneider T, Winther SV, Thomsen MB. Sinoatrial node dysfunction induces cardiac arrhythmias in diabetic mice. *Cardiovasc Diabetol*. 2014;13:122.

46. Bucchi A, Baruscotti M, Robinson RB, DiFrancesco D. Modulation of rate by autonomic agonists in SAN cells involves changes in diastolic depolarization and the pacemaker current. *J Mol Cell Cardiol*. 2007;43:39–48.

47. Shibata EF, Giles W, Pollack GH. Threshold Effects of Acetylcholine on Primary Pacemaker Cells of the Rabbit Sino-Atrial Node. *Proc R Soc Lond B Biol Sci*. 1985;223:355–378.

48. Gulick T, Chung MK, Pieper SJ, Lange LG, Schreiner GF. Interleukin 1 and tumor necrosis factor inhibit cardiac myocyte beta-adrenergic responsiveness. *Proc Natl Acad Sci U A*. 1989;86:6753–6757.

49. Chung MK, Gulick TS, Rotondo RE, Schreiner GF, Lange LG. Mechanism of cytokine inhibition of beta-adrenergic agonist stimulation of cyclic AMP in rat cardiac myocytes. Impairment of signal transduction. *Circ Res*. 1990;67:753–763.

50. Abcouwer SF, Shanmugam S, Gomez PF, Shushanov S, Barber AJ, Lanoue KF, Quinn PG, Kester M, Gardner TW. Effect of IL-1beta on survival and energy metabolism of R28 and RGC-5 retinal neurons. *Invest Ophthalmol Vis Sci*. 2008;49:5581–5592.

51. Han X, Light PE, Giles WR, French RJ. Identification and properties of an ATP-sensitive K+ current in rabbit sino-atrial node pacemaker cells. *J Physiol*. 1996;490:337–350.

52. Sharpe EJ, Larson ED, Proenza C. Cyclic AMP reverses the effects of aging on pacemaker activity and If in sinoatrial node myocytes. *J Gen Physiol*. 2017;149:237–247.

53. Nunes SS, Miklas JW, Liu J, Aschar-Sobbi R, Xiao Y, Zhang B, Jiang J, Massé S, Gagliardi M, Hsieh A, Thavandiran N, Laflamme MA, Nanthakumar K, Gross GJ, Backx PH, Keller G, Radisic M. Biowire: a platform for maturation of human pluripotent stem cell-derived cardiomyocytes. *Nat Methods*. 2013;10:781–787.

54. Lieu DK, Fu J-D, Chiamvimonvat N, Tung KC, McNerney GP, Huser T, Keller G, Kong C-W, Li RA. Mechanism-based facilitated maturation of human pluripotent stem cell-derived cardiomyocytes. *Circ Arrhythm Electrophysiol*. 2013;6:191–201.

55. Yang X, Pabon L, Murry CE. Engineering Adolescence: Maturation of Human Pluripotent Stem Cell–Derived Cardiomyocytes. *Circ Res*. 2014;114:511–523.

56. Bakker ML, Moorman AFM, Christoffels VM. The Atrioventricular Node: Origin, Development, and Genetic Program. *Trends Cardiovasc Med*. 2010;20:164–171.

57. Hoogaars WM, Engel A, Brons JF, Verkerk AO, de Lange FJ, Wong LY, Bakker ML, Clout DE, Wakker V, Barnett P, Ravesloot JH, Moorman AF, Verheijck EE, Christoffels

VM. Tbx3 controls the sinoatrial node gene program and imposes pacemaker function on the atria. *Genes Dev*. 2007;21:1098–1112.

58. Hoogaars WMH, Tessari A, Moorman AFM, de Boer PAJ, Hagoort J, Soufan AT, Campione M, Christoffels VM. The transcriptional repressor Tbx3 delineates the developing central conduction system of the heart. *Cardiovasc Res*. 2004;62:489–499.

59. Christoffels VM, Smits GJ, Kispert A, Moorman AFM. Development of the pacemaker tissues of the heart. *Circ Res*. 2010;106:240–254.

60. Hao X, Zhang Y, Zhang X, Nirmalan M, Davies L, Konstantinou D, Yin F, Dobrzynski H, Wang X, Grace A, Zhang H, Boyett M, Huang CL-H, Lei M. TGF-β1-Mediated Fibrosis and Ion Channel Remodeling Are Key Mechanisms in Producing the Sinus Node Dysfunction Associated With SCN5A Deficiency and AgingClinical Perspective. *Circ Arrhythm Electrophysiol*. 2011;4:397–406.

FIGURES

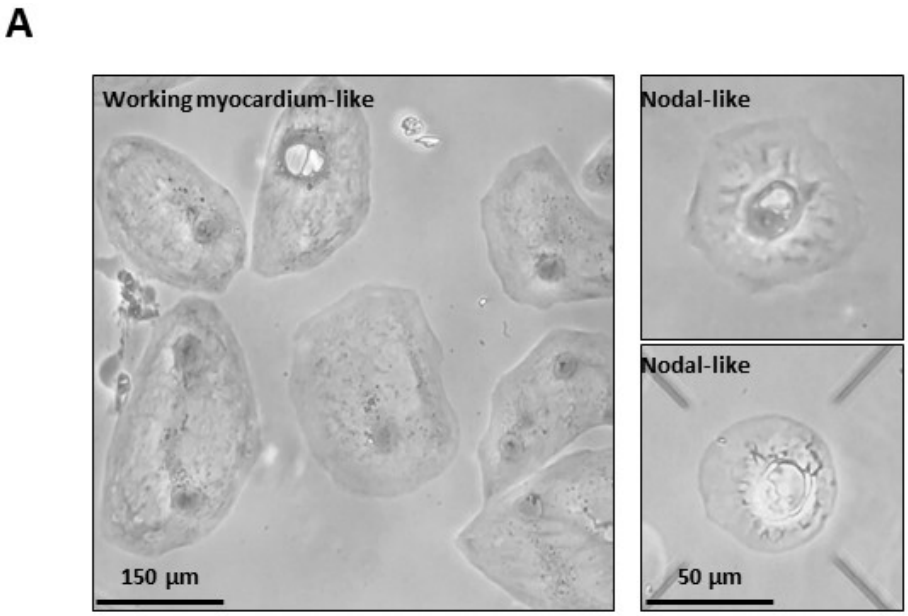
A
Working myocardium-like
150 µm
Nodal-like
Nodal-like
50 µm
B
Mean capacitance (pF)
350
300
250
200
150
100
50
0
*
N-hiPSC-CM
WM-hiPSC-CM

Figure 1. ***Morphological characteristics of N-hiPSC-CMs***. **(A)** Bright-field images of hiPSC-CMs are shown. Examples of large, polygonal, typical WM-hiPSC-CMs are shown on the left panel. Two examples of N-hiPSC-CMs are shown on the right. Note the significantly smaller size, round shapes and distinct morphology. **(B)** Mean capacitance of WM-hiPSC-CMs and N-hiPSC-CMs obtained from voltage-clamp experiments reveal significantly larger cell capacitance of WM-hiPSC-CMs compared to nodal-like cells. (N-hiPSC-CMs, n=20 and WM-hiPSC-CMs n=18, *$p<0.05$).

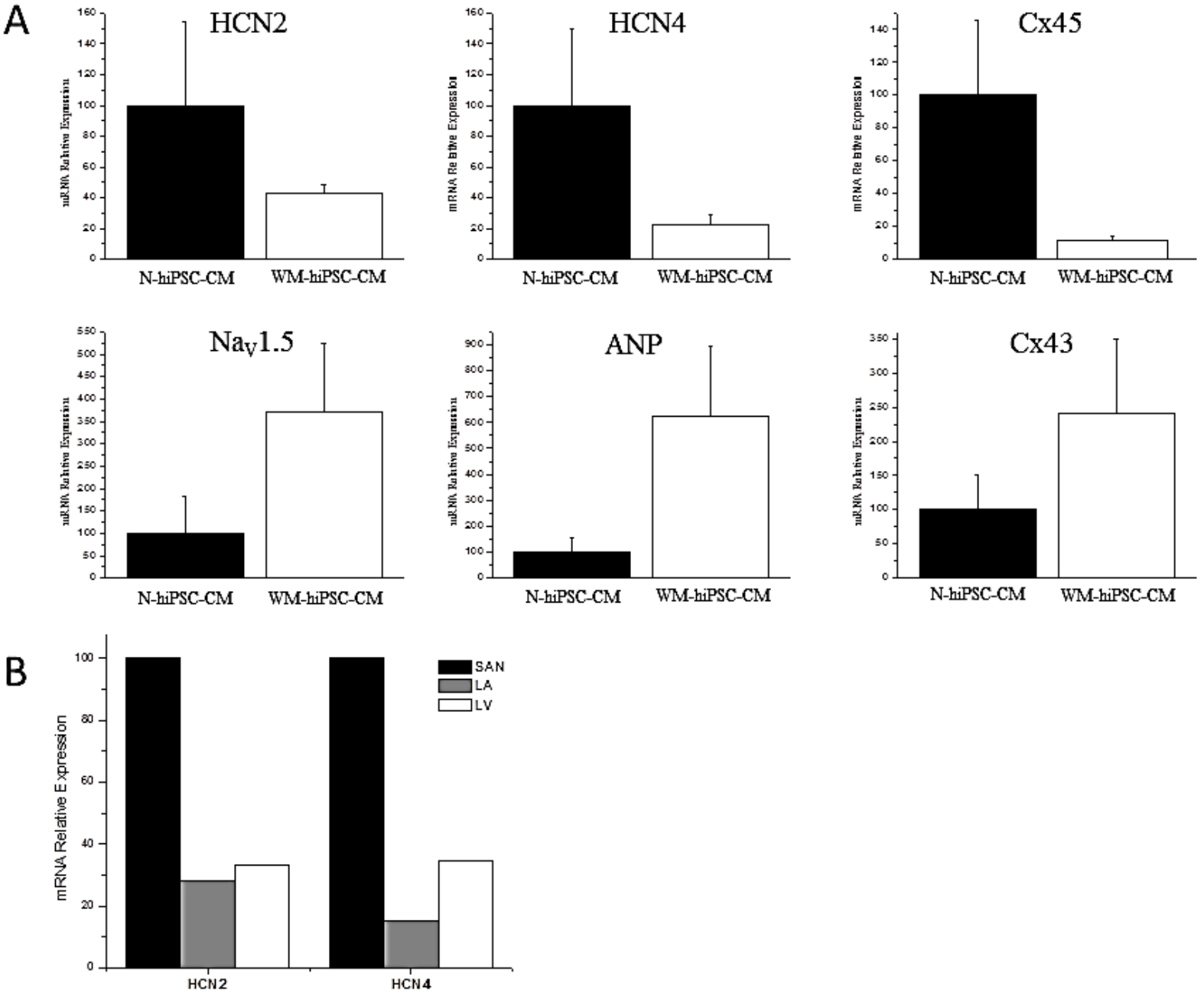
A
HCN2
HCN4
Cx45
Na$_V$1.5
ANP
Cx43
mRNA Relative Expression
N-hiPSC-CM
WM-hiPSC-CM
B
SAN
LA
LV
mRNA Relative Expression
HCN2
HCN4

Figure 2. ***Comparison of gene expression between N-hiPSC-CMs and WM-hiPSC-CMs.*** **(A)** Significant differences in expression of SAN-positive markers HCN2, HCN4, and Cx45 and working-myocardium-positive markers ANP, Cx43 and NaV1.5 were found using single-cell qPCR data that is represented in bar graphs for the two cell types. **(B)** Gene expression of pacemaker channels HCN2 and HCN4 in human SAN, atria and ventricles are compared, revealing high expression of HCN in the SAN compared to left atria (LA) and left ventricle (LV). Tissues were obtained from freshly explanted heart and expression analyzed by qPCR, n=1.

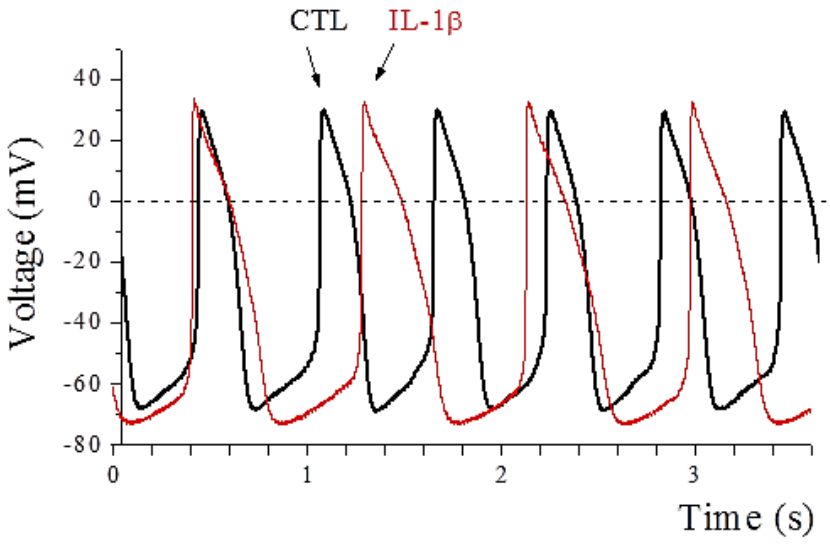

	CTL	IL-1β	*p*-value
Rate (bpm)	91.5 ± 4.2	73.6 ± 3.3 *	0.003
DDR (mV/s)	46.1 ± 3.5	31.4 ± 2.4 *	0.003
MDP (mV)	-53.6 ± 1.4	-61.6 ± 2.0 *	0.004
Eth (mV)	-44.1 ± 0.6	-51.5 ± 1.9 *	0.001
APA (mV)	79.5 ± 3.8	90.7 ± 2.5 *	0.02
APD (ms)	312 ± 15	376 ± 15 *	0.008

Figure 3. ***AP parameters in CTL and IL-1β-treated N-hiPSC-CMs.*** **(A)** Recordings of spontaneous AP in perforated current-clamp mode obtained from CTL and IL-1β-treated cells are superimposed. Note slower rate, DDR and the hyperpolarized MDP, threshold and longer APD. **(B)** Mean data of the various AP parameters summarized in the table show significant changes in all parameters induced by IL-1β. (CTL n=10-15; IL-1β, n=9-12) (*p<0.05)

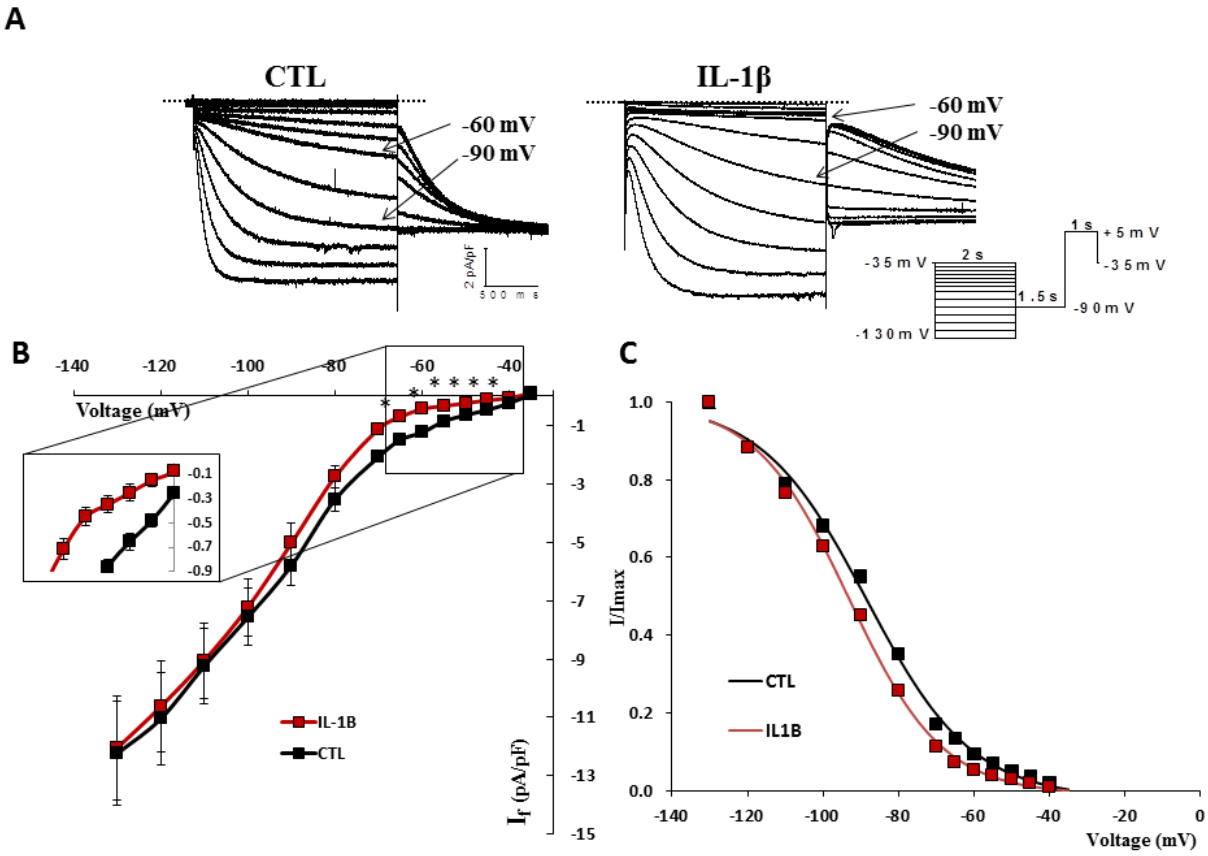

Figure 4. ***Effects of IL-1β on I_f in N-hiPSC-CMs.*** **(A)** Typical recordings of I_f obtained from CTL and IL-1β-treated N-hiPSC-CMs are shown while the mean IV relationship curves is shown on panel **B** (CTL, n=8; IL-1β, n=7, *p<0.05). **(C)** Mean data for the steady-state activation curves of I_f recorded under CTL and IL-1β conditions were fitted with Boltzmann equation. IL-1β results in a significant -4.8 mV shift.

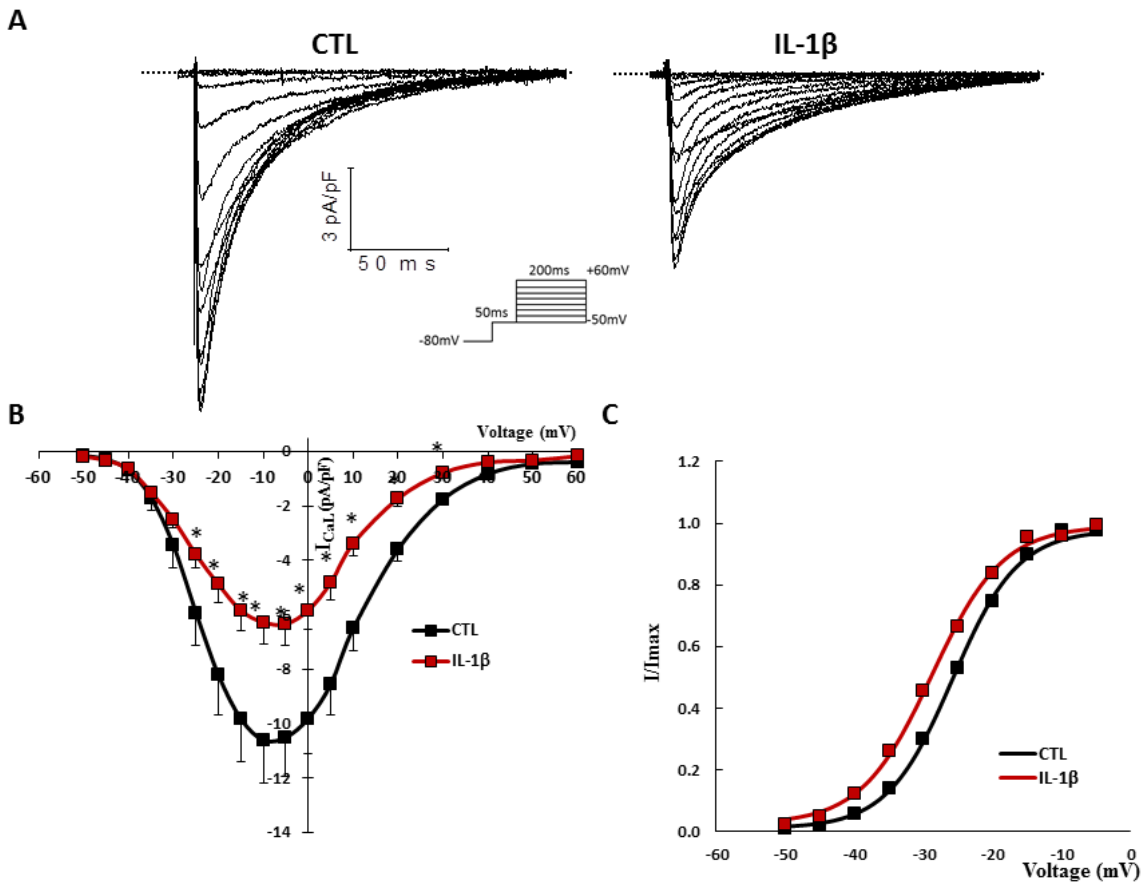

Figure 5. ***Effects of IL-1β on I_{CaL} in N-hiPSC-CMs.*** **(A)** Typical recordings of I_{CaL} obtained from CTL and IL-1β-treated N-hiPSC-CMs are shown, where significant decrease in current density is noticeable. **(B)** Mean IV relationship curves for I_{CaL} show ~40% reduction in peak current density in IL-1β-treated cells compared to CTL. (CTL, n=13; IL-1β, n=16, *p<0.05) **(C)** Mean macroscopic current activation curves for I_{CaL} constructed and fitted with Boltzmann equation, reveal significant a negative shift in I_{CaL} activation.

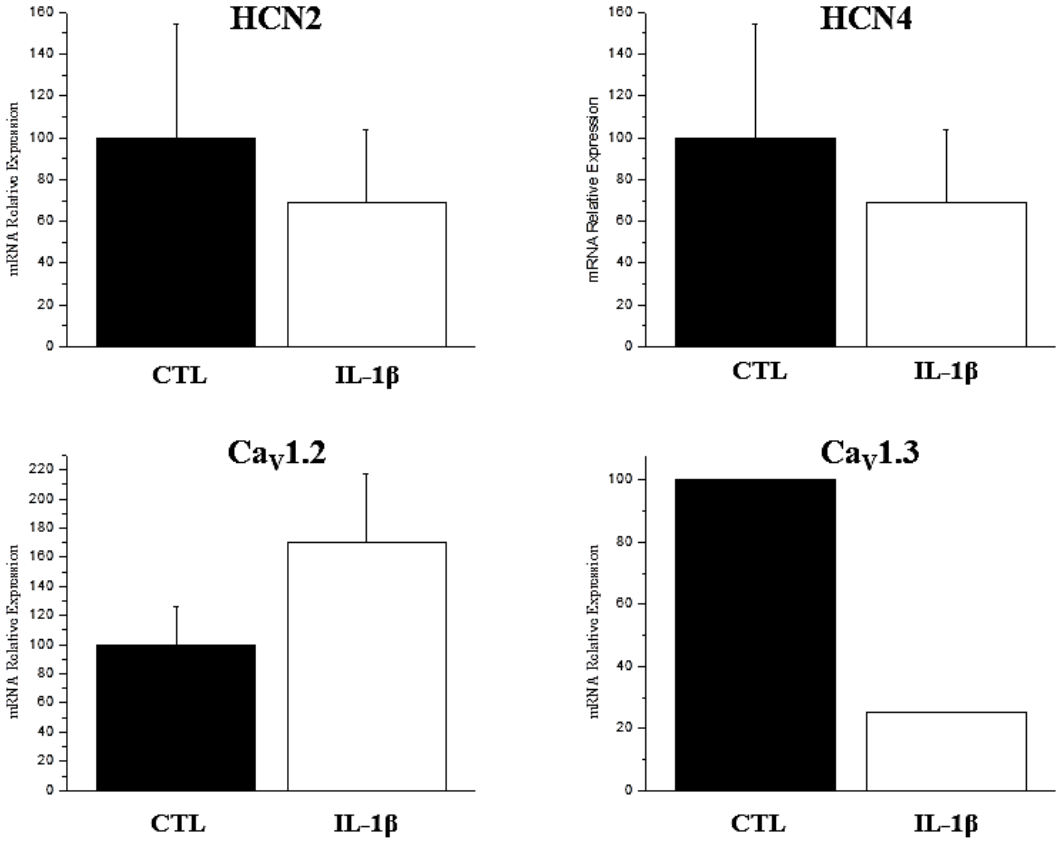

Figure 6. ***Regulation of gene expression by IL-1β.*** Single cell qPCR testing gene expression of major α-subunit of ion channels underlying I_f and I_{CaL} were performed on CTL and IL-1β-treated N-hiPSC-CMs. Data reveals that IL-1β induces no significant difference in global gene expression of HCN2, HCN4, while differentially modulating $Ca_V1.2$ and $Ca_V1.3$.

5 Discussion

This thesis has been entirely dedicated to the advancement of knowledge of the SAN and its regulation. Although initially discovered more than 100 years ago, the SAN is a small, extremely complex and difficult structure to study and much remains to be known about its organization, function and role in physiological processes and disease. The SAN is the natural pacemaker of the heart that dictates rhythm while carrying the substantial responsibility of adjusting cardiac frequency to meet the physiological demands of the organism.[3] Needless to say, failure to do so might result in devastating outcomes including shortness of breath, hypoperfusion, syncope, various arrhythmias, chronotropic incompetence and inability to perform the most simple physical activities, especially in the elderly population.[20,156] Considering the fact that the population is progressively ageing, it is estimated that the proportion of individuals suffering from SND will more than double in the next 50 years and currently, the only approved treatment for SND is the implantation of electronic pacemaker.[97,156] Therefore, understanding how the SAN is regulated is becoming increasingly important and accordingly, we attempt to fill some of this knowledge gap with three studies presented in this work. Indeed, by using both physiological and pathophysiological models, we provide new evidence and mechanistic insight on the regulation of cardiac pacemaking during health and disease and lay a foundation with exciting new ideas that we will build on and extend in our future studies.

5.1 Highlights, main findings and implications

5.1.1 Pacemaking during pregnancy

Starting with physiological mechanisms, the first two studies explored the influence of pregnancy on SAN function. It has been long known that during pregnancy there is an increase in resting heart rate and although several mechanisms explaining this adaptation have been proposed, none implicated SAN remodelling. To our knowledge, the findings reported here represent the first evidence in the literature clearly demonstrating that the SAN undergoes electrical remodelling to increase and sustain an elevated heart rate throughout pregnancy and that delivery results in a rapid and near complete reversal of this adaptation. In other words,

our findings support a new notion proposing that the SAN is a dynamic cardiac tissue capable of undergoing extensive remodelling in order to meet physiological demands and not, as historically thought, a static pacemaker which is simply regulated through autonomic tone balance and circulating catecholamines.

Specifically, using a mouse model of pregnancy we first show that these mice exhibit an increase in heart rate similarly to pregnant women and when the hearts were perfused *ex vivo*, this increase persisted, indicating that that the faster heart rate was due to an intrinsic change to the heart and was not attributable to enhanced sympathetic tone, as previously suggested.[157] Additional evidence supporting our observation came from hemodynamic measurements and blood work performed on pregnant mice revealing that neither arterial pressure nor circulating catecholamines differed compared to controls. Since the SAN is the intrinsic cardiac pacemaker, following these results, SANs of pregnant mice were dissected, enzymatically digested and individual SAN cells were isolated and subjected to several analyses in order to determine whether and how they contribute to an accelerated heart rate. Of note, obtaining individual cells represents a major challenge in exploring the SAN. Being no larger than 1.5 mm^2 in mice, dissecting and digesting the SAN is a technique that requires dexterity, patience and years of optimization and yields only a little number of cells even when well executed (~10 on average) compared to ventricular or atrial cell preparations. Fortunately, we have managed to successfully record spontaneous APs from individual SAN cells and found that the ones isolated from pregnant mice had a significantly higher automaticity, with faster diastolic depolarization compared to controls.

Subsequently, we explored the role of membrane ion channels and intracellular Ca^{2+} handling in this increased AP rate and reported that pregnancy induces a substantial increase in I_f and I_{CaL} along with faster Ca^{2+} transient rates and SR Ca^{2+} release. Molecularly, these changes were correlated with a significant increase in HCN2 protein expression and $Ca_V1.3$ and RyR2 mRNA expression. Of note, no changes in mRNA expression of HCN2 were detected and the reason behind this remains unknown, however since this is not a major isoform in the SAN but has a key role in accelerating pacemaking during pregnancy it is possible that HCN2 channel turnover was reduced instead of initiating transcription.

The molecular work has been performed on whole SAN and due to its tiny size this required isolating and pooling several samples in order to extract enough material. Through technique optimization we were able to reduce the required number of animals for a single "n" number from 10-12 to 4-6 SANs, thereby cutting the amount of required animals and work by half and permitting the development of Western blot techniques optimized for SAN proteins including membrane-bound ion channels.

The coupled-clock, the current model of SAN pacemaking, is based on the principle that both membrane voltage and Ca^{2+} clocks are locked in together and mutually entrained to generate automaticity (introduced p.28 and summarized in Figure 7). Here, we report electrophysiological and molecular changes that highlight a specific circumstance where a complete modulation of the coupled-clock system occurs, providing additional support for a coupled-clock model of pacemaking. Specifically, it was demonstrated how several constituents of this system were regulated while working collectively through a pregnancy-induced upregulation in order to accelerate and sustain rapid heart rates.

Interestingly, the fast heart rates, being a known risk factor for arrhythmias also correlated with an increased arrhythmia risk in pregnant mice which was uncovered through *in vivo* electrophysiological testing. These findings are consistent with reports of arrhythmia susceptibility in pregnant women[84,85] thus, our studies also provide a novel molecular determinant that explains, at least in part, why childbearing women may suffer from rhythm disturbances. We believe understanding the basic physiological mechanisms in health is crucial in order to identify how they are altered in pathology. Hence, a clear understanding of SAN function during pregnancy provides an important step towards the future of managing electrical disturbances in pregnant women, specifically and women's health generally. With the constantly increasing average age of first pregnancy[158] and presence of progressively more comorbidities during this critical period, a clear understanding of the basic mechanisms underlying cardiac electrical function is becoming ever more relevant.[157]

Another important aspect that we also reported was that these changes were rapidly reversible upon delivery. Indeed, when we performed all of the experimentation and analysis on 24-48H postpartum mice, we found a normalization and return to baseline of the examined parameters including heart rate, AP frequency, I_f, I_{CaL} as well as Ca^{2+} transients frequency

indicating that pregnancy-related factors are contributing to this remodelling of the SAN. The brief postpartum period during which we performed our analysis was sufficient for ECG parameters, arrhythmia susceptibility, ionic currents and gene expression to return to control values, attesting to the rapidity of the events. Interestingly, a similar swift return to baseline is also observed in pregnant women, where heart rate has been reported to return to the pre-pregnancy values within two weeks after delivery. Overall, these observations provide additional evidence in support of the pregnant mouse as a model with applicability and high relevance to human electrophysiology.[61,159]

5.1.1.1 Role of hormones in regulating pacemaking

Analysis of arrhythmia risk during various phases of pregnancy in women appears to coincide with moments of substantial fluctuation levels of hormones such as the ones observed during postpartum period. This observation suggests a major role for hormones as instigator of electrophysiological remodelling of the SAN. Hormones are the subject of current work in our laboratory in order to evaluate their role in regulating pacemaking and determine through which pathways they signal.

Indeed, as mentioned in the previous sections and studies several hormones including, estrogen, progesterone, relaxin and thyroid hormones have been shown to affect ion channels in various ways. However, previously shown to have pleiotropic effects and regulate various ion channels and even excitability of neurones,[78,90–93] oestrogen is likely to be a potent regulator of cardiac ion channels. Recently, we showed that oestrogen receptor α negatively regulate Kv4.3 subunit in the ventricles and prolongs repolarization.[160] Furthermore, oestrogen was also shown to reduce Kv4.3 expression in ovariectomized mice and induce cardiac hypertrophy.[161] Previously, we have used various mouse models including oestrogen administration, deficiency (ovariectomy) and oestrogen receptor knockout mice, to generate an extensive amount of results determining the role of oestrogen and oestrogen receptors in regulating ventricular K^+ channels, repolarization, and QT interval. Accordingly, using these models and approaches we have begun investigating the role of oestrogen in modulating the SAN. Preliminary data suggests that chronic treatment of mice with oestrogen significantly

increases heart rate (data not shown) and our subsequent step will be to evaluate the electrophysiological properties on the SAN and determine how they compare to pregnant mice. Moreover, it will be interesting to determine the effects of pregnancy on SAN automaticity in oestrogen receptor knock-out mice considering in these mice all the other hormones and associated regulatory pathways are present.[162] Although female oestrogen receptor α knock-out mice are completely sterile, pregnant β receptor knock-outs can be studied. Alternatively, it will also be possible to administer chronic oestrogen treatment to both α and β knock-out mice in order to determine which receptor and underlying pathways are activated in the SAN, contributing to the increase in heart rate.

Thyroid hormone is another major factor to be considered owing to its ability to regulate ion channels as well.[94,95] We have started using propylthiouracil in pregnant mice in order to uncover the effects of thyroid hormones and the preliminary data thus far does not suggest a major role for this hormone in increasing heart rate during pregnancy (data not shown), despite its ability to induce several changes in electrophysiological parameters, similarly to what is observed in the general population.[163] Lastly, relaxin, a key female hormone that has previously been shown to have various cardiac effects[164,165] will be examined in more depth although we showed in our first study that it was not responsible for changes in I_f activation kinetics and did not increase cAMP significantly in the SAN. Nonetheless, there are reports showing that it can increase I_{CaL} density making it a potential contributor to the faster heart rate during pregnancy.[157,165]

5.1.1.2 Pregnancy affects other parts of the conduction system

Interestingly, when closely analysing the ECGs it was noted that, compared to control mice, the rapid heart rate of the pregnant animals was also accompanied by a significantly shorter PR interval without any change in P wave duration. Since the duration of the PR interval comprises the P wave and impulse conduction through the atrio-ventricular junction, we concluded that the shorter PR interval in pregnant mice is likely to be a consequence of a faster AV node conduction with a preserved atrial conduction time as suggested by the similar values of the P wave durations between control and pregnant mice. This finding is not

completely surprising considering the atrio-ventricular node is regarded as an accessory pacemaker that shares numerous properties with the SAN including spontaneous pacemaking activity, expression of HCN channels, slow conducting connexins and several other ion channels.[4] Thus, it is very likely that the changes that pregnancy brings about to the SAN also extend to the AV node and other parts of the conduction system in order to support propagation of the rapid heart rate throughout the entire heart.

5.1.1.3 Role of autonomic nervous system in regulating heart rate

The SAN is innervated by both sympathetic and parasympathetic branches of the autonomic nervous system allowing for precise heart rate control.[166] Indeed, sympathetic stimulation causes the release of catecholamines that accelerate heart rate by augmenting conductance of key pacemaking ion channels in the SAN including HCN and $Ca_V1.2/1.3$. Conversely, parasympathetic stimulation by means of the vagal nerves induces an opposite effect resulting in a slowing of heart rate.[37] After the first trimester of pregnancy, several studies have previously shown that women exhibit lower heart rate variability and a blunted response to Valsalva manoeuvres.[167–169] This indicates that there is an enhancement of sympathetic and reduction in vagal parasympathetic tones. The overactive sympathetic branch overrides vagal input, hence reducing the heart rate variability while also blunting the response to a vagal stimulation that normally rapidly decreases heart rate. Therefore, it has been suggested that the increase in heart rate during pregnancy could be explained by the increase in sympathetic tone. However, our study performed in mice, where sympathetic drive is already dominant, shows that an intrinsic change to the heart is responsible for the increase in heart rate during pregnancy.[157] As such, when hearts were perfused *ex vivo* the rate dropped by ~30% highlighting the strong sympathetic tone in mice, yet a difference in heart rate between control and pregnant mice remained. In fact, the difference between the two groups was somewhat even larger *ex vivo* most likely due to the loss of the vagal influence that was slightly dampening the heart rate increase in pregnant animals.[157] Indeed, we have shown presence of vagal tone in pregnant mice through atropine administration (unpublished data).

We thus, conclude that although sympathetic tone in pregnant women might be contributing to some extent to the increased heart rate, it is acting over an electrically remodelled SAN.

In additional support of an intrinsic regulating of heart rate in women, it was shown that women have a higher heart rate and that the intrinsic heart rate i.e. after autonomic blockade, is higher than in men, suggesting an inherent difference in the hearts of men and women.[170,171] This observation would also be consistent with the previously discussed role of female hormones, notably oestrogen, in regulating cardiac electrical properties.

5.1.1.4 Comparison of pregnancy to other physiological adaptations

In many ways similar to pregnancy, an interesting physiological adaptation to be considered is exercise. Indeed, chronic exercise activates pathways that lead to physiological eccentric hypertrophy. Eccentric hypertrophy develops as a result of increased venous return and preload resulting in parallel replication of sarcomeres in the ventricles, thus, expanding the cardiac chamber for enhanced blood capacity.[172] This hypertrophy can be paralleled to the one observed during pregnancy where a similar hemodynamic changes to exercise occur. For instance, stroke volume, cardiac output, myocardial contractility and total vascular compliance are all increased in order to provide adequate blood supply to the organs and muscles.[173,174] Conversely to pregnancy however, resting heart rate is reduced by exercise and in high performing endurance athletes bradycardic rates lower than 30 bpm having been reported.[175] Historically, this profound bradycardia has been attributed to enhanced vagal tone in athletes. However, evidence now shows that bradycardia persists after complete autonomic blockade, indicating that an intrinsic remodelling of the SAN is responsible for slow heart rates.[22] Interestingly, denervating either rats or dogs and subjecting them to physical training completely prevents the exercise-induced bradycardia, underlining the essential role for the autonomic system in inducing remodelling of the SAN. Furthermore, it was also shown that in athletes, AV node recovery time was significantly prolonged suggesting AV node dysfunction and indicating that the electrophysiological remodelling also extended to other parts of the conduction system.[176] Thus, even though both pregnancy and exercise training appear to be physiological states that share several similarities, there is a sharp contrast when it comes to

the regulation of the SAN and the conduction system whereby intense aerobic exercise, ironically, promotes deep bradycardia and other pathological remodelling of atria often requiring implantation of pacemaker later in life.[20]

Indeed, molecular analysis and vis-à-vis comparison of athlete and pregnant hearts reveal that in pregnancy, high levels of oestrogen induce a physiological eccentric hypertrophy that is negative for changes in pathological markers of hypertrophy such as α- and β-myosin heavy chain, atrial natriuretic factor, phospholamban, and SERCA2a that are normally affected in heart disease. The increase in cardiac hypertrophy was previously attributed to lower Kv4.3 and c-Src tyrosine kinase activation, a kinase that can be activated by stretch.[161] On the other hand, during exercise hypertrophy, a significant increase in insulin growth factor activates downstream PI3K(p110α) and Akt1, leading to increase in cardiac mass, output and improved overall function.[177] This implies that the molecular signature underlying the hypertrophy in exercise and pregnancy are different. Thus, although the outcome in both of these physiological states is a beneficial hypertrophy, the evidence points to a major role for hormones in regulating mechanical and electrophysiological properties of the heart and the SAN. This also highlights a main difference in the instigating factors and underlying signalling pathways between these two physiological states where a strong dependence on autonomic control for exercise-induced remodelling is required. Overall, these findings could explain why the SAN function is enhanced by pregnancy and diminished during chronic intense exercise.

Recently, the molecular mechanisms underlying pathological remodelling during exercise were the subject of several studies that triggered worldwide discussion.[178–180] However, it is essential to note that the benefits of physical exercise are in no case being questioned nor is exercise being portrayed as a pathological condition. Importantly, a distinction must be made between moderate physical activity and intense endurance exercise seen at the professional level such as in Olympians or Tour de France athletes. In a group of retired cyclists, higher rates of SND were observed and generally, in extremely athletic individuals, irreversible bradycardia and SND associated with atrial fibrillation is often observed, requiring the implantation of cardiac pacemaker.[22,181] In order to determine the

underlying mechanisms of this pathological electrical remodelling, rodents were subjected to intense and long training times of treadmill running or swimming. Examination of these animals revealed that endurance exercise training in rodents results in slower automaticity of the SAN attributable to a lower expression of HCN4 correlating with a downregulation of Tbx3.[182] Furthermore, the significant lowering in resting heart rate was associated with higher susceptibility to atrial fibrillation that was explained by electrical remodelling, increased fibrosis and atrial enlargement.[183,184] Interestingly, it was shown that the pathological remodelling of the atria associated with exercise was dependent on the pro-inflammatory cytokine tumour necrosis factor α.[183] Thus, it appears that intense physical activity can also induce remodelling of supraventricular tissues and contributes to SND through inflammatory pathways, thereby supporting our hypothesis that inflammation might be a common denominator between seemingly unrelated diseases that result in SND.

5.1.2 Pacemaking and inflammation

The second theme of this thesis focused on understanding the cellular and molecular mechanisms that result in SND. Bradycardia and SND are affecting more and more people as the population is getting older and the current treatment options are limited to the implantation of electronic pacemaker. In fact, the estimate that over the next 50 years the rate of SND will more than double might even be an understatement of the prevalence of the condition. Considering there are many challenges in examining, diagnosing and reporting SND in large epidemiological studies, this means projections are based on current numbers that are currently underestimated.[97,156] The consequences of SND can vary from mild discomforting symptoms such as shortness of breath to atrial fibrillation, syncope, and chronotropic incompetence, rendering affected individuals incapable of completing any task that requires the slightest effort and increase in heart rate.[20] Several years ago, while analysing telemetry and ECG data in an HIV mouse model in our laboratory, data revealed several types of electrical disturbances. Although we were particularly interested in the ventricle, we noted sinus pauses and arrhythmias consistent with SND in these mice.[132,133] Following these observations, we showed that circulating pro-inflammatory cytokines that were elevated in HIV mice were able to cause electrical remodelling and alter properties of several major ventricular ion channels including K^+, Na^+ and Ca^{2+} channels.[69,133,134] Interestingly, by examining the literature later on, several reports showing clear SAN dysfunction in infectious conditions were noted. Furthermore, SND was also present in autoimmune inflammatory conditions, diabetic conditions and even ageing.[122,185,156,186] With our previous data showing that pro-inflammatory cytokines can alter ionic currents in the heart, we were able to propose the hypothesis that inflammation is a key process that is shared by multiple pathologies and even ageing that can lead to SND. As pointed out earlier, even intense exercise associated with deleterious electrical remodelling and bradycardia involved a pro-inflammatory cytokine.[183] Although a plethora of cytokines are upregulated in various disease states, we began evaluating the effects of IL-1β on pacemaking in our first study. There are several reasons behind this. IL-1β is a major cytokine that is activated early on in the inflammatory cascades. We initially detected it in HIV mice and at high concentrations it was shown to induce cardiomyopathy. Conversely, its blocking was shown to be protective in myocardial

infarction, heart failure and several other conditions.[133,187–191] Analysis of blood samples of patients suffering from inflammatory conditions such as rheumatoid arthritis, heart failure and relapsing pericarditis, also revealed that the levels of IL-1β are particularly elevated and importantly, we previously showed that IL-1β was a potent suppressor of ventricular I_{CaL}, a current that also plays a critical role in pacemaking.[69,192] In addition, the presence of anti-IL-1β treatments approved for human administration increases potential usefulness and translational potential of the study should IL-1β be validated as a SND target.

Accordingly, we began our investigation with IL-1β in hiPSC-CM nodal myocytes using previously tested conditions where a prolonged treatment was to be administered considering no acute effects on ionic currents could be observed (data not shown). Following a 72H-treatment with IL-1β recordings of spontaneous action potentials revealed a significant slowing in their rate. Analysis of the various parameters revealed that the DDR (or slope of phase 4) of the APs was dramatically reduced. Since the DDR is a key regulator of rate, this was the first evidence that IL-1β adversely affects automaticity.

The voltage-dependent molecular determinants of the DDR being I_f, T and L-type Ca^{2+} currents we subsequently examined these individual currents in order to determine whether they were affected. T-type Ca^{2+} channels are known to be expressed and contribute to automaticity of mouse and rabbit SAN. They were also shown to be expressed in humans SAN.[9,193] However, no current was detected in nodal hiPSC-CM although it was shown to be expressed at the mRNA level ($Ca_V3.1$).[194] This could either mean that these cells lack a functional current or that human SAN expresses non-functional T-type channels. Although the T-type channel blocker mibefradil was shown to lower heart rate in humans,[195] to our knowledge the very little data from adult human SAN that exists is limited to I_f and a few other currents with no direct evidence or recordings attesting to the existence of I_{CaT} current in the SAN. Thus, no conclusion can be made about this subject at present and it would be tempting to resolve this issue in the future. Historically, expression of T-type Ca^{2+} channels have been widely known to be repressed in the adult cardiac tissue and only reactivated during pathology and in N-hiPSC-CM we found that IL-1β induces re-expression of CaV3.1 (preliminary data not shown).[193] Since most human SAN data is derived from elderly patients it is possible that ion channel expression was noted to be more elevated than normal due to

presence of some form of pathological reactivation of gene expression. Arguably, T-type Ca^{2+} channels may not be necessary for human pacemaking owing to the low depolarization frequency compared to smaller animals and rodents where fast Ca^{2+} kinetics, supported by $Ca_V3.1$, are absolutely necessary to sustain rapid rates. Thus, a transition in depolarizing current from I_f to I_{CaL} may be possible and in support of this view smaller I_f and NCX current with weaker Ca^{2+} transients have been noted in the human SAN compared to the rabbit, potentially indicating that the slower rates found in human might not require large conductance and very rapid channel kinetics.[196–198] Of course, this aspect remains purely speculative and remains to be validated in the future.

Nonetheless, a robust I_{CaL} could be recorded and data showed that IL-1β causes a near 40% reduction in its density, consistent with our observed effect in ventricular cells.[69] The smaller I_{CaL} is consistent with a lower DDR and reduced AP rate. Lastly, the pacemaker current I_f was recorded in both groups and mean data showed that IL-1β caused a near 70% reduction in its density at voltage range close to the maximal diastolic potential, i.e. the functionally relevant range. Analysis of I_f activation revealed that IL-1β causes a significant negative shift in activation, consistent with the slower automaticity and lower conductance that were observed compared to the controls. Overall, our findings indicates that IL-1β through its effects on ionic currents involved in pacemaking adversely affects automaticity and may well be a factor in the development of bradycardia and SND. With the data reported in human cardiac cells, this provides an increased relevance and human applicability aspect to the results.

5.1.2.1 hiPSC-CMs as an *in vitro* SAN cell model

Early stages of any project ideally require a robust, fast and cost-effective way of determining whether there is any merit to extensively testing a particular hypothesis. Since we needed to determine if a chronic exposure to IL-1β had any effect on SAN and pacemaking, not many options were available. Considering isolation of SAN cells and their subsequent culture was not a feasible choice (extremely low cell number, culture conditions undefined, etc.), a pre-established *in vitro* model or *in vivo* experimentation was necessary. Since defined

in vitro models of SAN cells do not really exist *per se*, this made the situation rather difficult. *In vivo* models are interesting and a viable option but they present many limitations for early studies, especially in our case where long term IL-1β treatments are required. Large quantities of recombinant cytokines, animals, housing during entire treatment duration and subsequent reagents and experimentation proves globally to be extremely costly for initial and pilot studies.

Incidentally, we had in the laboratory a relatively new source of human cardiac cells derived from induced pluripotent stem cells that were being used for other projects. Through characterization work, a subpopulation of spontaneously beating cells was identified. These cells were already labelled as nodal-like myocytes in previous studies due to their action potential morphology[200] however, very little information other than that was known. This finding presented itself as an opportunity to advance the characterization of these cells as they might carry the potential to become a novel and unique *in vitro* model of human SAN cells. Indeed, the extremely limited availability of human SAN tissues with the technically challenging isolation of individual SAN cells from animals make these cells a highly interesting and appreciated model to individuals interesting in studying regulation of pacemaking properties.

Accordingly, a new strategy was devised in order to determine the electrophysiological and molecular signature of nodal-like hiPSC-CMs. First, using current-clamp technique, spontaneous action potentials were recorded and their various parameters were analysed. Our data is consistent with the values recorded from adult human SAN. Overall, cycle length, action potential duration, maximal diastolic potential and diastolic depolarization rate all seemed to be, although not identical, within an acceptable range and comparable to AP data recorded from isolated individual human SAN cells.[196] These parameters are compared between the two cell types in Figure 10.

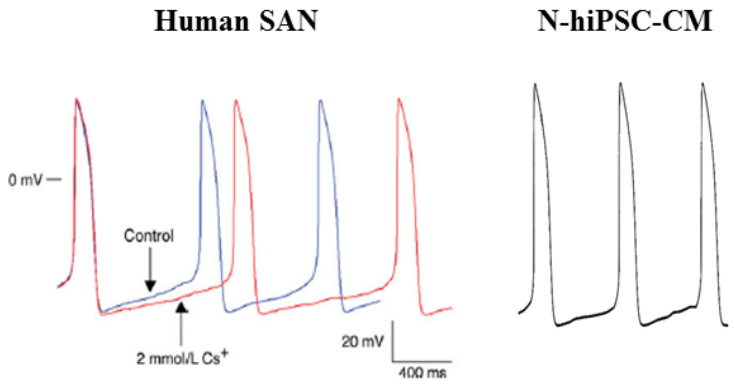

7

	Human SAN	CTL (IL-1β) N-hiPSC-CM	% Difference
Capacitance	56.6 ± 8.7	77.8 ± 8.6	27%
Rate (bpm)	72.5 ± 1.1	91.5±4.2 (73.6±3.3)	21% (1.5%)
DDR (mV/s)	48.9 ± 18*	46.1±3.5 (31.4±2.4)	6% (36%)
MDP (mV)	-61.7 ± 4.3	-53.6±1.4 (-61.6±2.0)	15% (0.1%)
APA (mV)	78.0 ± 4.5	79.5 ± 3.8 (90.7±2.5)	2% (29%)

Figure 10. Comparison between AP recordings obtained from human SAN cells to APs we recorded in N-hiPSC-CM. *Top*- Examples of adult human AP recordings (from (Verkerk et al. 2007) are shown on the left while N-hiPSC-CM are on the right. Fresh human SAN cells were isolated from arrhythmic patient. Note extremely long DD in human SAN not necessarily representative of mean data. Red traces indicate AP with 2mM Cs^{2+} to block I_f. *Bottom*- Mean data shows that several parameters between the two groups are comparable. Even more so following IL-1β treatment for rate and MDP. Highly comparable parameters are represented in red. *Highly variable parameter which might also be consistent with IL-1β-treated N-hiPSC-CM DDR values. Modified from Verkerk et al. 2007.[197]

It is important to evaluate human data with caution. For instance, a major limitation is that the cells in this previously mentioned study were isolated from a patient suffering from supraventricular arrhythmias requiring SAN ablation, indicating potentially severe SAN electrical remodelling and SND. This factor alone would account for many of the observed differences between AP parameters. Furthermore, APs were recordings under different experimental conditions. A remarkable observation however, is that several AP parameters from IL-1β treated cells are more consistent and much closer to the values reported for adult

human SAN APs. Heart failure and SND might also account for the slower AP rate in human SAN cells. Although the AP frequency in N-hiPSC-CM appears to be faster than previously reported in adult human cells, it is consistent with intrinsic heart rates of otherwise healthy adults 20–40 years of age (Figure 7) obtained either by pharmacological autonomic blockade or denervation.[201,202] Lastly, with the existence of other human SAN AP reports, it will be noteworthy eventually to compare all of this data while ensuring that similar recording conditions were maintained. Overall, we conclude that AP parameters of hiPSC-CM show a highly interesting resemblance and are consistent with adult human data of SAN AP, this observation was further supported by the presence of robust I_f and I_{CaL} currents.

A novel aspect of this characterization was the ability to determine the molecular signature of these nodal cells and establish whether they express known markers of human SAN and if indeed they differed from the working myocardium cells. In order to complete this objective, developing a method to separate the two cell populations and analysing their gene expression was necessary. Using the patch-clamp setup, individual myocytes could be picked up using a modified electrode fitted on an electronic micromanipulator that would allow rapid removal of adherent cells. Cells were promptly deposited in tubes filled with required reagents for single-cell qPCR technique. Although qPCR reactions are possible with the content of one cell, in order to reduce variability and chance of no detection resulting in experimental error, several cells were pooled per "n" number up to maximum of 5 cells. qPCR data showed that nodal hiPSC-CM had a high expression of the SAN hallmark genes, pacemaker channel HCN4 and slow conducting Cx45, compared to their working myocardium counterpart. Furthermore, negative markers of SAN were also tested. We report lower expression of atrial marker ANP, fast conducting Cx43 and cardiac $Na_V1.5$ Na^+ channel. Some of these results were also compared to explanted human heart tissues obtained from patients undergoing surgery. As an example, the data shows expectedly high expression of HCN isoforms in the SAN and dramatically lower expression in atrial and ventricular tissues validating the single cell technique and conditions.

The HCN expression in different human cardiac tissues is nonetheless not consistent with the results obtained in working myocardium hiPSC-CMs that show relatively high expression of HCN4. Indeed, this result does not invalidate the nodal phenotype but rather points out to an already widely known phenomenon, the immaturity of hiPSC-CM.[154,155,203]

It is likely that nodal-like myocytes are not necessarily immature like their working myocardium counterparts. During embryogenesis, at the tube heart stage, the myocardium contracts poorly, has very low T-tubule density, poorly developed sarcomeres and SR, slow conduction and automaticity, essentially resembling nodal cells. As early as E10.5-12.5, contractions within the tube trigger initial chamber formation and the sinus venous region progressively becomes more and more isolated as working myocytes mature.[13] The sinus venous region retains expression of repressive transcription factor that prevent its differentiation into working myocardium cells, eventually getting encircled and developing into a mature SAN. In other words, the nodal fate is established early on in embryogenesis and through complex transcriptional networks that progressively lead to loss of pacemaker channels and slow conducting gap junctions, working myocardium cells form.[204]

Thus, in hiPSC-CM working myocardium cells might be in the early stages of development where they still share properties of both working and nodal-like cells. In support of this view, we analysed expression of Nkx2.5 in hiPSC-CM. Nkx2.5 is a key transcription factor involved in septation, chamber development and expression of contractile proteins (see p.28).[3] Our preliminary data shows lower expression of Nkx2.5 in nodal cells compared to the working type (data not shown) indicating a maintained repression of Nkx2.5 that prevents the development of various proteins required for contractility. Interestingly, it has been reported that culturing hiPSC-CM for long periods of time matures the working myocardium phenotype.[205] It is possible that this is the result of long-term expression of Nkx2.5.

Overall, the electrophysiological data combined with gene expression supports the notion that nodal hiPSC-CM might be a novel and useful *in vitro* model to study mechanisms of human cardiac automaticity. Currently, a comprehensive approach to fully characterize these cells is undergoing development. Functionally, Ca^{2+} homeostasis will be examined and compared to current available data in animal models and molecularly, additional expression profiling of other key genes will be performed. For instance, expression of key cardiac

proteins that are differentially expressed between the SAN and working myocardium tissues including Cx40, Cav1.3, Shox2, Tbx3, MLC2v, MLC2a as well as RyR2, SERCA2a and various K^+ channels will all be assessed and we hope that an enrichment of nodal factors with a reduced expression of working myocardium genes will be observed. Eventually, this expression profile will also be compared to that of adult human SAN thereby completing a major milestone in the characterization of nodal hiPSC-CM.

5.1.2.2 In vivo effects of IL-1β

While human cellular models are highly interesting, akin to every model, they have limitations. Considering they are *in vitro* models of disease, they are missing major circulating factors and the complex physiological milieu of a whole organ system. Thus, *in vivo* and animal validation is also required in order to generate a complete functional approach that encompasses multiple models thereby increasing the translational potential and substantiating the data. Accordingly, with the *in vitro* data serving as a starting point we have begun testing chronic administration of IL-1β into adult mice. Mouse recombinant IL-1β solution or saline were filled into miniosmotic pumps. The pumps were primed and implanted subcutaneously between the scapulae, release rate was calibrated for 3 μg/kg daily.[191] Pumps were implanted for either 7 or 14 days in order to determine appropriate timeline required to obtain an effect. At the end of the treatment, ECG measurements for every animal were taken and were compared to baseline values obtained prior to pump implantation. In the future, live telemetry devices will be implanted in order to monitor heart rates continuously. Using telemetry data we can determine whether the effects of IL-1β are variable within a day or with activity level. Heart variability analysis correlated with day-night cycles and activity levels will allow determining how the heart rate fluctuates with IL-1β and uncover influence of sympathetic and vagal tones. Since there is evidence that IL-1β uncouples the β-adrenergic response, these results might prove to be noteworthy.[199] Interestingly, our preliminary data on 14 days and not 7-day treated animals reveals that the delta-decrease in heart rate was significantly larger in mice treated with IL-1β compared to saline, suggesting that chronic infusion of IL-1β into mice might progressively induce bradycardia. Once these results are validated with a larger

number of animals, a full *ex vivo* and cellular analysis of the SAN similar to the studies present will be performed. In addition, optical mapping through use of voltage sensitive dyes on intact isolated SAN will be performed. This will allow determining whether conduction velocity, lead pacemaker and arrhythmogenic potential are affected by chronic IL-1β. Eventually, Ca^{2+} homeostasis will also be examined in both N-hiPSC-CM and mouse SAN cells. We anticipate that the use of an approach combining animal data and human cellular model of the SAN will prove to be additional benefit and advantage in drawing a complete picture on the role of IL-1β in SND.

5.2 Future directions

It is certain that the studies presented here constitute merely the beginning of large projects filled with new and exciting work to come in the near future. Eventually, we hope that the outcomes to be valuable across multiple disciplines ranging from pregnancy, hormonal regulation of SAN and women's health to the elderly and patients suffering from SND. In regards to the SND-related studies, much work remains to be done in terms of characterizing nodal hiPSC-CM, *in vivo* testing and gaining mechanistic insight. Adopting a multidisciplinary approach in order to build an integrative and comprehensive model of disease will be an essential requirement for the development of new therapies. As an example, diseases where inflammatory cascades are activated induce the production of a plethora of cytokines that can have redundant, synergistically or antagonistic functions to each other. Indeed, there are more than 40 different cytokines in the interleukin family alone and while cytokines like IL-1β, TNFα or interleukin-6 are pro-inflammatory others such as interleukin-10 have anti-inflammatory effects.[206] Integrating their individual effect into an equation that yields a net outcome will therefore be an extremely challenging aspect. In heart disease, tumour necrosis factor α, TGF-β and platelet-derived growth factor, to name a few, have been shown to induce ionic current remodelling, fibrosis and activate hypertrophic pathways [134,140,207,208,183,209,210] and teasing out their role in influencing pacemaking or SAN remodelling will be essential.

As a strategy for the future, once we have clarified the role of IL-1β in inducing SND, we will refer to various animal models such as mouse models of HIV, arthritis or other inflammatory conditions where pacemaking is affected and attempt to rescue the phenotype through IL-1β blockade. Alternatively, this approach could also be complemented using new technologies that permit profiling of hundreds of cytokines at once in order to identify the ones that are particularly highly expressed. I trust this will prove to be particularly useful in determining the role of inflammation in ageing-induced SND. Recently, it was shown frailty and not chronological age correlated with decline in SAN function. Indeed, the frailest animals, identified by means of a reproducible frailty index, had the most extensive electrical and structural remodelling with the worse SAN function.[126] Consequently, use of large scale profiling on these animals might reveal particular cytokines that are highly active and are contributing to the rapid decline in SAN function. Previously, we have shown that TNFα and IL-1β induce oxidative stress in the ventricular myocytes, it would therefore be unsurprising if they were found to be elevated in frail animals and contributing to SAN senescence.[69] In short, there might be a strong link between frailty, inflammation and SND that is certainly worth investigating.

In regards to physiological mechanisms and adaptation to pregnancy, several undergoing experiments in our laboratory are attempting to determine the role of hormones in regulating electrophysiological properties of the heart and the SAN in particular. New models of oestrogen administration are being tested while the use of oestrogen receptor knockout mice will also be very useful in determining the downstream signalling pathways that lead to electrical remodelling. These *in vivo* and cellular approaches will also be combined with nodal hiPSC-CM data generated from cells treated under various conditions. The *in vitro* analysis of nodal myocytes will facilitate the elucidation of molecular changes and signalling pathways in response to various hormones within a human myocyte context in order to eventually generate a comprehensive view of the physiological changes that occur during pregnancy. This will allow us to establish how the adaptations extend to changes seen in women's lifespan and whether any of these changes can be used to our advantage during disease states.

6 Conclusions

In conclusion, this thesis has been entirely dedicated to the understanding of the SAN. Despite its modest size, the SAN proves to be a fascinatingly complex pacemaking structure. Overall, we have shown compelling evidence that, far from being a static pacemaker controlled by autonomic balance, the SAN is an adaptive tissue that has evolved to respond to varying external stimuli. Our work identified novel physiological mechanisms that allow the SAN to adapt to the increasing physiological demands during pregnancy. We believe that understanding the regulatory pathways during health is a necessity in order to grasp the changes brought by disease. To that end, we have also begun a new chapter in understanding the mechanisms underlying the pathology of the SAN with the help of cutting edge technologies and development of novel cellular models to study human pacemaking mechanisms. Eventually, we hope that this work will contribute to advancing new therapeutic options, improving women health and the wellbeing of the ageing population.

7 List of publications

First and co-first papers:

- Upregulation of the hyperpolarization-activated current increases pacemaker activity of the sinoatrial node and heart rate during pregnancy in mice.

  El Khoury N, Mathieu S, Marger L, Ross J, El Gebeily G, Ethier N, Fiset C.

  Circulation. 2013 May 21;127(20):2009-20.

- Interleukin-1β reduces L-type Ca2+ current through protein kinase Cϵ activation in mouse heart.

  El Khoury N, Mathieu S, Fiset C.

  J Biol Chem. 2014 Aug 8;289(32):21896-908

- Estrogen regulation of the transient outward K(+) current involves estrogen receptor α in mouse heart.

  El Gebeily G, El Khoury N, Mathieu S, Brouillette J, Fiset C.

  J Mol Cell Cardiol. 2015 Sep;86:85-94.

- Reduction in Na(+) current by angiotensin II is mediated by PKCα in mouse and human-induced pluripotent stem cell-derived cardiomyocytes.

  Mathieu S, El Khoury N, Rivard K, Gélinas R, Goyette P, Paradis P, Nemer M, Fiset C.

  Heart Rhythm. 2016 Jun;13(6):1346-54.

- Characterization of a new mutation in KCNJ2 using human cardiomyocytes from induced pluripotent stem cells

  Gélinas R, El Khoury N, Chaix M, Goyette P, Beauchamp C, Alikashani A, Ethier N, Boucher G, Villeneuve L, Robb L, Latour F, Mondesert B, Rivard L, Talajic M, Fiset C, Rioux J.D.

  Circ Arrhythm Electrophysiol. 2017. Awaiting final acceptance.

- Alterations in sinoatrial node Ca^{2+} homeostasis sustain an accelerated heart rate during pregnancy in mice

  El Khoury N, Ross J, Long V, Thibault S, Ethier N, Fiset C.

  Circulation. 2017, pending submission.

- Interleukin-1β contributes pacemaking dysfunction in human nodal myocytes derived from pluripotent stem cells

  El Khoury N, Naud P, Fiset C.

  Circulation Arrhythm Electrophysiol. 2017, in preparation.

Co-author:

- Nestin is a marker of lung remodeling secondary to myocardial infarction and type I diabetes in the rat.

  Chabot A, Meus MA, Naud P, Hertig V, Dupuis J, Villeneuve L, El Khoury N, Fiset C, Nattel S, Jasmin JF, Calderone A.

  J Cell Physiol. 2015 Jan;230(1):170-9.

- Female Mice with Human Angiotensin II Type 1 Receptor Overexpression are More Susceptible to Develop Dilated Cardiomyopathy and Mortality

  Mathieu S, El Khoury N, Rivard K, Paradis P, Nemer M, Fiset C.

  Circ Heart Fail. 2017, in revision.

8 References

1 Bugnitz C, Bowman J. Cardiac Conduction System. In: Abdulla R, Bonney W, Khalid O, Awad S (eds). *Pediatric Electrocardiography: An Algorithmic Approach to Interpretation*. Springer International Publishing: Cham, 2016, pp 31–33.

2 Dobrzynski H, Anderson RH, Atkinson A, Borbas Z, D'Souza A, Fraser JF *et al.* Structure, function and clinical relevance of the cardiac conduction system, including the atrioventricular ring and outflow tract tissues. *Pharmacol Ther* 2013; **139**: 260–288.

3 Park DS, Fishman GI. 29 - Cell Biology of the Specialized Cardiac Conduction System. In: Zipes DP, Jalife J (eds). *Cardiac Electrophysiology: From Cell to Bedside (Sixth Edition)*. W.B. Saunders: Philadelphia, 2014, pp 287–296.

4 Bakker ML, Moorman AFM, Christoffels VM. The Atrioventricular Node: Origin, Development, and Genetic Program. *Trends Cardiovasc Med* 2010; **20**: 164–171.

5 Silverman ME, Hollman A. Discovery of the sinus node by Keith and Flack: on the centennial of their 1907 publication. *Heart Br Card Soc* 2007; **93**: 1184–1187.

6 Keith A. The sino-auricular node: a historical note. *Br Heart J* 1942; **4**: 77–79.

7 Keith A. The Auriculo-ventricular bundle of His. *The Lancet* 1906; **167**: 623–625.

8 Keith A, Flack M. The Form and Nature of the Muscular Connections between the Primary Divisions of the Vertebrate Heart. *J Anat Physiol* 1907; **41**: 172–189.

9 Chandler NJ, Greener ID, Tellez JO, Inada S, Musa H, Molenaar P *et al.* Molecular Architecture of the Human Sinus Node: Insights Into the Function of the Cardiac Pacemaker. *Circulation* 2009; **119**: 1562–1575.

10 Verheijck EE, Wessels A, Ginneken ACG van, Bourier J, Markman MWM, Vermeulen JLM *et al.* Distribution of Atrial and Nodal Cells Within the Rabbit Sinoatrial Node. *Circulation* 1998; **97**: 1623–1631.

11 Sánchez-Quintana D, Cabrera JA, Farré J, Climent V, Anderson RH, Ho SY. Sinus node revisited in the era of electroanatomical mapping and catheter ablation. *Heart Br Card Soc* 2005; **91**: 189–194.

12 Boyett MR, Honjo H, Kodama I. The sinoatrial node, a heterogeneous pacemaker structure. *Cardiovasc Res* 2000; **47**: 658–687.

13 Christoffels VM, Smits GJ, Kispert A, Moorman AFM. Development of the pacemaker tissues of the heart. *Circ Res* 2010; **106**: 240–254.

14 Schuessler RB, Boineau JP, Bromberg BI. Origin of the sinus impulse. *J Cardiovasc Electrophysiol* 1996; **7**: 263–274.

15 Mangoni ME, Nargeot J. Genesis and Regulation of the Heart Automaticity. *Physiol Rev* 2008; **88**: 919–982.

16 Lei M, Zhang H, Grace AA, Huang CL. SCN5A and sinoatrial node pacemaker function. *Cardiovasc Res* 2007; **74**: 356–365.

17 Tellez JO, Dobrzynski H, Greener ID, Graham GM, Laing E, Honjo H *et al.* Differential Expression of Ion Channel Transcripts in Atrial Muscle and Sinoatrial Node in Rabbit. *Circ Res* 2006; **99**: 1384–1393.

18 Coppen SR, Kodama I, Boyett MR, Dobrzynski H, Takagishi Y, Honjo H *et al.* Connexin45, a major connexin of the rabbit sinoatrial node, is co-expressed with connexin43 in a restricted zone at the nodal-crista terminalis border. *J Histochem Cytochem Off J Histochem Soc* 1999; **47**: 907–918.

19 Dobrzynski H, Li J, Tellez J, Greener ID, Nikolski VP, Wright SE *et al.* Computer Three-Dimensional Reconstruction of the Sinoatrial Node. *Circulation* 2005; **111**: 846–854.

20 Choudhury M, Boyett MR, Morris GM. Biology of the Sinus Node and its Disease. *Arrhythmia Electrophysiol Rev* 2015; **4**: 28–34.

21 Chandler N, Aslanidi O, Buckley D, Inada S, Birchall S, Atkinson A *et al.* Computer Three-Dimensional Anatomical Reconstruction of the Human Sinus Node and a Novel Paranodal Area. *Anat Rec Adv Integr Anat Evol Biol* 2011; **294**: 970–979.

22 Boyett MR. 'And the beat goes on' The cardiac conduction system: the wiring system of the heart. *Exp Physiol* 2009; **94**: 1035–1049.

23 Lakatta EG, DiFrancesco D. What keeps us ticking: a funny current, a calcium clock, or both? *J Mol Cell Cardiol* 2009; **47**: 157–170.

24 Clark RB, Mangoni ME, Lueger A, Couette B, Nargeot J, Giles WR. A rapidly activating delayed rectifier K+ current regulates pacemaker activity in adult mouse sinoatrial node cells. *Am J Physiol Heart Circ Physiol* 2004; **286**: H1757–H1766.

25 Herrmann S, Hofmann F, Stieber J, Ludwig A. HCN channels in the heart: lessons from mouse mutants. *Br J Pharmacol* 2012; **166**: 501–509.

26 DiFrancesco D. The role of the funny current in pacemaker activity. *Circ Res* 2010; **106**: 434–446.

27 Swedberg K, Komajda M, Böhm M, Borer JS, Ford I, Dubost-Brama A *et al.* Ivabradine and outcomes in chronic heart failure (SHIFT): a randomised placebo-controlled study. *The Lancet* 2010; **376**: 875–885.

28 Barbuti A, DiFrancesco D. Control of Cardiac Rate by 'Funny' Channels in Health and Disease. *Ann N Acad Sci* 2008; **1123**: 213–223.

29 Baruscotti M, Barbuti A, Bucchi A. The cardiac pacemaker current. *J Mol Cell Cardiol* 2010; **48**: 55–64.

30 Altomare C, Terragni B, Brioschi C, Milanesi R, Pagliuca C, Viscomi C *et al.* Heteromeric HCN1-HCN4 channels: a comparison with native pacemaker channels from the rabbit sinoatrial node. *J Physiol* 2003; **549**: 347–359.

31 Wainger BJ, DeGennaro M, Santoro B, Siegelbaum SA, Tibbs GR. Molecular mechanism of cAMP modulation of HCN pacemaker channels. *Nature* 2001; **411**: 805–810.

32 Moosmang S, Stieber J, Zong X, Biel M, Hofmann F, Ludwig A. Cellular expression and functional characterization of four hyperpolarization-activated pacemaker channels in cardiac and neuronal tissues. *Eur J Biochem* 2001; **268**: 1646–1652.

33 Bucchi A, Barbuti A, DiFrancesco D, Baruscotti M. Funny Current and Cardiac Rhythm: Insights from HCN Knockout and Transgenic Mouse Models. *Front Physiol* 2012; **3**. doi:10.3389/fphys.2012.00240.

34 Mangoni ME, Traboulsie A, Leoni AL, Couette B, Marger L, Le QK *et al.* Bradycardia and slowing of the atrioventricular conduction in mice lacking CaV3.1/alpha1G T-type calcium channels. *Circ Res* 2006; **98**: 1422–1430.

35 Mangoni ME, Couette B, Bourinet E, Platzer J, Reimer D, Striessnig J *et al.* Functional role of L-type Cav1.3 Ca2+ channels in cardiac pacemaker activity. *Proc Natl Acad Sci U A* 2003; **100**: 5543–5548.

36 Cho HS, Takano M, Noma A. The electrophysiological properties of spontaneously beating pacemaker cells isolated from mouse sinoatrial node. *J Physiol* 2003; **550**: 169–180.

37 Irisawa H, Brown HF, Giles W. Cardiac pacemaking in the sinoatrial node. *Physiol Rev* 1993; **73**: 197–227.

38 Lei M, Honjo H, Kodama I, Boyett MR. Heterogeneous expression of the delayed-rectifier K+ currents iK,r and iK,s in rabbit sinoatrial node cells. *J Physiol* 2001; **535**: 703–714.

39 Fearnley CJ, Roderick HL, Bootman MD. Calcium Signaling in Cardiac Myocytes. *Cold Spring Harb Perspect Biol* 2011; **3**. doi:10.1101/cshperspect.a004242.

40 Bers DM. Cardiac excitation-contraction coupling. *Nature* 2002; **415**: 198–205.

41 Lakatta EG, Maltsev VA, Vinogradova TM. A Coupled SYSTEM of Intracellular Ca2+ Clocks and Surface Membrane Voltage Clocks Controls the Timekeeping Mechanism of the Heart' Pacemaker. *Circ Res* 2010; **106**: 659–673.

42 Kong H, Jones PP, Koop A, Zhang L, Duff HJ, Wayne Chen SR. Caffeine Induces Ca2+ Release by Reducing The Threshold for Luminal Ca2+ Activation of the Ryanodine Receptor. *Biochem J* 2008; **414**: 441–452.

43 Miller L, Steele D, Hart G, D'Souza A, Dobrzynski H, Boyett M. A comparison of Ca2+ spark properties in rat sinoatrial node and ventricular myocytes. *Proc Physiol Soc* 2014; **Proc Physiol Soc 31**. 8

44 Sirenko SG, Maltsev VA, Yaniv Y, Bychkov R, Yaeger D, Vinogradova T *et al.* Electrochemical Na+ and Ca2+ gradients drive coupled-clock regulation of automaticity of isolated rabbit sinoatrial nodal pacemaker cells. *Am J Physiol Heart Circ Physiol* 2016; **311**: H251–H267.

45 Yaniv Y, Lakatta EG, Maltsev VA. From two competing oscillators to one coupled-clock pacemaker cell system. *Front Physiol* 2015; **6**: 28.

46 Bucchi A, Baruscotti M, Robinson RB, DiFrancesco D. Modulation of rate by autonomic agonists in SAN cells involves changes in diastolic depolarization and the pacemaker current. *J Mol Cell Cardiol* 2007; **43**: 39–48.

47 Vinogradova TM, Lyashkov AE, Zhu W, Ruknudin AM, Sirenko S, Yang D *et al.* High basal protein kinase A-dependent phosphorylation drives rhythmic internal Ca2+ store oscillations and spontaneous beating of cardiac pacemaker cells. *Circ Res* 2006; **98**: 505–514.

48 Vinogradova TM, Zhou YY, Maltsev V, Lyashkov A, Stern M, Lakatta EG. Rhythmic Ryanodine Receptor Ca2+ Releases During Diastolic Depolarization of Sinoatrial Pacemaker Cells Do Not Require Membrane Depolarization. *Circ Res* 2004; **94**: 802–809.

49 Masumiya H, Yamamoto H, Hemberger M, Tanaka H, Shigenobu K, Chen SRW *et al.* The mouse sino-atrial node expresses both the type 2 and type 3 Ca2+ release channels/ryanodine receptors. *FEBS Lett* 2003; **553**: 141–144.

50 Murayama T, Kurebayashi N. Two ryanodine receptor isoforms in nonmammalian vertebrate skeletal muscle: Possible roles in excitation–contraction coupling and other processes. *Prog Biophys Mol Biol* 2011; **105**: 134–144.

51 Wiese C, Grieskamp T, Airik R, Mommersteeg MTM, Gardiwal A, Vries C de G *et al.* Formation of the Sinus Node Head and Differentiation of Sinus Node Myocardium Are Independently Regulated by Tbx18 and Tbx3. *Circ Res* 2009; **104**: 388–397.

52 Mommersteeg MTM, Domínguez JN, Wiese C, Norden J, Vries C de G, Burch JBE *et al.* The sinus venosus progenitors separate and diversify from the first and second heart fields early in development. *Cardiovasc Res* 2010; **87**: 92–101.

53 Wilson V, Conlon FL. The T-box family. *Genome Biol* 2002; **3**: reviews3008.1-reviews3008.7.

54 Kapoor N, Liang W, Marbán E, Cho HC. Direct conversion of quiescent cardiomyocytes to pacemaker cells by expression of Tbx18. *Nat Biotechnol* 2013; **31**: 54–62.

55 Mori AD, Zhu Y, Vahora I, Nieman B, Koshiba-Takeuchi K, Davidson L *et al.* Tbx5-dependent rheostatic control of cardiac gene expression and morphogenesis. *Dev Biol* 2006; **297**: 566–586.

56 Espinoza-Lewis RA, Yu L, He F, Liu H, Tang R, Shi J *et al.* Shox2 is essential for the differentiation of cardiac pacemaker cells by repressing Nkx2-5. *Dev Biol* 2009; **327**: 376–385.

57 Akazawa H, Komuro I. Cardiac transcription factor Csx/Nkx2-5: Its role in cardiac development and diseases. *Pharmacol Ther* 2005; **107**: 252–268.

58 Potthoff MJ, Olson EN. MEF2: a central regulator of diverse developmental programs. *Development* 2007; **134**: 4131–4140.

59 Jouven X, Empana JP, Schwartz PJ, Desnos M, Courbon D, Ducimetiere P. Heart-rate profile during exercise as a predictor of sudden death. *N Engl J Med* 2005; **352**: 1951–1958.

60 Leeper NJ, Dewey FE, Ashley EA, Sandri M, Tan SY, Hadley D *et al.* Prognostic value of heart rate increase at onset of exercise testing. *Circulation* 2007; **115**: 468–474.

61 Hunter S, Robson SC. Adaptation of the maternal heart in pregnancy. *Br Heart J* 1992; **68**: 540–543.

62 Clapp JF, Capeless E. Cardiovascular Function Before, During, and After the First and Subsequent Pregnancies. *Am J Cardiol* 1997; **80**: 1469–1473.

63 Blanco PG, Batista PR, Re NE, Mattioli GA, Arias DO, Gobello C. Electrocardiographic changes in normal and abnormal canine pregnancy. *Reprod Domest Anim* 2012; **47**: 252–256.

64 Knotts RJ, Garan H. Cardiac arrhythmias in pregnancy. *Semin Perinatol* 2014; **38**: 285–288.

65 Medzhitov R. Origin and physiological roles of inflammation. *Nature* 2008; **454**: 428–435.

66 Libby P, Ridker PM, Maseri A. Inflammation and atherosclerosis. *Circulation* 2002; **105**: 1135–1143.

67 Dinarello CA, Pomerantz BJ. Proinflammatory cytokines in heart disease. *Blood Purif* 2001; **19**: 314–321.

68 Kalogeropoulos AP, Georgiopoulou VV, Butler J. From risk factors to structural heart disease: the role of inflammation. *Heart Fail Clin* 2012; **8**: 113–123.

69 El Khoury N, Mathieu S, Fiset C. Interleukin-1beta Reduces L-type Ca2+ Current through Protein Kinase C Epsilon Activation in Mouse Heart. *J Biol Chem*. 2014;289:21896–21908.

70 Costantine MM. Physiologic and pharmacokinetic changes in pregnancy. *Front Pharmacol* 2014; **5**. doi:10.3389/fphar.2014.00065.

71 Granger JP. Maternal and fetal adaptations during pregnancy: lessons in regulatory and integrative physiology. *Am J Physiol - Regul Integr Comp Physiol* 2002; **283**: R1289–R1292.

72 Fujime M, Tomimatsu T, Okaue Y, Koyama S, Kanagawa T, Taniguchi T *et al.* Central aortic blood pressure and augmentation index during normal pregnancy. *Hypertens Res* 2012; **35**: 633–638.

73 van Oppen AC, Stigter RH, Bruinse HW. Cardiac output in normal pregnancy: a critical review. *Obstet Gynecol* 1996; **87**: 310–318.

74 Atkins AF, Watt JM, Milan P, Davies P, Crawford JS. A longitudinal study of cardiovascular dynamic changes throughout pregnancy. *Eur J Obstet Gynecol Reprod Biol* 1981; **12**: 215–224.

75 Melchiorre K, Sharma R, Thilaganathan B. Cardiac structure and function in normal pregnancy. *Curr Opin Obstet Gynecol* 2012; **24**: 413–421.

76 Geva T, Mauer MB, Striker L, Kirshon B, Pivarnik JM. Effects of physiologic load of pregnancy on left ventricular contractility and remodeling. *Am Heart J* 1997; **133**: 53–59.

77 Desai DK, Moodley J, Naidoo DP. Echocardiographic assessment of cardiovascular hemodynamics in normal pregnancy. *Obstet Gynecol* 2004; **104**: 20–29.

78 Eghbali M, Wang Y, Toro L, Stefani E. Heart Hypertrophy During Pregnancy: A Better Functioning Heart? *Trends Cardiovasc Med* 2006; **16**: 285–291.

79 Regitz-Zagrosek V, Gohlke-Barwolf C, Iung B, Pieper PG. Management of cardiovascular diseases during pregnancy. *Curr Probl Cardiol* 2014; **39**: 85–151.

80 Adamson DL, Nelson-Piercy C. Managing palpitations and arrhythmias during pregnancy. *Heart* 2007; **93**: 1630–1636.

81 Fox K, Borer JS, Camm AJ, Danchin N, Ferrari R, Lopez Sendon JL *et al.* Resting Heart Rate in Cardiovascular Disease. *J Am Coll Cardiol* 2007; **50**: 823–830.

82 Page RL. Treatment of arrhythmias during pregnancy. *Am Heart J* 1995; **130**: 871–876.

83 Silversides CK, Harris L, Haberer K, Sermer M, Colman JM, Siu SC. Recurrence rates of arrhythmias during pregnancy in women with previous tachyarrhythmia and impact on fetal and neonatal outcomes. *Am J Cardiol* 2006; **97**: 1206–1212.

84 Shotan A, Ostrzega E, Mehra A, Johnson JV, Elkayam U. Incidence of arrhythmias in normal pregnancy and relation to palpitations, dizziness, and syncope. *Am J Cardiol* 1997; **79**: 1061–1064.

85 Widerhorn J, Widerhorn AL, Rahimtoola SH, Elkayam U. WPW syndrome during pregnancy: increased incidence of supraventricular arrhythmias. *Am Heart J* 1992; **123**: 796–798.

86 Brodsky M, Doria R, Allen B, Sato D, Thomas G, Sada M. New-onset ventricular tachycardia during pregnancy. *Am Heart J* 1992; **123**: 933–941.

87 Brickner ME. Cardiovascular management in pregnancy: congenital heart disease. *Circulation* 2014; **130**: 273–282.

88 Rashba EJ, Zareba W, Moss AJ, Hall WJ, Robinson J, Locati EH *et al.* Influence of pregnancy on the risk for cardiac events in patients with hereditary long QT syndrome. LQTS Investigators. *Circulation* 1998; **97**: 451–456.

89 Gowda RM, Khan IA, Mehta NJ, Vasavada BC, Sacchi TJ. Cardiac arrhythmias in pregnancy: clinical and therapeutic considerations. *Int J Cardiol* 2003; **88**: 129–133.

90 Song M, Helguera G, Eghbali M, Zhu N, Zarei MM, Olcese R *et al.* Remodeling of Kv4.3 potassium channel gene expression under the control of sex hormones. *J Biol Chem* 2001; **276**: 31883–31890.

91 Chu Z, Takagi H, Moenter SM. Hyperpolarization-activated currents in gonadotropin-releasing hormone (GnRH) neurons contribute to intrinsic excitability and are regulated by gonadal steroid feedback. *J Neurosci* 2010; **30**: 13373–13383.

92 Bosch MA, Tonsfeldt KJ, Ronnekleiv OK. mRNA expression of ion channels in GnRH neurons: Subtype-specific regulation by 17b-estradiol. *Mol Cell Endocrinol* 2013; **10**: 85–97.

93 Zhang C, Bosch MA, Rick EA, Kelly MJ, Ronnekleiv OK. 17Beta-estradiol regulation of T-type calcium channels in gonadotropin-releasing hormone neurons. *J Neurosci* 2009; **29**: 10552–10562.

94 Shimoni Y, Fiset C, Clark RB, Dixon JE, McKinnon D, Giles WR. Thyroid hormone regulates postnatal expression of transient K+ channel isoforms in rat ventricle. *J Physiol* 1997; **500.1**: 65–73.

95 Le Bouter S, Demolombe S, Chambellan A, Bellocq C, Aimond F, Toumaniantz G *et al.* Microarray analysis reveals complex remodeling of cardiac ion channel expression with altered thyroid status: relation to cellular and integrated electrophysiology. *Circ Res* 2003; **92**: 234–242.

96 Dobrzynski H, Boyett MR, Anderson RH. New insights into pacemaker activity: promoting understanding of sick sinus syndrome. *Circulation* 2007; **115**: 1921–1932.

97 Jensen PN, Gronroos NN, Chen LY, Folsom AR, deFilippi C, Heckbert SR *et al.* Incidence of and Risk Factors for Sick Sinus Syndrome in the General Population. *J Am Coll Cardiol* 2014; **64**: 531–538.

98 Zipes DP, Jalife J. *Cardiac Electrophysiology: From Cell to Bedside*. Elsevier Health Sciences, 2013.

99 Ferrer MI. The Sick Sinus Syndrome in Atrial Disease. *JAMA* 1968; **206**: 645–646.

100 Sanders P, Lau DH, Kalman JM. 72 - Sinus Node Abnormalities. In: Jalife J (ed). *Cardiac Electrophysiology: From Cell to Bedside (Sixth Edition)*. W.B. Saunders: Philadelphia, 2014, pp 691–697.

101 Jose AD, Collison D. The normal range and determinants of the intrinsic heart rate in man. *Cardiovasc Res* 1970; **4**: 160–167.

102 National Institute for Health and Clinical Excellence N. Dual-chamber pacemakers for symptomatic bradycardia due to sick sinus syndrome and/or atrioventricular block | Guidance and guidelines. 2015.

103 Sanders P, Morton JB, Kistler PM, Spence SJ, Davidson NC, Hussin A *et al.* Electrophysiological and electroanatomic characterization of the atria in sinus node disease: evidence of diffuse atrial remodeling. *Circulation* 2004; **109**: 1514–1522.

104 Kang PS, Gomes JAC, El-Sherif N. Differential effects of functional autonomic blockade on the variables of sinus nodal automaticity in sick sinus syndrome. *Am J Cardiol* 1982; **49**: 273–282.

105 Kang PS, Gomes JA, Kelen G, El-Sherif N. Role of autonomic regulatory mechanism in sinoatrial conduction and sinus node automaticity in sick sinus syndrome. *Circulation* 1981; **64**: 832–838.

106 Ruan Y, Liu N, Priori SG. Sodium channel mutations and arrhythmias. *Nat Rev Cardiol* 2009; **6**: 337–348.

107 Schulze-Bahr E, Neu A, Friederich P, Kaupp UB, Breithardt G, Pongs O *et al.* Pacemaker channel dysfunction in a patient with sinus node disease. *J Clin Invest* 2003; **111**: 1537–1545.

108 Nof E, Luria D, Brass D, Marek D, Lahat H, Reznik-Wolf H *et al.* Point Mutation in the HCN4 Cardiac Ion Channel Pore Affecting Synthesis, Trafficking, and Functional Expression Is Associated With Familial Asymptomatic Sinus Bradycardia. *Circulation* 2007; **116**: 463–470.

109 Milanesi R, Baruscotti M, Gnecchi-Ruscone T, DiFrancesco D. Familial Sinus Bradycardia Associated with a Mutation in the Cardiac Pacemaker Channel. *N Engl J Med* 2006; **354**: 151–157.

110 Le Scouarnec S, Bhasin N, Vieyres C, Hund TJ, Cunha SR, Koval O *et al.* Dysfunction in ankyrin-B-dependent ion channel and transporter targeting causes human sinus node disease. *Proc Natl Acad Sci U S A* 2008; **105**: 15617–15622.

111 Knollmann BC, Chopra N, Hlaing T, Akin B, Yang T, Ettensohn K *et al.* Casq2 deletion causes sarcoplasmic reticulum volume increase, premature Ca2+ release, and catecholaminergic polymorphic ventricular tachycardia. *J Clin Invest* 2006; **116**: 2510–2520.

112 Sanders P, Morton JB, Davidson NC, Spence SJ, Vohra JK, Sparks PB *et al.* Electrical Remodeling of the Atria in Congestive Heart Failure. *Circulation* 2003; **108**: 1461–1468.

113 Sanders P, Kistler PM, Morton JB, Spence SJ, Kalman JM. Remodeling of Sinus Node Function in Patients With Congestive Heart Failure. *Circulation* 2004; **110**: 897–903.

114 Verkerk AO, Wilders R, Coronel R, Ravesloot JH, Verheijck EE. Ionic Remodeling of Sinoatrial Node Cells by Heart Failure. *Circulation* 2003; **108**: 760–766.

115 Shinohara T, Park H-W, Han S, Shen MJ, Maruyama M, Kim D *et al.* Ca2+ clock malfunction in a canine model of pacing-induced heart failure. *Am J Physiol - Heart Circ Physiol* 2010; **299**: H1805–H1811.

116 Zicha S, Fernández-Velasco M, Lonardo G, L'Heureux N, Nattel S. Sinus node dysfunction and hyperpolarization-activated (HCN) channel subunit remodeling in a canine heart failure model. *Cardiovasc Res* 2005; **66**: 472–481.

117 Alboni P, Baggioni GF, Scarfò S, Cappato R, Percoco GF, Paparella N *et al.* Role of sinus node artery disease in sick sinus syndrome in inferior wall acute myocardial infarction. *Am J Cardiol* 1991; **67**: 1180–1184.

118 Ando' G, Gaspardone A, Proietti I. Acute thrombosis of the sinus node artery: arrhythmological implications. *Heart* 2003; **89**: e5.

119 Evans R, Shaw DB. Pathological studies in sinoatrial disorder (sick sinus syndrome). *Br Heart J* 1977; **39**: 778–786.

120 Thery C, Gosselin B, Lekieffre J, Warembourg H. Pathology of sinoatrial node. Correlations with electrocardiographic findings in 111 patients. *Am Heart J* 1977; **93**: 735–740.

121 Shiraishi I, Takamatsu T, Minamikawa T, Onouchi Z, Fujita S. Quantitative histological analysis of the human sinoatrial node during growth and aging. *Circulation* 1992; **85**: 2176–2184.

122 Yanni J, Tellez JO, Sutyagin PV, Boyett MR, Dobrzynski H. Structural remodelling of the sinoatrial node in obese old rats. *J Mol Cell Cardiol* 2010; **48**: 653–662.

123 Jones S., Lancaster M., Boyett MR. Ageing-related changes of connexins and conduction within the sinoatrial node. *J Physiol* 2004; **560**: 429–437.

124 Jones SA, Boyett MR, Lancaster MK. Declining into failure: the age-dependent loss of the L-type calcium channel within the sinoatrial node. *Circulation* 2007; **115**: 1183–1190.

125 Larson ED, St Clair JR, Sumner WA, Bannister RA, Proenza C. Depressed pacemaker activity of sinoatrial node myocytes contributes to the age-dependent decline in maximum heart rate. *Proc Natl Acad Sci U S A* 2013; **110**: 18011–18016.

126 Moghtadaei M, Jansen HJ, Mackasey M, Rafferty SA, Bogachev O, Sapp JL *et al.* The impacts of age and frailty on heart rate and sinoatrial node function. *J Physiol* 2016.

127 Tellez JO, Mczewski M, Yanni J, Sutyagin P, Mackiewicz U, Atkinson A *et al.* Ageing-dependent remodelling of ion channel and Ca2+ clock genes underlying sino-atrial node pacemaking. *Exp Physiol* 2011; **96**: 1163–1178.

128 Demoulin JC, Servais JC, Bury J. A case of diphtheritic myocarditis. Pathology and histology of the conductive system. *Acta Cardiol* 1978; **33**: 143–154.

129 Elizari MV, Chiale PA. Cardiac Arrhythmias in Chagas'Heart Disease. *J Cardiovasc Electrophysiol* 1993; **4**: 596–608.

130 McAlister HF. Lyme Carditis: An Important Cause of Reversible Heart Block. *Ann Intern Med* 1989; **110**: 339.

131 Varghese MJ, Ramakrishnan S, Kothari SS, Parashar A, Juneja R, Saxena A. Complete heart block due to diphtheritic myocarditis in the present era. *Ann Pediatr Cardiol* 2013; **6**: 34–38.

132 Grandy SA, Brouillette J, Fiset C. Reduction of ventricular sodium current in a mouse model of HIV. *J Cardiovasc Electrophysiol* 2010; **21**: 916–922.

133 Brouillette J, Grandy SA, Jolicoeur P, Fiset C. Cardiac repolarization is prolonged in CD4C/HIV transgenic mice. *J Mol Cell Cardiol* 2007; **43**: 159–167.

134 Grandy SA, Fiset C. Ventricular K+ currents are reduced in mice with elevated levels of serum TNFa. *J Mol Cell Cardiol* 2009; **47**: 238–246.

135 Yilmazer B, Sali M, Cosan F, Cefle A. Sinus node dysfunction in adult systemic lupus erythematosus flare: A case report. *Mod Rheumatol* 2013.

136 Lin Y, Liou YM, Chen JY, Chang KC. Sinus node dysfunction as an initial presentation of adult systemic lupus erythematosus. *Lupus* 2011; **20**: 1072–1075.

137 Rus V, Atamas SP, Shustova V, Luzina IG, Selaru F, Magder LS *et al.* Expression of cytokine- and chemokine-related genes in peripheral blood mononuclear cells from lupus patients by cDNA array. *Clin Immunol* 2002; **102**: 283–290.

138 Scuderi F, Convertino R, Molino N, Provenzano C, Marino M, Zoli A *et al.* Effect of pro-inflammatory/anti-inflammatory agents on cytokine secretion by peripheral blood mononuclear cells in rheumatoid arthritis and systemic lupus erythematosus. *Autoimmunity* 2003; **36**: 71–77.

139 Suzuki H, Takemura H, Kashiwagi H. Interleukin-1 receptor antagonist in patients with active systemic lupus erythematosus. Enhanced production by monocytes and correlation with disease activity. *Arthritis Rheum* 1995; **38**: 1055–1059.

140 Dobaczewski M, Chen W, Frangogiannis NG. Transforming growth factor (TGF)-β signaling in cardiac remodeling. *J Mol Cell Cardiol* 2011; **51**: 600–606.

141 Inamura J, Ikuta K, Jimbo J, Shindo M, Sato K, Torimoto Y *et al.* Upregulation of hepcidin by interleukin-1beta in human hepatoma cell lines. *Hepatol Res* 2005; **33**: 198–205.

142 Salminen A, Ojala J, Kaarniranta K, Kauppinen A. Mitochondrial dysfunction and oxidative stress activate inflammasomes: impact on the aging process and age-related diseases. *Cell Mol Life Sci* 2012; **69**: 2999–3013.

143 Nelson TJ, Martinez-Fernandez A, Terzic A. Induced pluripotent stem cells: developmental biology to regenerative medicine. *Nat Rev Cardiol* 2010; **7**: 700–710.

144 Gilbert SF. *Developmental Biology*. 6th ed. Sinauer Associates, 2000.

145 Priori SG, Napolitano C, Di Pasquale E, Condorelli G. Induced pluripotent stem cell-derived cardiomyocytes in studies of inherited arrhythmias. *J Clin Invest* 2013; **123**: 84–91.

146 Acimovic I, Vilotic A, Pesl M, Lacampagne A, Dvorak P, Rotrekl V *et al.* Human pluripotent stem cell-derived cardiomyocytes as research and therapeutic tools. *BioMed Res Int* 2014; **2014**: 512831.

147 Davis RP, Casini S, van den Berg CW, Hoekstra M, Remme CA, Dambrot C *et al.* Cardiomyocytes derived from pluripotent stem cells recapitulate electrophysiological characteristics of an overlap syndrome of cardiac sodium channel disease. *Circulation* 2012; **125**: 3079–3091.

148 Takahashi K, Yamanaka S. Induction of pluripotent stem cells from mouse embryonic and adult fibroblast cultures by defined factors. *Cell* 2006; **126**: 663–676.

149 Kim JB, Sebastiano V, Wu G, Araúzo-Bravo MJ, Sasse P, Gentile L *et al.* Oct4-induced pluripotency in adult neural stem cells. *Cell* 2009; **136**: 411–419.

150 Sartiani L, Bettiol E, Stillitano F, Mugelli A, Cerbai E, Jaconi ME. Developmental changes in cardiomyocytes differentiated from human embryonic stem cells: a molecular and electrophysiological approach. *Stem Cells Dayt Ohio* 2007; **25**: 1136–1144.

151 Zhang J, Wilson GF, Soerens AG, Koonce CH, Yu J, Palecek SP *et al.* Functional Cardiomyocytes Derived from Human Induced Pluripotent Stem Cells. *Circ Res* 2009; **104**: e30–e41.

152 Ma JG Liang Fiene, Steve. High purity human-induced pluripotent stem cell-derived cardiomyocytes: electrophysiological properties of action potentials and ionic currents. *Am J Physiol - Heart Circ Physiol* 2011; **301**: H2006–H2017.

153 Knollmann BC. Controversies in Cardiovascular Research: Induced pluripotent stem cell-derived cardiomyocytes – boutique science or valuable arrhythmia model? *Circ Res* 2013; **112**: 969–976.

154 Kamakura T, Makiyama T, Sasaki K, Yoshida Y, Wuriyanghai Y, Chen J *et al.* Ultrastructural maturation of human-induced pluripotent stem cell-derived cardiomyocytes in a long-term culture. *Circ J Off J Jpn Circ Soc* 2013; **77**: 1307–1314.

155 Nunes SS, Miklas JW, Liu J, Aschar-Sobbi R, Xiao Y, Zhang B *et al.* Biowire: a platform for maturation of human pluripotent stem cell-derived cardiomyocytes. *Nat Methods* 2013; **10**: 781–787.

156 Monfredi O, Boyett MR. Sick sinus syndrome and atrial fibrillation in older persons - A view from the sinoatrial nodal myocyte. *J Mol Cell Cardiol* 2015; **83**: 88–100.

157 El Khoury N, Mathieu S, Marger L, Ross J, El Gebeily G, Ethier N *et al.* Upregulation of the hyperpolarization-activated current increases pacemaker activity of the sinoatrial node and heart rate during pregnancy in mice. *Circulation* 2013; **127**: 2009–2020.

158 Hamilton E. B, Martin A. J, Osterman J.K. M, Curtin C. S, Mathews TJ. Births: Final Data for 2014. *National Vital Statistics Reports* 2015; **64**.http://www.cdc.gov/nchs/data/nvsr/nvsr64/nvsr64_12.pdf (accessed 5 Dec2016).

159 San-Frutos L, Engels V, Zapardiel I, Perez-Medina T, Almagro-Martinez J, Fernandez R *et al.* Hemodynamic changes during pregnancy and postpartum: a prospective study using thoracic electrical bioimpedance. *J Matern Fetal Neonatal Med* 2011.

160 El Gebeily G, El Khoury N, Mathieu S, Brouillette J, Fiset C. Estrogen regulation of the transient outward K+ current involves estrogen receptor a in mouse heart. *J Mol Cell Cardiol* 2015; **86**: 85–94.

161 Eghbali M, Deva R, Alioua A, Minosyan TY, Ruan H, Wang Y *et al.* Molecular and functional signature of heart hypertrophy during pregnancy. *Circ Res* 2005; **96**: 1208–1216.

162 Cooke PS, Buchanan DL, Lubahn DB, Cunha GR. Mechanism of estrogen action:Lesson from the estrogen receptor-alpha knockout mouse. *Biol Reprod* 1998; **59**: 470–475.

163 Zhang Y, Post WS, Cheng A, Blasco-Colmenares E, Tomaselli GF, Guallar E. Thyroid Hormones and Electrocardiographic Parameters: Findings from the Third National Health and Nutrition Examination Survey. *PLoS ONE* 2013; **8**. doi:10.1371/journal.pone.0059489.

164 Du XJ, Bathgate RAD, Samuel CS, Dart AM, Summers RJ. Cardiovascular effects of relaxin: from basic science to clinical therapy. *Nat Rev Cardiol* 2010; **7**: 48–58.

165 Han X, Habuchi Y, Giles WR. Relaxin increases heart rate by modulating calcium current in cardiac pacemaker cells. *Circ Res* 1994; **74**: 537–541.

166 Speranza G, Verlato G, Albiero A. Autonomic changes during pregnancy: Assessment by spectral heart rate variability analysis. *J Electrocardiol* 1998; **31**: 101–109.

167 Ekholm EM, Erkkola RU. Autonomic cardiovascular control in pregnancy. *Eur J Obstet Gynecol Reprod Biol* 1996; **64**: 29–36.

168 Ekholm EM, Erkkola RU, Piha SJ, Jalonen JO, Metsala TH, Antila KJ. Changes in autonomic cardiovascular control in mid-pregnancy. *Clin Physiol* 1992; **12**: 527–536.

169 Kuo CD, Chen GY, Yang MJ, Lo HM, Tsai YS. Biphasic changes in autonomic nervous activity during pregnancy. *Br J Anaesth* 2000; **84**: 323–329.

170 Wolbrette D, Patel H. Arrhythmias and women. *Curr Opin Cardiol* 1999; **14**: 36–43.

171 Burke JH, Goldberger JJ, Ehlert FA, Kruse JT, Parker MA, Kadish AH. Gender differences in heart rate before and after autonomic blockade: Evidence against an intrinsic gender effect. *Am J Med* 1996; **100**: 537–543.

172 Grossman W, Paulus WJ. Myocardial stress and hypertrophy: a complex interface between biophysics and cardiac remodeling. *J Clin Invest* 2013; **123**: 3701–3703.

173 Hellsten Y, Nyberg M. Cardiovascular Adaptations to Exercise Training. *Compr Physiol* 2015; **6**: 1–32.

174 Evans DL. Cardiovascular adaptations to exercise and training. *Vet Clin North Am Equine Pract* 1985; **1**: 513–531.

175 Estes NA, Link MS, Cannom D, Naccarelli GV, Prystowsky EN, Maron BJ *et al.* Report of the NASPE policy conference on arrhythmias and the athlete. *J Cardiovasc Electrophysiol* 2001; **12**: 1208–1219.

176 Stein R, Medeiros CM, Rosito GA, Zimerman LI, Ribeiro JP. Intrinsic sinus and atrioventricular node electrophysiologic adaptations in endurance athletes. *J Am Coll Cardiol* 2002; **39**: 1033–1038.

177 Weeks KL, McMullen JR. The Athlete's Heart vs. the Failing Heart: Can Signaling Explain the Two Distinct Outcomes? *Physiology* 2011; **26**: 97–105.

178 Coote JH, White MJ. CrossTalk proposal: bradycardia in the trained athlete is attributable to high vagal tone. *J Physiol* 2015; **593**: 1745–1747.

179 D'Souza A, Sharma S, Boyett MR. CrossTalk opposing view: bradycardia in the trained athlete is attributable to a downregulation of a pacemaker channel in the sinus node. *J Physiol* 2015; **593**: 1749–1751.

180 Guasch E, Nattel S. CrossTalk proposal: Prolonged intense exercise training does lead to myocardial damage. *J Physiol* 2013; **591**: 4939–4941.

181 Baldesberger S, Bauersfeld U, Candinas R, Seifert B, Zuber M, Ritter M *et al.* Sinus node disease and arrhythmias in the long-term follow-up of former professional cyclists. *Eur Heart J* 2008; **29**: 71–78.

182 D'Souza A, Bucchi A, Johnsen AB, Logantha SJ, Monfredi O, Yanni J *et al.* Exercise training reduces resting heart rate via downregulation of the funny channel HCN4. *Nat Commun* 2014; **5**: 3775.

183 Aschar-Sobbi R, Izaddoustdar F, Korogyi AS, Wang Q, Farman GP, Yang F *et al.* Increased atrial arrhythmia susceptibility induced by intense endurance exercise in mice requires TNFα. *Nat Commun* 2015; **6**: 6018.

184 Guasch E, Benito B, Qi X, Cifelli C, Naud P, Shi Y *et al.* Atrial fibrillation promotion by endurance exercise: demonstration and mechanistic exploration in an animal model. *J Am Coll Cardiol* 2013; **62**: 68–77.

185 Monfredi O, Dobrzynski H, Mondal T, Boyett MR, Morris GM. The anatomy and physiology of the sinoatrial node--a contemporary review. *Pacing Clin Electrophysiol* 2010; **33**: 1392–1406.

186 Liu J, Noble PJ, Xiao G, Abdelrahman M, Dobrzynski H, Boyett MR *et al.* Role of pacemaking current in cardiac nodes: Insights from a comparative study of sinoatrial node and atrioventricular node. *Prog Biophys Mol Biol* 2001; **96**: 294–304.

187 Dinarello CA. Blocking IL-1 in systemic inflammation. *J Exp Med* 2005; **201**: 1355–1359.

188 Abbate A, Kontos MC, Grizzard JD, Biondi-Zoccai GG, Van Tassell BW, Robati R *et al.* Interleukin-1 blockade with anakinra to prevent adverse cardiac remodeling after acute myocardial infarction (Virginia Commonwealth University Anakinra Remodeling Trial [VCU-ART] Pilot study). *Am J Cardiol* 2010; **105**: 1371–1377.

189 Van Tassell BW, Toldo S, Mezzaroma E, Abbate A. Targeting interleukin-1 in heart disease. *Circulation* 2013; **128**: 1910–1923.

190 Van Tassell BW, Raleigh JM, Abbate A. Targeting Interleukin-1 in Heart Failure and Inflammatory Heart Disease. *Curr Heart Fail Rep* 2014.

191 Van Tassell BW, Seropian IM, Toldo S, Mezzaroma E, Abbate A. Interleukin-1beta induces a reversible cardiomyopathy in the mouse. *Inflamm Res* 2013.

192 Dinarello CA. Interleukin-1 in the pathogenesis and treatment of inflammatory diseases. *Blood* 2011; **117**: 3720–3732.

193 Ono K, Iijima T. Cardiac T-type Ca2+ channels in the heart. *J Mol Cell Cardiol* 2010; **48**: 65–70.

194 Rao C, Prodromakis T, Kolker L, Chaudhry UAR, Trantidou T, Sridhar A *et al.* The effect of microgrooved culture substrates on calcium cycling of cardiac myocytes derived from human induced pluripotent stem cells. *Biomaterials* 2013; **34**: 2399–2411.

195 Levine TB, Bernink PJLM, Caspi A, Elkayam U, Geltman EM, Greenberg B *et al.* Effect of Mibefradil, a T-Type Calcium Channel Blocker, on Morbidity and Mortality in Moderate to Severe Congestive Heart Failure. *Circulation* 2000; **101**: 758–764.

196 Verkerk AO, Borren MMGJ van, Peters RJG, Broekhuis E, Lam KY, Coronel R *et al.* Single Cells Isolated from Human Sinoatrial Node: Action Potentials and Numerical Reconstruction of Pacemaker Current. *ResearchGate* 2007; **2007**: 904–7.

197 Verkerk AO, Wilders R, Borren MMGJ van, Peters RJG, Broekhuis E, Lam K *et al.* Pacemaker current (If) in the human sinoatrial node. *Eur Heart J* 2007; **28**: 2472–2478.

198 Verkerk AO, van Borren MMGJ, Wilders R. Calcium transient and sodium-calcium exchange current in human versus rabbit sinoatrial node pacemaker cells. *ScientificWorldJournal* 2013; **2013**: 507872.

199 Gulick T, Chung MK, Pieper SJ, Lange LG, Schreiner GF. Interleukin 1 and tumor necrosis factor inhibit cardiac myocyte beta-adrenergic responsiveness. *Proc Natl Acad Sci U A* 1989; **86**: 6753–6757.

200 Ma J, Guo L, Fiene SJ, Anson BD, Thomson JA, Kamp TJ *et al.* High purity human-induced pluripotent stem cell-derived cardiomyocytes: electrophysiological properties of action potentials and ionic currents. *Am J Physiol Heart Circ Physiol* 2011; **301**: H2006-2017.

201 Strobel JS, Epstein AE, Bourge RC, Kirklin JK, Kay GN. Nonpharmacologic validation of the intrinsic heart rate in cardiac transplant recipients. *J Interv Card Electrophysiol Int J Arrhythm Pacing* 1999; **3**: 15–18.

202 Opthof T. The normal range and determinants of the intrinsic heart rate in man. *Cardiovasc Res* 2000; **45**: 177–184.

203 Lieu DK, Fu J-D, Chiamvimonvat N, Tung KC, McNerney GP, Huser T *et al.* Mechanism-based facilitated maturation of human pluripotent stem cell-derived cardiomyocytes. *Circ Arrhythm Electrophysiol* 2013; **6**: 191–201.

204 Nguyen-Tran VT, Kubalak SW, Minamisawa S, Fiset C, Wollert KC, Brown AB *et al.* A novel genetic pathway for sudden cardiac death via defects in the transition between ventricular and conduction system cell lineages. *Cell* 2000; **102**: 671–682.

205 Yang X, Pabon L, Murry CE. Engineering Adolescence: Maturation of Human Pluripotent Stem Cell–Derived Cardiomyocytes. *Circ Res* 2014; **114**: 511–523.

206 Akdis M, Burgler S, Crameri R, Eiwegger T, Fujita H, Gomez E *et al.* Interleukins, from 1 to 37, and interferon-γ: Receptors, functions, and roles in diseases. *J Allergy Clin Immunol* 2011; **127**: 701–721.e70.

207 Kaur K, Zarzoso M, Ponce-Balbuena D, Guerrero-Serna G, Hou L, Musa H *et al.* TGF-beta1, released by myofibroblasts, differentially regulates transcription and function of sodium and potassium channels in adult rat ventricular myocytes. *PLoS One* 2013; **8**: e55391.

208 Musa H, Kaur K, O'Connell R, Klos M, Guerrero-Serna G, Avula UMR *et al.* Inhibition of platelet-derived growth factor-AB signaling prevents electromechanical remodeling of adult atrial myocytes that contact myofibroblasts. *Heart Rhythm* 2013; **10**: 1044–1051.

209 Ferrari R. The role of TNF in cardiovascular disease. *Pharmacol Res* 1999; **40**: 97–105.

210 Fiset C. Platelet-derived growth factor: A promising therapeutic target for atrial fibrillation. *Heart Rhythm* 2013; **10**: 1052–1053.